Development of tissue engineered blood vessels using cell-seeded acellular porcine arterial scaffolds

By

Dr Mark Richard Tatterton

Submitted in accordance with the requirements for the degree of Doctor of Medicine

School of Medicine

University of Leeds

September 2015

The candidate confirms that the work submitted is his own, except where work which has formed part of jointly authored publications has been included. The contribution of the candidate and the other authors to this work has been explicitly indicated below. The candidate confirms that appropriate credit has been given within the thesis where reference has been made to the work of others.

Chapter 1 contains work from a jointly-authored publication:

M. Tatterton, S-P. Wilshaw, E.Ingham, S Homer-Vanniasinkam. ***The use of antithrombotic therapies in reducing synthetic small-diameter vascular graft thrombosis,*** *Journal of Vascular and Endovascular Surgery****,*** *2012;* ***46:3;*** *212-222.*

The work attributable to me was that of performing the literature review for the publication and writing the manuscript for the publication. The remaining co-authors provided guidance on the final editing and layout of the publication.

Acknowledgements

Firstly I would like to extend my sincere gratitude to my supervisors Professor Homer-Vanniasinkam, Professor Eileen Ingham and Dr Stacy-Paul Wilshaw for allowing me to undertake this project in tissue engineering. I would also like to thank my supervisors for all their help, support, guidance and patience during my project.

I would also like to thank my father, Keith Tatterton for his help in tissue procurement and both my parents, Judy and Keith Tatterton, for all their love and support over the years. They have both been a constant source of help and guidance throughout my career.

I would like to thank all members of the iMBE department for all their help, with special thanks to Taha Khan, Kirsty Owen, Robert Guilliatt, Chris Brown and Dan Thomas. They all made me feel very welcome in the laboratory and were a constant source of help and guidance.

Abstract

The patency rate of small diameter synthetic bypass grafts remains poor. The aim of this study was to develop a biocompatible, acellular, arterial scaffold, assess the scaffolds regenerative capacity using ovine vascular cells and begin preliminary studies of a vascular tissue bioreactor for the development of a tissue engineered graft for peripheral and coronary arterial bypass.

Porcine carotid arteries were decellularised using a protocol developed at the University of Leeds. Arteries were incubated sequentially in disodium ethylenediaminetetraacetic acid, hypotonic solution, sodium dodecyl sulphate [0.1% w/v], DNAse and RNAse, hypertonic solution and 0.1% (v/v) peracetic acid.

To ensure decellularisation, representative arterial histological sections were stained using haematoxylin and eosin and 4',6-diamidino-2-phenylindole to confirm removal of cells and cell nuclei. The total DNA content of treated arteries was also determined. Biocompatibility of the acellular scaffolds was assessed using contact and extract cytotoxicity assays using both primary cells (porcine and ovine endothelial cells and smooth muscle cells) and two distinct cell lines (murine 3T3 and BHK cells).

Ovine endothelial cells were harvested from the femoral arteries of sheep following digestion with collagenase. Ovine smooth muscle cells were isolated from ovine arterial explant cultures. To determine correct cell phenotype, immuno-staining was performed using a variety of primary antibodies to vascular cell markers by indirect immunofluorescence. Ovine vascular cells were then seeded onto the luminal surface of the decellularised vessels in both a two-dimensional and three-dimensional manner. A cell viability assay (Live / Dead Stain ®) was performed to confirm the viability of seeded cells.

A vascular bioreactor was successfully assembled and preliminary sterility runs were performed in preparation for future scaffold pre-conditioning.

The decellularisation protocol resulted in porcine carotid arteries that were free from cells with >90% of the total DNA being removed. The decellularised porcine carotid artery was not cytotoxic to any test cells. Indirect immunofluorescence performed on the harvested cells confirmed correct ovine endothelial cell and smooth muscle cell phenotype after cell isolation using magnetic bead separation. Ovine vascular cells were successfully seeded onto the luminal matrix of decellularised arteries in both two-dimensional and three-dimensional experiments. Seeded cells were viable at 48 hours post incubation. A

vascular bioreactor was successfully assembled and was kept free from macroscopic microbial contamination for a maximum of fourteen days.

In conclusion, porcine carotid arteries were successfully decellularised using an established decellularisation protocol. The remaining acellular scaffolds demonstrated capability in allowing the attachment and proliferation of xenogeneic vascular cells onto the scaffold surface. Further work developing a vascular bioreactor in order assess the functionality and ongoing cell viability of the seeded scaffold will be needed to assess the efficacy of decellularised porcine carotid artery as a viable conduit for arterial bypass.

Table of Contents

List of Tables

List of Figures

List of Abbreviations

AK	Above knee
ATP	Adenosine-5-triphosphate
BK	Below knee
BHK	Baby hamster kidney
CABG	Coronary artery bypass grafting
CHD	Coronary heart disease
CO_2	Carbon dioxide
CV	Cardiovascular
DABCO	1,4-diazobicyclo-(2,2,2)-octane
Dacron	Polyethylene terephthalate
DAPI	4',6-diamidino-2-phenylindole
DMEM	Dulbecco's Modified Eagle's Medium
DMSO	Dimethylsulfoxide
DNA	Deoxyribonucleic acid
DPBSa	Dulbecco's Phosphate Buffered Saline
EC	Endothelial cell
ECM	Extracellular matrix
EDTA	Disodium ethylenediaminetetraacetic acid
EPC	Endothelial progenitor cells
ePTFE	Expanded polytetrafluoroethylene

FBS	Foetal bovine serum
GAG	Glycosaminoglycans
H+E	Haemotoxylin and Eosin
iMBE	Institute of Medical and Biological Engineering
MSC	Mesenchymal stem cells
NIH	Neointimal hyperplasia
NO	Nitric oxide
P	Passage
PAA	Peracetic acid
PAD	Peripheral arterial disease
PC	Porcine carotid
SD	Small diameter
SMC	Smooth muscle cell
TBS	Tris buffered saline
UK	United Kingdom

Chapter 1

Literature Review

1. Introduction

Cardiovascular (CV) disease remains the most common cause of death within the Western population (Campbell *et al*., 1999). In the US, two million deaths a year are caused by CV disease and in the UK, one in three deaths (Punshon *et al*., 2008).

The Western lifestyle of excess, lipid-laden foods, smoking and lack of exercise are the leading causes of CV disease (American Heart Association, 2010). In order to treat such prevalent disease, worldwide, over 800,000 coronary artery bypass (CABG) procedures and 3,000,000 peripheral bypass procedures are performed annually (Fields *et al*., 2002; Nalysnyk *et al*., 2003).

Autologous saphenous vein remains the most commonly used graft for performing peripheral and coronary revascularisation (Izzat *et al*., 1994; Nigri *et al*., 2004). Saphenous vein has mechanical strength, resistance against infection and antithrombogenic properties. Unfortunately, in up to a third of cases, the vein is unsuitable for use or has been harvested previously (Sayers *et al*., 1998).

For coronary bypass, if vein is not available, other conduits such as the internal mammary artery or radial artery may be harvested. However when multiple or revision grafts are required (15% of cases), there may be a lack of autogenous material, necessitating use of synthetic material (Farrar, 2000). For peripheral bypass, surgeons must turn to the use of synthetic grafts when performing bypass procedures if vein is not available. The two synthetic grafts which are widely used clinically in bypass surgery are polyethylene terepthalate (Dacron) and expanded polytetrafluroethylene (ePTFE). Synthetic medium and large-diameter grafts with higher flow rates and lower resistance have been shown to have much higher patency rates than small-diameter (SD) grafts (Kannan *et al*., 2005; Kasisis *et al*., 2005). The patency of synthetic SD grafts (<6mm) is poor, largely as a result of thrombosis and neointimal hyperplasia (NIH) within the graft (Ishii *et al*., 2008). At four years, the primary patency rates of ePTFE infra-popliteal and aorto-coronary grafts are 12% and 14% (Weyand *et al.*, 1999; Biancari *et al.*, 2001). SD grafts are the conduits required most often for coronary and peripheral arterial revascularisation (Mitchell *et al.*, 2003). In addition to their poor performance when implanted into small diameter arteries,

synthetic grafts lack favourable biomechanical properties and display much higher rates of infection compared to vein grafts.

Although vein grafts have been shown to have superior patency rates compared to synthetic grafts (75% patency at five years), they are not without complications, 7-13% of grafts occlude within the first year, 15% fail within five years and 25% fail thereafter (Hatar *et a.l*, 2007; Punshon *et al.*, 2008; Thomas *et al.*, 2009). Furthermore, veins produce less heparin sulphate, nitric oxide (NO) and tissue plasminogen activator (tPA) compared to arterial tissue, increasing their thrombogenic potential (Angelini *et al.*, 1989; Cox *et al.*, 1991; Allaire *et al.*, 1997). In addition, vein harvest sites are associated with wound complications and post-operative leg oedema.

For both peripheral and coronary artery bypass grafting, causes of graft failure can be divided into early, mid-term and late. Early failure (within 30 days) is as a result of surgical error or graft thrombosis (Conte *et al*., 2002). Mid-term failure (between 3 months to 2 years) occurs as a result of neointimal hyperplasia, a process of smooth muscle proliferation that occurs predominantly at/around the distal anastomosis, narrowing the graft lumen (Sottiurai *et al*., 1983; Moneta *et al*., 1995;). Long-term graft failure (after 2 years) results from ongoing active atherosclerosis within the graft (Moneta *et al*., 1995).

There is an urgent need therefore for the development of novel SD vascular grafts and efforts are currently focused on developing a superior SD conduit that addresses the key issues of biocompatibility, thrombogenicity and patency. The key attributes of an ideal vascular graft are given in Table (1).

Non-thrombogenic	Easy to manufacture
Non-immunogenic	Easy to transport
Non-carcinogenic	Easy to store
Bacteriostatic	Easy to handle
Displays effective endothelialisation	Long-term mechanical stability
Inhibits neointimal hyperplasia	Unlimited size availability
Reasonable cost	Biomechanical properties similar to native artery

Table 1. Attributes of the 'Ideal' Vascular Graft.

1.1 Structure and function of human arterial blood vessels

A typical artery is comprised of three main layers: the tunica intima, tunica media and tunica adventitia (Figure 1). The intima is made up of a monolayer of endothelial cells (EC), collectively called the 'endothelium'. The integrity and function of the endothelium is vitally important for maintaining the haemodynamics of blood flow and the balance between thrombosis and fibrinolysis. The medial layer consists of smooth muscle cells (SMC) embedded in an extracellular matrix (ECM) of collagens (type I and III), proteoglycans and other proteins such as elastin. The medial layer provides mechanical strength and gives functionality to the artery by controlling luminal diameter. Proteoglycans provide resistance to compression, collagens provide tensile strength and elastin fibres provide recoil and deformability and determine the vessel compliance. The outer layer, the adventitia, is separated from the medial layer by the external elastic lamina. The adventia is mainly comprised of loose collagen fibres and fibroblasts. It serves to adhere the artery to surrounding tissue and provides access for the vasa vasorum (Mitchell *et al.*, 2003; Stegemann *et al*., 2007).

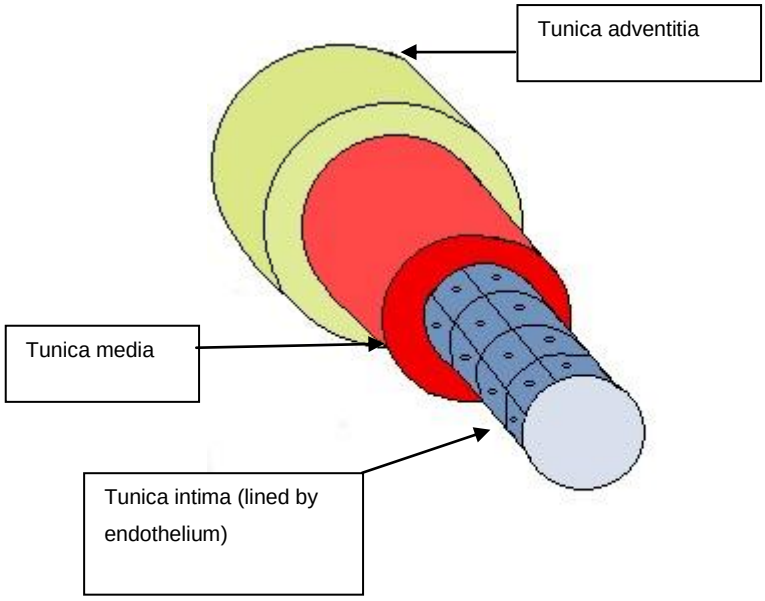

Figure 1. Basic cross-sectional structure of a human artery.

1.1.1 Importance of the endothelium

The endothelium provides many anti-thrombogenic functions. It contains anticoagulants such as heparins and thrombomodulin and produces inhibitors of platelet aggregation such as prostacyclin (Mitchell *et al*., 2003; Sarkar *et al*., 2007). It serves an important barrier function between circulating proteins of the coagulation cascade and the thrombogenic subendothelium. Damage to, or activation of, the endothelium by procoagulants such as thrombin and fibrin leads to attenuation of its anti-thrombotic nature (Yang *et al*., 2007). The endothelium is also important for regulating the movement and proliferation of underlying SMC, by the release of transforming growth factors (Sprague *et al*., 2005).

1.2 Atherosclerosis

Atherosclerosis is the process responsible for both peripheral arterial disease (PAD) and coronary heart disease (CHD). It is a complex process that can be identified as early as infancy. Major risk factors for atherosclerosis include age, gender, smoking, hypercholesterolaemia, hypertension, diabetes and homocysteinaemia. The process is initiated by endothelial dysfunction as a result of injury (see above). The injured endothelium releases pro-inflammatory mediators that lead to several key processes in the arterial wall: 1) chronic inflammation (characterised by chronic inflammatory cell infiltrates such as T lymphocytes and macrophages), 2) deposition of lipid [mainly low-density lipoprotein (LDL)], 3) vascular SMC migration and proliferation and 4) remodelling of the arterial ECM. The net result of these four processes is the formation of an intimal plaque, characterized by a fibrous cap and a lipid-laden core (Libby *et al*., 2011). The mediators that lead to these four key events are numerous and complex and include, in particular: the tumour necrosis factor α (TNF-α) / NO pathway, the renin-angiotensin axis, secretion of matrix metalloproteinase (MMP-9 and MMP- 12), membrane receptors such as LOX-1 (lectin-like oxidized LDL receptor-1) , RAGE (receptor for advanced glycation end products, TLRs (toll-like receptors) and NLRs (nod-like receptors) (Mehta *et al*., 2007).

The atherosclerotic plaque tends to cause pathology in two main ways. The plaque can grow in size ultimately leading to stenotic disease and chronic ischaemia or it can undergo thrombosis as a result of unstable plaque rupture, leading to acute ischaemia.

1.2.1 Peripheral arterial disease and peripheral arterial bypass

Almost 10 million Americans suffer currently from symptomatic PAD (Alexy *et al*., 2008). Surgical revascularisation is performed in patients with PAD who develop critical limb ischaemia or have severe, debilitating symptoms. For the former, a bypass procedure may offer the only hope against the threat of amputation. Two hundred and twenty thousand patients a year in the US require peripheral arterial bypass, the majority of whom will require infrainguinal revascularisation (National Centre for Health Statistics., 1996). Autologous saphenous vein is considered the gold standard graft for infrainguinal bypass due to superior patency rates over prosthetic grafts (Norgren *et al*., 2007). In the third of patients in whom autologous vein is not available, surgeons turn to synthetic grafts as alternatives. At present, ePTFE is used most frequently for infrainguinal bypass. A recent Cochrane review however found that Dacron had superior primary patency rates over PTFE in above-knee infrainguinal bypass (Twine *et al*., 2010). The reported patency rates of ePTFE, however, remain inferior when compared to saphenous vein. In above-knee (AK) bypass, 5-year primary patency rates of 39% have been reported for ePTFE against 74% for saphenous vein (Klinkert *et al*., 2004). In below-knee (BK) bypass, results are significantly worse with ePTFE demonstrating less than 50% primary patency rates at two years (Albers *et al*., 2003). For infrainguinal bypass, early and late graft occlusions remain the most common causes of failure (Pulli *et al*., 2010).

1.2.2 Coronary heart disease and coronary artery bypass grafting

Despite the increasing use of coronary angioplasty and stenting to treat symptomatic coronary heart disease, worldwide, just under a million patients still require coronary artery bypass grafting (CABG) each year (Nalysnyk *et al*., 2003).
Grafts between 2-3 mm are most frequently required for patients undergoing CABG (Dempsey *et al*., 1998). Grafts used for CABG include autologous internal mammary (thoracic) artery, radial artery and saphenous vein. Arterial grafts demonstrate greater patency rates than saphenous vein, however, saphenous vein continues to be utilised in over 70% of UK CABG surgery due to its ease of accessibility, harvesting and handling (Izzat *et al*., 1994).

When utilising saphenous vein, technical issues such as anastomotic angle, size mis-match and thrombosis are largely responsible for the 12% of patients who develop graft failure within the first year (Burton *et al*., 2006). At ten years, 50% of vein grafts have

occluded due to accelerated atherosclerosis (Suma, 1999). Synthetic SD conduits are avoided in coronary revascularisation due to poor patency and high failure rates (Jones *et al*.,1991; Ishii *et al*., 2008). Comparing ePTFE with autologous saphenous vein for example, Hehrlein *et al* reported patency at one year at 86% for saphenous vein and 59% for ePTFE. At 4 years, Chard *et al* reported a patency rate of just 14% for ePTFE aorto-coronary grafts (Hehrlein *et al*., 1984; Chard *et al*., 1987).

Lesions within the coronary arteries are generally repaired by circulating endothelial progenitor cells (EPC) which are attracted to damaged epithelium by chemotaxis. As synthetic grafts do not release chemokines, EPC are not attracted to the graft surface and so thrombosis often ensues due to a lack of an EC monolayer (Hoffmann *et al*., 2008). Synthetic CABG is therefore only attempted when autogenous material is not available.

1.2.3 Use of allogeneic tissue

The use of cardiovascular allografts such as cryopreserved saphenous vein and glutaraldehyde-tanned human umbilical vein, theoretically, have two obvious advantages compared to synthetic graft materials. Allografts possess a functioning endothelium and display a reduced tendency for infection (Wilshaw *et al*., 2012). Unfortunately such materials have failed to achieve widespread clinical use due to low patency rates (19%-42% at 6 years) and complications such as aneurysmal dilatation, calcification, degradation (thought to be due to elastin depletion) and allosensitisation. Aldehyde-tanned tissue in particular was shown to demonstrate high rates of thrombogenicity as a result of collagen exposure (Sawyer *et al*., 1987; Strobel *et al*., 1996; Benedetto *et al*., 2001; Harris *et al*., 2001; Thomas *et al*., 2003; Swartz et al., 2005). Furthermore, the general feeling from vascular surgeons when using such tissues is that the tissue handling properties and expense of production cannot justify their commercial use (Devine *et al*., 2001).

1.3 Graft thrombosis and neointimal hyperplasia

As discussed earlier, graft thrombosis and neointimal hyperplasia (NIH) are the two main processes responsible for the poor patency rates of SD grafts.

1.3.1 Graft thrombosis

Formation of graft thrombus is dependent upon the inherent properties and thrombogenicity of the graft surface, the haemodynamics of the graft itself, the degree of graft healing (neo-intimal formation and endothelialisation), blood flow, surgical technique and the thrombotic profile of the recipient patient (Ariyoshi *et al*., 1997; Haruguchi *et al*., 2003; Zhan *et al*., 2010).Graft endothelialisation is an important factor influencing thrombogenesis. It has been extensively shown that the generation of a confluent endothelium on the surface of SD synthetic grafts reduces their thrombogenicity and improves short and long-term patency (Zilla *et al*., 1994; Meinhart *et al*., 2001; Sarkar *et al*., 2007).

EC are able to migrate and adhere to the graft from the anastomosis, the recipient's bloodstream and from neocapillary formation (Greisler, 1982). Exposure to arterial pressure and flow however, significantly limits this process (Giudiceandrea *et al*., 1998). Unlike other animals, in humans, synthetic grafts display minimal rates of spontaneous and trans-anastomotic endothelialisation. ePTFE for example, the most favoured synthetic graft for peripheral revascularisation, has been shown to have poor rates of endothelialisation, even up to five years post-implantation (Camilleri *et al*., 1985; Formichi *et al*., 1988). The lack of this process is a key factor that contributes to graft thrombosis and NIH in synthetic grafts.

1.3.1.1 Events following vascular graft implantation

Synthetic

The presence of a synthetic vascular graft initiates a complex system of prothrombotic activity within the local circulation. Following implantation, the *Vroman effect* leads to the adsorption of coagulation factors and adhesive proteins on synthetic graft surfaces such as glycoprotein IIb-IIIa, fibrinogen, thrombin and von Willebrand factor (Vroman, 1962; Ikeda *et al*., 1996; Spijker *et al*., 2003). These proteins cause adherence of platelets, leading to platelet aggregation and activation, and generation of further fibrin (Suzuki *et al*., 1996). Following activation, platelets will release further thrombogenic products such as thromboxane B_2 and β-thromboglobulin leading to thrombus propagation (Spijker *et al*., 2003). Platelet adhesion and activation is also influenced by the 'wettability' of the surface

material. Hydrophillic materials have been shown to lead to higher rates of platelet adhesion whilst hydrophobic materials lead to greater rates of platelet activation (Spijker *et al*., 2002). If the Vroman process propagates exponentially, thrombosis will ensue. If it is limited, the laid down fibrin and proteins will form neointima, with the graft lumen remaining patent (Scharn *et al*., 2006).

In 1979, Sauvage *et al*. developed the notion of a 'thrombotic threshold velocity (TTV)' for a material surface, essentially, the relationship between blood flow velocity and thrombosis. A higher blood flow leads to increased shear forces acting on the graft surface, reducing thrombus formation. Blood flow above the TTV prevents thrombosis whilst flow below results in thrombus formation. Pouiselles's law states that flow through small diameter grafts is low. The low flow present in a SD synthetic graft therefore leads to less shear forces on the graft surface and may mean that the TTV for that material is not reached. As a consequence, thrombosis can ensue.

Synthetic / Vein

Implantation of either a synthetic or venous graft inevitably involves injury to native blood vessels. When veins are used as grafts, substantial injury can occur to the venous endothelium prior to implantation, during the harvesting process. Following harvesting, implantation of the hypoxic vein graft into the arterial circulation exposes the vein not only to increased pressures, but also to higher oxygen tensions within the blood. This rapid change in oxygen tension leads to the creation of free radical species that cause damage to tissue and the endothelium (Motwani *et al*., 1989). Following damage, endothelial cells up-regulate the production of adhesion molecules and procoagulants such as von-Willebrand factor, thrombin, plasminogen activator inhibitor and tissue factor (TF). In addition, there is a down-regulation of antithrombotics such as thrombomodulin, NO and tPA expression by damaged endothelium (Motwani *et al*., 1989; Fields *et al*., 2002; Hagemeyer *et al*., 2009). Plasmin is formed from plasminogen in a fibrin environment mainly by the action of tPA, and to a lesser extent urokinase-type plasminogen activator (uPA). Plasmin acts on fibrin to cause thrombus dissolution via proteolysis (Potter *et al*., 1992; Novokhatny, 2008). Loss of tPA therefore elevates the vein graft to an already heightened thrombotic state. When synthetic grafts are implanted, damage will occur to native vessels at the sites of the proximal and distal anastomosis. An important net result of endothelial damage in these cases is the release of TF and initiation of the TF-pathway of coagulation (Figure 2). Factor VII (FVII) and factor VIIa (FVIIa) from the circulation form

a complex with exposed TF, leading to the activation of factor X (FX) and factor IX (FIX). FIXa up-regulates the formation of FXa**.** FXa complexes with factor V (FV) on platelet membranes, forming the prothrombinase complex, which cleaves prothrombin to thrombin. Thrombin converts fibrinogen to fibrin and activates platelets, leading to thrombus generation (Rubin *et al*., 1996). Feedback activation by thrombin of FVIII, FIX and FV leads to further thrombin production (Mann *et al*., 2003). Bound thrombin remains active within a clot, cleaving additional fibrinogen to fibrin. In addition, there is no inhibition by antithombin III on thrombin in this form. Thrombin therefore is considered a dominant procoagulant in the aetiology of graft thrombogenesis (Weitz *et al*., 1990). There is an inhibitory protein present in the circulation produced by the endothelium to counteract the TF pathway of coagulation. The tissue factor pathway inhibitor protein (TFPI) circulates alone or complexed with plasma lipoproteins. It binds to and inhibits the TF / FVIIa complex preventing FX activation. Damage to the endothelium however, leads to the down-regulation of TFPI expression (Broze *et al*., 1988; Sarkar et al., 2007).

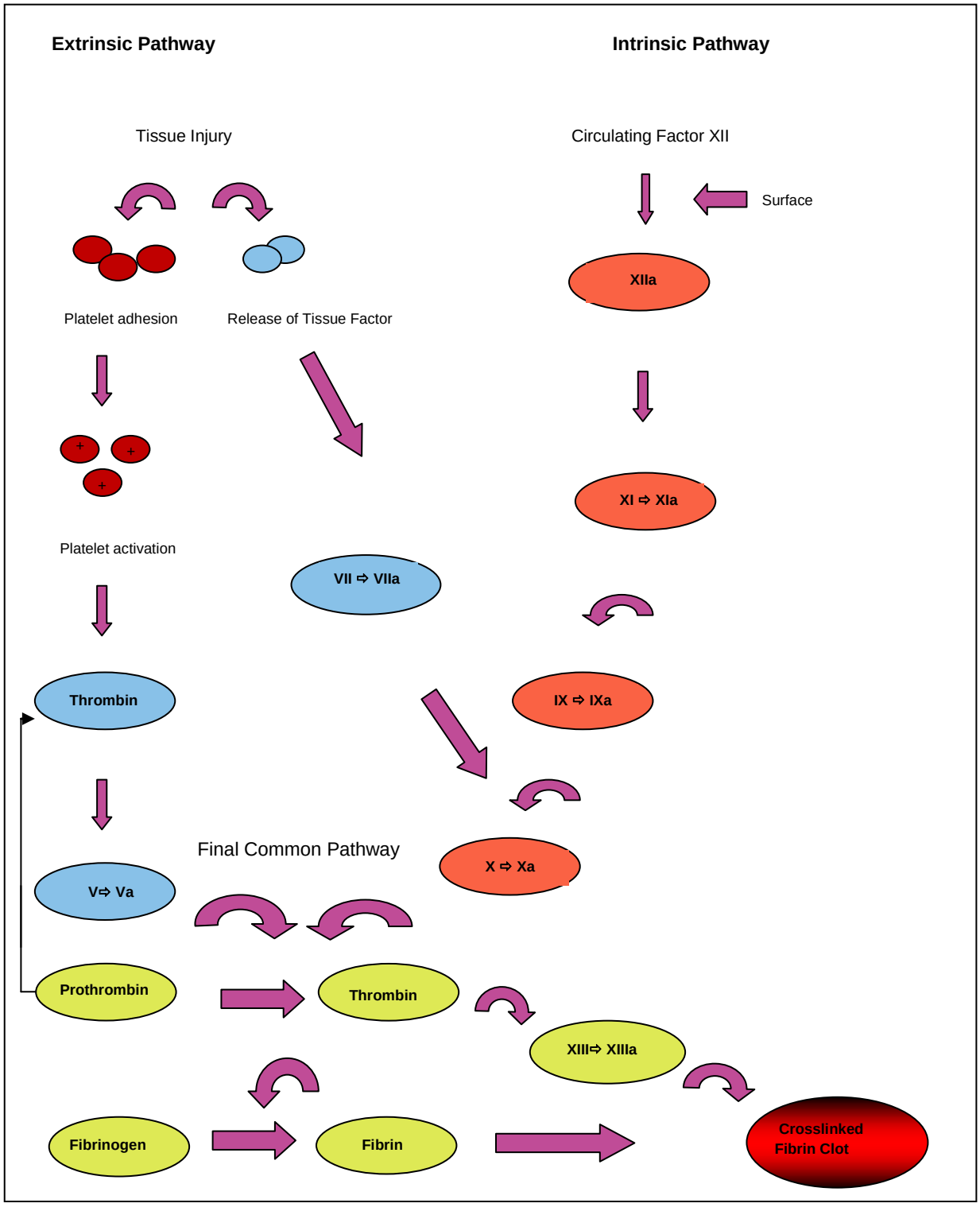

Figure 2. The coagulation cascade (adapted from Sakar *et al*., 2007). VII to XIII, Prothrombin and Thrombin = coagulation factors.

The net effect of these complex processes following SD graft implantation is the rapid activation of the coagulation cascade and subsequent formation of graft surface thrombus. Certainly in synthetic grafts, Toursarkissian *et al*. (2007) have demonstrated that such procoagulant activity continues for at least 24 hours post-implantation.

1.3.2 Neointimal hyperplasia

Neointimal hyperplasia is a process that occurs in both synthetic and vein grafts and alongside thrombosis, is a major cause of graft failure. It predominantly occurs at sites of anastomoses, causing narrowing of the lumen initially and then eventually leading to occlusion. The pathogenesis of NIH is complex and involves the migration and proliferation of SMC, myofibroblasts, macrophages, platelets, inflammatory pathways and deposition of extracellular matrix (Schachner *et al*., 2006). The initiating step in the development of NIH is endothelial damage. Damage occurs in several ways. In vein-grafts, damage occurs initially during harvesting. For both synthetic and vein grafts, damage to the endothelium of the native artery occurs during creation of the anastomosis. Implantation of vein or synthetic graft into the arterial circulation leads to turbulent flow as a result of a radial compliance mismatch between the graft and native artery and altered or increased vessel wall forces and stresses (Kannan *et al*., 2005; Desai *et al*., 2010;). Such altered haemodynamics damages the endothelium lining the graft. Damage to endothelium has been shown to lead to the widespread release of factors that promote NIH. Damaged endothelia release inflammatory mediators, growth factors (platelet-derived growth factor, vascular-endothelial growth factor) and cytokines. These substances cause proliferation and migration of vascular SMC and myofibroblasts from the media and adventitia to the intima. They also promote modification of the ECM and deposition of new ECM and endothelial cell proliferation within the intima (Schachner, 2006; Ahanchi *et al*., 2010; Desai *et al*., 2010). The net effect is thickening of the ‘neointima” lining the graft, a reduction in cross-sectional area and eventual luminal occlusion.

Reducing or preventing the development of NIH is an area under active research. Examples of simple strategies to date include external stenting of grafts, which aims to reduce compliance mismatch and distensibility and drug therapy with agents such as immunosuppressants and statins (Schachner, 2006; Desai *et al*., 2010). More complex strategies include the use of growth factor modulators, nitric oxide donors and gene therapy (Nigri *et al*., 2004). Simple surgical techniques to reduce NIH when using vein

grafts include minimising the handling of vein during harvesting and limiting the ischaemic time (Schachner, 2006).

1.4 Strategies to improve SD arterial bypass grafting

There are three main strategies focused on improving the outcomes of SD arterial bypass:

1) Modification of existing synthetic grafts e.g. graft functionalisation
2) Creation of new synthetic grafts e.g. nanocomposites
3) Creation of engineered blood vessels or hybrid synthetic grafts using tissue engineering.

With each strategy comes a large volume of research and literature too extensive to fully discuss here. As this thesis focuses on the third strategy, that of tissue engineering, this strategy forms the basis of this review.

1.5 Tissue engineering of blood vessels

Tissue engineering began in the late 70's and at its simplest, is the manipulation of cells to create functional tissue. Cardiovascular tissue engineering techniques range from modifying existing synthetic grafts, creating novel functionalised acellular biological scaffolds derived from allogeneic arteries and fully tissue engineered blood vessels comprising cell-seeded natural and synthetic scaffolds. Early and current cardiovascular tissue engineering strategies include the seeding of EC onto the surface of synthetic grafts in an attempt to recreate the innately anti-thrombogenic endothelium ('hybrid' grafts).

1.5.1 Hybrid graft development

It is now recognised that the generation of a confluent endothelium on the surface of synthetic grafts reduces their thrombogenicity and improves short and long-term patency. At present therefore, the endothelium is considered the gold-standard lining for vascular grafts (Zilla *et al*., 1994; Clowes *et al*., 1997; Meinhart *et al*., 2001; Sarkar *et al*., 2007). It was Herring *et al.* in 1978 who were the first to develop the idea of seeding autogenous EC onto the surface of prosthetic grafts in an attempt to reduce graft thrombogenicity. Following Herring *et al*. a large number of cell-seeding studies were performed in the 1980's and demonstrated that whilst feasible, EC-seeding and subsequent adhesion on

synthetic grafts was poor (Meinhart *et al*., 2001). During these initial studies, up to 70% of EC were lost from the graft surface following exposure to fluid shear forces (Rosenman *et al*., 1985). Difficulties faced in the development of such grafts included sourcing of EC, growing sufficient numbers in culture and as mentioned, maximising the adherence and retention of EC to the graft surface (Rashid *et al*., 2004).

The key elements for successful EC adherence have been suggested to be 1) the development of favourable interactions between the EC's and synthetic surface, 2) allowing sufficient time for EC adhesion and 3) ensuring appropriate distribution and density of EC's on the graft surface prior to exposure to shear forces (Pratt *et al*., 1988).

Ideally, a single-stage process of EC procurement and graft seeding followed by implantation would be optimal for the patient. However early studies showed this technique to yield low EC numbers and rates of adherence (Falk et al., 1998; Giudiceandrea *et al*., 1998). To combat these problems, two-stage EC seeding was developed in which the EC's were first extracted and then cultured *in vitro* to increase cell numbers prior to seeding. Using this two-stage technique, the clinical series by Zilla *et al.* (1994), Meinhart *et al.* (1997, 2001), Deutsch *et al.* (1997, 1999) and Laube *et al.* (2000) all unanimously demonstrated that endothelial seeding improved patency of synthetic grafts for both peripheral and coronary arterial bypass. When used for infra-inguinal bypass for example, endothelialised ePTFE had a primary patency of 84.7% at three years, compared to 55.4% for standard ePTFE (Zilla *et al*., 1994). At nine years, the primary patency of endothelialised grafts was 65% compared to 16% for standard ePTFE grafts (Deutsch *et al*.,1999).The improvement in patency was not just due to a reduction in graft thrombogenicity, but also a result of reduced rates of SMC proliferation and NIH within the grafts (Clowes, 1997).

The limitations of two-stage seeding are that it is expensive, the patient requires two procedures (EC procurement then implantation) and the patient must wait while the cells undergo culture (negating use in acute ischaemia) (Rashid *et al*., 2004; Punshon *et al*., 2008). Furthermore, cell populations are often mixed (fibroblasts, SMC and EC) and must be separated prior to culture and seeding (Knetsch *et al*., 2004). EC maintained in culture have been shown to become senescent at low passage values (ten and above) and so rapidly become unsuitable for graft seeding (Shi *et al*., 2004). As a result, two-stage cell seeding has not been widely adopted. Current techniques are aimed at modifying the two-stage process or creating new methods that aid endothelialisation. The seeding

techniques for any scaffold (biological or synthetic) can be divided simply into two broad categories- static or dynamic. In static seeding, the cells are simply placed in or onto the scaffold surface and left to attach under culture conditions. In dynamic seeding, the scaffold and cells undergo forces to aid attachment (radial/cyclical stress) using instruments such as roller plates and perfusion bioreactors. Under dynamic seeding conditions, greater seeding efficiencies have been reported (Hsu *et al*., 2005). For successful EC seeding of synthetic (and biological) grafts, cell densities of around 10^4-10^5 cells.cm^{-2} have been reported to be required to achieve confluent graft coverage (Salacinski *et al*., 2001). At present no EC-seeded synthetic graft has achieved widespread clinical use.

1.5.1.1 Cell attachment and interaction

The formation of ECM on a graft surface is vitally important for cell attachment. The ECM is secreted by both EC and SMC and includes molecules such as fibronectin and collagen. These molecules possess surface ligands that allow for cell attachment (Yu *et al*., 2003; Wallace *et al*., 2007). Several studies have shown that lining a synthetic graft with SMC prior to the seeding of EC improves the subsequent retention of EC to the graft by limiting EC aniokis (apoptosis due to deficient ECM) (Yu *et al*., 2001, 2003). This has been reported to be due to the more favourable attributes that SMC possess over EC for cell attachment. SMC produce more ECM than EC (allowing for greater numbers of EC cell attachment) and have been shown to adhere more readily to graft surfaces and resist the shear forces of bloodflow (Yu *et al*., 2003). Furthermore, the ECM laid down by SMC will provide the graft with elastic recoil and tensile strength, two essential attributes required particularly in biological grafts for mechanical integrity (Stephan *et al*., 2006). EC reciprocally interact with SMC, leading to the expression of growth factors responsible for the maintenance of and geometric orientation of, the ECM (Aper *et al*., 2007).

In their study, Yu *et al.* (2003) reported EC retention rates of 90% on ePTFE grafts at 24 hours post implantation into rabbit aortas when pre-coated with SMC, compared to only a 51% retention rate in grafts seeded with EC only.

There have been concerns that lining a graft with SMC will lead to significant NIH, reducing the luminal diameter and subsequent graft patency. However data suggests that with dual seeding, the EC limit SMC migration and proliferation as they do normally *in vivo* (Fillinger *et al*., 1993; Powell *et al*., 1996). In the study by Yu *et al.* (2003), although

neointimal thickness was greater in dual seeded grafts at 30 days, at 100 days there was no significant difference in thickness between dual seeded or single (EC) seeded grafts. If dual seeding is to be used, it is important to assess the effects of such seeding on 1) individual cell phenotype and 2) overall thrombogenicity. Particularly as it is quite clear from the literature that the interactions of EC and SMC show different species-specific behavior (Wallace *et al*., 2007; Pang *et al*., 2010; Zhao *et al*., 2010).

Pang *et al.* (2010) studied the thrombogenicity of a co-culture of porcine SMC and EC by measuring TF activity. SMC/EC co-cultures displayed higher levels of TF activity than EC cultured alone. The increased TF activity correlated with contraction of the SMC/EC co-culture. Contraction of the co-culture disrupted the EC monolayer allowing the exposure of high levels of TF present on the surface of SMC. The authors were able to demonstrate an association between contraction of the co-culture with increased levels of reactive oxygen species. Indeed, incubating the co-culture with an antioxidant (N-acetyl-L-cysteine) lead to a reduction in contraction of the co-culture. Interestingly, in a similar study using co-cultures of human SMC and EC, Wallace *et al.* (2007) demonstrated a reduction in TF activity in co-cultures compared to an EC monolayer. These *in vitro* findings cannot be extrapolated to an *in vivo* model however as the cells were not seeded onto scaffolds in these *in vitro* studies and therefore the studies did not examine the effects of the scaffold itself on cell phenotype. Certainly in studies in which both EC and SMC have been seeded onto biological scaffolds, a significant reduction in thrombogenicity was seen (Tiwari *et al*., 2001; Zhao *et al*., 2010).

There is no definitive optimal seeding density for seeding grafts with EC and SMC in the literature. Optimal cell densities are dependent on many variables, including: species, type and processing of graft and utilisation of dual or single cell seeding. In general, cell densities between 10^4-10^6 cells.ml^{-1} tend to be used. The range of cell seeding densities found within the literature for both biological and synthetic grafts is demonstrated in Table (2).

Cell type	Seeding Density	Scaffold (all tissue decellularised)	Culture	Authors
Human EC	$1.1x10^4$ + - $6x10^3$ cells. cm^{-1}	Porcine carotid artery (luminal)	Dynamic	Heine *et al*., 2011
Human SMC	5.7 $x10^3$ +- $2.8x10^2$ cells.cm^{-1}	Porcine carotid artery (adluminal)	Dynamic	Heine *et al*., 2011
Human EC	1.8x 10^4 cells.ml^{-1}	Porcine carotid artery (luminal)	Static	McFetridge *et al*., 2004
Human SMC	$6.7x10^4$ cells. ml^{-1}	Porcine carotid artery (adluminal)	Static	McFetridge *et al*., 2004
Ovine SMC	1 $x10^6$ cells.ml^{-1}	Porcine carotid artery (luminal)	Static	Nitsan *et al*., 2012
Human EC	1 $x10^6$ cells.ml^{-1}	Porcine carotid artery (adluminal)	Static	Nitsan *et al*., 2012
Human SMC & Fibroblasts	$1x10^6$ cells.ml^{-1}	Porcine carotid artery (luminal)	Dynamic	Shimizu *et al*., 2007
Human EC	1.2 x 10^5 cells.cm^{-1}	Porcine aorta	Dynamic	Bader *et al*., 2000
Human saphenous vein EC	5 x 10^6 cells.ml^{-1}	Porcine aorta	Dynamic	Amiel *et al*., 2006
Ovine EC	1 x 10^7 cells.ml^{-1}	Ovine carotid artery (luminal)	Static	Zhao *et al*., 2010
Ovine SMC-like cells	2 $x10^7$cells.ml^{-1}	Ovine carotid artery (luminal)	Static	Zhao *et al*., 2010
Porcine SMC	6-10$x10^4$ cells .cm^{-1}	Porcine SMC	Static	Pang *et al*., 2010
Porcine EPC	$1x10^6$ cells.ml^{-1}	Fibrin scaffold	Dynamic	Aper *et al., 2007*
Human umbilical vein SMC	10^6-10^7 cells.ml^{-1}	Type I Collagen	Static	Leung *et al*., 2007
Canine EC	1 x 10^6 cells.cm^{-1}	PGA/PLA	Dynamic	Iwai *et al*., 2005
Human EC & SMC	$1x10^5$ cells.cm^{-1}	Polyurethane	Static	Rashid *et al*., 2008
Human EC	6 x 10^4cells.cm^{-1}	Polyurethane	Static	Hsu *et al*., 2005
Human Fibroblasts, EC & SMC	4.4-7.7$x10^6$cells.cm^{-1}	Polyurethane	Dynamic	Gulbins *et al*., 2004
Human EC	7.6 $x10^4$ cells.cm^{-1}	PTFE	Static	Gumpenberger *et al*., 2003
Rabbit EC & SMC	$3x10^5$ cells .ml^{-1}	PTFE	Dynamic	Yu *et al*., 2003
Human EC & SMC	3 x 10^5 cells.ml^{-1}	PTFE	Dynamic	Yu *et al., 2001*
Ovine EPC	3 x 10^6 cells.cm^{-1}	Porcine heart valve	Static	Lee *et al*., 2009

Table 2. Examples of vascular-cell seeding densities used in the seeding of synthetic and acellular scaffolds (EC= endothelial cell, SMC = smooth muscle cell).

1.5.1.2 Maximising cell adhesion

Several techniques have been developed to maximise EC adhesion and retention to synthetic graft surfaces, as EC adherence to such grafts is often not strong enough to withstand the shear stress of the blood circulation (Knetsch *et al*., 2004). The use of specific endothelial adhesion proteins such as fibrin, gelatine, laminin and the Arg-Gly-Asp (RGD) binding sequence of fibronectin have all demonstrated improved EC adhesion and retention onto synthetic grafts following seeding (Kumar *et al*., 2002; Hsu *et al*., 2003) Alternate strategies include the use of antibodies, electrostatic techniques, alterating graft porosity and graft irradiation (Bowlin *et al*., 2001; Gumpenberger *et al*., 2003; Zhang *et al*., 2004; Rotmans *et al*., 2005). Recent studies on EC adhesion are summarised in Table (3).

Conduit	Technique	Outcome	In vivo / In vitro	Authors
Polyurethane	Electrospun with gelatin to create composite mesh	Improved EC adherence + proliferation compared to controls.	In vitro	Detta *et al*., 2010
Polyurethane	RGD containing recombinant protein(CBD-RGD) + gelatin coating	Enhanced EC retention. 63% retention rate after 3 hrs perfusion. Reduced platelet activation + adhesion compared to controls.	In vitro	Hsu *et al.*, 2003
Polyurethane	Rotational (dynamic) seeding	90% surface cell adhesion (4mm polyurethane). Retention enhanced by perfuse culture	In vitro	Hsu *et al.*, 2005
PTFE	UV Irradiation	Increased EC adherence. Confluent EC graft seeding in 8 days	In vitro	Gumpenberger *et al.*, 2003
PTFE & Dacron	Freeze-dried fibrin glue with gelatin and growth factor	Improved EC adhesion and proliferation compared to controls.	In vitro	Kumar *et a.l*, 2002
ePTFE	Electrostatic seeding	Increased EC seeding compared to control.	In vivo (Dogs)	Bowlin *et a.l*, 2001
PTFE	EC seeding under perfusion	Increased proliferation of EC + expression of fibronectin under pulsatile flow conditions compared to static conditions	In vitro	Rademacher *et al.*, 2001
Polyurethane & ePTFE	Porosity- PTFE with 60µm and polyurethanes with 5-30 µm pores	Perigraft tissue ingrowth may accelerate endothelialisation. Greatest endothelialisation seen in 30 µm pore size polyurethane grafts.	In vivo (Rats)	Zang *et al.*, 2004
ePTFE	Coated with anti-CD34 antibodies	85% EC coverage at 28 days implantation in anti-CD34 grafts compared to 32% for controls.	In vivo (Pigs)	Rotmans *et al.*, 2005
ePTFE	Coated with fibrin & vascular endothelial growth factor	No change in EC seeding density. Increased narrowing at proximal anastomoses and increased NIH in coated grafts compared to untreated (ePTFE) controls.	In vivo (Pigs)	Walpoth *et al.*, 2007

Table 3. Examples of techniques used to maximise endothelialisation of synthetic grafts (EC=Endothelial cells, RGD= Arg-Gly-Asp sequence, CBD=cellulose-binding domain, RPM= revolutions per minute, G-CSF= Granulocyte-colony stimulating factor, UV=Ultraviolet, PTFE= polytetrafluroethylene, CD= cluster of differentiation, ePTFE= expanded polytetrafluroethylene).

1.5.1.3 Cell Procurement

The early procurement of EC/SMC for two-stage seeding required an invasive procedure for the patient on tissues such as vein, fat or omentum. Furthermore, often the populations of harvested cell lines were not pure (Tiwari *et al*., 2001).

Alternate cell types have been studied in seeding experiments, such as mesothelial cells and stem cells (Verhagen *et al*., 1996; Campbell *et al*, 1999; Cho *et al*., 2005; Zhao *et al*., 2010). Mesothelial cells can be harvested in high numbers, grow well in culture and possess anticoagulant activity (Verhagen *et al*., 1996). In animal studies, mesenchymal stem cells have been reported to be induced to differentiate into SMC and EC and thus may be an alternate source for the acquisition of vascular cells (Cho *et al*., 2005; Zhao *et al*., 2010). Once again however, invasive procedures for procurement are required.

It is now known that human blood contains both circulating endothelial cells and EPC (Punshon *et al*., 2008). EPC have been shown to demonstrate high proliferation rates, a valuable trait for rapid graft endothelialisation (Avci-Adali *et al*., 2011). Punshon *et al.* (2008) were able to isolate both types of cell from volunteer human blood and maintain them in culture. Furthermore, they were able to seed the EC onto a nanocomposite graft (UCL-Nano™) and achieved confluent graft endothelialisation after fourteen days of culture.

A great deal of research into methods of attaining a confluent endothelium is now focusing on the development of grafts that may self endothelialise, either by recruiting cells from the site of anastomosed vessel or neocapillaries or indeed by recruiting circulating progenitor cells. The technique consists of implanting a functionalised scaffold into the circulation containing various adhesion peptides (discussed earlier) that will capture circulating EPC / EC and allow endothelialisation to occur (Rotmans *et al*., 2005; Walpoth *et al*., 2007; Avci-Adali *et al*., 2011).

1.5.1.4 Gene therapy

Some researchers have taken the cell-seeding of synthetic grafts one step further by utilising gene therapy to transduce EC with anticoagulant/antithrombotic genes in order to improve synthetic graft patency (Huber *et al*., 1995; Dichek *et al*., 1996; Dunn *et al*., 1996; Kimura *et al*., 2000). Following seeding onto synthetic grafts, it is hoped the transduced EC will express additional antithrombotic gene products leading to more potent inhibition of

thrombogenesis. Dichek *et al.* in 1997 successfully transduced EC from Baboons with retroviral vectors expressing human tPA or urokinase-type plasminogen activator (uPA).Transduced EC were then seeded onto collagen-coated 4 mm PTFE grafts. Grafts were then implanted into arterio-venous (AV) shunts created within the baboons. Compared to un-seeded grafts, both the tPA and uPA grafts displayed reduced levels of platelet and fibrin deposition secondary to a ten-fold increase in plasminogen activator. These effects were only observed for a 60-minute period and so it is unknown how long antithrombotic gene expression would continue for. Dunn *et al.* (1996) and Huber *et al.* (1995) however reported significantly reduced EC adherence onto Dacron and ePTFE grafts following seeding with EC transduced with a retroviral vector encoding tPA. In these studies, EC with high passage numbers were used. Kimura *et al*. (2000) transduced canine EC with tPA and LacZ, using low EC passage numbers, and found no significant difference in EC adhesion rates onto 4 mm ePTFE. They postulated that tPA expression would only affect EC adherence when EC with high passage numbers were used. Techniques that have shown efficacy in improving transduced-EC adherence to grafts include graft surface modification and [EC] seeded graft preconditioning. Falk *et al*. (1998) demonstrated increased EC retention onto ePTFE following luminal coating with fibronectin. Dardik *et al.* (1999) reported improved EC retention rates when seeded grafts were subjected to shear stress prior to implantation. The main limitation of using retroviral vectors for gene transduction is that subsequent gene expression declines rapidly within seven days of transduction (Quiniones *et al*., 1996). Therefore using grafts seeded with transduced EC may only be effective in reducing short-term graft failure rates.

At present, only animal studies have been performed. Human trials involving the seeding of transduced EC will be some way off yet whilst further work continues on the refinement of conventional EC seeding.

Limitations of synthetic hybrid grafts mainly relate to their inorganic component and include the ongoing risk of infection, lack of biodegradability and complete incorporation into host tissue and the inability to grow. Furthermore, the endothelialisation of prosthetic grafts often remains limited to areas adjacent to the anastomoses (Berger *et al*., 1972; Bader *et al*., 2000).

It is important to iterate here that many of the principles of synthetic graft cell-seeding pertain to cell-seeded biological grafts and that many of the advances that have been

made in the development of tissue engineered blood vessels have come from cell-seeding research using synthetic grafts. The limitation of synthetic hybrid grafts is that seeded vascular cells do not remodel them as effectively as biological scaffolds (Thomas *et al*., 2003).

1.6. Total-engineered blood vessels (TEBV)

The ideal TEBV will integrate with host tissue, possess a functioning endothelial lining capable of cellular remodelling and regeneration and possess mechanical integrity (tensile strength and elasticity).

It has been suggested that the development of a TEBV requires the successful integration of three components: scaffold, matrix and vascular cells (Baguneid *et al*., 2006). Weinberg and Bell in 1986 were the first group to develop a TEBV. They utilised a collagen gel scaffold seeded with bovine EC, SMC and fibroblasts.

The importance of the ECM for cell attachment has been discussed earlier. Furthermore, an ideal TEBV will contain ECM proteins such as elastin and collagen in proportions similar to the native artery to ensure mechanical integrity (Mitchell *et al*., 2003). In addition to these roles, the ECM is essential for cellular differentiation, a function which is important for maintaining the correct phenotype of seeded vascular cells (Ziegler *et al*., 1994). It is not just the components of the ECM themselves that are important for this regulation of cellular differentiation, but also how they are geometrically configured (Bader *et al*., 2000). Although a lot of emphasis has been placed on the importance of a cellular lining for a TEBV, it must also be emphasised that the biocompatibility of the scaffold itself is extremely important for long-term graft function (Ogle *et* al., 2002; Walles *et al*., 2003; Baguneid *et al*., 2006). Immunological attack and lack of tissue ingrowth are just two potential mechanisms by which an implanted TEBV may degrade and fail.

1.6.1 Techniques used to create a TEBV

Decellularisation of natural tissue

One of the forefront techniques in CV tissue engineering is the decellularisation of allogeneic and xenogeneic tissue to create acellular scaffolds. Decellularisation is the process of removing all cells, cellular proteins and debris and coding DNA from a tissue to leave an immunologically ‘inert’ scaffold comprised of ECM. Many protocols for the

decellularisation of tissues have been developed in the literature, however most will involve the use of enzymic cleavage, detergents, and hypertonic/hypotonic solutions

The decellularisation of xenogeneic cardiovascular tissue in particular is attractive to tissue engineers for several reasons. Firstly, animal tissue is readily available. Secondly, the natural ECM of cardiovascular tissue is innately orientated to withstand pulsatile flow and shear stress. Thirdly, the ECM or scaffold itself can be manipulated / modified by a vast array of biological techniques e.g. cell seeding or binding of antibodies or antithrombotic agents to the luminal surface. Finally, the main ECM proteins that comprise decellularised cardiovascular tissue (e.g. collagen and elastin) display close sequence homology across species and are immunologically well-tolerated by xenogeneic recipients (Liao *et al*., 2009). Decellularisation of allogeneic tissue has been shown to produce acellular scaffolds with reasonable biomechanical and regenerative properties (Schaner *et al*., 2004). However, the large amount of legislation governing the use of human tissue and the difficulty of large-scale procurement of healthy tissue from young donors (compared to xenogeneic tissue) currently makes its use less favourable than xenogeneic tissue.

Early decellularised vascular xenografts lacked a cellular component and studies using these grafts without seeded cells demonstrated high thrombosis rates and poor patency (Walles *et al*., 2003; Hilbert *et al*., 2004; Zhao *et al*., 2010). This has led to the development of pre-treated or cell-seeded acellular grafts in an attempt to improve graft patency. For example, using heparin treated and non-heparin treated decellularised canine carotid arteries, Wang *et al.* (2007) demonstrated significantly reduced rates of thrombosis following implantation into rabbits (3 weeks; 4% vs 25%, 6 months; 8% vs 58%). In their elegant ovine study, Zhao *et al.* (2010) clearly demonstrated the impact of cell- seeding an acellular vascular xenograft to aid patency. Firstly, instead of harvesting EC and SMC cells directly, they harvested ovine bone marrow-derived mesenchymal stem cells (MSC) and were able to induce them to differentiate into endothelial-like (ELC) and smooth muscle-like cells (SMLC). The authors then seeded the ELC and SMLC onto decellularised ovine carotid arteries and implanted them into the sheep that had donated the MSC. Grafts were assessed by angiography at two and five month's post-implantation and then explanted at five months. Unseeded [control] acellular grafts were occluded at two weeks as a result of thrombosis. Cell-seeded grafts at both two and five months post-implantation were all patent and showed regeneration of intimal, media and adventitial layers.

Many xenogeneic tissues have been successfully decellularised for vascular tissue engineering and include bovine and porcine ureter, porcine arterial and venous tissue and canine arterial tissue (Clarke *et al*., 2001; Widmer *et al*., 2004; Wang *et al*., 2007; Derham *et al*., 2008; Yang *et al*., 2009).

Use of autologous tissue

The issue of scaffold biocompatibility has lead researchers to look at the feasibility of creating a TEBV using varying types of autologous tissue and engineering techniques. Instead of focusing on arterial tissue as a conduit, Schaner *et al.* (2004) decellularised human saphenous vein using a detergent (SDS) based protocol. Mechanical and histological assessment demonstrated preservation of strength and ECM composition of the decellularised vein compared to native tissue. They did not however attempt cell-seeding of the conduit.

Aper *et al.* (2007) were able to harvest both a scaffold and cells from a 100 ml peripheral porcine blood sample. They created a fibrin scaffold by isolating fibrinogen from the blood sample and mixing with a thrombin solution. The fibrin was then placed onto a customised mould to create a tube shape. Next, they isolated EPC from the blood sample and successfully seeded them onto the fibrin tubes. As is the case for many protein-based conduits, the mechanical properties of the tubes did not, however, match those required for an arterial bypass conduit. Campbell *et al.* (1999) created autogenous vascular grafts by implanting silastic tubing into the peritoneal cavity of rats for two weeks. The implanted tubes became coated in connective tissue and mesothelial cells. The authors removed and reversed the lining tissue so that the mesothelium became the inner lining of the tube. Histologically, the tubes possessed an inner mesothelial lining, a ‘media’ consisting of myofibroblasts and an ‘adventitia’ of connective tissue. The tube-grafts were implanted into rat carotid and rat aorta and demonstrated a 50% patency rate at 6 months. Explanted grafts demonstrated arterialisation and response to contractile agents.

Although these studies fall short of creating a TEBV for wide-spread clinical use, they do demonstrate what can be achieved in tissue engineering using modest starting materials and techniques.

Biodegradable synthetic scaffolds

The development of biodegradable synthetic polymer scaffolds is a viable goal in vascular tissue engineering. Three of the most commonly used materials include polyglycolic acid (PGA), polylactic acid (PLA) and polycaprolactone (PCL) (Iwai *et al*., 2005; Isenberg *et al*., 2006; Torikai *et al*., 2008; Seifu *et al*., 2013;). Other materials have also been used such as bacterial cellulose (Innocente *et al*., 2009; Wippermann *et al*., 2009). The idea of a graft degrading over time eventually to be replaced by autologous tissue is certainly advantageous in terms of achieving long-term graft patency and biocompatability. Different materials degrade at differing rates, with polycaprolactone degrading slowly over a period of up to six months (Innocente *et al*., 2009).

Iwai *et al.* (2005) fabricated a PGA/PLA collagen micro-sponge mesh and implanted two patches (one large and one small) into canine and porcine circulations. Grafts were explanted at 2 and 6 months for the small and large patches respectively and were analysed using histology and immunohistochemistry. Characterisation of the explanted mesh revealed no evidence of aneurysmal degradation, thrombus formation or neointimal hyperplasia. Small patches were nearly fully degraded at 2 months and demonstrated uniform cellularisation with both EC and SMC following immunohistochemical analysis. Large patches displayed similar cellular re-modelling with a confluent endothelium visible by scanning electron microscopy.

At present however, much is still to be learnt with regards to the biology of synthetic polymer scaffold degradation. For example, what remodelling takes place post implantation in humans? What happens to waste products? How are they eliminated from the body? Do they effect cellular phenotype? Do they have any carcinogenic/toxic systemic effects? PGA and PLA for example, have both been shown to create degradation products *in vitro* that induce inflammation and immunoreactivity, create acidic conditions, inhibit cellular proliferation and cause de-differentiation of cells (Gao *et al*., 1998; Swartz *et al*., 2005; Seifu *et al*., 2013). Furthermore, the timing of degradation and the degree of subsequent tissue regeneration is crucial. In their study with PGA/ PLA scaffolds, Torikai *et al.* (2008) reported complete collagen regeneration in degraded scaffolds but insufficient elastin remodelling (compared to native tissue) at 6 months post implantation. Elastic discrepancies between native artery and graft will lead to compliance mismatch, a major factor in the pathogenesis of NIH (Desai et al., 2010).

A graft that degrades prior to host integration and stabilisation is doomed to fail. PGA for example is rapidly resorbed *in vivo*. Degradable scaffolds must therefore be engineered to degrade predictively whilst, in addition, retain some degree of biomechanical integrity. Furthermore, it is still not known whether the autologous tissue that forms around such biodegradable scaffolds can withstand systemic blood pressures in the long-term (Higgins *et al*., 2003; Torikai *et al*., 2008).

Self-assembled vascular constructs

Following on from the seminal work of Weinberg and Bell (1986), some tissue engineers continue to focus on the use of self-assembled tissue engineered blood vessel constructs (L'Heureux *et al*., 1998; Gauvin *et al*., 2010).

To date, the best assembled TEBV was that created by L'Heureux *et al.* (1998) in their pioneering work using human umbilical vein endothelial cells (HUVEC), human SMC and human dermal fibroblasts. Cells were seeded separately onto gelatine-coated culture flasks and cultured for 30 days. Following culture, a self-assembled sheet containing cells and synthesized ECM was created which could be peeled away from the flask surface. Firstly, the fibroblast sheet was wrapped around a tubular PTFE mandrel which was then covered by a sheet of SMC. The construct was then placed into a bioreactor for preconditioning and maturation for one week (see Section 1.8 Bioreactors in tissue engineering). After maturation, a further sheet of fibroblasts was wrapped around the sheet of SMC to finally create a construct with three layers- a luminal lining of fibroblasts, a medial layer of SMC and a [adventitial] layer of fibroblasts. The constructs were then cultured for a further eight weeks. After eight weeks, constructs were seeded with HUVEC for one week. Subsequent histological analysis demonstrated a construct comprised of three layers histologically analogous to the intimal, medial and adventitial layers of an artery. The endothelium was metabolically active and immunostaining confirmed the fibroblast, SMC and EC phenotypes of each layer, together with an ECM comprised of components seen in typical arterial tissue (collagen I,III,IV, laminin and fibronectin). Biomechanical assessment of the constructs demonstrated burst pressures (a surrogate marker of long-term mechanical integrity) greater than the current gold standard- human saphenous vein (2594 ± 501 mmHG vs 1680 ± 307 mmHG). The graft has been used in early human clinical trials as an AV graft for haemodialysis access with primary patencies of 75% and 60% at one and six months respectively (McAllister *et al*., 2009).

Gauvin *et al.* (2010) recently developed a TEBV using human SMC, dermal fibroblasts and saphenous vein fibroblasts. Cells were seeded onto gelatine-coated culture flasks and cultured for 14 and 28 days. Following culture, a self-assembled sheet containing cells and synthesized ECM was created which could be removed and wrapped around a tubular mandrel. Following incubation, the constructs were subjected to biomechanical analysis. Although constructs demonstrated mechanical strength above human physiological parameters, they failed to achieve burst pressures (a surrogate marker of long-term mechanical integrity) comparable to the current gold standard- human saphenous vein.

Nemcova *et al.* (2001) used type I collagen (porcine intestinal submucosa and bovine type I collagen) to assemble tubular constructs for *in vivo* implantation to assess their cellularisation ability and efficacy as vascular grafts. Porcine intestinal submucosa constructs (0.4cm diameter x 5cm) were implanted into the femoral arteries of mongrel canines for 9 weeks and then explanted for histological characterisation. One graft had occluded with the remaining eight remaining patent and displaying cellularisation by SMC, EC and myofibroblasts. Huynh *et al.* (1999) constructed a scaffold using both collagen type I from porcine intestinal submucosa and bovine type I collagen together and implanted them into rabbits. Once again, grafts were found to be cellularised by EC and SMC and displayed patency at 90 days. The burst pressure of such grafts was low however (931 mmHg) compared to other biomaterials such as decellularised PCA (2338mmHg) and human saphenous vein (1800 mmHg), which may indicate a lack of long-term durability (Huynh *et al*., 1999; Roy *et al*., 2005; Seifu *et al*., 2013). Clearly longer term studies are required to assess the efficacy of such constructs.

Fibrin constructs have also been investigated as potential vascular grafts (Swartz *et al*., 2005; Yao *et al*., 2005). Fibrin is an attractive protein to use as it is readily available from a sample of patient blood, is cheap to isolate and stimulates re-modelling in a variety of cell types (Stegemann *et al*., 2007). One of the seminal experiments to date involving the creation of a fibrin scaffold, was that performed by Swartz and colleagues (Swartz *et al*., 2005). They created a fibrin tube embedded with ovine SMC and EC and implanted them into the jugular vein of sheep. At 15 weeks post implantation, harvested scaffolds demonstrated remarkable re-modelling with the formation of collagen and elastin fibres and the laying down of SMC in an orientation consistent with blood flow, covered by an endothelial monolayer. Furthermore implanted grafts demonstrated vaso-reactivity and displayed patency rates similar to those of native vessels (Mehta *et al*., 2007).

The variations in the mechanical strengths of self-assembled TEBV, lack of long-term patency data and the time and expense required for their construction again limits their widespread commercial and clinical availability as a vascular graft.

1.6.2 The use of porcine arterial tissue for vascular tissue engineering

Porcine carotid arteries (PCA)

PCA are ideal conduits for the tissue engineering of small-diameter vascular grafts. They are innately designed to function under pulsatile flow, they are readily available and have luminal diameters 6 mm and below.

Recent studies have shown excellent biocompatibility of decellularised PCA with human vascular cells. Heine *et al.* (2011) successfully seeded decellularised PCA with human EC and SMC's in a bioreactor under co-culture. In the bioreactor, EC were seeded on the luminal surface (following pre-coating with gelatine) and the SMC on the abluminal surface. Re-seeded vessels demonstrated a confluent endothelial lining and vasomotor activity when stimulated pharmacologically.

McFetridge *et al.* (2004) demonstrated successful seeding of both human umbilical EC and SMC onto the surfaces of decellularised PCA that had undergone photo-oxidative crosslinking.

In their exciting study, Shimizu *et al.* (2007) successfully seeded decellularised PCA using magnetically labelled human SMC and fibroblasts (Mag-TE). By incubating cells with magnetic nanoparticles and subjecting them to a magnetic field, they were able to achieve high seeding densities of 94% for SMC and 73% for fibroblasts. Initial seeding times in the study took hours as opposed to days for conventional [vascular cell] seeding. In their study, Nitsan *et al.* (2012) were able to recellularise decellularised PCA with human EC and ovine SMC using both static and dynamic seeding techniques. No difference between static and dynamically seeded EC was shown in terms of cell proliferation, but EC under perfusion conditions displayed a more uniform surface. Both statically and dynamically seeded EC and SMC adhered well to the scaffold surface and not only expressed new ECM proteins, but remodelled existing ones (collagen I,III and laminin). They were also able to demonstrate that co-culturing both SMC and EC in a perfusion bioreactor created a thicker medial layer and a more confluent endothelial monolayer on the PCA scaffold.

Biomechanical performance of porcine carotid arteries

There is certainly varying and conflicting data within the literature regarding the biomechanical performance of decellularised PCA. In these studies, the decellularisation protocols all seem to be similar and involve osmotic, detergent, enzymic and mechanical steps.

Roy *et al.* (2005) compared the biomechanical characteristics of decellularised PCA's against fresh PCA's *in-vitro* and reported significant differences between the two. The decellularisation process lead to a significant reduction in wall thickness, most pronounced at the smaller, distal end of the PCA. Decellularised arteries were able to withstand a mean pressure of 2338 mmHg prior to rupture, compared to 3124 mmHg for fresh arteries. Up to the point of rupture, all arteries remained watertight. Between physiological pressures of 70-150 mmHg, compliance of the decellularised arteries was 50% lower than fresh arteries, leading to a reduction in distensibility by a factor of three, resulting in a much lower increase in diameter during pressure insufflation. Although the decellularised arteries were stiffer then fresh arteries, they still displayed a greater level of compliance compared to Dacron and ePTFE.

In their study with decellularised PCA's, Conklin *et al.* (2002) reported greater compliance rates with decellularised PCA's then fresh PCA's. Over a range of 0-200 mmHg, the diameters of decellularised PCA increased by 88%, compared to 73% in fresh vessels. Shimizu *et al.* (2007) reported equal compliance rates in their measurements in native and decellularised PCA. In their study, Nitsan *et al.* (2012) reported no difference in elasticity between control, decellularised and recellularised PCA.

What is clear is that removal of the cellular arterial elements leads to structural changes within the ECM, the degree of which will depend on each individual decellularisation method. Roy *et al.* (2005) suggested that the changes in compliance seen in decellularised arteries is to a large part, a result of the disruption between the bonds of SMC's and elastin in the arterial walls.

Surface-modification of porcine carotid arteries

As discussed earlier, many decellularised conduits that do not undergo surface modification or cell-seeding display high rates of thrombosis (Walles *et al*., 2003; Hilbert *et al*., 2004; Zhao *et al*., 2010). The alternative to cell-seeding is to bind antithrombotic agents to the graft wall to reduce overall thrombogenicity. Liao *et al.* (2009) were able to successfully bind heparin to the surface of decellularised porcine carotid arteries using covalent linkage between carboxyl groups of amino acids and hydroxylamine sulphate and heparin. Following the addition of fresh canine blood on the surface of heparin-bound and control decellularised arteries, control segments demonstrated 100% clot formation at 60 minutes, compared to 0% for heparin-bound segments. The authors then attached the heparin-bound and control arteries to femoral arteriovenous conduits of male baboons and measured (radio-labelled) platelet-deposition onto the grafts surfaces. At 60 minutes, there was a 54% reduction of platelet deposition on the surface of heparin-bound grafts compared to controls.

The use of heparin may not be restricted to merely performing an anticoagulant effect for the surface of biological grafts. In addition, it may aid the cell-seeding of such grafts. Following endothelial seeding, heparin present on the graft lumen may reduce early thrombus formation until a confluent endothelium is generated, thereby preventing early failure of cell-seeded grafts (Wissink *et al*., 2000). Furthermore, bound heparin serves as a substrate for heparin-binding growth factors such as vascular endothelial growth factor and basic fibroblast growth factor (bFGF) which can recruit SMC and EC to the graft surface creating a potentially autogenous self-seeding graft (Liao *et al*., 2009). Wissink *et al.* (2000) were indeed able to show such an effect using heparin-bound collagen films. The authors loaded bFGF onto heparin-bound and control collagen films and seeded HUVEC onto the collagen surfaces. They demonstrated increased bFGF binding and release and improved proliferation of HUVEC on the heparin-bound collagen films compared to controls.

Using PCA as a starting material, Hinds *et al.* (2006) were able to create a porcine elastin composite graft composed of porcine elastin and acellular porcine small intestinal submucosa (SIS). Tensile strength and burst pressures were comparable to native vessels. Following implantation as carotid interposition grafts in swine, the composite grafts remained patent longer than [ePTFE] controls (5.23 hours compared to 4.15 hours).

The study was limited however by the lack of assessing the capability of cells to seed onto the composite surface. Furthermore, the time and cost of vessel processing would be unlikely to make the composite a viable clinical product.

Decellularised porcine aorta

Bader *et al.* (2000) were able to decellularise porcine aortas using only enzymic cleavage with trypsin to reduce alterations in scaffold structure. They then successfully seeded the acellular scaffold with human EC and myofibroblasts. Using static culture conditions, only a poor EC monolayer covered the acellular scaffold specimens. When the seeded specimens were placed in a bioreactor for dynamic culturing, a fully confluent layer of EC developed. Furthermore, the EC were shown to secrete NO, an important compound in vascular biology, suggesting retention of cell phenotype.

Amiel *et al.* (2006) decellularised porcine aortic segments (3-4mm internal diameter segments) using a more ‘ conventional ’, detergent based decellularisation protocol and successfully seeded human saphenous vein EC onto the scaffold surface. Seeded scaffolds possessed respectable burst pressures (> 1300 mmHg) and demonstrated vaso-reactivity.

These studies highlight two important points. Firstly, human vascular cells can be seeded onto acellular arterial porcine tissue and secondly, the importance of shear stress for EC retention and differentiation.

Decellularised porcine iliac artery

Kaushal *et al.* (2001) decellularised porcine iliac artery and were able to seed ovine EPC onto the scaffold surface. Once seeded, scaffolds were implanted into the carotid arteries of sheep and demonstrated a minimum patency of four months together with development of a medial layer.

The studies using decellularised porcine material discussed above demonstrate two key attributes, firstly, that porcine tissue can be effectively decellularised using a range of protocols. Secondly, once decellularised, such scaffolds demonstrate effective seeding rates. Porcine arterial tissue therefore would seem to be a sensible starting material in the development of a tissue-engineered SD graft.

1.7 Limitations of using xenogeneic tissue

With the use of any xenogeneic tissue comes the risk of disease transmission. When using porcine tissue for example, there is a risk of porcine endogenous retrovirus transmission (Bader *et al*., 2000). It is vitally important therefore that xenogeneic tissue is effectively decellularised to remove any functional DNA to eliminate viral pathogens. Effective sterilisation is also important to prevent disease transmission. Again, many techniques for scaffold sterilisation exist in the literature, ranging from chemical sterilants to ethylene oxide (Derham *et al*., 2008; Zhao *et al*., 2010). Whatever type of xenogeneic tissue used and decellularisation protocol followed, it is vital that subsequent scaffolds are fully characterised to ensure sufficient decellularisation. One protein in particular, must be removed from xenogeneic tissue to prevent immunoreactivity and subsequent rejection- the α-gal epitope. This carbohydrate epitope is present on the glyco-proteins/lipids of all non-primate mammals, some monkeys and prosimians such as lemurs and bushbabies. Humans possess abundant circulating IgG antibodies against the α-gal epitope and so for xenogeneic tissue to be tolerated, the α-gal epitope must be removed during the decellularisation process (Galili, 2005).

1.8 Bioreactors in tissue engineering

Bioreactors range from basic to extremely complex and sophisticated instruments and are designed to reproduce an *in-vivo* environment that closely mimics target cell/organ physiology. There are rapidly becoming increasingly critical pieces of apparatus for vascular tissue engineering as they allow preconditioning of seeded conduits prior to *in-vivo* implantation (Goldstein *et al*., 2009). All bioreactors, no matter how sophisticated follow a basic design: a pump to propel circulating fluid / medium, a reservoir to contain the fluid /medium and a perfusion chamber to house the scaffold /construct. Large and expensive components should ideally be safe to sterilise to allow repeated use (Lee *et al*., 2009). Butler *et al.* (2009) describe the ideal characteristics that a bioreactor should possess, most importantly, a controlled culture environment and an ability to reproduce identical mechanical stimulation to tissue constructs.

1.8.1 Bioreactor Design

The culture environment within the bioreactor is extremely important as this will ultimately dictate whether seeded cells on a conduit will survive and maintain a correct phenotype. Temperature, humidity, O_2 and CO_2 levels (for acid / base balance) must be optimised whilst ensuring the environment remains free from contamination by micro-organisms. Appropriate circulating medium is needed to provide nutrition to cells and to remove waste products of cellular metabolism. The flow, pulsatility and shear stress provided by the circulating medium is important as they pre-condition the cells and construct (Rademacher *et al*., 2001; Rashid *et al*., 2008).

Preconditioning describes an *in vitro* process whereby a tissue-engineered construct is subjected to pulsatile flow and pressure to optimise the mechanical and biological characteristics of the construct (Rademacher *et al*., 2001; Rashid *et al*., 2008). Pulsatility creates and exposes hydrostatic pressure, circumferential stretch and importantly, shear stress to the seeded cells and ECM (Lehoux *et al*., 2006). Shear and cyclic stress is extremely important for tissue-engineered constructs as it enhances SMC and EC adhesion, regulates their differentiation, gene expression, viability and proliferation, and mechanically orientates the cells and ECM components (Dardik *et al*., 1999; Fisher *et al*., 2001; Rademacher *et al*., 2001; Rashid *et al*., 2004, 2008; Isenberg *et al*., 2006; Lee *at al*., 2009). The molecular biology of preconditioning remains far from understood, but increased NO production and expression of NO synthase and matrix metalloproteinase-9 appear to be important (Baguneid *et al*., 2004)

Gambillara *et al.* (2008) demonstrated the importance of cyclic stress on the vascular ECM of PCA in their *ex-vivo* study. They reported a 50% increase in matrix metalloproteinase (MMP) expression and activation in PCA exposed to low rates of cyclic stretch compared to normal physiological levels. MMP's are a group of proteases that can degrade the ECM, a process which could prove disastrous for a tissue-engineered construct in terms of cellular retention and mechanical integrity.

Optimal preconditioning parameters have not yet been defined and will likely differ for each type of construct. It does seem however that exposing a construct to a regimen of gradually increasing shear stress as opposed to constant [low stress] prior to exposure to physiological pressures results in greater cell attachment (Fillinger *et al*., 1993; Kaushal *et al*., 2001). An explanation for this is that by gradually increasing shear stress, the cells of

the construct have time to synthesise adhesion factors and ECM which allows for more effective cell-cell and cell-construct attachment (Fillinger *et al*., 1993).
Carnagey *et al.* (2003) used flow preconditioning to assess EC coverage on both a decellularised biological graft (ovine carotid artery) and a fibrin treated PTFE (4 mm) graft. Firstly, control experiments (seeded grafts with no flow preconditioning) demonstrated that biological grafts had an EC coverage rate up to 50% greater than the fibrin treated PTFE grafts. Secondly, following six hours of gradually increasing flow preconditioning (to a maximum flow rate of 300 mls.min^{-1}) biological grafts demonstrated a 24% increase in EC coverage compare to controls grafts.
Yazdani *et al.* (2009) demonstrated improved SMC proliferation and creation of a medial layer on decellularised PCA following preconditioning in a bioreactor for 1-2 weeks. Yazdani and colleagues have also demonstrated that bioreactor preconditioning improves EC adherence to the surface of decellularised PCA using *in vivo* and *ex-vivo* models. Furthermore, they found less blood product absorption to grafts exposed to higher rates of shear and cyclic stress, thereby lowering their thrombotic potential (Yazdani *et al*., 2010).

1.9 Aims and objectives

There is a clear, clinical need for a SD vascular graft if greater patency rates are to be achieved in vascular bypass. The presence of a functioning endothelium on the surface of the graft is clearly paramount in achieving superior patency rates over conventional grafts.

Tissue engineering strategies have all shown promise in producing an endothelial lined-SD graft. The decellularisation and subsequent re-cellularisation of analogous biological tissues appears to be one strategy that shows particular promise.
Porcine arterial tissue, amoungst others, can be successfully decellularised and performs biomechanically similar to native tissue.

The overall aim of this research was to develop an acellular biological vascular scaffold and develop methods for the seeding of the scaffolds with vascular cells with a view to future development of a tissue-engineered SD bypass graft.

Specific objectives:

- To decellularise porcine carotid arteries using a proprietary decellularisation protocol to create an acellular scaffold.

- To determine the success of the decellularisation process using a robust array of characterisation techniques.

- To determine the biocompatibility of the acellular scaffolds using cell lines and primary [vascular] cells.

- To isolate ovine EC and SMC and maintain them in culture.

- To develop a reproducible protocol to confirm ovine vascular cell phenotype.

- To perform two-dimensional (2D) static seeding of the acellular scaffolds with ovine vascular cells and if successful, subsequently characterise seeded scaffolds.

- To use knowledge gained from two-dimensional seeding, to develop approaches for three-dimensional (3D) dynamic seeding of the acellular scaffolds with ovine vascular cells and determine the viability and characteristics of the seeded cells.

- To commission a perfusion bioreactor for conditioning of the cell seeded acellular scaffolds.

Chapter 2

Materials and Methods

2.1 Materials

All glassware used was purchased from Fisher Scientific unless otherwise stated.

2.1.1 Chemicals and reagents

Chemicals and reagents used throughout the study are listed in Table (4).

Chemical/Reagent	Cat No.	Supplier
Acetone	LS8/1970/G	European Bios
Anti-Fibroblast Microbeads	130-050-601	Miltenyli Biotec
Anti-FITC Microbeads	130-048-701	Miltenyli Biotec
Aprotonin (10000 $KIU.ml^{-1}$	AP012	Mayfair house
ATPLite-M assay	6016941	Perkin-Elmer
Bovine serum albumin (BSA)	A7030-100G	Sigma-Aldrich
Calcium acetate	C/0920/50	Thermo Fisher Scientific Ltd.
Calcium chloride	C-7902	Sigma-Aldrich
Citric acid (anhydrous)	BP339-500	Thermo Fisher Scientific Ltd.
Collagen gel	N/A	N/A
Collagenase type 2 filtered (273 U/ml)	GEC2	MP Biomedical
Cyanoacrylate contact adhesive	Z105902-1EA	Sigma-Aldrich
DABCO (1,4-diazobicyclo-(2,2,2)-octane	290734	Sigma-Aldrich
DAPI stain (4',6-Diamidino-2-phenylindole Dihydrochloride)	D9564	Sigma-Aldrich
Dimethyl sulfoxide (DMSO)	D26650	Sigma-Aldrich

Disodium ethylenediaminetetraacetic acid (EDTA)	E/P140/53	Thermo Fisher Scientific Ltd.
DNAase	DN25-1	Sigma-Aldrich
DNeasy kit	69504	Qiagen
DPX mountant	M81330/C	Thermo Fisher Scientific Ltd.
Dulbecco's Modified Eagle Medium	BE12-604F	Lonza
Dulbecco's PBS (DPBSa) tablets	BR0014	Oxoid
Dulbecco's PBS (DPBSa) with calcium and magnesium	BE17-512F	Lonza
Dulbecco's PBS (DPBSa) without calcium and magnesium	17-512F	Lonza
Endothelial cell growth supplement	E2759	Sigma
Eosin	1.09844.1000	VWR International
Ethanol (100%;v/v)	E/0555DF/25	Thermo Fisher Scientific Ltd.
Foetal calf serum	French	Lonza
Gentamycin sulphate	345810	VWR International
Giemsa stain	352603R	VWR International
Glutaraldehyde	111-30-8	Sigma-Aldrich
Glycerol (100%;v/v)	G9012	Sigma-Aldrich
Haematoxylin	PS50/C	European Bios
Heparin (1000U/ml)	009878-06	Leo
Hydrochloric acid (6 M)	2611.5000	VWR International
Hydrogen peroxide	H1009	Sigma-Aldrich
ImmEdge Hydrophobic Barrier Pen	H-4000	Vector Laboratories
L-Glutamine (200mM)	25030032	Lonza
Liquid nitrogen		BOC
LIVE/DEAD ® Viability/Cytotoxicity Kit	L3224	Invitrogen

M-199 Medium	12-119F	Lonza
Magnesium chloride	22321-1000	Thermo Fisher Scientific Ltd.
Methanol	0428	Genta Medical
Methylated Spirits	GPS1000-K	Biostain Ready reagents
Molecular grade water	W4502-1L	Sigma-Aldrich
Neutral buffered formalin (10%; w/v)	BFN250	Genta Medical
Osmium tetroxide	20816-12-0	Sigma-Aldrich
Paraffin wax	PS138/E	Thermo Fisher Scientific Ltd.
Penicillin/streptomycin solution (10,000U.ml^{-1} penicillin and 10,000U.ml^{-1} streptomycin)	DE17-602E	Lonza
Peracetic acid	269336	Sigma-Aldrich
Polymyxin B	81334-5G	Sigma-Aldrich
RNase A (17,500 U)	19101	Qiagen
Scott's tap water	PS138/E	Thermo Fisher Scientific Ltd.
Sodium acetate	S/2080/60	Thermo Fisher Scientific Ltd.
Sodium azide	438456	Sigma-Aldrich
Sodium chloride	42429-5000	Thermo Fisher Scientific Ltd.
Sodium dodecyl sulphate (SDS)	71727	Sigma-Aldrich
Sodium heparin 1000U/ml	018891-04	Leo
Sodium hydrogen carbonate	102475W	VWR International
Sodium hydroxide	S/4920/53	Thermo Fisher Scientific Ltd.
Trizma base	T-1503	Sigma-Aldrich
Trypsin (porcine pancreas)	1001005154	Sigma-Aldrich
Trypan blue (0.4%)	72-57-1	Sigma-Aldrich
Tween 20	P1379	Sigma-Aldrich

Ultra vision One detection system: HRP Polymer DAB Plus substrate	 TL-125-HLJ TA-125-HDX	Thermo Scientific
Vancomycin hydrochloride	861987-1G	Sigma-Aldrich
Xylene	LS81950/G	Genta Medical
Zinc acetate	383317	Sigma-Aldrich
Zinc chloride	96470	Fluka

Table 4. Chemicals and reagents used throughout the study.

2.1.2 Antibodies

Antibodies used throughout the course of these studies are listed in Table (5).

Anti-Sheep CD31: FITC antibody	MCA1097F	AbD Serotec
CD31 antibody	M0823	Dako
Goat anti-mouse antibody	A11017	Invitrogen
Goat anti-rabbit antibody	A11070	Invitrogen
Isotype control antibody (IgG1)	MO75-4	MBL International
Isotype control antibody (IgG2)	MO75-1	MBL International
Smooth Muscle Myosin-Heavy Chain antibody	MAB3570	Chemicon International
Von Willebrand Factor antibody	Nr.A0082	Dako
α-Smooth Muscle Actin antibody	A2547	Sigma-Aldrich

Table 5. Primary and secondary antibodies used throughout the study.

2.1.3 Materials

Materials used in the course of these studies are listed in Table (6).

Material	Cat No.	Supplier
250ml sterile containers	CON7580S	Scientific Laboratory Supplies
2ml cryovials	72.380.992	Sarstedit
3T3 cells (+3)	89022402	National Collection of Type Cultures
75ml tissue culture flask	TKT-130-210-T	Thermo Fisher Scientific Ltd.
BHK cells (21, clone 13)	85011433	National Collection of Type Cultures
Culture slides tissue culture 4 wells	734-0088	VWR International
Delrin holding pc	Cross Tech	Custom Made
Delrin Three way pc	Cross Tech	Custom Made
Filter Flask Pyrex	CLS5340500	Sigma
Fine tip stainless steel forceps	E12	R.A. Lamb
Glass coverslips	MIC3228	Scientific Laboratory Supplies
Glass troughs	E105	Raymond A Lamb
Histology moulds	E10.8/4161	Raymond A lamb
Long hair brush No6	E6	R.A. Lamb
Micro tube I 1.5ml, loop cap- Simport	212-9573	VWR International
Microtome Blades	SD3050835	Fisher Scientific
One-way valves (luer fittings)	K-30600-01	Cole-palmer
Plastic histology cassettes	CMB-160-030R	Thermo Fisher Scientific Ltd.
Polycarbonate Y-branch fitting	K-30526-06	Cole-parmer
PP Male Luer Plug	EW-45503-56	Cole-parmer

PP 3-way stopcocks 4mm	K-06225-40	Cole-parmer
PTFE thread seal tape	EG-08782-27	Cole-parmer
Six-well culture plates	140675	Thermo Fisher Scientific Ltd.
Slide Holder	E102	Raymond A Lamb
Stainless steel rod	Cross Tech	Custom Made
Sterile containers (150ml)	CON7570S	Scientific Laboratory Supplies
Superfrost Microscope Slide	MIC3040	SLS
TopSeal 96 well plate	6005185	Perkin Elmer
Twistit stopper Filter Flask	EW-62992-26	Cole-parmer
Two-way valves (luer fittings)	K-30600-03	Cole-parmer
Tubing #1 (0.125 ID)	95702-05	Cole-parmer
Tubing #2 (0.188 ID)	95702-10	Cole-parmer
Universal tube	CON9000	Scientific Laboratory Supplies
White, 96 well tissue culture plate	6005680	Perkin Elmer

Table 6. List of materials used throughout the study.

2.1.4 Equipment

Equipment used during the course of these studies is listed in Table (7).

Equipment	**Model**	**Supplier**
Aspirator	Vacusafe Comfort	IBS (Integra Biosciences)
Automatic pipettes	Various	Gilson
Balance	GR-200-EC	AND
Centrifuge	Microcentaur	MSE

Class II Safety cabinet	CL2	Heraeus
Confocal microscope	LSM510 META	Zeiss
Digital colour camera	Evolution MP5	Media Cybernetics
Dissection equipment	Various	Thermo Fisher Scientific Ltd.
Dissection kit	N/A	Thackeray
Histology water bath	MH8515	Barnstead Electrothermal
Hot wax oven	E18/31	Raymond A Lamb
Hotplate	E18/1	R.A. Lamb
Image-Pro Plus	Version 5.1	Media Cybernetics
Incubator	Heraeus	Jencons PLC
Inverted microscope	IX71	Olympus UK
Liquid nitrogen dewar	Various	Various
MACS® MiniSeperator	130-042-102	Miltenyli Biotec
MACS® MS Columns	130-042-201	Miltenyli Biotec
Magnetic stirrer	CB161	Stuart scientific
Motor-bioreactor	GP232004	Baldor motors
Motor control-bioreactor	BC138	Baldor motors
Microtome	RM2125 RTF	Leica
Microwave	MOL5137	Scientific Laboratory Supplies
Nanodrop spectrophotometer	ND-100	Labtech
Orbital incubator shaker	SI50	Stuart Scientific
Orbital shaker	KSI30B	IKA
pH meter	3510	Jenway
Pipette boy	Integra acu	Integra Bioscience
Roller Mixer	SRT6D	Stuart

Scanning electron microscope	CamScan 3-30BM	Obducat CamScan Ltd
Sputter-Coater	208HR	Cressington
Table shaker	Ks 130	IKA
Tissue processor	TP11020	Leica
Top Count	C9902 NXT	Perkin Elmer
Upright fluorescent microscope	BX51	Olympus UK
Wax dispenser	E66	Raymond A Lamb
Whrli mixer	CM-1	Thermo Fisher Scientific Ltd.

Table 7. List of equipment used throughout the study.

2.2 Stock solutions

Antibiotic solution (300 U.ml^{-1} streptomycin, 300 U.ml^{-1} penicillin)

Penicillin/streptomycin solution (15 ml) was added to 500 ml DPBS containing calcium and magnesium. The solution was stored at 4°C for a maximum of one week.

Bovine serum albumin (BSA) solution (5 mg.ml^{-1} BSA)

Bovine serum albumin (250 mg) was dissolved into 50 ml of distilled water using a magnetic stirrer. The solution was then passed through a 0.2 µm pore size filter into a sterile container. Aliquots (5ml) were placed into sterile universals and stored at -20°C for up to six months.

Dulbecco's phosphate buffered saline (DPBSa)

Five Oxoid Dulbecco's PBS tablets were dissolved in 500 ml of distilled water using a magnetic stirrer. Whilst stirring, the pH was adjusted to lie within the range of 7.2-7.4 by adding drops of either 6 M hydrochloric acid or 6 M sodium hydroxide. The solution was then autoclaved at 121°C, 15psi, for twenty minutes. Solutions were stored for up to one month at room temperature.

Disinfection solution

Vancomycin hydrochloride (10 mg.ml^{-1}; 2.5 ml), 2.5 ml of gentamycin sulphate (0.5 mg. ml^{-1}) and 2 ml of polymyxin B (0.2 mg. ml^{-1}) were added to 100 ml of DPBSa. Using a magnetic stirrer, the pH was adjusted to lie within the range of 7.2-7.4 by adding drops of either 6 M hydrochloric acid or 6 M sodium hydroxide. The solution was then passed through a 0.2 µm pore size filter into a sterile container. The volume was then made up to 500 ml using sterile DPBSa. The solution was used immediately.

EDTA solution (200 mM)

EDTA (74.4 g) was dissolved into 1 L of distilled water using a magnetic stirrer and stirrer bar. The pH was adjusted to lie within the range of 7.2-7.4 by adding drops of either 6 M hydrochloric acid or 6M sodium hydroxide. The solution was then autoclaved at 121°C, 15psi, for twenty minutes. Solutions were stored for up to one month at room temperature.

DPBSa and EDTA (2.7 mM; 0.15; w/v)

Five Oxoid Dulbecco's PBS tablets were dissolved together with 0.5 g of EDTA in 500 ml of distilled water using a magnetic stirrer. The pH was adjusted to lie within the range of 7.2-7.4 by adding drops of either 6 M hydrochloric acid or 6 M sodium hydroxide. The solution was then autoclaved at 121°C, 15psi, for twenty minutes. Solutions were stored for up to one month at room temperature.

DPBSa EDTA (2.7mM) containing aprotonin (10KIU.ml^{-1})

Aprotonin (500 µl) was drawn up aseptically using a sterile needle and syringe. The aprotonin was then aseptically delivered into 500 ml of autoclaved DPBSa EDTA. Solutions were stored for up to one month at 4°C if required.

Sodium dodecyl sulphate (SDS) solution (10%; v/v SDS)

SDS (1 g) was dissolved into 10 ml of distilled water using a magnetic stirrer.

SDS hypotonic buffer (0.1%; w/v SDS 10 mM tris, 2.7 mM EDTA, 10 KIU.ml^{-1} aprotonin)

SDS solution (5 ml) was added to 495 ml of autoclaved hypotonic buffer. The solution was used immediately.

Hypertonic solution (50 mM tris, 1.5 M sodium chloride)

Sodium chloride (87.66 g) and 6.06 g of tris were dissolved in 900 ml of distilled water. The pH was adjusted to lie within the range of 7.5-7.7 by adding drops of either 6 M hydrochloric acid 6 M sodium hydroxide. A further 100 ml of distilled water was then added to make the volume up to one litre. The solution was then autoclaved at 121°C, 15psi, for twenty minutes and stored at room temperature for up to one month.

Hypotonic buffer (10 mM tris, 2.7 mM EDTA, 10 KIU.ml^{-1} aprotonin)

Trizma base (1.21 g) and 1 g of EDTA were dissolved in 900 ml of distilled water using a magnetic stirrer. The pH was adjusted to lie within the range of 8-8.2 by adding drops of either 6 M hydrochloric acid or 6 M sodium hydroxide. A further 100 ml of distilled water was then added to make the volume up to one litre. The solution was then autoclaved at 121°C, 15psi, for twenty minutes. Solutions were stored at room temperature for up to one month. Aprotonin solution (1ml; 10,000 KIU/ml) stock was added aseptically immediately prior to use.

DNAase stock solution

DNAase was rehydrated to a final concentration of 10,000 U.ml^{-1} using 5 mM sodium lactate, 1 mM calcium chloride and 50% (v/v) glycerol. The solution was then passed through a 0.2 µm pore size filter into a sterile container and placed in labeled aliquots and frozen at -20°C.

DNAase diluent (5 mM sodium acetate, 1 mM calcium chloride, 50%; w/v glycerol)

Sodium acetate (0.68 g) and 0.11 g of calcium chloride were dissolved in 500 ml of distilled water using a magnetic stirrer. Glycerol (500ml) was added to the solution which was then inverted to mix. The pH was adjusted to lie within the range of 4-5 by adding drops of either 6 M hydrochloric acid or 6 M sodium hydroxide. The solution was stored at room temperature for up to three months.

RNAase *A* stock solution

RNAase was rehydrated to a final concentration of 100 U.ml^{-1} using distilled water. The solution was then passed through a 0.2 µm pore size filter into a sterile container and placed in labeled aliquots and frozen at -20°C.

Nuclease solution (50 mM tris, 50 µg.ml^{-1} BSA, 50 U.ml^{-1} DNAase, 1 U.ml^{-1} RNAase)

The solution was made aseptically in a class II safety cabinet. Trizma base (6.1 g) and 2 g of magnesium chloride were dissolved in 80 ml of distilled water using a magnetic stirrer. The pH was adjusted to lie within the range of 7.5-7.7 by adding drops of either 6 M hydrochloric acid or 6 M sodium hydroxide. A further 910 ml of distilled water was added to the solution to make up the volume to 990ml. The solution was then autoclaved at 121°C, 15psi, for twenty minutes. Prior to use, 10 ml of stock BSA solution was defrosted and then added to 975 ml of solution. 10 ml of RNAase stock (100U.ml^{-1}) and 5 ml of DNAase (10,000 U.ml^{-1}) were then added to the solution. The solution was used within ten minutes of preparation.

Peracetic acid (PAA) solution (0.1%; v/v)

PAA solution (1.57 ml) was added to 500 ml of autoclaved DPBSa. The pH was adjusted to lie within the range of 7.2-7.5 by adding drops of either 6 M hydrochloric acid or 6 M sodium hydroxide. Solutions were used within one hour of preparation.

DAPI dye solution (1 mg.ml^{-1})

Following receipt of DAPI (10 mg), 10 ml of nuclease free water (1 mg.ml^{-1}) was immediately added. The solution was then stored at -20°C in a foil-wrapped container for a maximum of six months.

DAPI working dye solution (0.1 µg.ml^{-1})

DAPI dye solution (20 µl) was added to 200 ml of dye buffer in a dark bottle. The bottle was inverted to mix. Whilst stirring, the pH was adjusted to 7.4 by adding drops of either 6 M hydrochloric acid or 6 M sodium hydroxide. The solution was used immediately.

2.5% (w/v) DABCO

1,4-diazobicyclo-(2, 2, 2)-octane (2.5 mg) was dissolved in 100 ml of 0.1 M sodium hydrogen carbonate using a magnetic stirrer. The pH was adjusted to 9 by adding pellets of sodium hydroxide. The solution was stored for up to three months at room temperature.

DABCO: glycerol mountant

DABCO (10 ml) 2.5% (w/v) was mixed with 90 ml of glycerol using a magnetic stirrer. The solution was stored at 4°C in a foil-wrapped bottle for up to three months.

Sodium hydrogen carbonate buffer (0.1 M)

Sodium hydrogen carbonate (4.2 g) was dissolved into 500 ml of distilled water using a magnetic stirrer. The pH was adjusted to 9 by adding pellets of sodium hydroxide whilst stirring. The solution was stored for up to three months at room temperature.

Sodium hydroxide solution (6 M)

Sodium hydroxide (120 g) was added to 500 ml of distilled water using a magnetic stirrer. The solution was stored for up to three months at room temperature.

Sodium chloride solution (3 M)

Sodium chloride (175.32 g) was dissolved into 1 L of distilled water and autoclaved at 121°C, 15psi for 20 minutes. The solution was stored for a maximum of one month.

Endothelial cell culture medium (M-199, 20% (v/v) FBS, 100 U.ml^{-1} penicillin and 100µg.ml^{-1} streptomycin, 2mM L-glutamine, 30 U.ml^{-1} heparin, endothelial growth factor supplement)

The M-199 Medium, penicillin/streptomycin solution, L-glutamine solution and FBS were all pre-warmed to 37°C. To 100 ml of M-199 culture medium, 20 ml of FBS, 1.2 ml of penicillin/streptomycin, 1.2 ml of L-glutamine, 3 ml of sodium heparin (30 U.ml^{-1}) and 1 ml of 100X endothelial growth factor supplement were added. The solution was mixed and stored at 4°C for a maximum of one week.

3T3, BHK and SMC culture medium (10% FBS, 2 mM L-glutamine, 100 U.ml^{-1} penicillin and 100µg.ml^{-1} streptomycin).

The Dulbecco's modified Eagle's medium, penicillin/streptomycin solution, L-glutamine solution and FBS were all prewarmed to 37°C. Under aseptic precautions in a class II safety cabinet, 55 ml of FBS, 5.5 ml each of penicillin/streptomycin and L-glutamine solutions were added to 500 ml of Dulbecco's modified Eagle's medium. The medium was stored for a maximum of one week at 4°C.

Dimethyl sulfoxide (40% v/v)

Dimethyl sulfoxide [(DMSO), 8 ml] was added to 12 ml of Dulbecco's modified Eagle's medium and then filter-sterilised into a sterile universal.

Acetone: methanol solution

Acetone (100ml) was added to methanol (100ml) for immediate use.

Tris solution (2 M)

Trizma base (242.26 g) was added to 500 ml of distilled water and mixed using a magnetic stirrer. The pH was adjusted to 7.6 using 6 M hydrochloric acid or 6 M sodium hydroxide and then made up to 1 L using distilled water. The solution was then autoclaved at 121°C, 15psi for 20 minutes. The solution was stored for a maximum of one month.

Tris solution (0.1 M)

Trizma base (12.1 g) was dissolved in 1 L of distilled water using a magnetic stirrer. The solution was then autoclaved at 121°C, 15psi for 20 minutes.

Tris buffered saline (TBS)

To create TBS, 25 ml of tris solution (2 M) was added to 50 ml of sodium chloride (3 M) and mixed using a magnetic stirrer. The volume was then made up to 1 L using distilled water. The pH was adjusted to 7.6 using 6 M hydrochloric acid or 6 M sodium hydroxide. The solution was then autoclaved at 121°C, 15psi for 20 minutes and stored for a maximum of one month.

TBS containing 0.05 % (w/v) Tween 20

One litre of TBS was mixed with 500 µl of Tween 20 using a magnetic stirrer. The pH was adjusted to 7.6 using either 6 M hydrochloric acid or 6 M sodium hydroxide. The solution was stored for up to three months at room temperature.

Dye buffer (10 mM Tris, 1 mM Na_2EDTA, 1 mM NaCl)

Trizma base (1.211 g), 0.3724 g of EDTA and 0.0058 g of sodium chloride were all dissolved in one litre of distilled water using a magnetic stirrer. The solution was then autoclaved at 121°C, 15psi, for twenty minutes in a dark bottle and stored for up to six

months at room temperature. Just prior to use, the pH was adjusted to 7.4 by adding drops of either 6 M hydrochloric acid or 6 M sodium hydroxide.

Antibody diluent (TBS, 0.1 % (w/v) BSA, 0.1 % (w/v) sodium azide)

To create the diluent, 600 µl of sodium azide (10%; (w/v) and 59.1 ml of TBS were mixed with 300 µl of BSA (5 %; w/v) using a magnetic stirrer. The pH was adjusted to 7.6 using either 6 M hydrochloric acid or 6 M sodium hydroxide. The solution was stored for up to three months at 4°C.

Sodium azide (10%; w/v)

Sodium azide (10 g) was dissolved into 100 ml of distilled water using a magnetic stirrer and autoclaved at 121°C, 15psi for 20 minutes. The solution was stored for a maximum of one month at room temperature.

Glutaraldehyde solution (2.5%; v/v glutaraldehyde)

Glutaraldehyde (10 ml, 50%; v/v) was added to 100 ml of DPBSa. The solution was then made up to a final volume of 200 ml with distilled water.

Collagenase stock solution (1% collagenase type 2, 273 U.ml^{-1})

DPBSa (5 ml) without calcium or magnesium was added to 50 mg of collagenase type 2 and mixed until the collagenase had dissolved. The solution was stored at -20°C.

Collagenase working solution (0.1% collagenase type 2, 2.73 U.ml^{-1})

Collagenase stock solution (1 ml) was added to 9 ml of DPBSa without calcium and magnesium. The solution was used on the same day of production.

Magnetic separation buffer solution (BSA 5%; w/v)

EDTA (0.25 g) and BSA (12.5 ml) were added to 250 ml of DPBSa. The pH was adjusted to 7.2

Hydrogen peroxide solution (3%; v/v)

Hydrogen peroxide (20 ml, 30%;v/v) was added to 180 ml of distilled water.

Citrate buffer (10 mM citric acid, 0.05% (v/v) Tween 20)

Citric acid (1.92 g) and Tween 20 (0.5 ml) were dissolved in 1 L of distilled water. The pH was adjusted to pH6 using sodium hydroxide (6 M).

Trypsin working solution (0.1% (v/v) trypsin)

Porcine trypsin (100 mg) was dissolved in 10 ml of distilled water. Next, calcium chloride (100mg) was dissolved in 10 ml of distilled water. Then 1 ml of trypsin stock solution (1%) and 1 ml of calcium chloride solution (1%) was added to 10 ml of distilled water. The pH was adjusted to pH7.8 using sodium hydroxide (6 M).

Zinc fixative solution

Calcium acetate (0.5 g) was dissolved in 1 L of 0.1 M Tris solution using a magnetic stirrer. The pH was adjusted to 7-7.4 using either 6 M hydrochloric acid or 6 M sodium hydroxide. Next, 5 g of zinc acetate followed by 5 g of zinc chloride was added to the solution using a magnetic stirrer.

2.3 Methods

2.3.1 pH measurement

The pH measurement of all solutions was performed using a Jenway 3020 pH meter. Calibration was performed with pH 4, 7 and 10 buffer solutions. The pH of solutions was altered by adding either hydrochloric acid (6 M) or sodium hydroxide (6 M) in a dropwise fashion.

2.3.2 Bright field microscopy

Bright field microscopy was performed using an upright fluorescent BX51 microscope (Olympus, UK). For fluorescent microscopy, a vertical illuminator (BX51-RFA) was used. Images were captured using a digital colour camera (Evolution MP5, Media Cybernectics) in combination with Image-Pro Plus (Version 5.1, Media Cybernetics) software.

2.3.3 Scanning electron microscopy and tissue preparation

All steps were performed in a fume cupboard.

Specimens were placed into six-well plates. To fix the specimens, 2 ml of 2.5% (v/v) glutaraldehyde in DPBSa was added to each well for 24 hours at 4°C. Once fixed, the glutaraldehyde was removed and the segments washed with sterile DPBSa. Specimens were post-fixed in 2 ml of 1% (v/v) osmium tetroxide in DPBSa for 24 hours at room temperature.

Specimens were then dehydrated using ascending concentrations of acetone. To begin dehydration, 2 ml of 20% (v/v) acetone was added to each well for 30 minutes at room temperature. This step was then repeated for 40%, 60%, 80% and 100% acetone. Following dehydration, specimens were critical-point dried using a Polaron E3000 critical point drying machine using liquid carbon dioxide as the transition fluid. Each section was then mounted onto a 13 mm pin stub using carbon cement and coated in platinum using a Cressington 208HR sputter-coater. Specimens were then examined using a CamScan 3-30BM scanning electron microscope at a working distance of between 5-10 mm. Images were captured using Image Pro Plus software.

2.4 Sterilisation

2.4.1 Moist heat sterilisation

All solutions, bioreactor components and other materials not suitable for dry heat sterilisation were autoclaved at 121°C at fifteen pounds per square inch (psi) for twenty minutes.

2.4.2 Dry heat sterilisation

Items suitable for dry heat sterilisation included dissection instruments and multi-spot glass slides. Items were placed in an oven at 160°C for four hours.

2.4.3 Filter sterilisation

Small volume solutions and solutions unsuitable for moist heat sterilisation were passed through a 0.2 µm filters.

2.5 Tissue procurement

Porcine carotid arteries from English White Pigs were delivered from Sykes House Farm (Thorp Arch, Wetherby, UK) one day post-slaughter. Arteries were delivered with laryngeal and thoracic structures still attached. Residual and adventitial tissue was removed from

the arteries using sharp dissection. Arteries were then immediately washed three times in sterile DPBSa with EDTA (2.7 mM) and aprotonin (10 KIU.ml^{-1})] at 4°C for 30 minutes to remove any tissue debris and inhibit endogenous protease activity. Arteries were then placed in labeled sterile universals and stored at - 80°C ready for use.

2.6 Histological techniques

2.6.1 Specimen processing and fixation for paraffin wax embedding

The middle and distal ends of both decellularised and fresh arteries were analysed. Using a scalpel, each artery was cut in half. Samples (5 mm) were then cut from the distal ends of the two cut halves of each decellularised artery. Each tissue sample was placed into labeled individual plastic histology cassettes. The cassettes were placed into a metal holding basket and placed in a tissue processor. Program one was selected, which immersed the samples for an hour under vacumn into the following solutions:

1. 10% (w/v) neutral buffered formalin at 21°C
2. 70% (v/v) ethanol at 21°C
3. 90% (v/v) ethanol at 21°C
4. 100% (v/v) ethanol at 21°C
5. 100% (v/v) ethanol at 21°C
6. 100% (v/v) ethanol at 21°C
7. Xylene at 21°C
8. Xylene at 21°C
9. Xylene at 21°C
10. Paraffin wax at 50°C
11. Paraffin wax at 50°C
12. Paraffin wax. at 50°C

After completion of program one, the cassettes were removed from the tissue processor and transferred into fresh molten wax inside a wax oven. Metal wax block moulds were filled with molten wax and then specimens were positioned carefully into the centre of each mould, with the lumen facing upwards. The moulds were then placed onto ice packs to solidify the wax at the bottom of each mould (to hold the specimen in the correct

orientation). The plastic histology cassettes were then placed on top of the moulds and topped up with further molten wax. The moulds were then left to cool and harden at room temperature. After cooling, the wax block was removed from the mould, leaving it attached to the cassette base. Excess wax was removed from the edges of the cassette base using the flat edge of a metal spatula.

Blocks were then placed into the microtome and cut into 5 µm sections at an angle of 5°. Sections were removed and placed onto the surface of a hot water-bath at 45°C until wrinkles within the wax had disappeared. Sections were then collected onto labeled glass slides and placed onto hotplate rails at 50°C to dry for three hours.

2.6.2 Haemotoxylin and Eosin (H& E) staining of paraffin wax embedded tissue samples

Once the sections had dried they were placed in a slide holder and immersed into two consecutive pots of (dewax) xylene for ten minutes each. Sections were consecutively placed into separate pots of 100% ethanol for three, two and two minutes respectively. Sections were then placed in 70% (v/v) ethanol for two minutes and then immersed into running tap water for three minutes. Following this, sections were immersed into haemotoxylin for one minute and then immersed into running tap water, until water drained clear. Sections were placed in eosin for three minutes. Sections were placed again in 70% (v/v) ethanol for five seconds and then placed into consecutive pots of 100% ethanol for one, two and three minutes respectively. Sections were immersed into two consecutive pots of clean xylene for ten minutes each. Sections were mounted using glass coverslips and DPX mountant and left in a fume cupboard to dry for four hours.

2.6.3 DAPI staining of paraffin wax embedded tissue samples

Embedded tissue sections were stained using DAPI to visualise double-stranded DNA and cell nuclei. Slides were placed in a slide holder and immersed into two consecutive pots of (dewax) xylene for ten minutes each. Sections were consecutively placed into separate pots of 100% ethanol for three, two and two minutes respectively. Sections were placed in 70% (v/v) ethanol for two minutes and then immersed into running tap water for three minutes. In a dark room, the sections were immersed into 200 ml of DAPI working solution (0.1 $\mu g.ml^{-1}$) and incubated at room temperature for ten minutes. Sections were washed

three times in DPBSa for ten minutes in the dark. Sections were mounted using 1,4-diazobicyclo-(2,2,2)-octane(DABCO): glycerol mountant and glass cover slips. Sections were viewed using an upright fluorescent microscope and DAPI filter. Images were captured using a digital camera and Image-Pro Plus v 5.1.

2.6.4 Specimen processing and zinc fixation for paraffin wax embedding

Specimens (5mm) were cut from the distal end of each artery. Each tissue sample was then placed into labeled individual plastic histology cassettes. The cassettes were placed into zinc fixative solution for 24 hours at room temperature. The cassettes were placed into a metal holding basket and placed in a tissue processor. Program three was selected, which immersed the samples for an hour under vacumn into the following solutions:

1. 70% (v/v) ethanol at 21°C
2. 90% (v/v) ethanol at 21°C
3. 100% (v/v) ethanol at 21°C
4. 100% (v/v) ethanol at 21°C
5. 100% (v/v) ethanol at 21°C
6. Xylene at 21°C
7. Xylene at 21°C
8. Xylene at 21°C
9. Paraffin wax at 50°C
10. Paraffin wax at 50°C
11. Paraffin wax. at 50°C

After completion of program three, the specimens were wax embedded and sectioned as described in Section 2.6.1. H & E and DAPI staining was then performed as described in Sections 2.6.2-2.6.3.

2.7 Cell culture

All materials, equipment, reagents and solutions used are listed in Sections 2.1-2.2.

All methods were performed using full aseptic precautions in a class II safety cabinet.

2.7.1 Cell maintenance

Spent culture medium was aspirated from each T75 flask and replaced with 10 ml of cell-specific medium every 48 hours.

2.7.2 Cell passage

Cells were passaged when they became 70-80% confluent in the flasks. Medium was removed from the flasks carefully to prevent disruption of the cell monolayer. The flask surface was then washed with 10 ml of DPBSa without calcium or magnesium for five minutes. Trypsin (3 ml) was then added to each T75 flask of cells. Flasks were then gently rocked to ensure uniform coverage of the cell monolayer and incubated at 37°C with 5% (v/v) CO_2 in air for five minutes. Following incubation the sides of the flasks were gently tapped to dislodge the cells. Cell detachment was confirmed using an inverted microscope. Cell-specific medium (10 ml) was then added dropwise into the flask with contents then being placed into a sterile universal. To remove the trypsin and create a cell pellet, the solution was centrifuged at 150 g for ten minutes. Following centrifugation, the supernatant was removed and the cell pellet was resuspended in 1 ml of fresh medium. The cell suspension was diluted by addition of a further 4 ml of medium. The diluted cell suspension was then placed into a new, sterile T75 flask and placed back into incubation at 37°C with 5% (v/v) CO_2 in air.

2.7.3 Cell storage in liquid nitrogen

A cell pellet was created using the procedure described above for cell passage. The cell pellet was then resuspended in cell-specific medium (12 ml) containing 10% (v/v) dimethyl sulfoxide (DMSO). The following stages were performed quickly due to the toxicity of DMSO to the cells. The cell suspension was then aliqoted into 1 ml cryovials labelled with the cell name, date and passage number. The cryovials were then placed into a Mr Frosty containing isopropranol and stored at -80°C overnight. Cryovials were then placed in a cell-specific liquid nitrogen dewar for long-term storage. A cell log form was completed to allow update of the digital cell log database.

2.7.4 Cell resurrection

Cell-specific culture medium was pre-warmed to 37°C. The digital cell log database was inspected to confirm position of required cells. Cryovials were then warmed to room temperature and the cell suspension transferred into a sterile universal. Immediately, 10 ml of warmed medium was added dropwise (to prevent cell shock) into the universal. The suspension was then centrifuged at 150 g for ten minutes to remove the DMSO. Following centrifugation, the supernatant was removed and the cell pellet was resuspended in 1 ml of fresh medium. A further 9 ml of medium was then added to the universal and contents placed into a T75 flask. Cells were then incubated at 37°C with 5% (v/v) CO_2 in air and observed for growth.

2.7.5 Cell counting

A cell pellet was created using the procedure described above for cell passage. Cell specific medium (8 ml) was then added to create a cell suspension. Trypan blue (10 µl) was mixed with 90 µl of cell suspension in a sterile bijou. A haemocytometer was cleaned with 70% (v/v) ethanol and then a glass cover slide was placed over the top. Approximately 10-15 µl of the cell suspension containing trypan blue was then placed under the coverslip to lie over the central, triple-ruled area of the haemocytometer. Cells present in five of the twenty-five squares within the haemocytometer were counted using a cell counter (cells containing trypan blue were not counted as these represented non-viable cells). In order to calculate the number of cells present per ml of suspension, the following working was used.

Within the central ruled area of the haemocytometer, there were nine large squares each of 1 mm^2. The depth of the counting chamber with the glass coverslip appropriately in place was 0.1 mm. Therefore cells lying within one of the nine large squares came from a volume of 0.1 mm^3. Counting five of the twenty-five smaller squares was equivalent to counting 1/5 of 0.1 mm^3. The number of cells in 0.1 mm^3 was multiplied by 10^4 to estimate number of cells.ml^{-1}. Finally if only five small squares were counted, to estimate the number of cells per ml this was multiplied by 5 x 10^4 to estimate the number of cells.ml^{-1}.

2.7.6 Cell viability assay

2.7.6.1 Live / Dead ® Assay to assess for cell viability

The Live/Dead ® stain was prepared using DPBSa, 1 mM calcein AM and 1 mM ethidium homodimer-1. Sections of seeded scaffold (2 cm x 2 cm) were cut from the main scaffold and placed into individual wells of a six-well plate. Live / Dead ® stain solution was added into each well to completely cover the tissue. The plate was then incubated in the dark at room temperature for 45 minutes. The tissue was then washed three times using TBS (pH 7.6) for ten minutes on a plate rocker. The tissue was then wet mounted with DPBSa onto a microscope slide and covered with a glass coverslip. The tissue was viewed using a confocal microscope and a conventional fluorescent long pass filter.

2.8 Vascular cell harvest (ovine and porcine)

2.8.1 Tissue procurement and preparation

Fresh ovine and porcine hind-legs were delivered by a local abattoir (John Penny & Sons, Leeds, UK) immediately following slaughter. The superficial femoral artery from each leg was harvested using sterile dissecting instruments within a class II safety cabinet to minimize contamination. Once excised, the arteries were placed immediately into sterile DPBSa to wash away any adherent clot or tissue debris. Arteries were then incubated in an antibiotic solution (streptomycin 300 $U.ml^{-1}$, 300 $U.ml^{-1}$ penicillin) at 37°C for two hours.

2.8.2 Endothelial cell isolation

Following incubation, one end of the artery was tied off using a silk suture. A blunt needle was placed into the other end with a silk suture tied loosely around both artery and needle. A syringe containing collagenase solution (0.1% collagenase type II 273 $U.ml^{-1}$) was then attached to the needle and the contents then injected into the arterial lumen. The needle was then removed and the suture tightened to maintain the collagenase solution within the arterial lumen. The vessel containing collagenase was then incubated at 37°C for thirty minutes.

Following incubation, the vessel was cut along its axis and the contents emptied into a sterile universal tube. The arterial lumen was then washed with 10 ml of DPBSa to flush out any remaining endothelial cells. The collected cell suspension was then centrifuged at 250 g for 10 minutes. After centrifugation, the supernatant was discarded and the cells

washed in 20 ml of M-199 medium. Cells were then re-suspended in endothelial culture medium and split into two T75 culture flasks. Flasks were then incubated at 37 °C in 5% (v/v) CO_2 in air with the culture medium being changed every 48 hours. Flasks were examined for evidence of endothelial cell attachment, characterised initially by the growth of cells in colonies. Once cells had reached near-confluence, the characteristic 'cobblestone' appearance of an EC monolayer was observed.

2.8.3 Isolation of smooth muscle cells

The remaining arterial segments from the isolation of EC were macerated using a sterile scalpel blade and then placed into a T75 culture flask together with 10 ml of SMC medium and incubated at 37°C in 5% (v/v) CO_2 in air. Medium was changed every 48 hours. Flasks were examined from 72 hours to assess for SMC migration from the explant onto the flask surface.

2.9 Data analysis and statistics

All statistical analyses were performed using Microsoft Excel 2010 software. All values were displayed as the mean ± 95 % confidence intervals. To assess statistical significance between groups, a student's t-test was used to analyse data with two sets of mean values and a one way analysis of variance (ANOVA) test was use assess data with more than two sets of mean values. Following ANOVA, individual differences between group means were determined using the t-method to obtain the minimum significant difference. A p-value of <0.05 was considered statistically significant.

Chapter 3

Decellularisation and characterisation of porcine carotid arteries

3.1 Introduction

For the tissue engineering of SD grafts, the approach taken was to decellularise porcine carotid arteries since they are the correct diameter (<6 mm), are readily available and have been shown to be amenable to varying decellularisation protocols in the literature (McFetridge *et al.*, 2004; Roy *et al.*, 2005; Heine *et al.*, 2011; Nitsan *et al.*, 2012). The Institute of Medical and Biological Engineering (IMBE) at the University of Leeds had previously developed a decellularisation protocol that had been used to successfully decellularise a number of allogeneic and xenogeneic tissues (without significant alteration in tissue biomechanics) including heart valves, pericardium, amniotic membrane and ureter (Booth *et al.*, 2002; Wilcox *et al.*, 2003; Wilshaw *et al.*, 2006; Derham *et al.*, 2008).

The aim of decellularisation is to remove all cells from a tissue whilst preserving the composition of the remaining ECM. For this project therefore, the use of xenogeneic artery was an obvious choice given that its ECM is innately designed to withstand and adapt to the haemodynamics of blood circulation. In addition, the ECM proteins of arteries display close sequence homology across species, which has obvious importance in biocompatibility (Gilbert *et al.*, 2006). The ultimate goal at present in cardiovascular tissue engineering is to be able to re-cellularise a decellularised scaffold with vascular cells not only to provide a functioning endothelium, but also to give the scaffold functionality. Although decellularisation protocols differ within the literature, re-cellularisation studies on decellularised arteries have consistently shown successful re-cellularisation of scaffolds using a variety of cell types, most importantly, vascular cells. (Conklin *et al.*, 2002; McFetridge *et al.*, 2004; Shimizu *et al.*, 2007; Dahan *et al.*, 2011; Heine *et al.*, 2011).

3.2 Aims and Objectives

The aims and objectives of this chapter were:

1. To decellularise porcine carotid arteries 8-11cm in length

2. To determine the extent of decellularisation using histological analysis and DNA quantification

3. To determine the biocompatibility of decellularised arteries to ISO standard cell lines (BHK and 3T3 cells).

4. To determine the biocompatibility of decellularised arteries to (native) primary porcine vascular cells

3.3 Experimental approach

The standard iMBE decellularisation protocol was used in an attempt to decellularise the porcine carotid arteries.

Once the arteries had been harvested and prepared, they were sequentially washed in a series of buffers to decellularise the tissue. The first step was to wash the arteries in antibiotic solution to reduce the bio-burden. Arteries were then treated with EDTA to loosen the vascular cells from the extracellular matrix by inhibiting integrin function. Arteries were then washed in hypotonic buffer followed by low concentration SDS. The hypotonic buffer caused the cells to swell and then burst. SDS, a detergent, solubilised the cell membranes. These two steps were then repeated. The next step was treatment with a nuclease solution containing RNase and DNase enzymes to digest DNA and RNA. Arteries were then washed in a hypertonic buffer to remove any hydrophobic substances from the arteries such as the α-gal epitope. The α-gal epitope is a carbohydrate present on glycoproteins expressed by cells of non-primate mammals. It is not present in humans; indeed, all humans produce an antibody to the epitope (Galili, 2005). For the penultimate step, arteries were treated with PAA. PAA efficiently removes any residual cellular remnants and sterilises the tissue. The final step was three terminal washes with DPBSa to remove any residual cell debris.

To confirm decellularisation, histological staining methods and DNA quantification were used. H&E and DAPI stains were used to confirm decellularisation histologically. Both haemotoxylin and DAPI bind to nuclear (acidic) material and so demonstrate any cell nuclei remaining in the tissue. DNA quantification was also performed to assess the removal of nuclear material. To quantify the DNA remaining within the tissue, a standard

DNA extraction kit was used to extract DNA into solution. The concentration of the DNA in solution was then measured using spectrophotometry. In total, eight batches of between 2-22 porcine carotid arteries were subject to the decellularisation protocol in this study.

Once the porcine carotid arteries were successfully decellularised, the biocompatibility of the decellularised arteries was assessed using contact and extract cytotoxicity assays using two cell lines (murine 3T3 cells and BHK cells) and porcine EC and SMC. 3T3 and BHK cells are recommended by the ISO to assess the biocompatibility of medical devices.

3.4 Materials and Methods

All equipment, reagents, materials and solutions used in the study are listed in Chapter 2. The porcine cells were kindly gifted by a fellow University of Leeds MD student (Mr Taha Khan). They were harvested using the techniques described in Chapter 2.8 and subsequently characterised to confirm vascular cell phenotype.

3.4.1 Tissue procurement and preparation

Porcine carotid (PC) arteries were procured and prepared as described in Section 2.5. In total, 79 PC arteries were used in this study.

3.4.2 Decellularisation of porcine carotid arteries

All incubations in the process were performed using 200 ml of solution, with agitation at 240 rpm with the exception of the nuclease step, which was at 80 rpm. Prior to each incubation, the arteries were placed in sterile 250 ml containers. Two to four arteries were used in the first four decellularisation runs. Between six to twenty-two arteries were used in the proceeding runs (exact number based on artery availability at the time). Details of all solutions used are listed in Chapter 2, Section 2.2.

Frozen porcine carotid arteries were thawed in an incubator at 37°C for twenty minutes. Following thawing, the arteries were washed in disinfectant solution and incubated for 30 minutes at 37°C. Arteries were then incubated in EDTA solution for 24 hours at 4°C. Arteries were then incubated in hypotonic buffer for 24 hours at 4°C. Arteries were then incubated in 0.1% (w/v) SDS in hypotonic at 37°C for 24 hours. Arteries were then once again incubated in hypotonic solution at 4°C for 24 hours. Arteries were then incubated in DPBSa EDTA solution with aprotonin for 56 hours at 4°C. Arteries were then incubated in 0.1% (w/v) SDS in hypotonic buffer at 37°C. The arteries were then incubated three times

in DPBSa solution at 37°C for 30 minutes each. The arteries were then incubated in nuclease for three hours at 37°C. Following nuclease incubation, the arteries were incubated three times in DPBSa EDTA solution with aprotonin at 37°C for 30 minutes each. Arteries were then incubated in hypertonic buffer for 24 hours at 37°C. The arteries were then incubated three times in DPBSa EDTA solution with aprotonin at 37°C for 30 minutes each. The arteries were then sterilised in 0.1% (v/v) PAA solution for three hours at 27°C. The final two steps were performed aseptically in a class II safety cabinet. The arteries were incubated three times in DPBSa EDTA solution with aprotonin at 37°C for 30 minutes each. For the final step in the decellularisation process, the arteries were incubated with DPBSa for 24 hours at 4°C. Arteries were stored in DPBSa solution at 4°C until required, for a maximum of three months.

3.4.3 Characterisation of decellularised arteries

To determine whether decellularisation was successful, the processed arteries were characterised histologically using H&E and DAPI staining and DNA content was quantified. To ensure fully representative analysis, samples were taken from the end and middle section of each artery.

3.4.3.1 Histological characterisation

Processed arteries were compared to fresh control arteries using the histological techniques described in Chapter 2, Sections 2.6.1-2.6.3

3.4.3.2 Isolation and quantification of total DNA

The DNeasy kit (Qiagen) was used for this process.

Four (25 mg) sections from two decellularised arteries (two end sections and two middle sections) and four (25 mg) sections from two control arteries were macerated using a scalpel. Each sample of tissue was then placed in a labeled 1.5 ml micro-centrifuge tube. Buffer ATL (180 µl) and 20 µl of proteinase K were added to the tubes. The contents of each tube were mixed thoroughly using pulsed-vortexing for 10 seconds. All tubes were then incubated in a waterbath at 56°C for three and a half hours to achieve complete tissue lysis.

Buffer AL (200 µl) was then added to each tube and then mixed using pulse-vortexing, and 200 µl of ethanol (100%; v/v) was added to each tube. Tubes were mixed using pulse-

vortexing immediately following addition of ethanol to ensure a homogenous solution. Each sample was then placed in a DNeasy mini spin column and placed in a 2 ml collecting tube. Samples were then centrifuged at 6000 x g for one minute. The flow-through material was then discarded and the samples were placed in new collection tubes. Buffer AW1 (500 µl) was added to each tube and centrifuged again at 6000 x g for one minute. Flow-through was again discarded and the samples transferred to new collection tubes. Buffer AW2 (500 µl) was added to each tube, centrifuged this time at 16,000 x g for three minutes, to dry the DNeasy membrane. Again flow-through was discarded and samples placed into 2ml micro-centrifuge tubes. Buffer AE (100 µl) was then added onto the DNeasy membrane. Samples were incubated at room temperature for one minute and then centrifuged at 6000 x g for one minute. This time, flow-through was not discarded. A further 100 µl of Buffer AE was added to the samples which were again centrifuged at 6000 x g for one minute following incubation at room temperature. This latter step was performed twice in order to maximise DNA yield. The resultant DNA samples were stored for a short period at 4°C prior to quantification. The concentration of DNA in each sample was determined by loading 2 µl aliquots onto a Nanodrop™ spectrophotometer (which determined absorbance at 260 nm wavelength of light). Nuclease free water from the DNeasy kit was used to blank. Each sample was tested in triplicate. The concentration of each sample was normalised for volume and initial tissue mass to determine DNA concentration in $\mu g.mg^{-1}$.

3.4.4 Assessment of the biocompatibility of decellularised porcine carotid arteries

3.4.4.1 Extract cytotoxicity

This procedure describes the process of assessing the cytotoxicity of decellularised porcine carotid artery using adherent 3T3 cells, BHK cells, porcine EC and SMC compared to a positive control of 40% (v/v) DMSO and negative control of culture medium. Any soluble components present in the artery were extracted and cultured with a monolayer of cells. The ATP content of the cells was then determined as an indicator of cell viability. The procedure was performed using full aseptic precautions in a class II safety cabinet.

Three [300 mg] sections from three separate decellularised arteries from batch 8 were macerated using a scalpel and placed into a sterile labeled bijou containing 3 ml of DMEM. The tissue and medium was then incubated at 37°C with agitation at 240 rpm for 72 hours. Following this, the supernatant from each bijou was aspirated and divided into three sterile

microtubes. To ensure sterility, a specimen of supernatant from each bijou was plated onto four different agar plates each- fresh blood agar, heated blood agar, nutrient agar and Sabouraud dextrose agar which were then placed to culture. All plates except the latter were incubated at 37°C, the Sabouraud dextrose agar plate was incubated at 30°C. The extracts were stored at -20°C ready for use. Plates were inspected at 48 hours to confirm no growth had occurred. Subconfluent 3T3 cells (Passage [P] =13), BHK cells (P=12), porcine EC (P=2) and SMC (P=3) were subcultured into pre-labeled white 96 well tissue culture plates (n= 3 replicates). Cells were placed in labeled wells to test both extract samples and in wells for positive and negative controls. Cells were then incubated in 5% (v/v) CO_2 at 37°C until approximately 80% confluent. On the day of the assay, the extracts were defrosted ready for use. The medium was aspirated from each well in the culture plate and replaced with 100 µl of culture medium containing twice the normal FBS concentration (110 ml ; Section 2.2). For the medium-only controls, 200 µl of culture medium was placed into each set of wells (Section 2.2). Each extract (100 µl) was then placed into labeled wells in the well plate. Culture media (100 µl) was placed in labeled wells together with 100 µl of DMSO for the positive control. The plate was then incubated for 48 hours in 5% (v/v) CO_2 in air at 37°C. After incubation, the well-plate was ready for the ATPLite-M assay to quantify ATP levels.

ATPLite-M reagents were equilibrated to room temperature. The lyophilised substrate solution was reconstituted by adding 5 ml of substrate buffer. The contents of all wells were then aspirated and replaced with 50 µl of DMEM. Following this, 50 µl of mammalian cell lysis solution was then added to each well and agitated at 500 rpm for five minutes. Following agitation, 50 µl of substrate solution was added to each test well and again agitated at 500 rpm for five minutes. After agitation, luminescence was determined using TopCount. Data (counts per second) was analysed using one-way ANOVA.

3.4.4.2 Contact cytotoxicity assay

This procedure describes the process of assessing the cytotoxicity of decellularised porcine carotid artery using adherent 3T3 cells, BHK cells, porcine EC and SMC compared to collagen type I and cyanoacrylate contact adhesive. This assay tests for any toxic components leeching from the intact tissue. The procedure was performed using full aseptic precautions within a class II safety cabinet.

Three 10 mm^2 sections from two separate decellularised arteries from batch 4 were cut using a scalpel and placed in sterile DPBSa to prevent dehydration. For the positive control, a drop of cyanoacrylate contact adhesive was placed into the centre of one well in a six-well plate. As the negative control, 20 µl of collagen gel neutralized with 10 µl of sodium hydroxide (0.1 M) was placed into the centre of a well within a six well plate. One of the square sections of artery was then placed into the centre of one of the wells using the collagen gel and sodium hydroxide as an adhesive (2:1 ratio). All wells were then washed three times for ten minutes using sterile DPBSa. 3T3 cells (P=13) were harvested from culture and suspended in culture medium . 3T3 cells (1 ml) were then added to each well. Cells were then incubated in 5% (v/v) CO_2 in air at 37°C for 48 hours. The whole process was repeated using BHK cells (P=12) and porcine EC (P=2) and SMC (P=3).

Following incubation, the plates were examined under a microscope and examined for changes in cell morphology and density. Medium was then aspirated from the wells which were then washed with sterile DPBS containing calcium and magnesium.

The cell layers were then fixed using 10% (v/v) neutral buffered formalin for ten minutes. Following fixation, the formalin was removed and then the cell layer was stained using Giemsa solution for five minutes. Each well was then rinsed in running tap water until it ran clear. The plate was then left to air dry. Once dry, the plate was again examined using microscopy for changes in cell morphology and density and for cell growth to the edges of the arterial specimen. Images were then taken using a digital microscope.

3.5 Results

3.5.1 Histological evaluation of decellularised porcine carotid arteries [Batches 1-3]

The first three batches of treated arteries were incompletely decellularised. Figure (3) shows H&E and DAPI staining of representative samples from batches 1-3 confirming the presence of cell nuclei remaining in all three arterial layers as compared to controls, although the cell density in each layer was less then untreated controls.

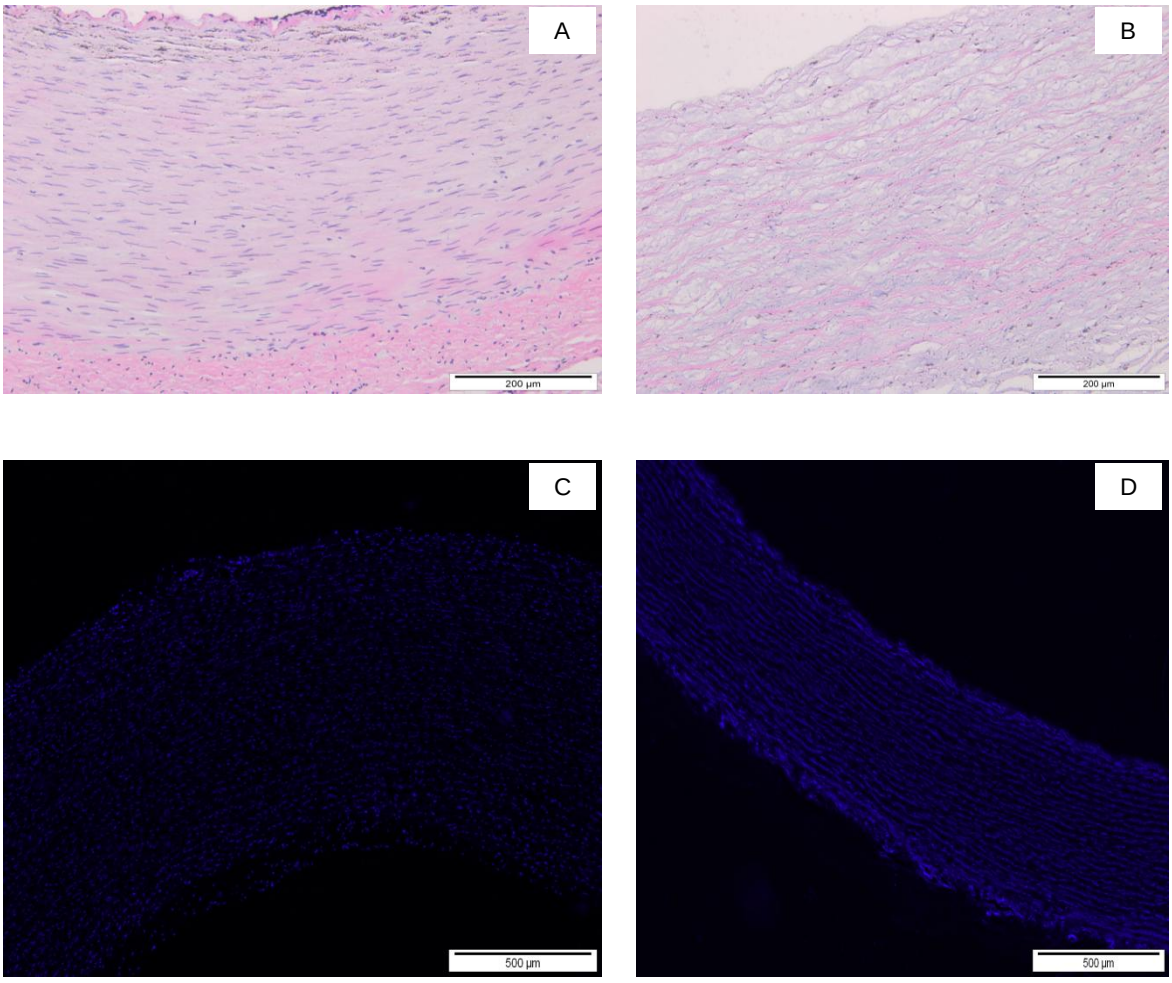

Figure 3. Representative sections of porcine arteries from decellularisation Batches 1-3 stained with H&E and DAPI. A; Fresh PCA (H&E), B; Treated PCA (H&E). Both micrographs clearly demonstrate the presence of cell nuclei through all layers of the arterial wall in both control and treated specimens. C; Fresh PCA (DAPI), D; Treated PCA (DAPI). DAPI staining confirms the presence of DNA (indicating cellular nuclear material) again through all layers of the arterial wall in both control and treated specimens.

3.5.2 Total DNA content of decellularised porcine carotid arteries [Batches 1-3]

Unsurprisingly, only an average DNA removal of 12-28% was achieved during the first three decellularisation batches (Figure 4), which was well below the target of >90% DNA removal.

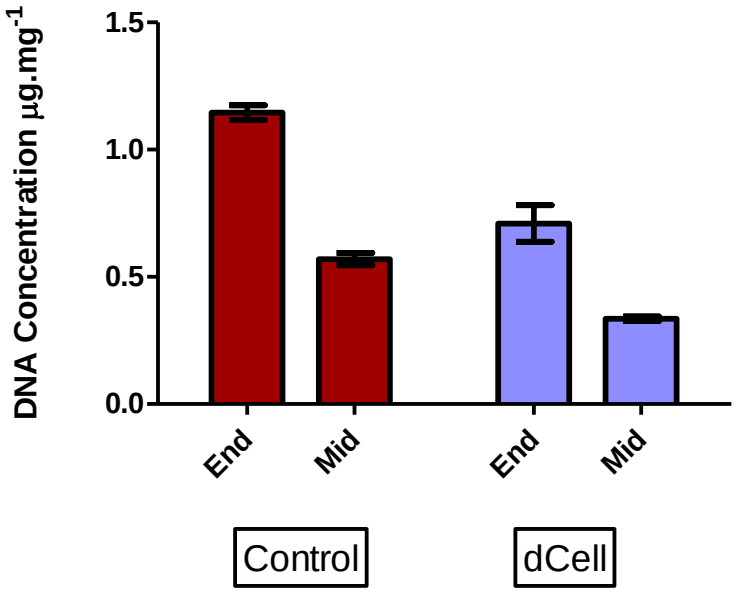

Figure 4. DNA content of fresh and decellularised porcine carotid artery from Batches 1-3. Data is expressed as the mean [n=6 (two decellularised arteries and two control arteries from each batch tested) ± 95% confidence limits]. End; end of artery, Mid; middle of artery.

3.5.3 Histological evaluation of decellularised porcine carotid arteries [Batches 4-8]

Following analysis of the histological sections from batches 1-3, it was felt that the failure to decellularise was as a result of insufficient detergent (SDS) activity on the cell membranes, most likely as a result of error in preparing the SDS solution. The error was likely as a result of the filtration step where SDS is passed through a 0.2µm filter. To confirm whether it was an error with filtration of the SDS, it was decided to add 1g of SDS powder directly into one litre of sterile hypotonic buffer. Following this modification, the following five subsequent decellularisation batches all demonstrated successful decellularisation of arteries and so this method of SDS production was adopted throughout the rest of the study. As can be seen in Figures (5) and (6), H&E staining of the end and middle sections of representative samples from batchs 4-8 demonstrate a complete lack of cell nuclei in all three arterial layers, confirming successful decellularisation.

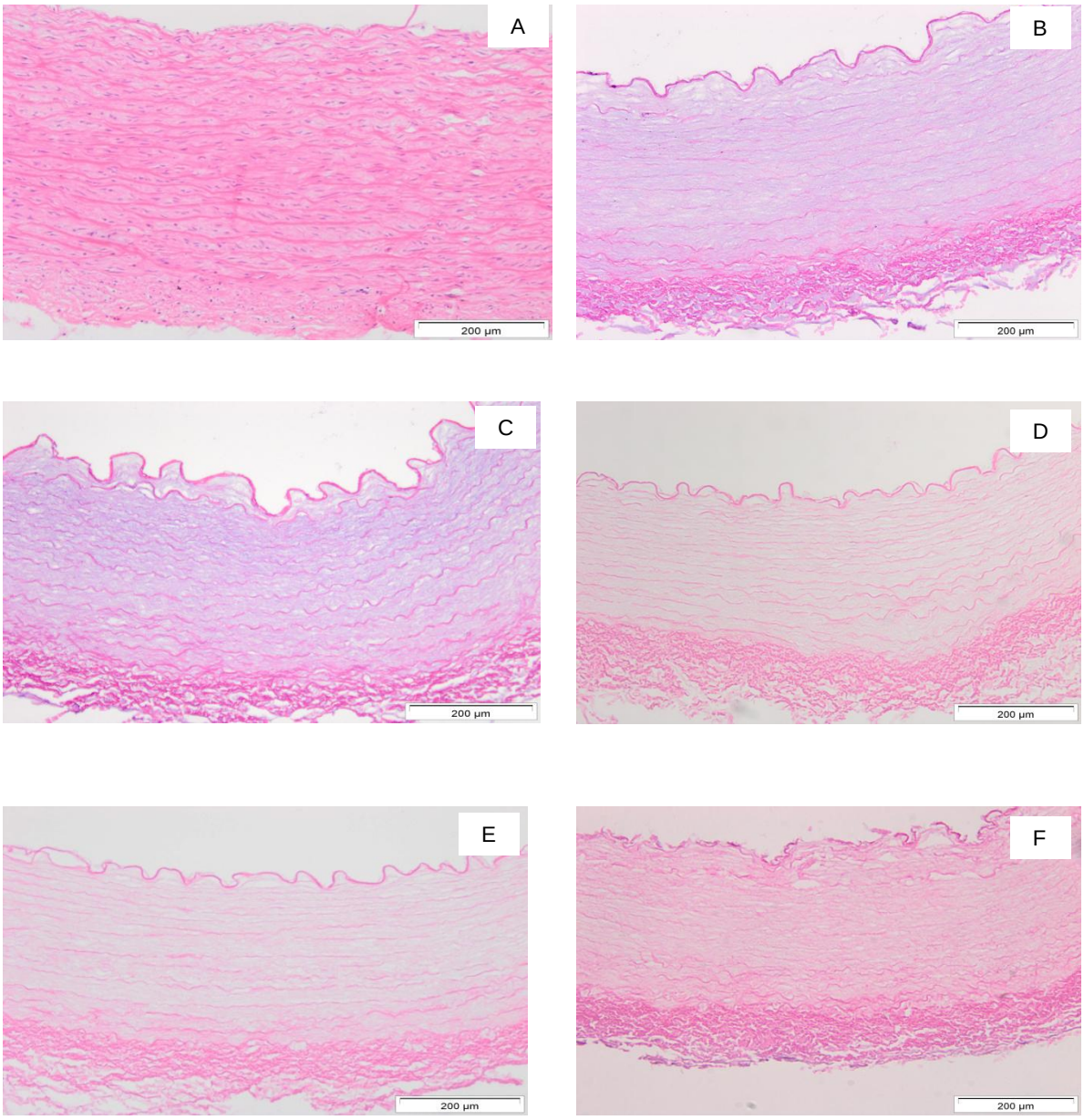

Figure 5. Representative end sections of porcine arteries from decellularisation Batches 4-8 stained with H&E. A; Fresh PCA (H&E) demonstrating the presence of nuclear material in all arterial layers, B; Decellularised PCA (H&E) Batch 4, C; Decellularised PCA (H&E) Batch 5, D; Decellularised PCA (H&E) Batch 6, E; Decellularised PCA (H&E) Batch 7, F; Decellularised PCA (H&E) Batch 8. Micrographs B-F demonstrate a lack of cell nuclei in all layers of the arterial wall, representing successful decellularisation.

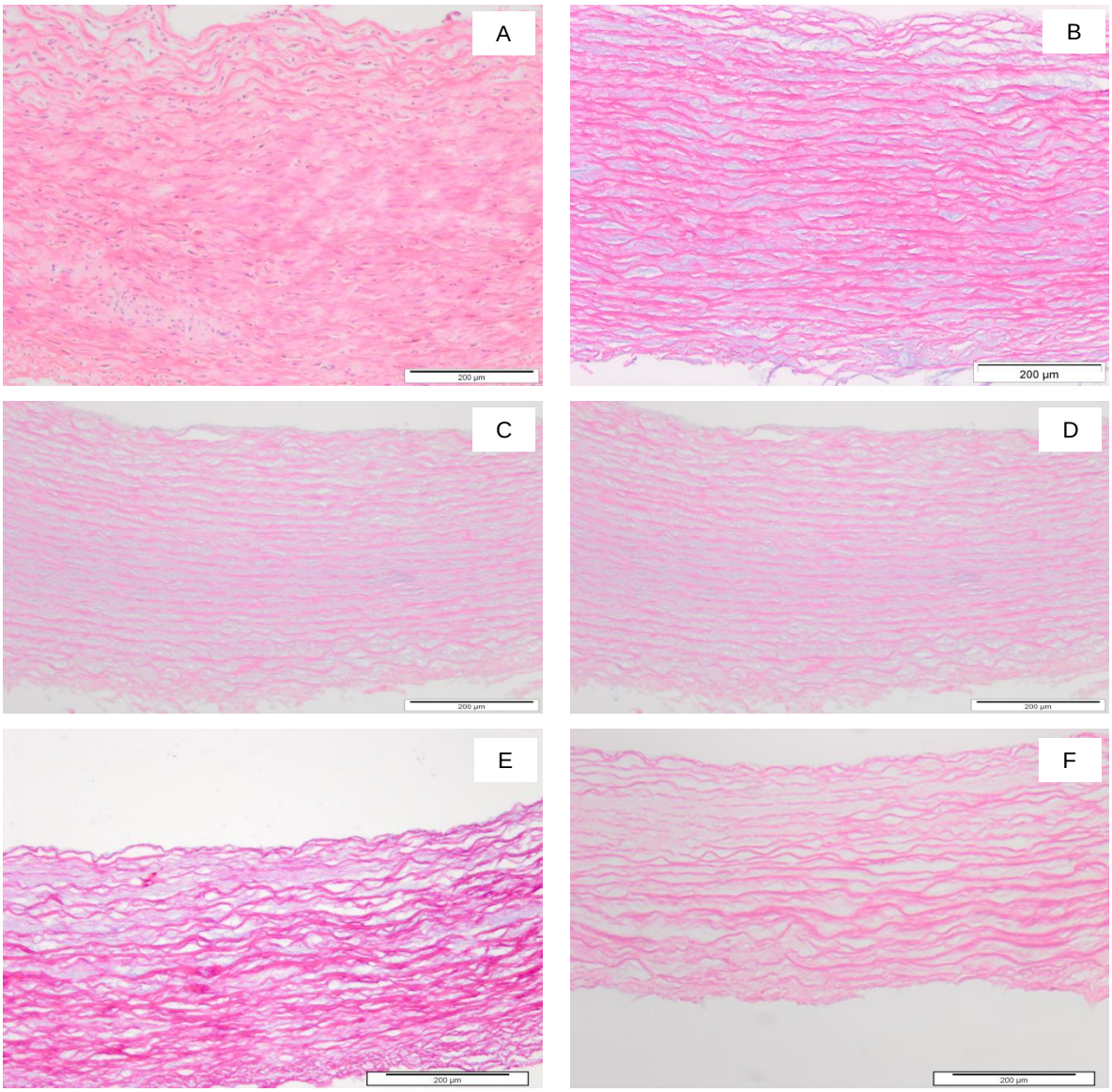

Figure 6. Representative middle sections of porcine arteries from decellularisation Batches 4-8 stained with H&E. A; Fresh PCA (H&E) demonstrating the presence of nuclear material in all arterial layers, B; Decellularised PCA (H&E) Batch 4, C; Decellularised PCA (H&E) Batch 5, D; Decellularised PCA (H&E) Batch 6, E; Decellularised PCA (H&E) Batch 7, F; decellularised PCA (H&E) Batch 8. Micrographs B-F demonstrate a lack of cell nuclei in all layers of the arterial wall, representing successful decellularisation.

DAPI staining of the end and middle sections of representative samples from batchs 4-8 also demonstrated a complete lack of cell nuclei in all three arterial layers, confirming

successful decellularisation (Figures 7-8). Autofluorescence was seen secondary to residual SDS within the ECM of the scaffolds following the decellularisation process.

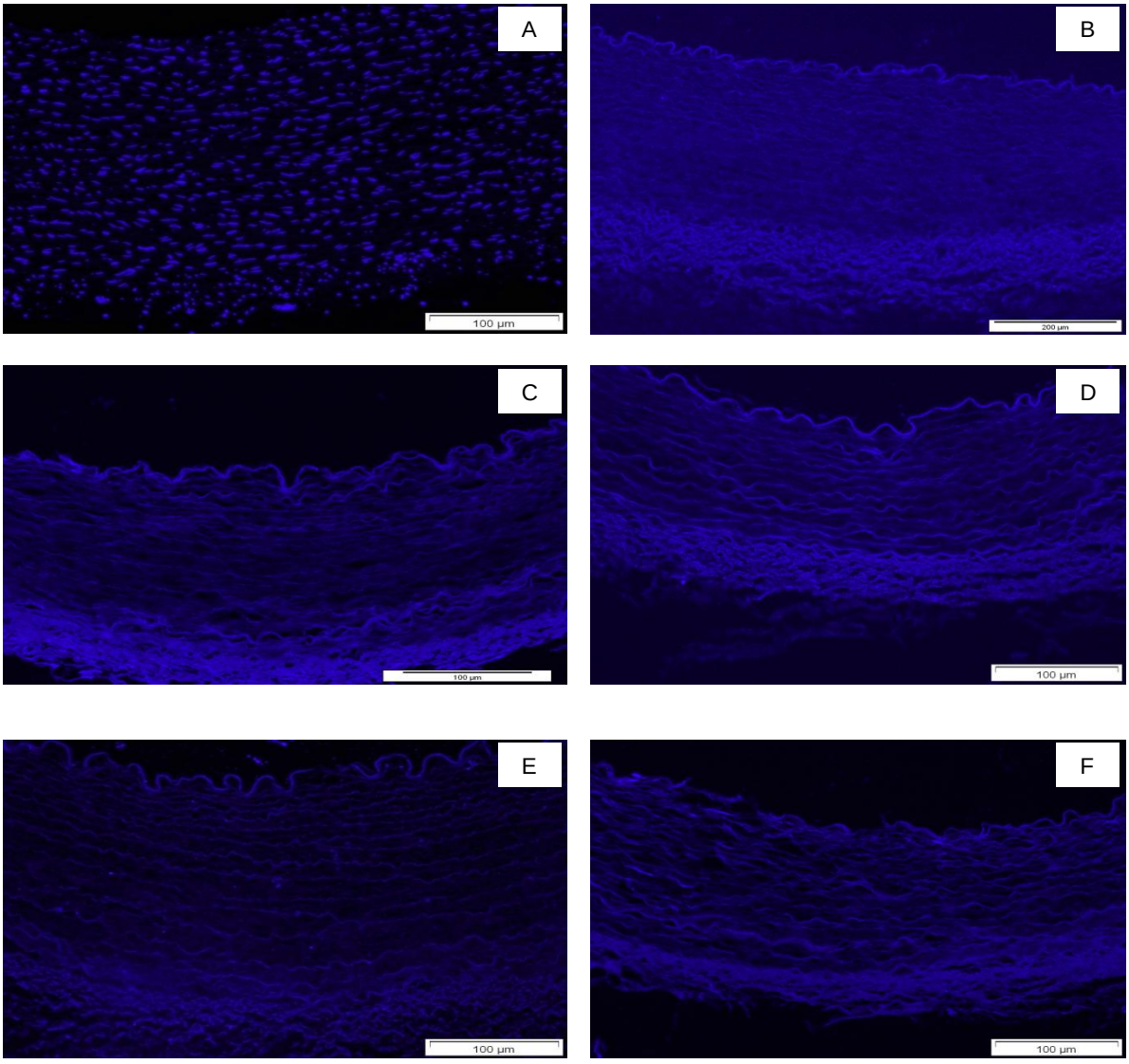

Figure 7. Representative end sections of porcine arteries from decellularisation Batches 4-8 stained with DAPI. A; Fresh PCA (DAPI) demonstrating the presence of nuclear material in all arterial layers, B; Decellularised PCA (DAPI) Batch 4, C; Decellularised PCA (DAPI) Batch 5, D; Decellularised PCA (DAPI) Batch 6, E; Decellularised PCA (DAPI) Batch 7, F; Decellularised PCA (DAPI) Batch 8. Micrographs B-F demonstrate a lack of nuclear staining (cell nuclei) in all layers of the arterial wall, representing successful decellularisation.

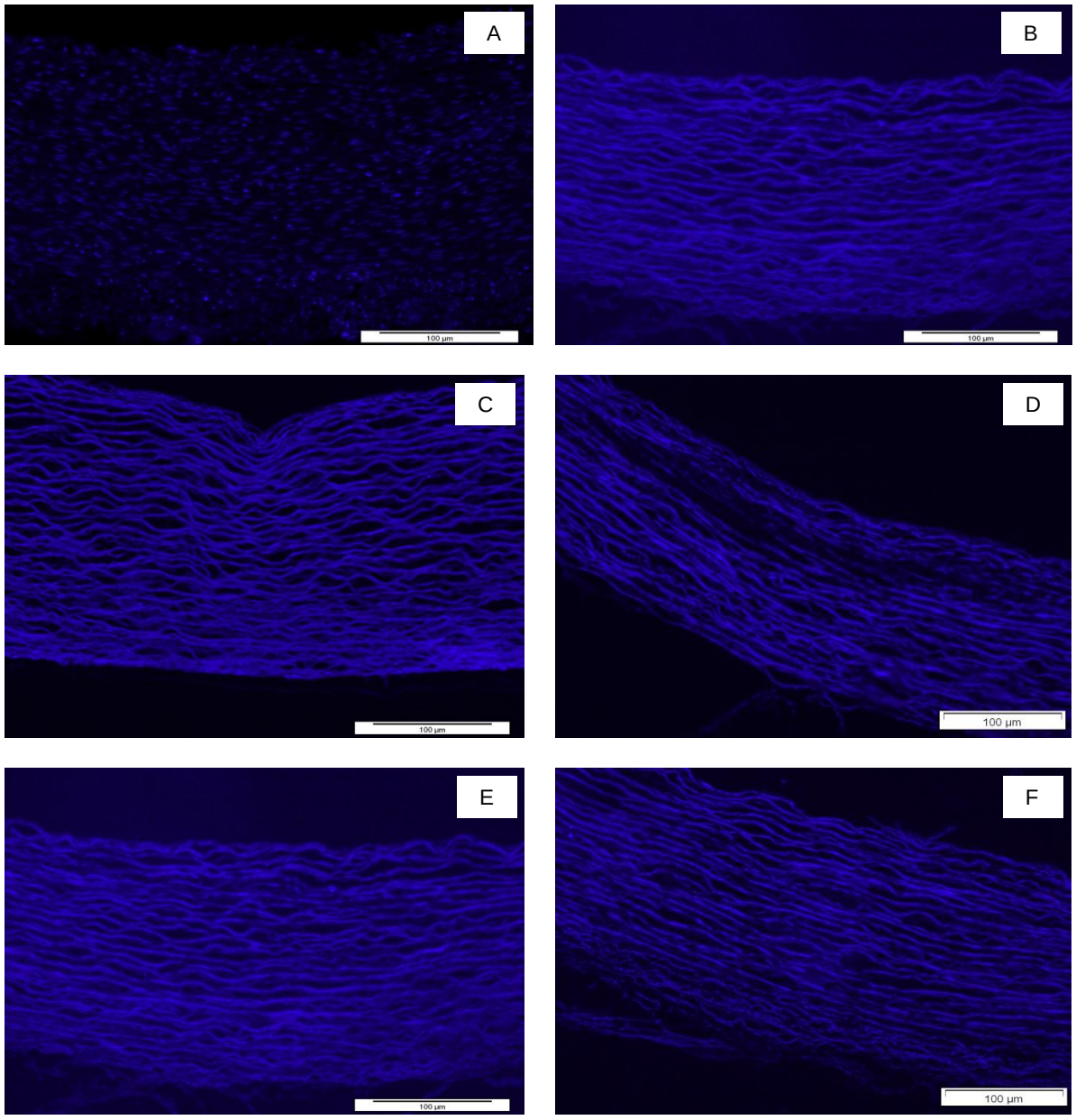

Figure 8. Representative middle sections of porcine arteries from decellularisation Batches 4-8 stained with DAPI. A; Fresh PCA (DAPI) demonstrating the presence of nuclear material in all arterial layers, B; Decellularised PCA (DAPI) Batch 4, C; Decellularised PCA (DAPI) Batch 5, D; Decellularised PCA (DAPI) Batch 6, E; Decellularised PCA (DAPI) Batch 7, F; Decellularised PCA (DAPI) Batch 8. Micrographs B-F demonstrate a lack of nuclear staining (cell nuclei) in all layers of the arterial wall, representing successful decellularisation.

3.5.4 Total DNA content of decellularised porcine carotid arteries [Batches 4-8]

Following the modification of the SDS step in the decellularisation protocol, an average DNA removal of 90-99% was achieved during the last five decellularisation batches, successfully reaching the target of >90% DNA removal (Figure 9).

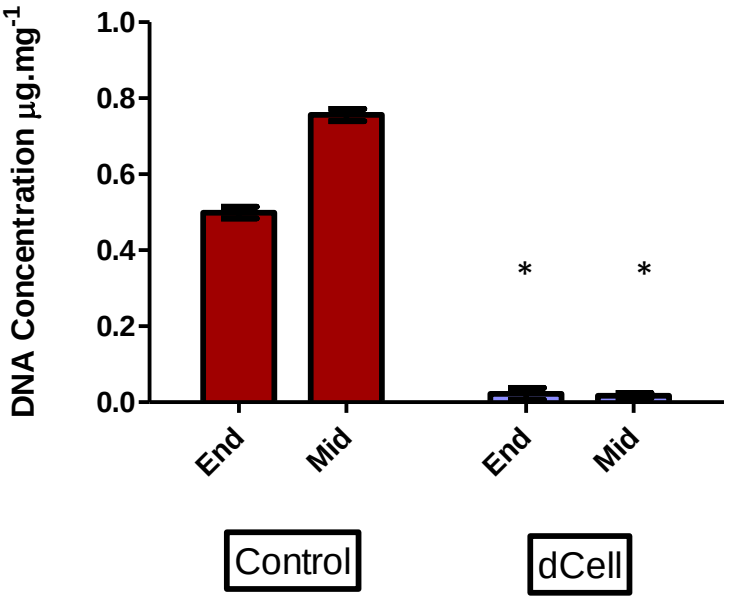

Figure 9. DNA content of fresh and decellularised porcine carotid artery from (representative) Batch 7. Data is expressed as the mean [n=3 (three decellularised arteries and three control arteries) ± 95% confidence limits. * Significantly different to control (Student's t-test)]. End; end of artery, Mid; middle of artery.

3.5.5 Summary of results for decellularised porcine carotid arteries [Batches 1-8]

Characterisation of arteries from the first three batches of arteries confirmed a lack of decellularisation likely as a result of ineffective detergent activity on the cell membranes (Figures 3-4). Following modification of the SDS step, the subsequent five batches of arteries were all successfully decellularised (Figures 5-9).

The data from the analysis of eight batches of arteries subject to decellularisation are presented in Table (8). The means of the controls for both mid and end sections (for each separate batch) were used to calculate the percentage DNA removal. It can be seen that

once the decellularisation process was successful (Run's 4 and onwards), the target DNA removal rate of ≥ 90% was achieved (range 90-99.5%).

Decellularisation Batch	Arterial Portion	H & E	DAPI	Mean DNA content ($\mu g.mg^{-1}$) n=3	% DNA removal
1 (Control artery 1)	End	+	+	0.5	-
1 (Control artery 1)	Mid	+	+	0.38	-
1 (Control artery 2)	End	+	+	1.14	-
1 (Control artery 2)	Mid	+	+	0.57	-
1 (Decell artery 1)	End	+	+	0.72	12.2
1 (Decell artery 1)	Mid	+	+	0.34	28
1 (Decell artery 2)	End	+	+	0.03	97
1 (Decell artery 2)	Mid	+	+	0.87	0
2 (Control artery 1)	End	+	+	0.34	-
2 (Control artery 1)	Mid	+	+	0.29	-
2 (Control artery 2)	End	+	+	0.37	-
2 (Control artery 2)	Mid	+	+	0.37	-
2 (Decell artery 1)	End	+	+	0.44	0
2 (Decell artery 1)	Mid	+	+	0.47	0
2 (Decell artery 2)	End	+	+	0.44	0
2 (Decell artery 3)	End	+	+	0.27	25
2 (Decell artery 4)	End	+	+	0.35	3
3 (Control artery 1)	End	+	+	0.50	-
3 (Control artery 1)	Mid	+	+	0.49	-
3 (Control artery 2)	End	+	+	0.73	-
3 (Control artery 2)	Mid	+	+	0.66	-
3 (Decell artery 1)	End	+	+	1.08	0
3 (Decell artery 1)	Mid	+	+	0.72	0
3 (Decell artery 2)	End	+	+	0.71	0
3 (Decell artery 2)	Mid	+	+	0.66	0
4 (Control artery 1)	End	+	+	0.75	-
4 (Control artery 1)	Mid	+	+	0.64	-
4 (Control artery 2)	End	+	+	0.6	-

4 (Control artery 2)	Mid	+	+	0.7	-
4 (Decell artery 1)	End	-	-	0.06	91
4 (Decell artery 1)	Mid	-	-	0.04	94
4 (Decell artery 2)	End	-	-	0.06	91
4 (Decell artery 2)	Mid	-	-	0.07	90
5 (Control artery 1)	End	+	+	0.74	-
5 (Control artery 1)	Mid	+	+	0.66	-
5 (Control artery 2)	End	+	+	0.59	-
5 (Control artery 2)	Mid	+	+	0.82	-
5 (Decell artery 1)	End	-	-	0.01	98.5
5 (Decell artery 1)	Mid	-	-	0.02	97.3
5 (Decell artery 2)	End	-	-	0.02	97
5 (Decell artery 3)	End	-	-	0.02	97.3
5 (Decell artery 4)	End	-	-	0.01	98.5
5 (Decell artery 5)	End	-	-	0.05	92.5
5 (Decell artery 6)	End	-	-	0.03	95.5
6 (Control artery 1)	End	+	+	0.64	-
6 (Control artery 1)	Mid	+	+	0.34	-
6 (Control artery 2)	End	+	+	0.99	-
6 (Control artery 2)	Mid	+	+	0.86	-
6 (Decell artery 1)	End	-	-	0.03	96.3
6 (Decell artery 1)	Mid	-	-	0.03	95
6 (Decell artery 2)	End	-	-	0.005	99.4
6 (Decell artery 2)	Mid	-	-	0.003	99.5
6 (Decell artery 3)	End	-	-	0.02	97.5
6 (Decell artery 4)	End	-	-	0.02	97.5
6 (Decell artery 5)	End	-	-	0.03	96.3
6 (Decell artery 6)	End	-	-	0.005	99.4
6 (Decell artery 7)	End	-	-	0.03	96.3
7 (Control artery 1)	End	+	+	0.5	-
7 (Control artery 1)	Mid	+	+	0.75	-
7 (Control artery 2)	End	+	+	0.72	-
7 (Control artery 2)	Mid	+	+	0.63	-

7 (Decell artery 1)	End	-	-	0.02	96.7
7 (Decell artery 1)	Mid	-	-	0.01	98.5
7 (Decell artery 2)	End	-	-	0.02	96.7
7 (Decell artery 2)	Mid	-	-	0.004	99.4
7 (Decell artery 3)	End	-	-	0.01	98.3
7 (Decell artery 4)	End	-	-	0.02	96.7
7 (Decell artery 5)	End	-	-	0.02	96.7
7 (Decell artery 6)	End	-	-	0.01	98.3
7 (Decell artery 7)	End	-	-	0.04	93.5
7 (Decell artery 8)	End	-	-	0.04	93.5
7 (Decell artery 9)	End	-	-	0.02	96.7
7 (Decell artery 10)	End	-	-	0.05	92.2
7 (Decell artery 11)	End	-	-	0.04	93.5
7 (Decell artery 12)	End	-	-	0.04	93.5
7 (Decell artery 13)	End	-	-	0.003	99.5
7 (Decell artery 14)	End	-	-	0.04	93.5
7 (Decell artery 15)	End	-	-	0.03	95
7 (Decell artery 16)	End	-	-	0.01	98.3
7 (Decell artery 17)	End	-	-	0.007	98.9
7 (Decell artery 18)	End	-	-	0.02	96.7
7 (Decell artery 19)	End	-	-	0.04	93.5
7 (Decell artery 20)	End	-	-	0.006	99
8 (Control artery 1)	End	+	+	0.62	-
8 (Control artery 1)	Mid	+	+	0.76	-
8 (Control artery 2)	End	+	+	0.59	-
8 (Control artery 2)	Mid	+	+	0.75	-
8 (Decell artery 1)	End	-	-	0.03	95.1
8 (Decell artery 1)	Mid	-	-	0.05	93.5
8 (Decell artery 2)	End	-	-	0.02	96.7
8 (Decell artery 2)	Mid	-	-	0.02	97.4
8 (Decell artery 3)	End	-	-	0.02	96.7
8 (Decell artery 4)	End	-	-	0.05	92
8 (Decell artery 5)	End	-	-	0.03	95

8 (Decell artery 6)	End	-	-	0.03	95
8 (Decell artery 7)	End	-	-	0.04	93.5
8 (Decell artery 8)	End	-	-	0.01	98.4
8 (Decelll artery 9)	End	-	-	0.04	93.5
8 (Decell artery 10)	End	-	-	0.02	97.4
8 (Decell artery 11)	End	-	-	0.03	95
8 (Decell artery 12)	End	-	-	0.04	93.5
8 (Decell artery 13)	End	-	-	0.04	93.5
8 (Decell artery 14)	End	-	-	0.04	93.5
8 (Decell artery 15)	End	-	-	0.03	95
8 (Decell artery 16)	End	-	-	0.05	93.5
8 (Decell artery 17)	End	-	-	0.05	93.5
8 (Decell artery 18)	End	-	-	0.04	93.5
8 (Decell artery 19)	End	-	-	0.03	95
8 (Decell artery 20)	End	-	-	0.03	95
8 (Decell artery 21)	End	-	-	0.03	95
8 (Decell artery 22)	End	-	-	0.05	93.5

Table 8. Characterisation of fresh and decellularised arteries from eight different batches. (+ve = H & E or DAPI staining confirmed presence of cell nuclei; -ve = H & E or DAPI staining confirmed absence of cell nuclei).

3.5.6 Biocompatibility of decellularised porcine carotid arteries

3.5.6.1 Extract biocompatability

Prior to performing the extract biocompatibility assays, extract samples from decellularisation run 5 were plated on agar and incubated to confirm a lack of gross microbial contamination. Following 48 hours incubation, no visible bacterial or fungal growth was seen on the fresh blood agar, heated blood agar, nutrient agar and Sabouraud dextrose plates (Figure 10).

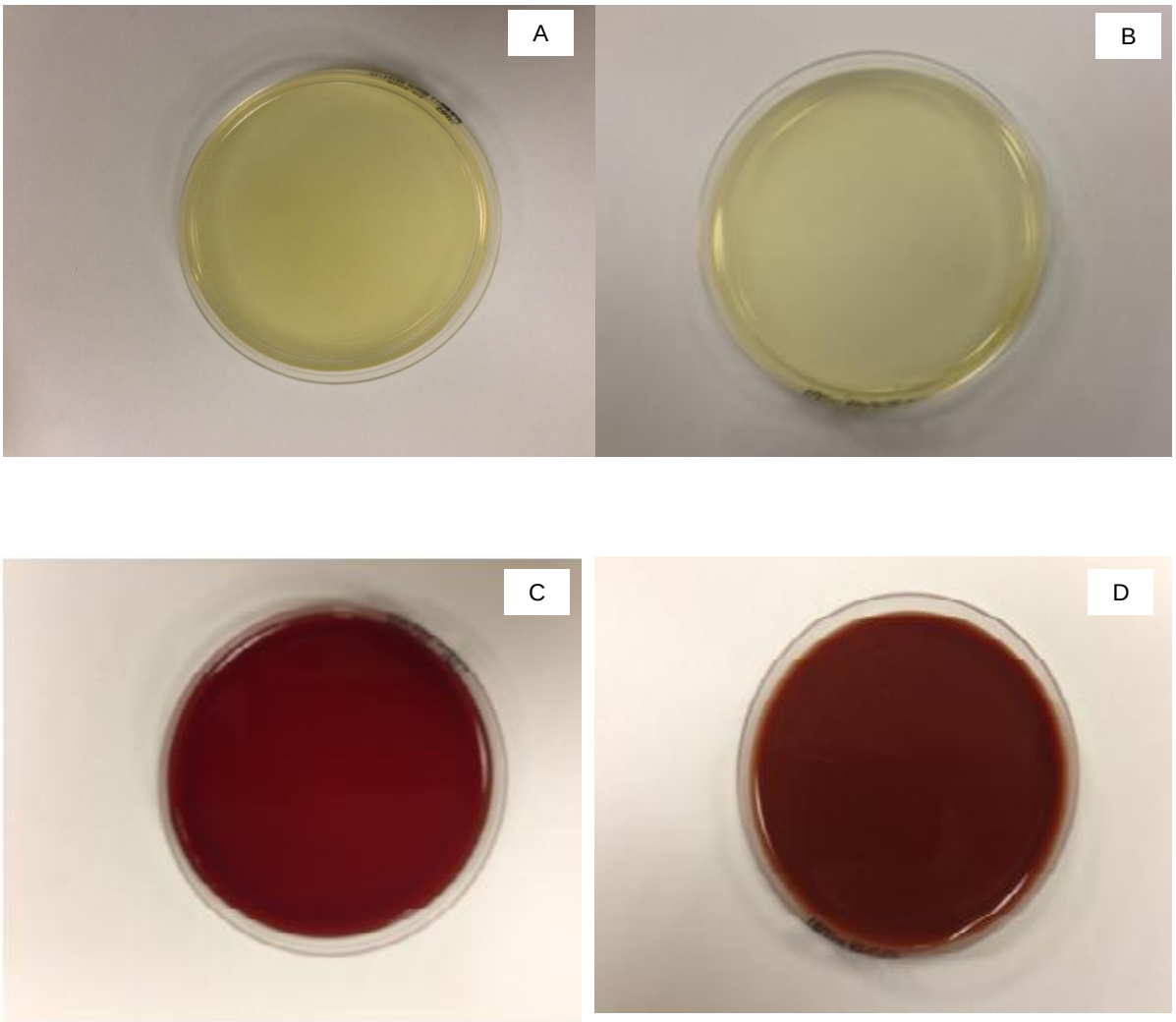

Figure 10. Agar plates with representative samples of decellularised arterial extracts from decellularisation run 5. A**;** Sabouraud dextrose agar, B; Nutrient agar, C; Fresh blood agar, D; Heated blood agar. All plates demonstrated a lack of microbial growth at 48 hours.

The extracts were then tested for their effects on the growth of BHK cells, 3T3 cells and porcine EC and SMC over 48 hours. Cell growth was assessed by ATP assay. No significant difference (one-way ANOVA) was seen in ATP levels (n = 3 replicates [decellularised arteries 1-3]) between the extracts and the negative control (normal cells in cell-specific medium) confirming a lack of cytotoxicity of any soluble components of the arteries to BHK cells, 3T3 cells porcine EC and SMC. Significant differences were seen

with the positive control and medium-only wells compared to the negative control following statistical analysis using one-way ANOVA and post hoc testing (Figures 11-14).

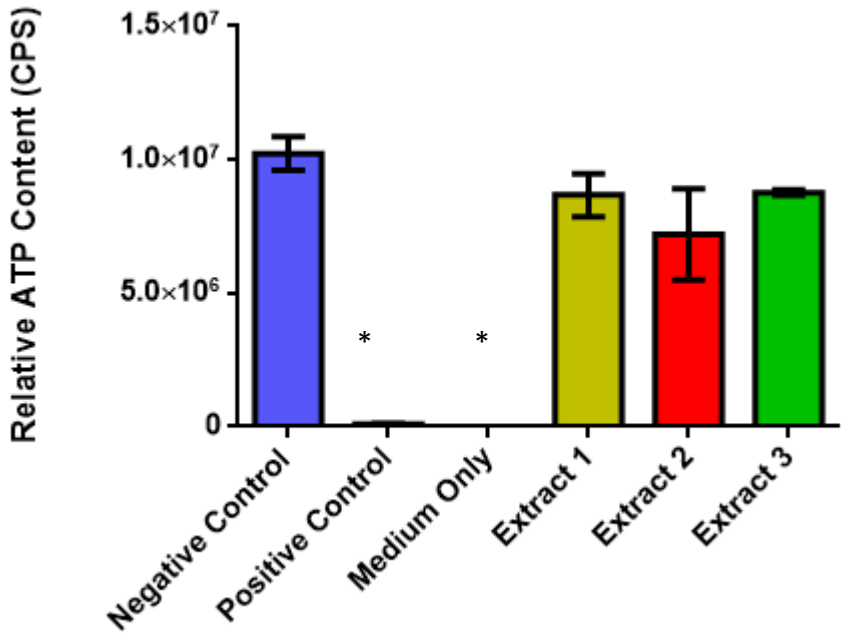

Figure 11. Extract cytotoxicity of decellularised PC arteries to 3T3 cells. Data represents mean values ± 95 % confidence limits (n = 3 replicates). ***** Significantly lower than negative control (one-way ANOVA and post hoc testing $p < 0.05$).

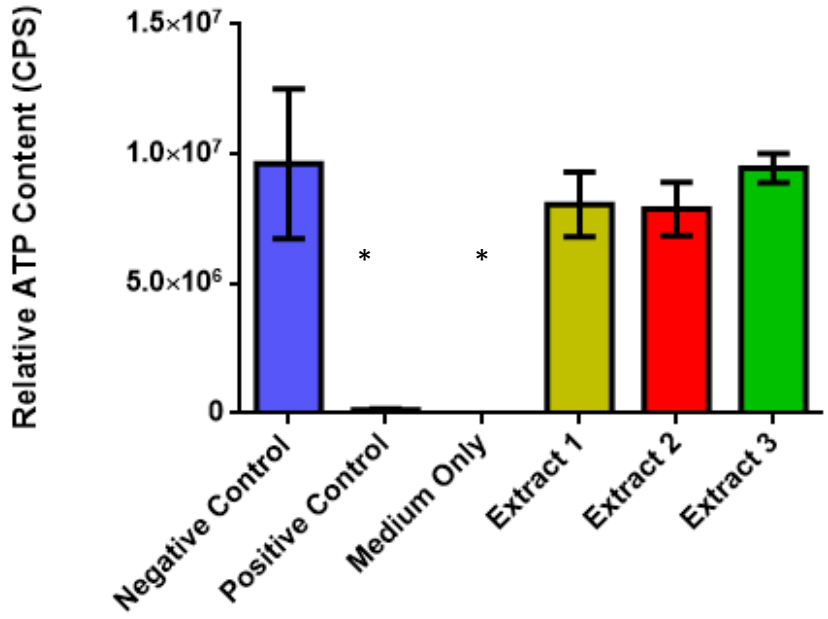

Figure 12. Extract cytotoxicity of decellularised PC arteries to BHK cells. Data represents mean values ± 95 % confidence limits (n = 3 replicates). ***** Significantly lower than negative control (one-way ANOVA and post hoc testing $p < 0.05$).

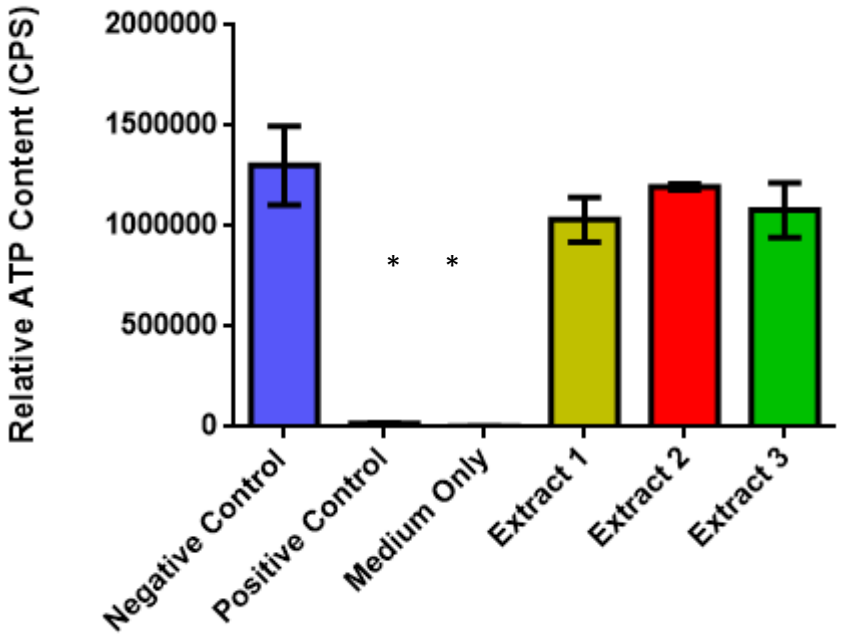

Figure 13. Extract cytotoxicity of decellularised PC arteries to porcine endothelial cells. Data represents mean values ± 95 % confidence limits (n = 3 replicates). ***** Significantly lower than negative control (one-way ANOVA and post hoc testing $p < 0.05$).

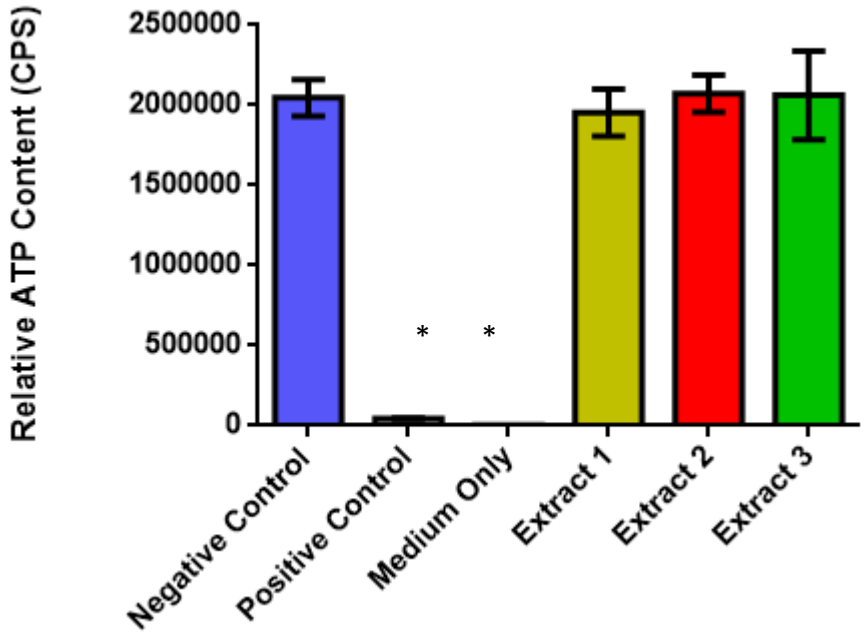

Figure 14. Extract cytotoxicity of decellularised PC arteries to porcine smooth muscle cells. Data represents mean values ± 95 % confidence limits (n = 3 replicates). ***** Significantly lower than negative control (one-way ANOVA and post hoc testing $p < 0.05$).

3.5.6.2 Contact Biocompatability

All contact assays demonstrated clear growth of cells to the arterial edges with no evident change in cellular morphology. The results demonstrated a lack of cytotoxicity of the decellularised arteries to 3T3 cells, BHK cells and porcine EC and SMC (Figures 15-18).

In Figure (15), clear growth is visible to the edge of the artery (B) with retention of the spindle-shaped appearance and size typical of 3T3 monolayers, as seen in photomicrograph A. Confluent growth is visible across collagen gel (C), again demonstrating a spindle-shaped appearance of the cells. No cell growth is visible near cyanoacrylate (D).

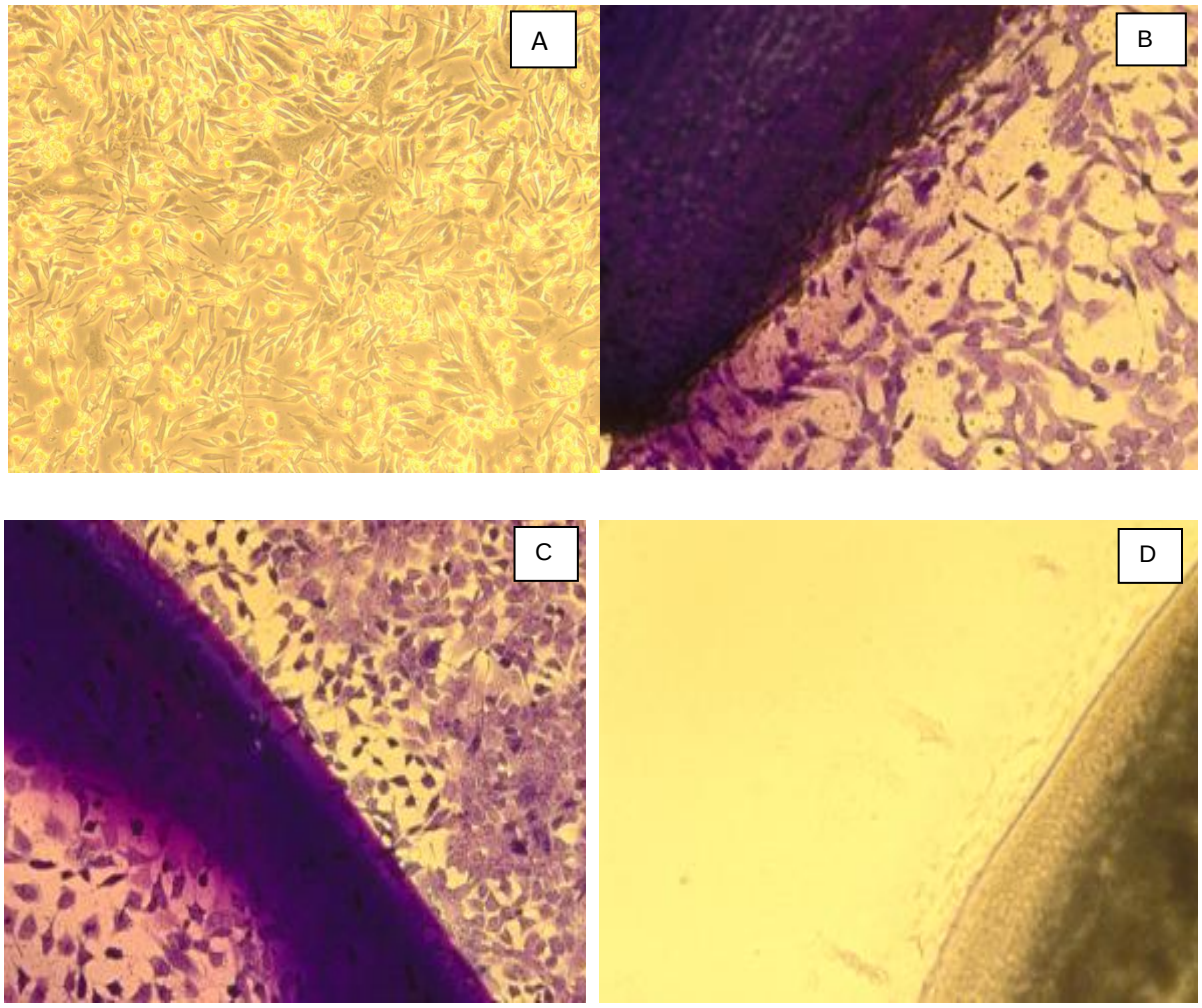

Figure 15. Contact cytotoxicity of decellularised PC arteries to 3T3 cells. A; 3T3 cells in culture demonstrating spindle-shaped morphology, B; Decellularised artery, C; Collagen gel, D; Cyanoacrylate.

In Figure (16), clear growth is visible to the edge of the artery in (B) with retention of the cobblestone appearance and size typical of BHK monolayers as seen in photomicrograph A. Confluent growth is visible across collagen gel (C), again demonstrating a cobblestone appearance of the cells. No cell growth is visible near cyanoacrylate (D).

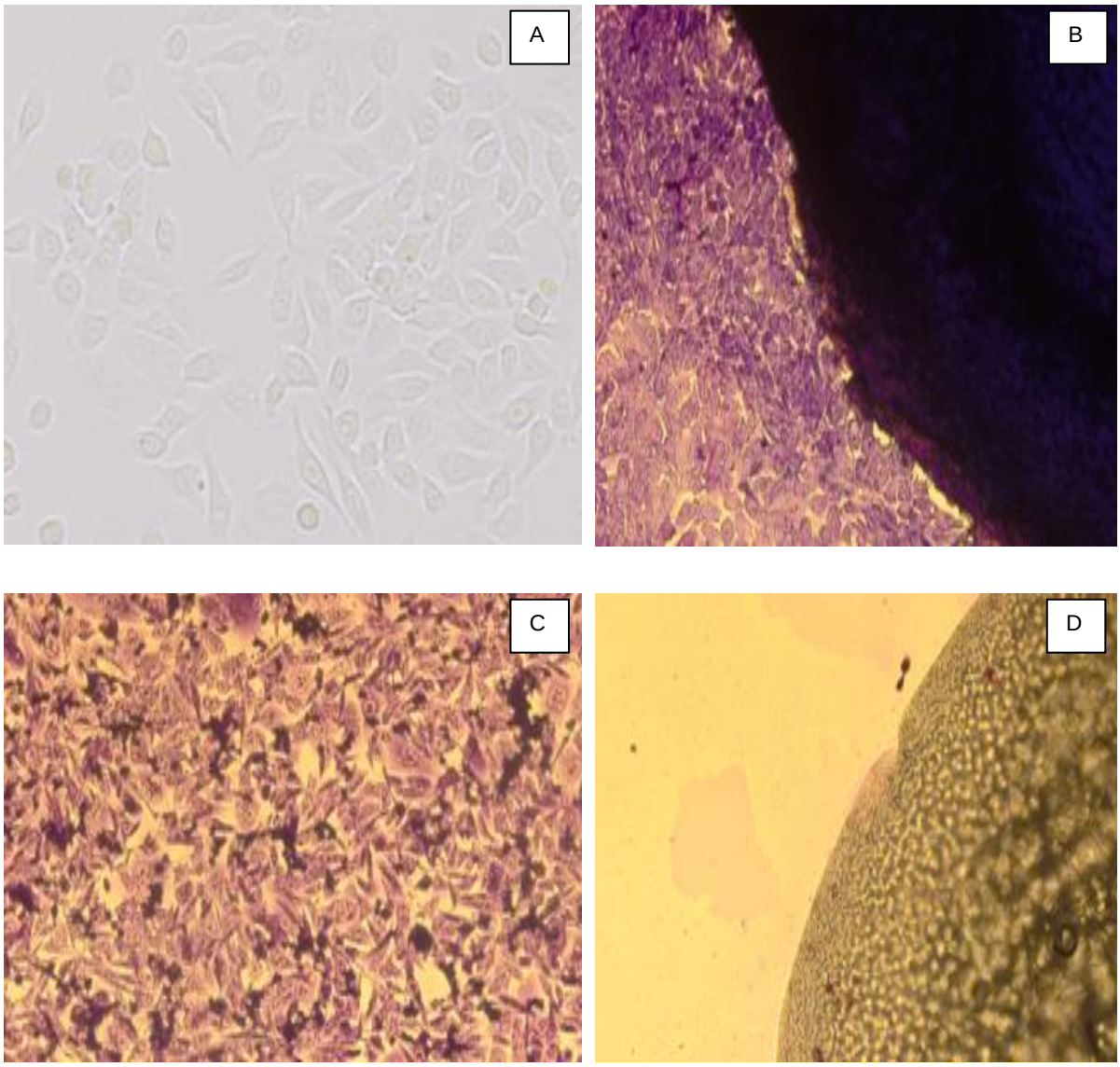

Figure 16. Contact cytotoxicity of decellularised PC arteries to BHK cells. A; BHK cells in culture demonstrating cobblestone appearance, B; Decellularised artery, C; Collagen gel, D; Cyanoacrylate.

In Figure (17), clear growth is visible to the edge of the artery in (B) with retention of the cobblestone appearance and size typical of EC monolayers, as seen in photomicrograph A. Confluent growth is visible across collagen gel (C), again demonstrating a cobblestone appearance of the cells. No cell growth is visible near cyanoacrylate (D).

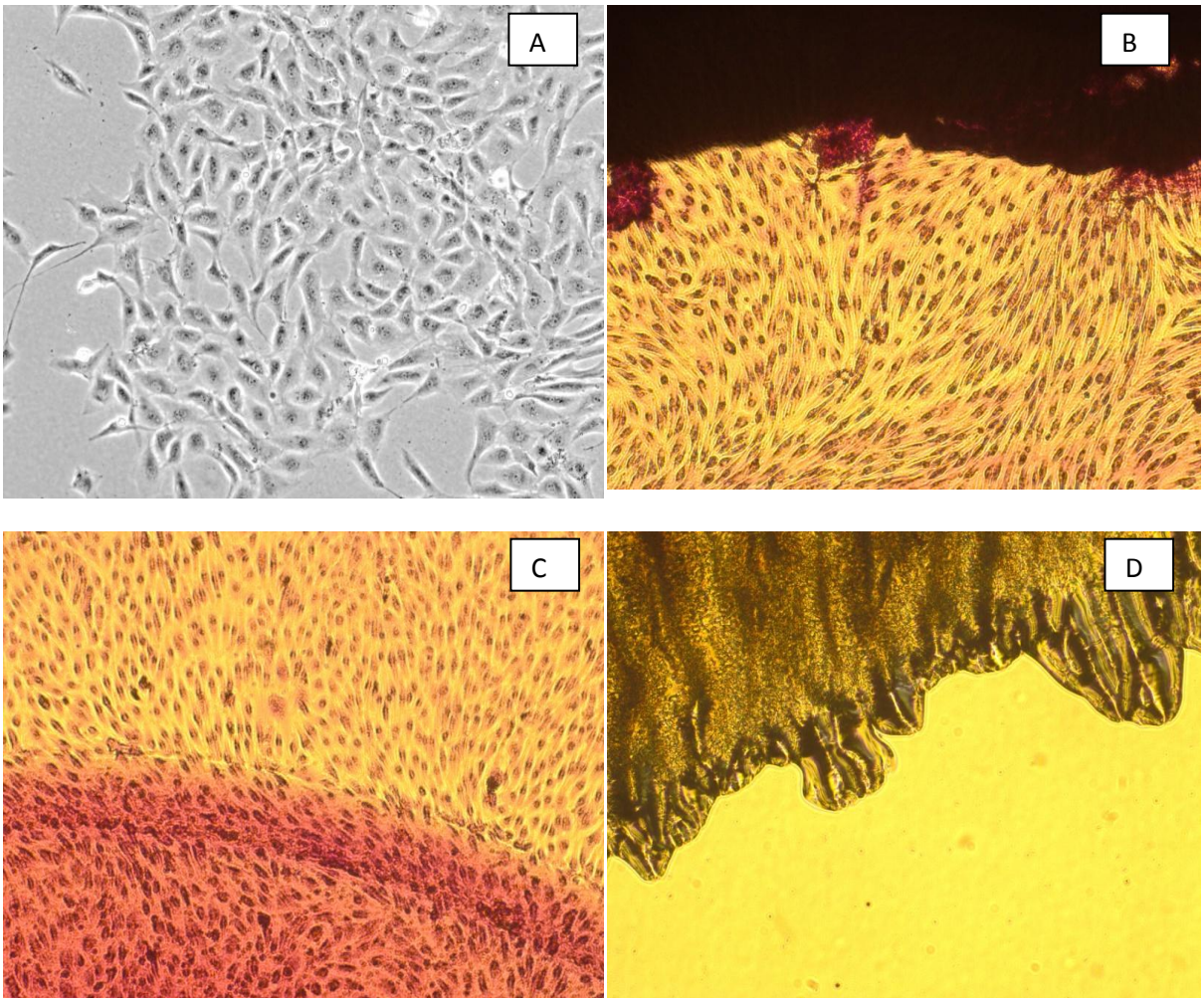

Figure 17. Contact cytotoxicity of decellularised PC arteries to porcine endothelial cells. A; PC EC in culture demonstrating cobblestone appearance, B; Decellularised artery, C; Collagen gel, D; Cyanoacrylate.

In Figure (18), clear growth is visible to the edge of the artery in (B) with retention of the spindle-shaped appearance and size typical of SMC monolayers, as seen in photomicrograph A. Confluent growth is visible across collagen gel (C), again demonstrating a spindle-shaped appearance of the cells. No cell growth is visible near cyanoacrylate (D).

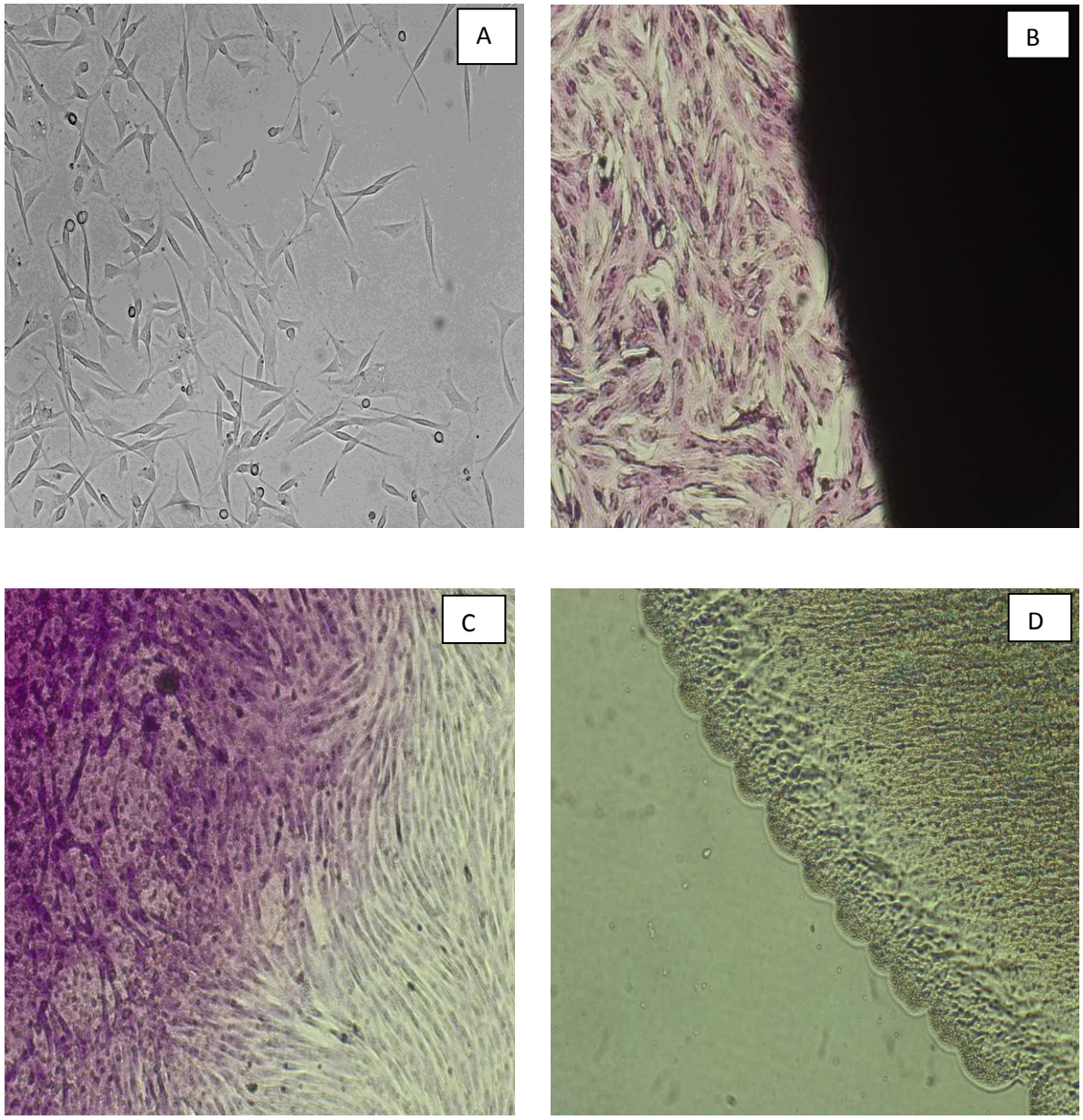

Figure 18. Contact cytotoxicity of decellularised PC arteries to porcine smooth muscle cells. A; Porcine SMC in culture demonstrating spindle-shaped morphology, B; Decellularised artery, C; Collagen gel, D; Cyanoacrylate.

3.6 Discussion

The aim of decellularisation is to remove all cellular and nuclear material from a tissue, whilst, minimising disruption of scaffold architecture and preserving components of the ECM. The technique developed by iMBE involves physical, chemical and enzymatic methods.

After a minor modification in the production of the SDS solution, all subsequent decellularisation runs resulted in acellular scaffolds, confirmed by histological absence of cell nuclei and DNA quantification. A small amount of residual SDS was retained within the ECM following decellularisation and this was responsible for the autofluorescence seen within the scaffolds following DAPI staining. The amount of SDS retained in decellularised tissues is small however and well below cytotoxic levels (Gratzer *et al*., 2006). Histological assessment of the acellular scaffolds also confirmed excellent preservation of the histioarchitecture of the scaffold with a tri-layer structure remaining intact following the decellularisation process. Demonstrating the preservation of the remaining ECM was important for two reasons, firstly, the ECM contains the structural proteins that will give the artery biomechanical strength (e.g. elastin, collagen, laminin). Secondly, an intact ECM is essential for future re-cellularisation of the scaffolds as vascular cells will adhere to the ECM via integrin binding. Integrins are transmembrane glycoproteins found on the surface of cells, the ligands of which include collagen, fibronectin and laminin. They have many functions in addition to mediating cell-ECM binding, they are also important in signal transduction pathways that regulate the migration and proliferation of cells (Kokubo *et al.*, 2007).

Decellularisation of batches 4-8 of arteries resulted in removal rate of 90% or greater porcine DNA levels. Removal of remnant DNA is important for several reasons, most importantly to prevent an innate reaction following implantation into a xenogeneic recipient [ECM components share close sequence homology across species and are therefore immune-tolerated (Gilbert *et al.*, 2006)]. Furthermore, retainment of large fragments of DNA within the scaffold could incite calcification within the scaffold matrix leading to a marked effect on the biomechanical durability and function of the scaffold (Wilshaw *et al.*, 2011). Many decellularisation protocols exist within the literature and most utilise physical, mechanical, osmotic, enzymic and detergent based treatments. The iMBE protocol uses all modalities and has shown effective decellularisation of a number of tissues (Booth *et*

al., 2002, Wilcox *et al.*, 2003, Wilshaw *et a.l*, 2006, Derham *et al.*, 2008), now including porcine carotid artery.

Decellularised scaffolds were assessed for and found to be biocompatible with ISO standard cell lines and primary porcine vascular cells. Porcine cells were used in the assays in addition to cell lines as they could provide initial data on scaffold biocompatibility to primary [vascular] cell lines, and in particular, to the primary vascular cells originating from the pre-treated decellularised scaffold. Ensuring the scaffolds were biocompatible was essential to ensure that the decellularisation process had not inferred any toxicity to the acellular scaffolds.

Chapter 4

Ovine vascular cell characterisation

4.1 Introduction

The importance of an endothelial lining and presence of SMC in providing a TEVG with antithrombotic characteristics and functionality has been discussed in Chapter 1. Given that the decellularised scaffolds are of porcine origin, it was important to attempt cell seeding of the scaffolds with cells from a different species to investigate the biocompatibility of the scaffold to xenogeneic vascular cells. When deciding on a species for testing a vascular scaffold, several important factors must be taken into account. Cost is always important in research, animals such as sheep and pigs are more economical compared to non-human primates and canines. Secondly, for the assessment of thrombogenicity, the haematology and haemodynamics of the species must either be comparable to that of the human circulation or possess key attributes that highlight either limitations or superiority of the vascular scaffold. Sheep have a clotting system that is closer to that of a human when compared to canines and pigs (Konya *et al.*, 2008). They also possess similar systolic and diastolic blood pressures and heart rates (Bianco *et al.*, 2004). The ovine circulation possesses a higher number of platelets with high adhesiveness compared to many species, including human ($3\text{-}8 \times 10^5.ml^{-1}$ vs $2\text{-}5 \times 10^5.ml^{-1}$). Furthermore, the fibrinolytic system in sheep is less pronounced than human. The net effect of these differences is that the ovine circulation is more coaguable than the human circulation (Gross, 1994; Bianco *et al*., 2004). This fact is important when assessing the antithrombogenic attributes of a vascular graft following implantation, as if indeed the scaffold does display antithrombogenic efficacy in a hypercoaguable circulation, it may be predicted to do so in a lesser coaguable system i.e. human.

Very little work has been performed on the characterisation of ovine vascular cells in the literature. Almost all research has involved the use of primary antibodies to specific cell

markers. Furthermore, many of the antibodies are manufactured for reactivity to epitopes expressed in humans and other species, and cross-reactivity to ovine cells is often unknown. In reviewing the literature available for ovine cell characterisation, unsurprisingly, anti-VWF was the most commonly used antibody to identify EC in view of its specificity. For SMC, anti-SMC α-actin was the most commonly used antibody (Abdi *et al.*, 1995; Grooby *et al.*, 1997; Afting *et al.*, 2003; Zhao *et al.*, 2010).

Other markers that have been used successfully for vascular ovine cell characterisation are listed below in Table (9).

Cell marker	Function	Antibody (Ab)	Authors
Smooth Muscle Myosin Heavy Chain (MHC-B)	Biomarker for SMC proliferation	_	Hutanu *et al.*, 2007
VCAM-1 (CD31)	Vascular cell adhesion	Mouse anti-human Ab to VCAM-1 (IgG1)	Grooby *et al.*, 1997
P-selectin (CD62P)	Vascular cell adhesion	Mouse anti-human Ab to P-Selectin (IgG1)	Grooby *et al.*, 1997
CD29 (Integrin β1 subunit)	Cell adhesion molecule	Anti-CD29 Mouse IgG	Grooby *et al.*, 1997

Table 9. Antibodies that have shown specificity for ovine vascular cells in the literature (SMC=smooth muscle cell, VCAM= vascular cell adhesion molecule, Ab= antibody, Ig= Immunoglobulin, CD = cluster of differentiation).

Morphological appearances have also been used for EC characterisation. EC at confluence are often described as being ‘cobblestone’ in appearance (Abdi *et al.*, 1995; Grooby *et al.*, 1997; Ovine fibroblasts commonly contaminate EC populations, however they can be differentiated from EC by their elongated shape and swirling growth pattern (Grooby *et al.*, 1997). Based on research in the literature, antibody stocks and traditional EC and SMC markers known for humans, characterisation was performed using indirect immunofluorescence to identify antibodies that could be used to confirm correct cell phenotype (Blann *et al*, 2003; Orrico *et al.*, 2010).

4.2 Aims and Objectives

The aim of this chapter was to determine the phenotype of isolated ovine vascular cells using indirect immunofluorescence. The objectives were:

1) To isolate ovine vascular cells (EC and SMC) from ovine superficial femoral arteries

2) To develop a protocol to phenotype ovine EC and SMC.

3) To determine and ensure the purity of harvested ovine cells.

4) To investigate the biocompatibility of the decellularised PC arteries to ovine vascular cells

4.3 Materials and Methods

All equipment, reagents, materials and solutions used in the study are listed in Chapter 2. Three separate characterisation experiments using ovine vascular cells were performed in the study.

4.3.1 Tissue procurement and preparation

Four fresh ovine hind-legs (male, Texel breed, aged approximately ten months) were delivered by a local abattoir (John Penny & Sons, Leeds, UK) immediately following slaughter. The superficial femoral artery from each leg was harvested using sterile dissecting instruments within a class II safety cabinet to minimise contamination. Once excised, the arteries were placed immediately into sterile DPBSa to wash away any adherent clot or tissue debris. Arteries were then incubated in antibiotic solution (DPBSa, streptomycin 300 $U.ml^{-1}$, 300 $U.ml^{-1}$ penicillin) at 37°C for two hours. Four arteries in total were used during the study.

Ovine vascular cells were isolated twice using the techniques described in Section 2.8. Figure (19) demonstrates the appearance of the isolated ovine vascular cells in culture. Photomicrograph A demonstrates the typical cobblestone monolayer appearance of EC in

culture. Photomicrograph B demonstrates the typical spindle-shaped appearance of SMC in culture.

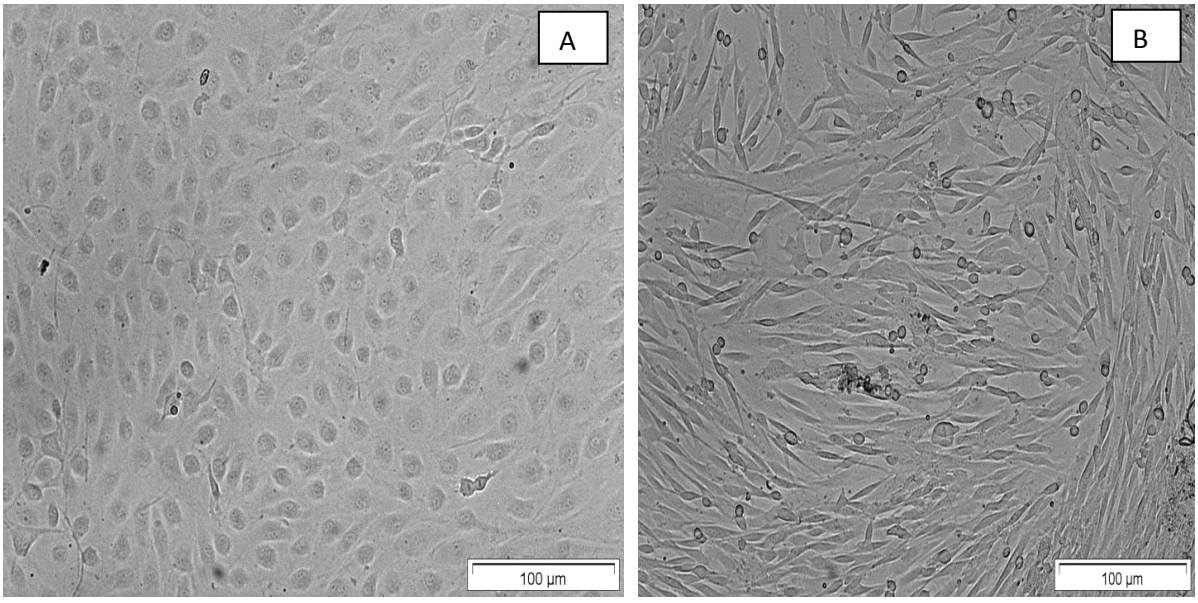

Figure 19. Photomicrographs of isolated ovine EC and SMC in culture. A; Ovine EC in culture. B; Ovine SMC in culture

4.3.2 Characterisation of ovine vascular cells using indirect immunofluoresence

Details of all reagents used in the study can be found in Chapter 2, Section 2.2.

Multi-spot glass slides were cleaned with 70% (v/v) ethanol, covered in foil and then sterilised using dry heat. Confluent ovine SMC and EC were then harvested and centrifuged to obtain a cell pellet. The cells were then suspended in 1ml of medium with 20 µl of the resulting cell suspension of each being subcultured onto the surface of each spot of the glass slide. Slides were then incubated for 48 hours at 37°C in 5% (v/v) CO_2 in air using the appropriate culture medium for each cell type. After incubation, the culture medium was aspirated and the cells were fixed in acetone: methanol (1:1) for one minute. After being left to air dry for five minutes, the slides were then washed gently in running tap water for ten minutes. Following this, the slides were then washed in tris buffered saline (TBS) for five minutes. After washing, the cells were then ready to receive the primary or isotype control antibodies. Prior to adding antibody, each specific primary antibody was diluted to its working concentration using antibody diluent. Once the correct concentration

for each antibody was achieved, 20 µl of primary antibody solution was carefully placed onto each spot (see Table [10] and [11] for antibodies used with concentrations). Slides were then incubated in the dark, in a moist environment, at room temperature, for one hour. Following incubation, slides were washed twice for ten minutes in TBS-Tween using agitation at 40 rpm. Following this, slides were washed twice for ten minutes in TBS using agitation at 40 rpm. Following the washes, the fluorescently labelled secondary antibodies against the primary antibodies were diluted to their working concentration using antibody diluents (see Table [12] for secondary antibodies used). Once the correct concentration for each antibody was achieved, 20 µl of fluorescently labelled antibody solution was carefully placed onto each spot. Slides were then incubated in the dark, in a moist environment, at room temperature, for thirty minutes. Following incubation, slides were washed twice for ten minutes in TBS-Tween using agitation at 40 rpm. Following this, slides were washed twice for ten minutes in TBS using agitation at 40 rpm. Following washes, the slides were then placed into 200 ml of DAPI dye buffer to counterstain the cells. The slides were incubated with the DAPI dye buffer for ten minutes in the dark. Following incubation, each slide was washed three times in DPBSa for ten minutes, again in the dark. After washing, slides were mounted with a glass cover slip using DABCO: glycerol mountant. Slides were then viewed as soon as possible using an upright fluorescent microscope and a DAPI filter. Images were captured in black and white using a digital camera. Image- Pro Plus v 5.1. software was then used to colour anti-actin and anti-myosin antibody staining red and all other antibodies green. The primary and secondary antibodies used in the characterisation of ovine cells from ovine vascular cell isolation run one and two are shown in Table's (10-12).

Antigen	Type	Isotype	Dilution	Positive Control tissue
CD31	Mouse anti-human	IgG1κ	1:20	Porcine EC
VWF	Rabbit anti-human	Polyclonal	1:200	Porcine EC
α-Smooth Muscle Actin	Mouse (PAN) antibody	IgG1	1:400	Porcine SMC
Smooth Muscle Myosin (Heavy Chain)	Mouse anti- human	IgG1	1:100	Porcine SMC
Isotype Control	Mouse	IgG1	1:20	-

Table 10. Details of primary antibodies used in the characterisation of cells from isolation run one (CD= cluster of differentiation, Ig= immunoglobulin, EC= endothelial cell, SMC= smooth muscle cell, VWF= von Willebrand factor).

Antigen	Type	Isotype	Dilution	+ve control tissue
CD31: FITC	Mouse anti-sheep	IgG2	1:10	Ovine EC
VWF	Rabbit anti-human	Polyclonal	1:200	Porcine EC
α-Smooth Muscle Actin	Mouse (PAN) antibody	IgG2	1:400	Porcine SMC
Smooth Muscle Myosin (Heavy Chain)	Mouse anti- human	IgG1	1:100	Porcine SMC
Isotype Control	Mouse	IgG1	1:20	-
Isotype Control	Mouse	IgG2	1:20	-

Table 11. Details of primary antibodies used in the characterisation of cells from isolation run two (CD= cluster of differentiation, FITC= fluorescein isothiocyanate, Ig= immunoglobulin, EC= endothelial cell, SMC= smooth muscle cell, VWF= von Willebrand factor).

Type	Conjugate	Isotype	Dilution
Goat anti-mouse: FITC	Alexa Fluor 488	IgG	1:200
Goat anti-rabbit: FITC	Alexa Fluor 488	IgG	1:200

Table 12. Details of secondary antibodies used in all characterisation runs (Ig= immunoglobulin).

4.3.3 Purification of ovine vascular cells using magnetic bead separation

All methods were performed using full aseptic precautions in a class II safety cabinet.

Ovine EC and SMC were placed into suspension using techniques described in Section 2.7. Two sets of magnetic beads and one antibody were used: Anti-Sheep CD31: FITC antibody, Anti-FITC Microbeads and Anti-Fibroblast Microbeads. As characterisation demonstrated mixed ovine SMC and EC, an Anti-Sheep CD31: FITC antibody and Anti-FITC microbead was used to separate these two cell types. In addition, an Anti-Fibroblast microbead was used to deplete any fibroblasts contained within the cultures as they are known to commonly contaminate harvested vascular cell populations.

4.3.4 Fibroblast depletion of ovine SMC and ovine EC

A buffer solution was prepared containing DPBSa, EDTA 2.7 mM and 0.5% (w/v) BSA. Ovine cells were diluted to a final density of 1 x 10^5 cells.ml^{-1} in cell-specific medium within a sterile universal. The cell suspension was then centrifuged for ten minutes at 100 xg. Supernatant was then discarded. The cell pellet was then resuspended in 80 µl of buffer solution. Next, 20 µl of Anti-Fibroblast Microbeads were added to the cell suspension and incubated for 30 minutes at room temperature. Cells were then washed by adding 1 ml of buffer and centrifuged at 100 x g for ten minutes. Supernatant was discarded and the cell pellet was then resuspended in 1 ml of buffer. The cell suspension was then loaded into a MACS® MS column which had been pre-washed with buffer and placed onto a magnetic MiniMACS® separator. The suspension was then passed through the MACS® MS column and MiniMACS® separator with the (unlabelled, ovine vascular cell) effluent being collected below in a sterile bijou. For purity, the process was repeated three times using a separate MACS® MS column each time. Immediately following separation, the cells were placed into T75 flasks containing 10 ml of cell-specific medium and placed into culture until subconfluent. Flasks were examined to confirm cell growth.

4.3.5 Purification of ovine SMC and ovine EC

A buffer solution was prepared containing DPBSa, EDTA 2.7 mM and 0.5% BSA. Ovine cells were diluted to a final density of 1 x 10^5 cells.ml^{-1} in cell-specific medium within a sterile universal. The cell suspension was then centrifuged for ten minutes at 100 x g. Cells were then resuspended in 300 µl of buffer. A 1:10 dilution of Anti-Sheep CD31:FITC Microbeads was made using the buffer solution. Then 10µl of Anti-Sheep CD31:FITC Microbeads / 100 µl cell suspension was added to the cell suspension (100 µl of cell suspension= 30 µl of Anti-Sheep CD31:FITC Microbeads) and incubated in the dark at room temperature for 30 minutes. Cells were then washed by adding 2 ml of buffer and centrifuged at 300 x g for ten minutes to remove unbound Anti-Sheep CD31:FITC antibody. Supernatant was then discarded and the cell pellet was then resuspended in 270 µl of buffer. Next, 30 µl of Anti-FITC Microbeads was added to the cell suspension and incubated at 4°C for 15 minutes on an orbital shaker. Following incubation, cells were washed by adding 2 ml of buffer and centrifuging at 300 x g for 10 minutes. Supernatent was then discarded and the cell pellet was resuspended in 500 µl buffer.

To isolate ovine SMC, the SMC cell suspension was loaded into a MACS® MS column which had been pre-washed with buffer and placed onto a magnetic MiniMACS® separator. The suspension was then passed through the MACS® MS column and MiniMACS® Seperator with the (unlabelled, ovine SMC) effluent being collected below in a sterile bijou. For purity, the process was repeated three times using a separate MACS® MS column each time. Immediately following separation, the cells were then placed into a T75 flask containing 10 ml of SMC medium and placed into culture until subconfluent. Flasks were examined to confirm cell growth.

To isolate ovine EC, the EC cell suspension was loaded into a MACS® MS column which had been pre-washed with buffer and placed onto a magnetic MiniMACS® separator. The suspension was then passed through the MACS® MS column and MiniMACS® separator with the effluent (containing any potential ovine SMC) being discarded. The MACS® MS column (containing labeled ovine EC) was rinsed with 2 ml of EC culture medium three times to wash the isolated EC into a sterile universal. The EC cell suspension (6 ml) was placed into a T75 flask containing 4 ml of EC medium and placed into culture. Flasks were examined to confirm cell growth.

4.3.6 Biocompatibility of porcine carotid arteries to ovine vascular cells

Contact and extract cytotoxicity assays were performed once pure isolates of ovine SMC (P=4) and EC (P=4) were confirmed. The techniques used were identical to those described in Sections 3.4.4.1-3.4.4.2.

4.4 Results

4.4.1 Ovine vascular cell characterisation from cell isolation run one

For the characterisation of isolated ovine cells from the first run, antibodies currently in laboratory stock were used to assess for any cross-reactivity to the sheep cells. The primary and secondary antibodies used in the characterisation of ovine cells from isolation run one are shown in Table's (10) and (12).

Figures (20-21) show a lack of reactivity of ovine SMC's to conventional EC markers (anti-CD31 and anti-VWF antibodies). Ovine EC demonstrated reactivity with anti-VWF antibody only. Positive staining to both markers in the positive controls (porcine EC) was seen. VWF was not expressed uniformly at all times by the Weibal-Palade bodies within EC, hence the scattered but characteristic positive staining pattern. No staining was seen in

the isotype control confirming lack of reactivity of the secondary antibody with the ovine vascular SMC.

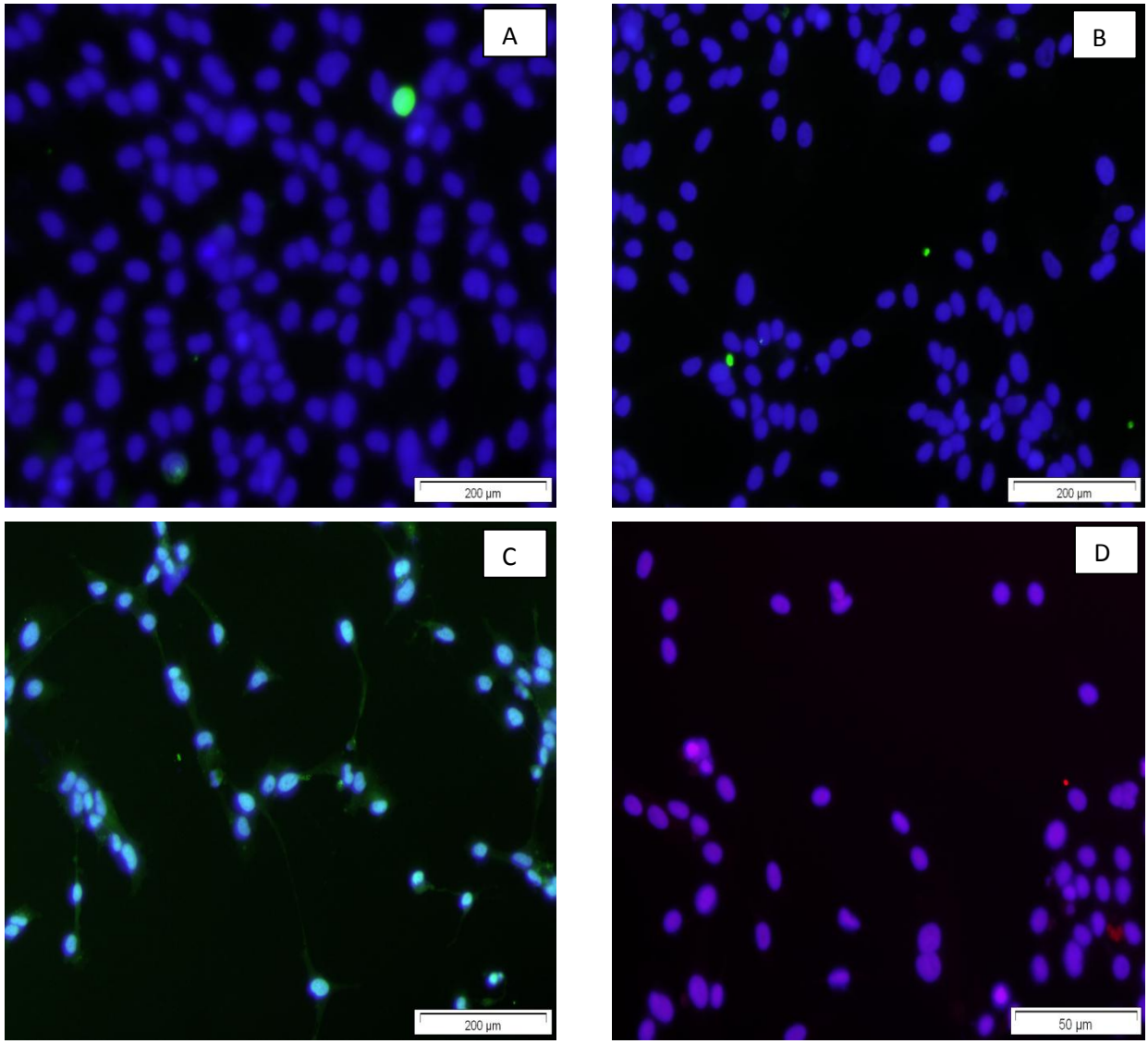

Figure 20. Indirect immunofluorescent antibody labelling with anti-CD31 antibody. A; Negative ovine SMC staining with anti- CD31, B; Negative ovine EC staining with anti-CD31, C; Positive staining of porcine EC with anti-CD31, D; Isotype control.

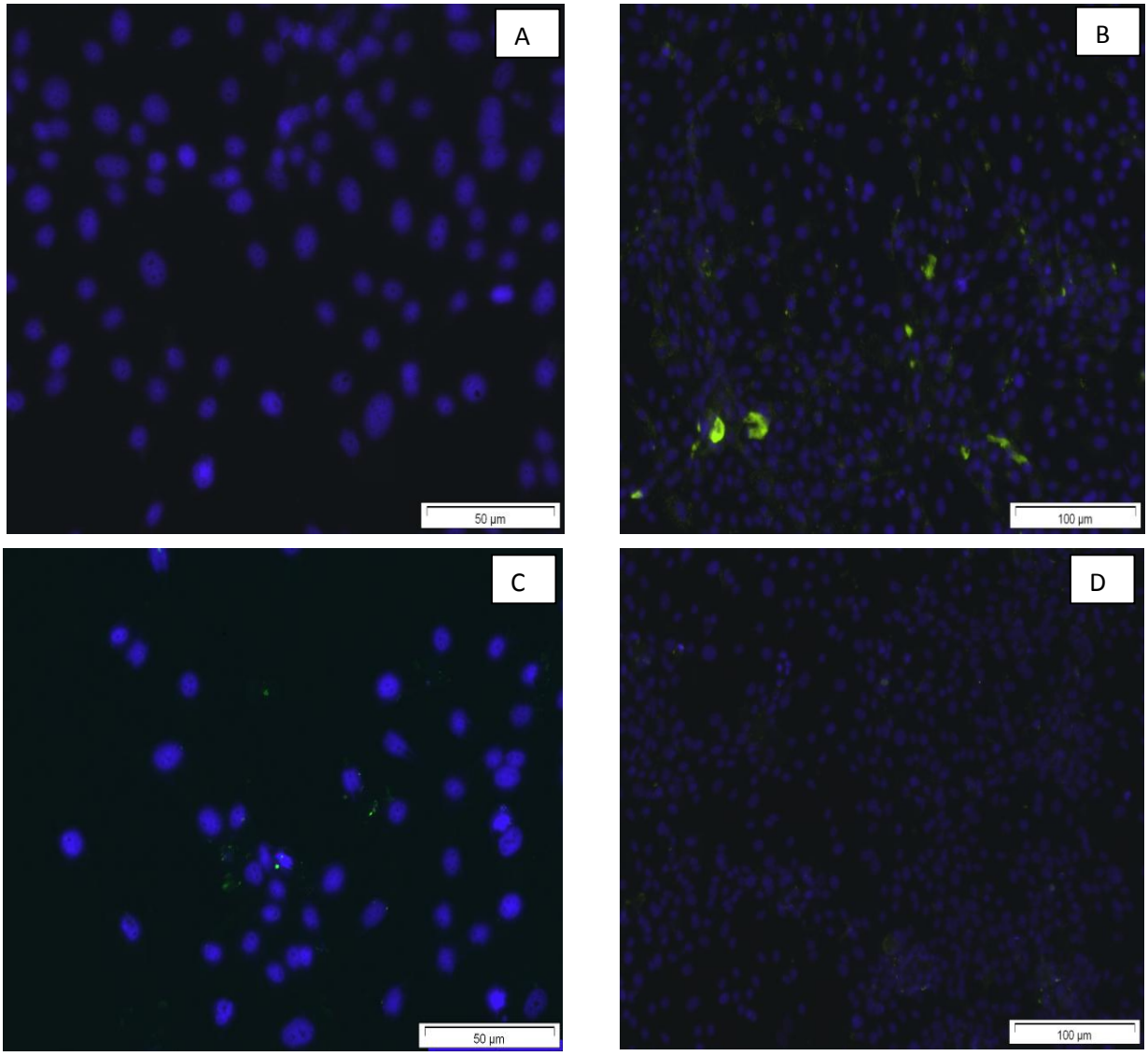

Figure 21. Indirect immunofluorescent labeling with anti-VWF antibody. A; Negative ovine SMC staining with anti- VWF, B; Positive ovine EC staining with anti-VWF, C; Positive staining of porcine EC with anti-VWF, D; Isotype control.

Figures (22-23) show reactivity of ovine SMC's and the positive controls (porcine SMC) to conventional SMC markers [anti-SMC α-actin and anti-SMC Myosin (Heavy Chain) antibodies]. Negative staining to both markers was seen for ovine EC. No staining was seen in the isotype control confirming specific binding of antibody.

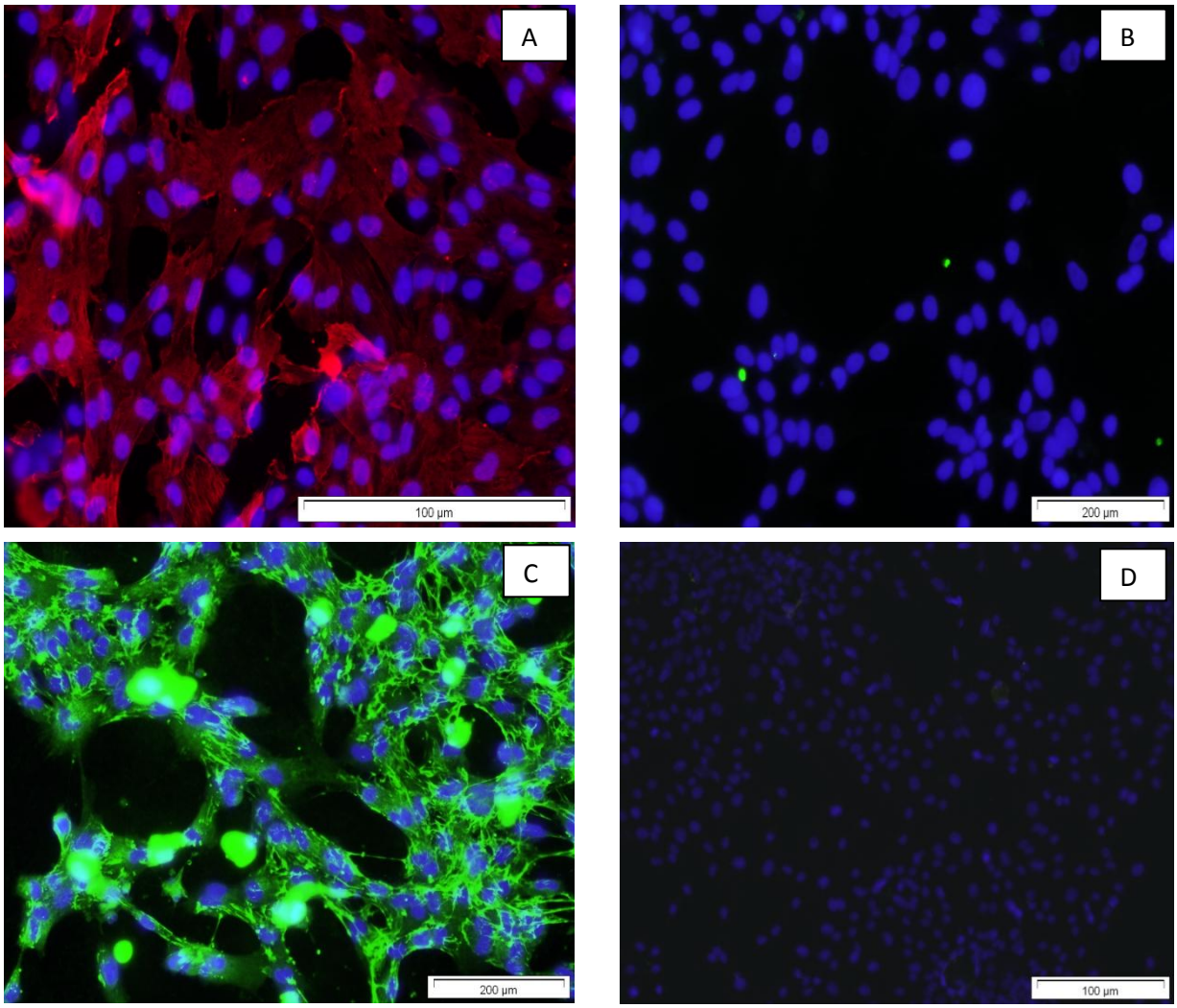

Figure 22. Indirect immunofluorescent antibody labelling with anti-SMC α-actin antibody. A; Positive ovine SMC staining with anti-SMC α-actin antibody, B; Negative ovine EC staining with anti-SMC α-actin antibody, C; Positive porcine SMC staining with anti-SMC α-actin, D; Isotype control.

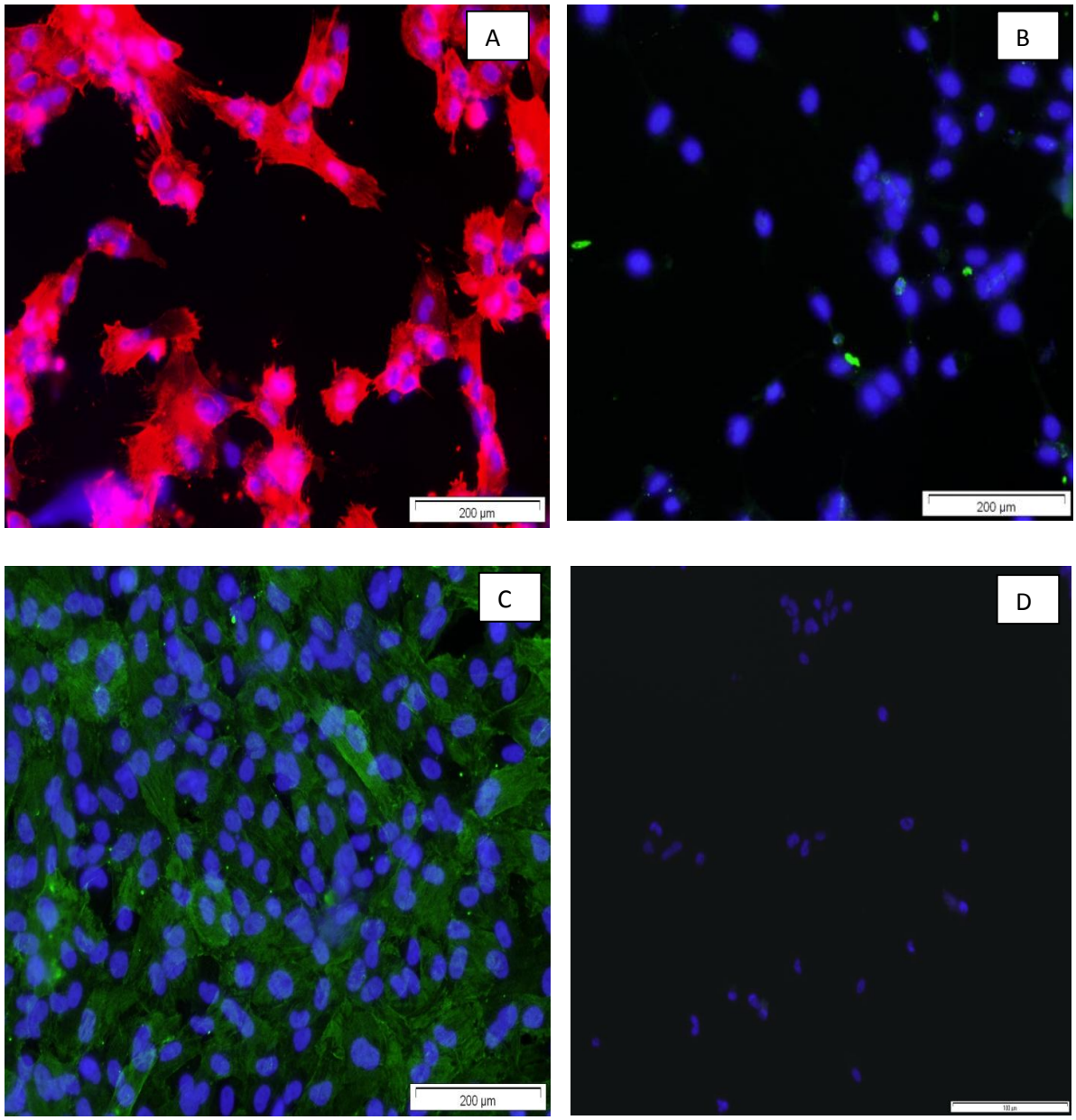

Figure 23. Indirect immunofluorescent antibody labelling with anti-SMC Myosin (Heavy Chain) antibody. A; Positive ovine SMC staining with anti-SMC Myosin (Heavy Chain) antibody, B; Negative ovine EC staining with anti-SMC Myosin (Heavy Chain) antibody, C; Positive porcine SMC staining with anti-SMC Myosin (Heavy Chain) antibody, D; Isotype control.

Results from the first characterisation experiments demonstrated that isolated cells showed positivity to traditional vascular cell markers e.g VWF for EC and actin and myosin

for SMC. Anti-CD31 did not cross react with ovine EC and this was not completely unexpected as the antibody data-sheet did not confirm goat or sheep cross-reactivity with the antibody. A second isolation run of ovine vascular cells was performed to confirm the isolation techniques were reproducible and to assess further primary antibodies for cross reactivity to ovine vascular cells in an attempt to demonstrate more robust confirmation of vascular cell phenotype.

4.4.2 Ovine vascular cell characterisation from cell isolation run two

An ovine specific anti-CD31 antibody was purchased and used to characterise the phenotype of isolated ovine EC. Figure (24) demonstrates confluent staining of ovine EC to anti-CD31 antibody. No staining was seen for the isotype control confirming specific binding of primary antibody.

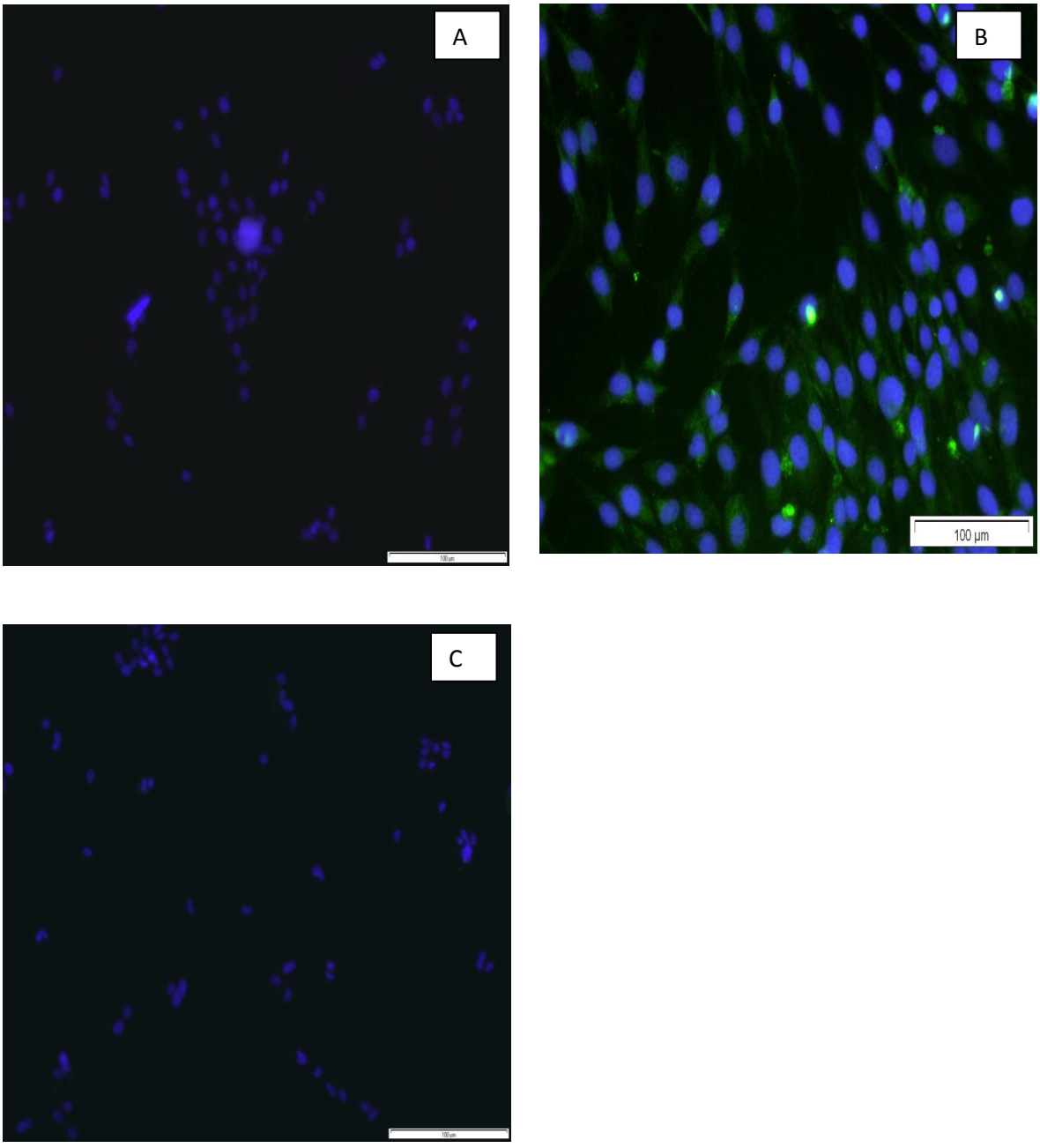

Figure 24. Direct Immunofluorescent antibody labelling with anti-sheep-CD31 antibody. A; Negative ovine SMC staining with antisheep-CD31 antibody, B; Positive ovine EC staining with antisheep-CD31 antibody, C; Isotype control.

Ovine SMC's once again demonstrated reactivity to anti-SMC α-actin and anti-SMC myosin (Heavy Chain) antibodies as in run one (Figures 25 and 27).

Figure (26) however demonstrated some positivity of the ovine EC isolates to anti-SMC myosin (Heavy Chain) antibody. As the results from both run one and two had confirmed specificity of the antibody for ovine SMC, the positive staining seen in this experiment was likely due to the presence of ovine SMC's within the EC isolates confirming a mixed population of cells.

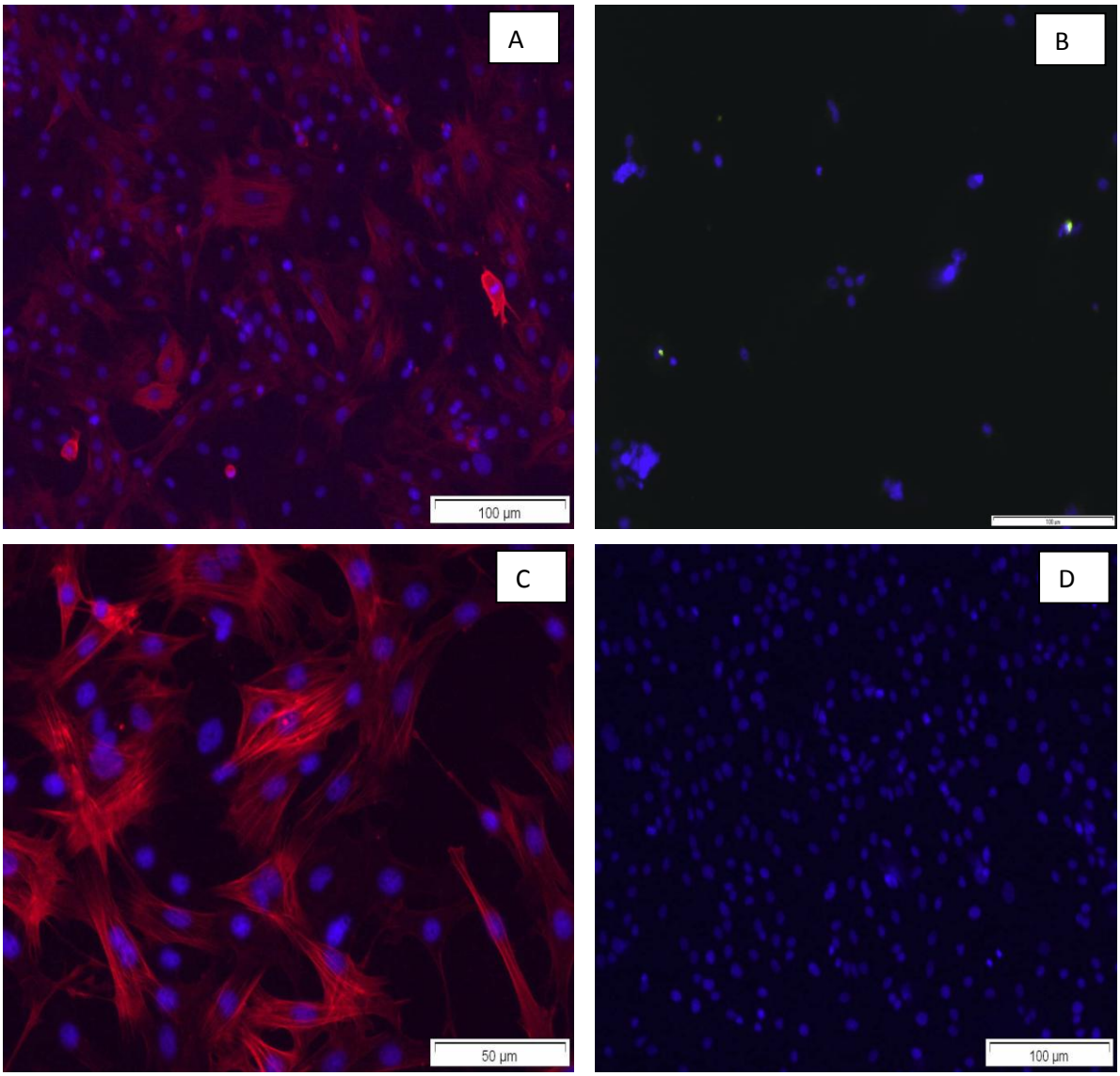

Figure 25. Indirect immunofluorescent antibody labelling with anti-SMC myosin (Heavy Chain) antibody. A; Positive ovine SMC staining with anti-SMC myosin (Heavy Chain) antibody, B; Negative ovine EC staining with anti-SMC myosin (Heavy Chain) antibody, C; Positive porcine SMC staining with anti-SMC myosin (Heavy Chain) antibody, D; Isotype control. No staining is seen confirming specific binding of primary antibody.

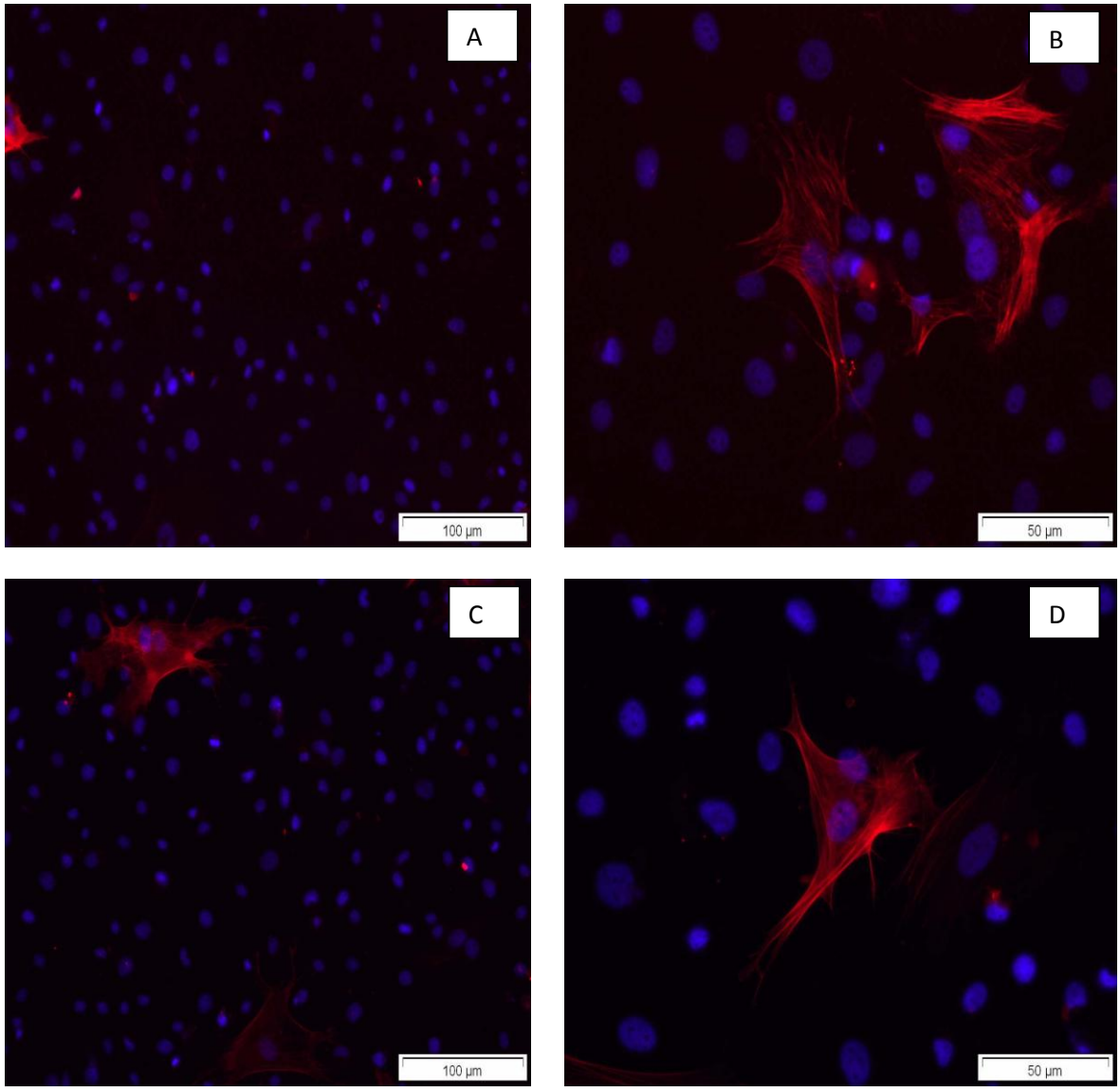

Figure 26. Indirect immunofluorescent antibody labelling with anti-SMC myosin (Heavy Chain) antibody labeling against ovine EC. Photomicrographs A-D all demonstrate negative staining of antibody for ovine EC but demonstrate positive staining of ovine SMC confirming a mixed population of both ovine EC and SMC.

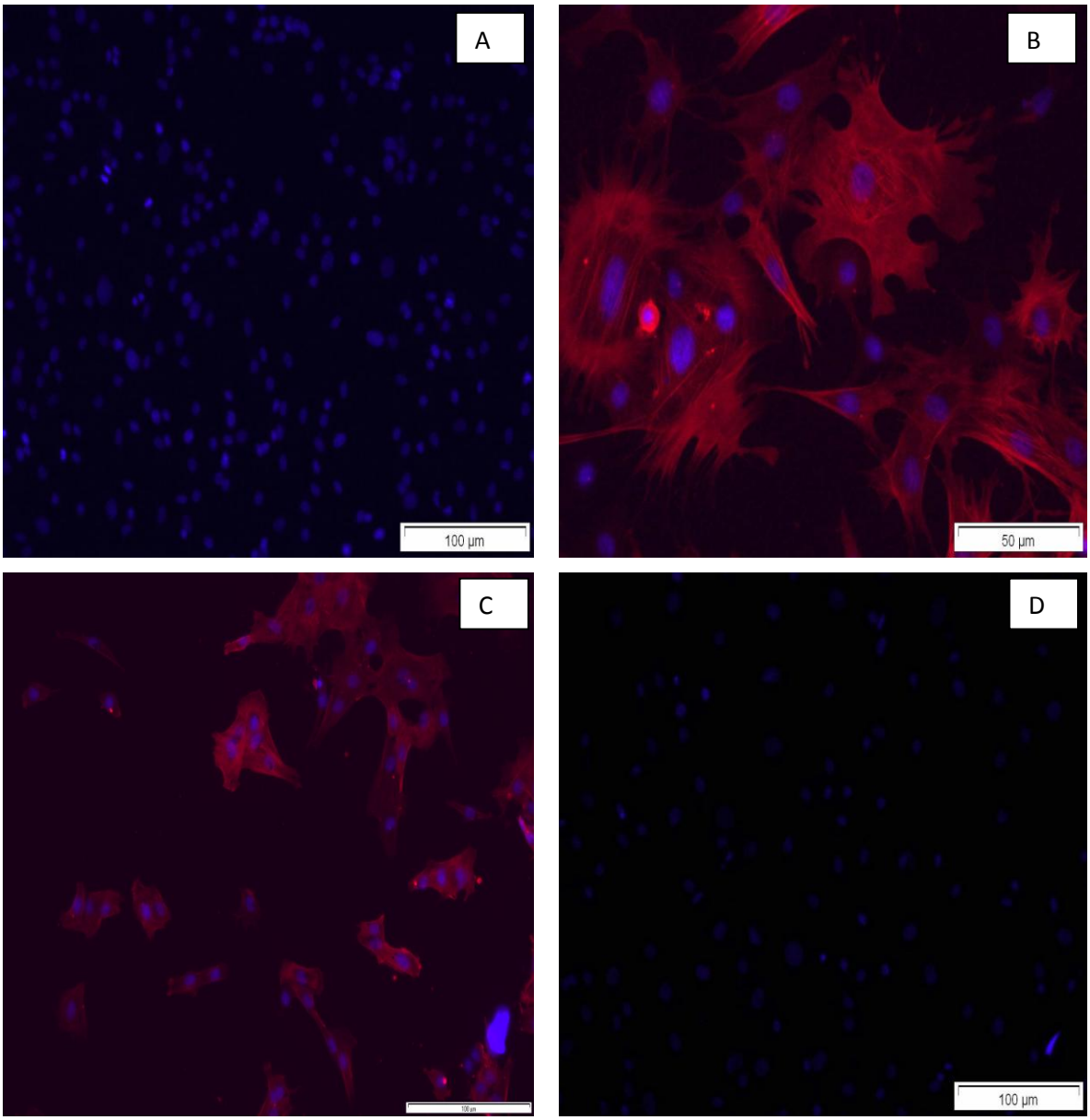

Figure 27. Indirect immunofluorescent antibody labelling with anti-SMC α-actin antibody. A; Negative ovine EC staining with anti-SMC α-actin antibody, B; Positive ovine SMC staining with anti-SMC α-actin antibody, C; Positive porcine SMC staining with anti-SMC α-actin, D; Isotype control. No staining is seen confirming specific binding of primary antibody.

Using antibodies that had been successfully used to identify ovine vascular cells in the literature and antibodies available in laboratory stock, a successful characterisation protocol was developed to identify both ovine SMC and EC. The results from cell isolation run two (the cells of which were for storage in liquid nitrogen for future studies) confirmed mixed cell populations. In an attempt to achieve pure cell isolates, it was decided to isolate cells using magnetic beads with bound (cell-specific) ligand and then re-characterise the cells using indirect immunofluoresence. Briefly, this involved incubating (ovine vascular) cell suspensions with magnetic beads bound with ligand and then passing the suspension through a magnetic column. This lead to either retention or depletion of a specific cell type based on the bound ligand. A more detailed description of magnetic bead separation is described in Section 4.3.3.

4.4.3 Characterisation of ovine vascular cells following magnetic bead purification

To assess whether magnetic bead separation had achieved pure cell isolates, cells were examined in culture for typical cellular morphology and underwent characterisation using immunofluoresence.

As shown in Figure (28), separated ovine SMC successfully grew in culture (the typical spindle shaped monolayer appearance of SMC in culture was clearly evident).

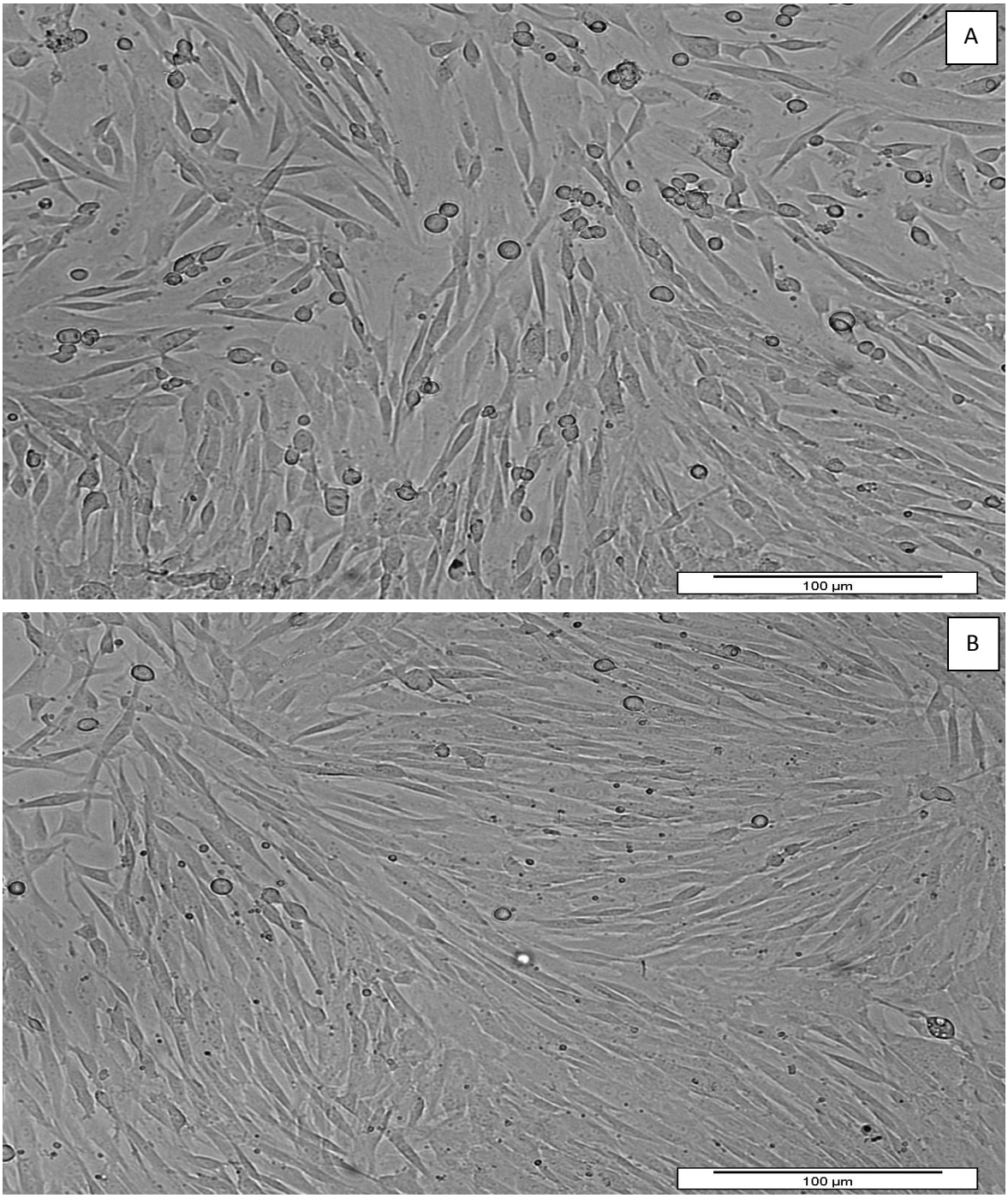

Figure 28. Magnetic-bead separated ovine SMC in culture displaying typical morphological (spindle shaped) appearances.

Unfortunately, despite two attempts of magnetic bead separation, separated EC failed to survive in culture. This was either as a result of experimental error or toxicity to one of the reagents used in the experiments. The photomicrographs in Figure (29) clearly show a lack of cell adherence to the flask surface with dead cells visible within the medium.

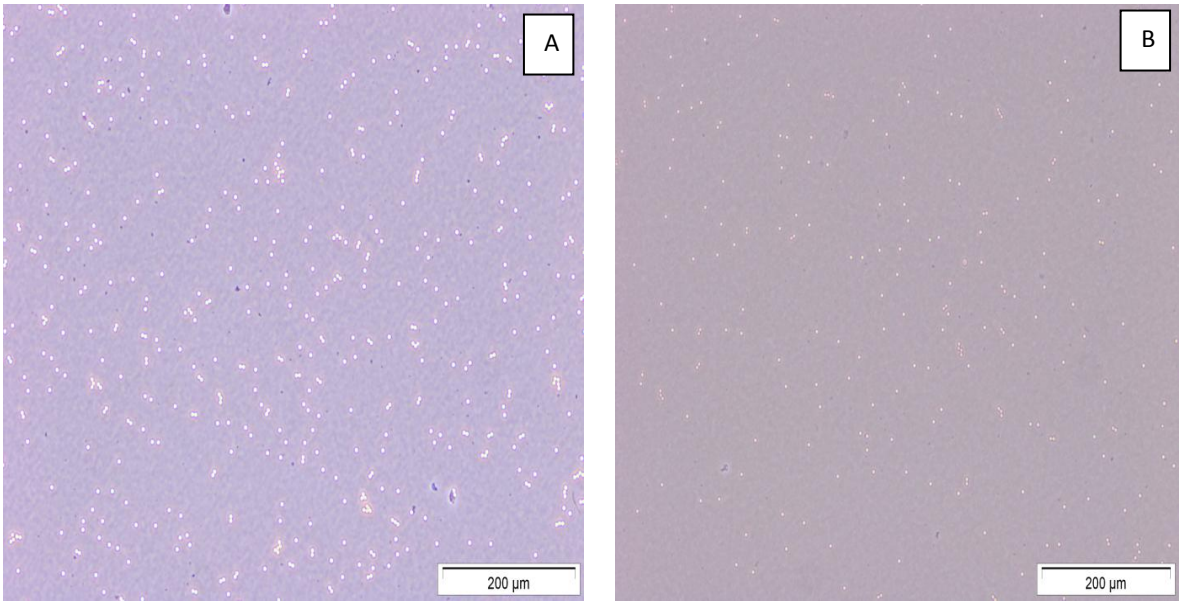

Figure 29. Appearance of ovine EC following 48 hours in culture post magnetic-bead separation. A; Ovine cells in culture following the first magnetic-bead separation. B; Ovine cells in culture following the second magnetic-bead separation.

4.4.4 Characterisation of gifted ovine vascular cells

To expedite progress of the study, a fellow (PhD) student within IMBE (Mr Robert Guilliatt), kindly gifted cultures of harvested pure isolates of ovine EC (P=4). To confirm pure isolates, gifted EC were scrutinised in the same manner as SMC, namely by morphological examination of cells in culture and by indirect immunofluoresence. The typical 'cobblestone' monolayer appearances of the gifted ovine EC is shown in Figure (30).

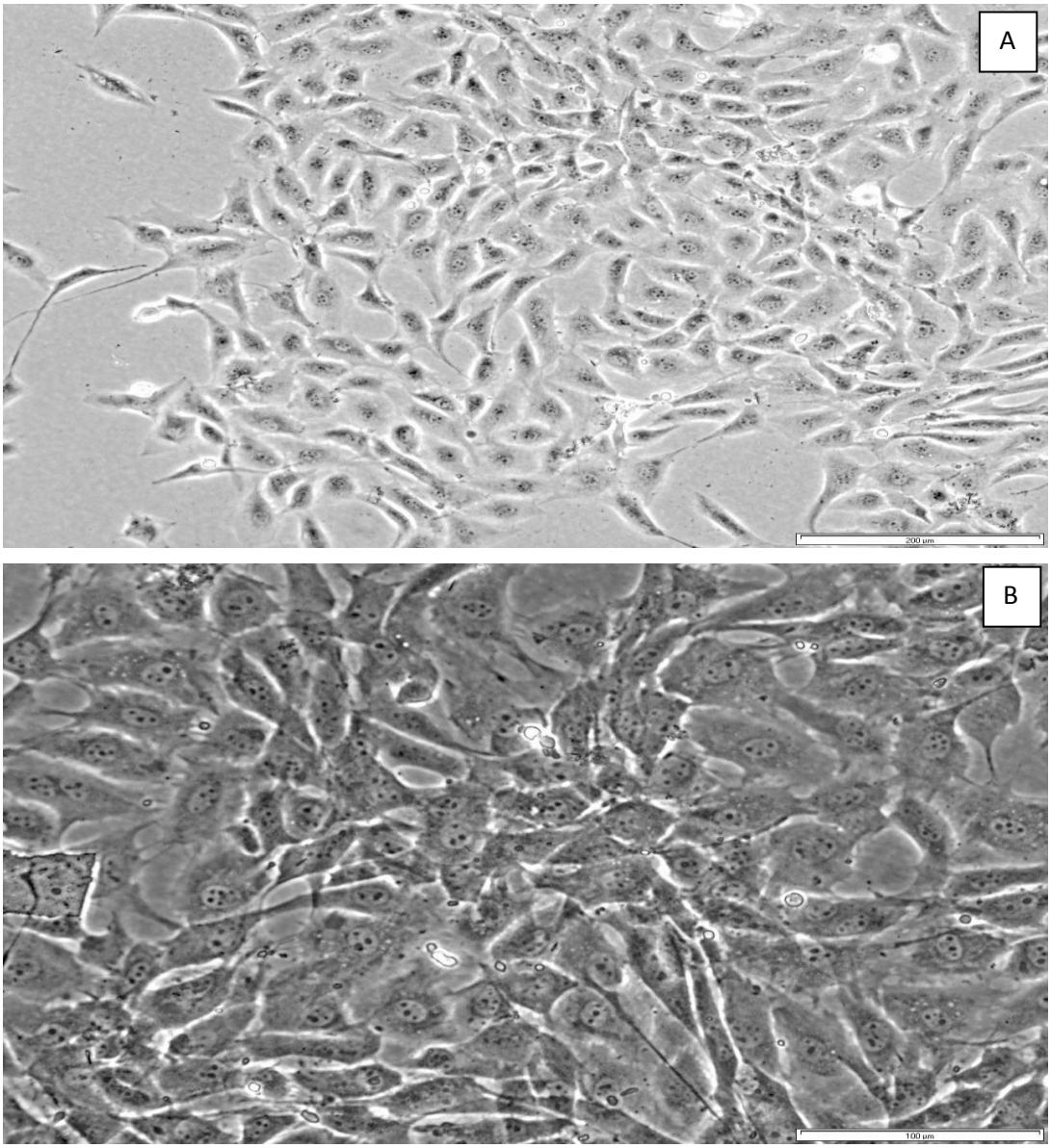

Figure 30. Gifted ovine EC in culture displaying typical (cobblestone) morphological appearances.

As the appearances of both SMC and EC displayed typical morphological appearances for their cell type, the cells then underwent characterisation using immunofluoresence to known reactive primary antibodies.

Figures (31) demonstrates confluent staining of gifted ovine EC to anti-sheep CD31 antibody. Figure (32) demonstrates clear, positive staining of the Weibal-Palade bodies present within EC to anti-VWF antibody. Both markers specific for EC demonstrated

positivity thereby confirming the phenotype of gifted cells to be those of EC origin. No staining was seen in the isotype controls, confirming specific binding of primary antibody.

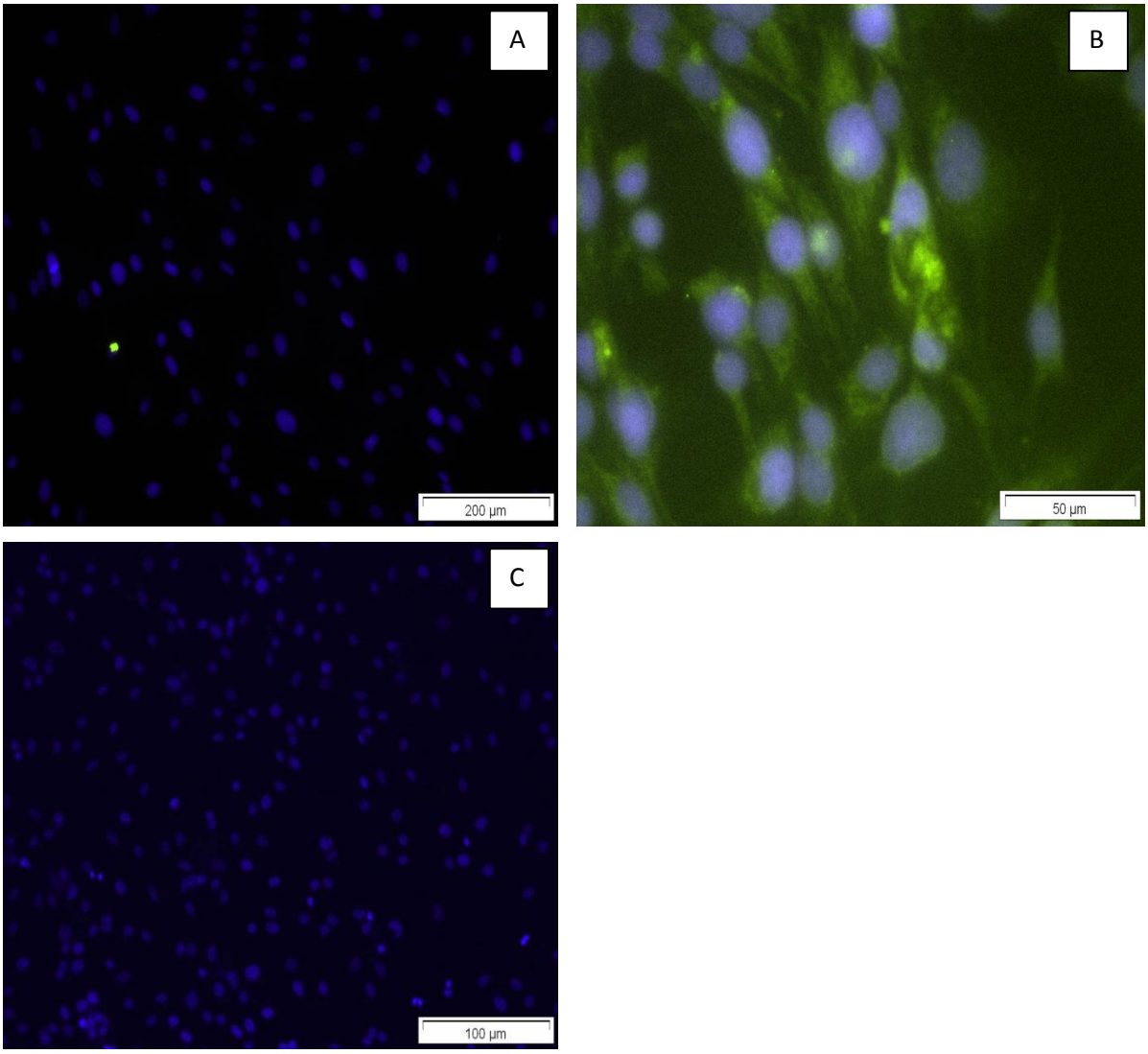

Figure 31. Direct immunofluorescent antibody labelling with antisheep-CD31 antibody. A; Negative ovine SMC staining with antisheep-CD31 antibody, B; Positive ovine EC staining with antisheep-CD31 antibody, C; Isotype control.

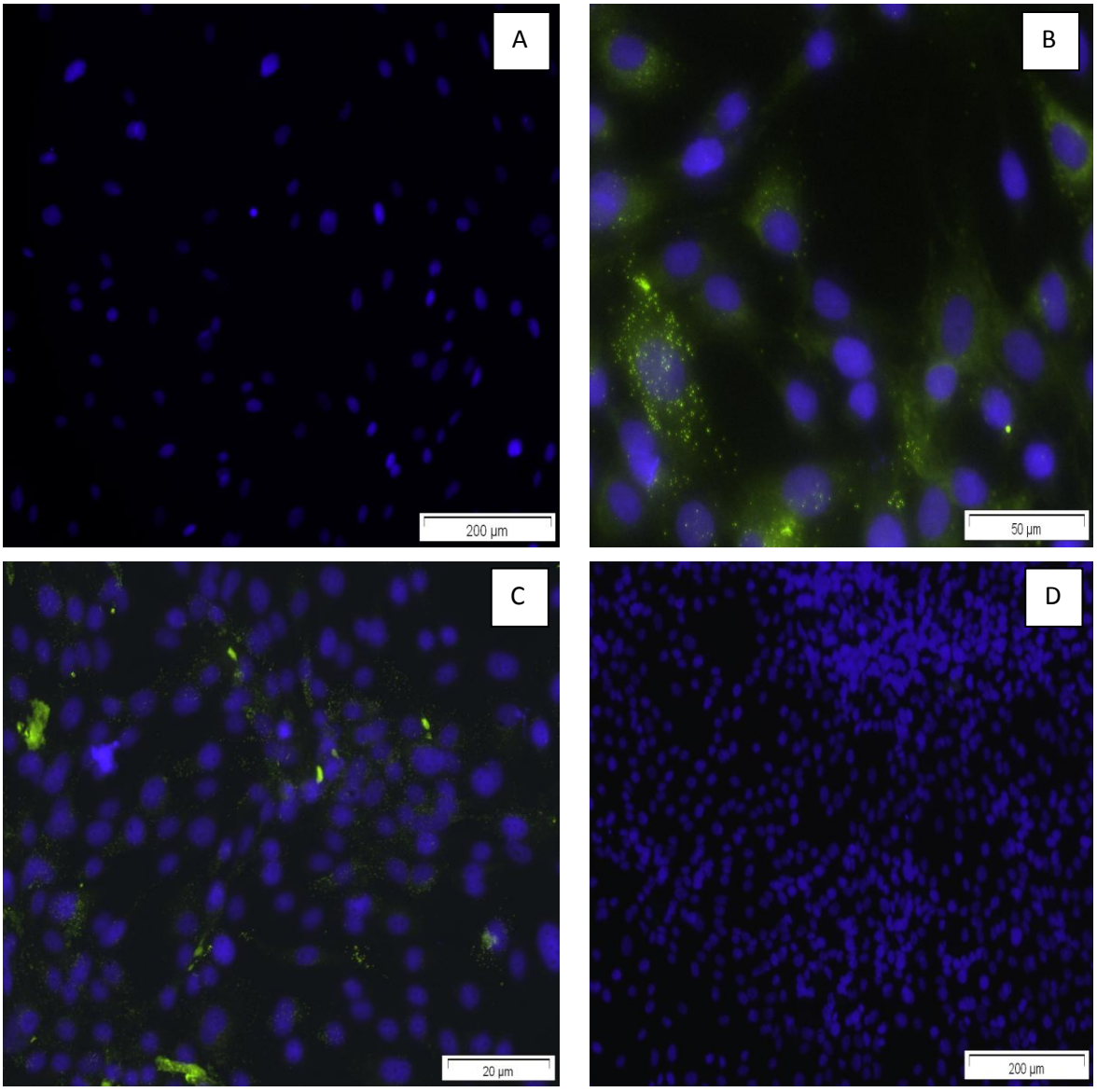

Figure 32. Indirect immunofluorescent antibody labelling with anti-VWF antibody. A; Negative ovine SMC staining with anti- VWF, B; Positive ovine EC staining with anti-VWF. C; Positive staining of porcine EC with anti-VWF, D; Isotype control.

Figures (33-34) again show reactivity of ovine SMC's and the positive controls (porcine SMC) to conventional SMC markers [anti-SMC α-actin and anti-SMC Myosin (Heavy Chain) antibodies]. Negative staining to both markers was seen in the ovine EC

populations confirming the presence of pure cell isolates. No staining was seen in the isotype control confirming specific binding of antibody.

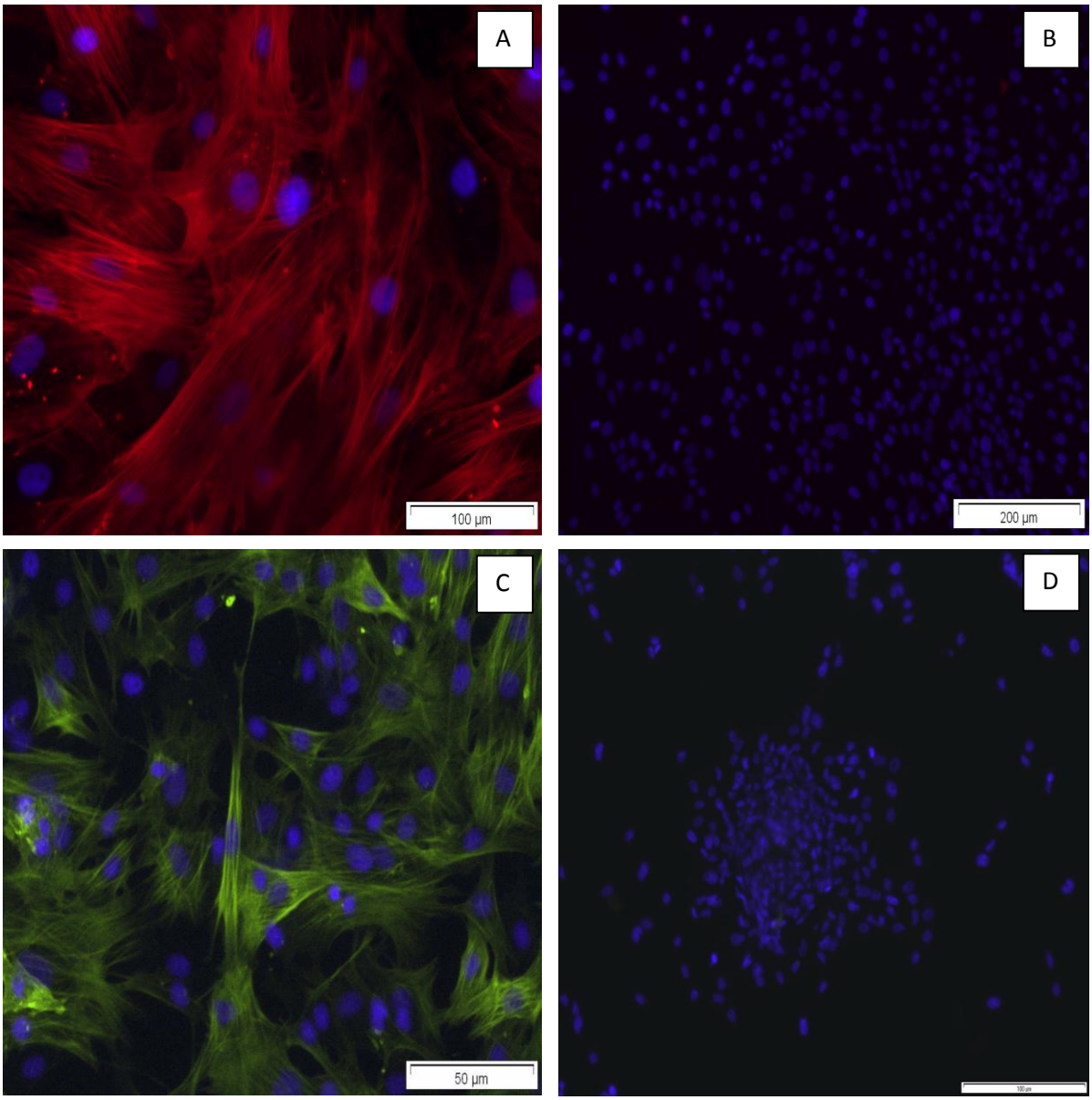

Figure 33. Indirect immunofluorescent antibody labelling with anti-SMC α-actin antibody. A; Positive ovine SMC staining with anti-SMC α-actin antibody, B; Negative ovine EC staining with anti-SMC α-actin antibody, C; Positive porcine SMC staining with anti-SMC α-actin, D; Isotype control.

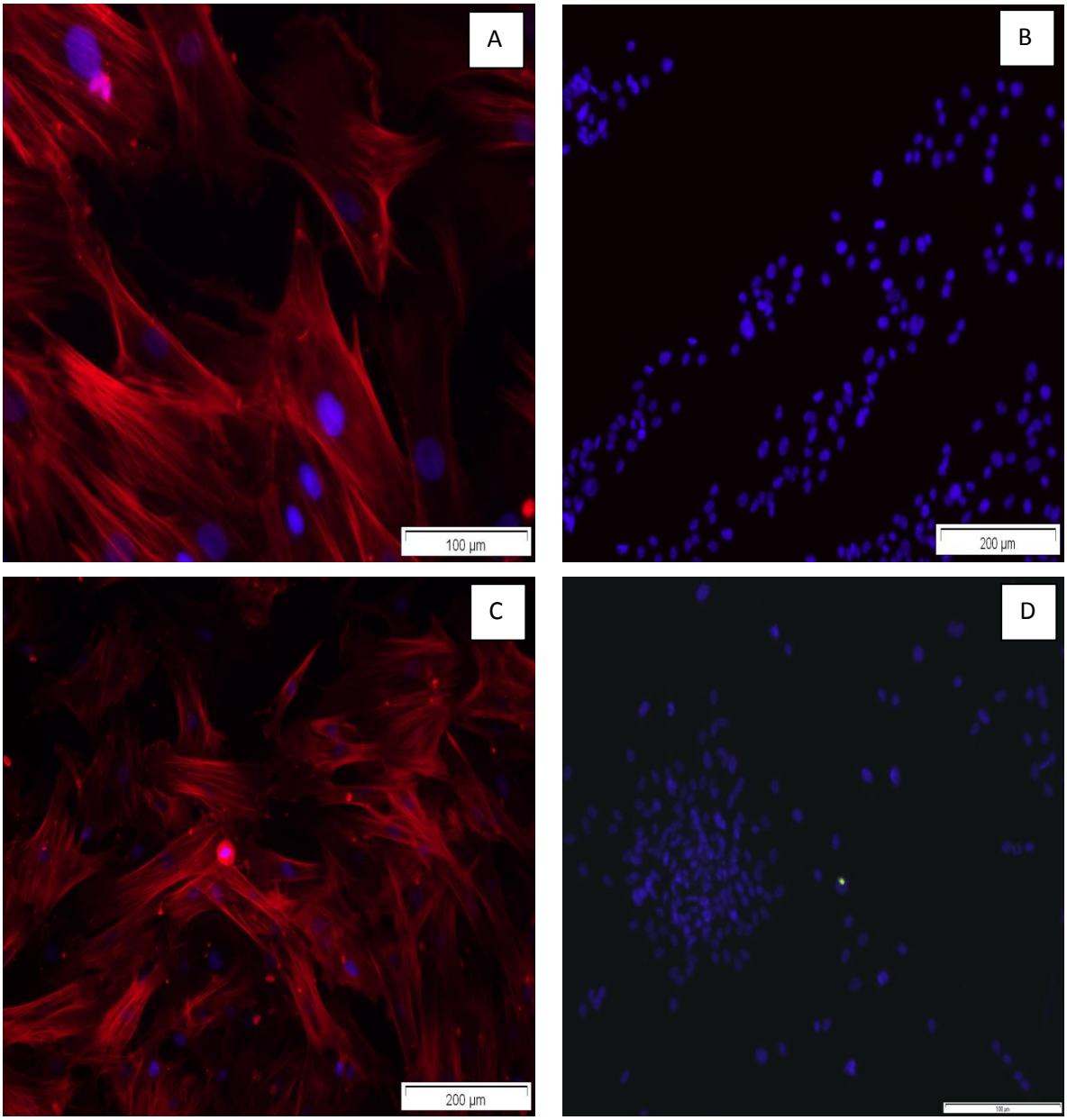

Figure 34. Indirect immunofluorescent antibody labeling with anti-SMC Myosin (Heavy Chain) antibody. A; Positive ovine SMC staining with anti-SMC Myosin (Heavy Chain) antibody, B; Negative ovine EC staining with anti-SMC Myosin (Heavy Chain) antibody, C; Positive porcine SMC staining with anti-SMC Myosin (Heavy Chain) antibody, D; Isotype control.

4.4.5 Biocompatibility of porcine carotid arteries to ovine vascular cells

4.4.5.1 Extract biocompatability

Prior to performing the extract biocompatibility assays, extract samples from decellularisation run 5 were plated on agar and incubated to confirm a lack of gross microbial contamination. Following 48 hours incubation, no visible bacterial or fungal growth was seen on the fresh blood agar, heated blood agar, nutrient agar and Sabouraud dextrose plates

The extracts were tested for their effects on the growth of ovine EC and SMC over 48 hours. Cell growth was assessed by ATP assay. No significant difference (one-way ANOVA) was seen in ATP levels (n = 3 replicates [decellularised arteries 4-6]) between the extracts and the negative control (normal cells in cell-specific medium) confirming a lack of cytotoxicity of any soluble components of the arteries to ovine EC and SMC. Although not significant, increased levels of ATP were seen in the presence of extract (2) for both ovine EC and SMC. Significant differences were seen with the positive control and medium-only wells compared to the negative control following statistical analysis using one-way ANOVA and post hoc testing (Figures 35 – 36).

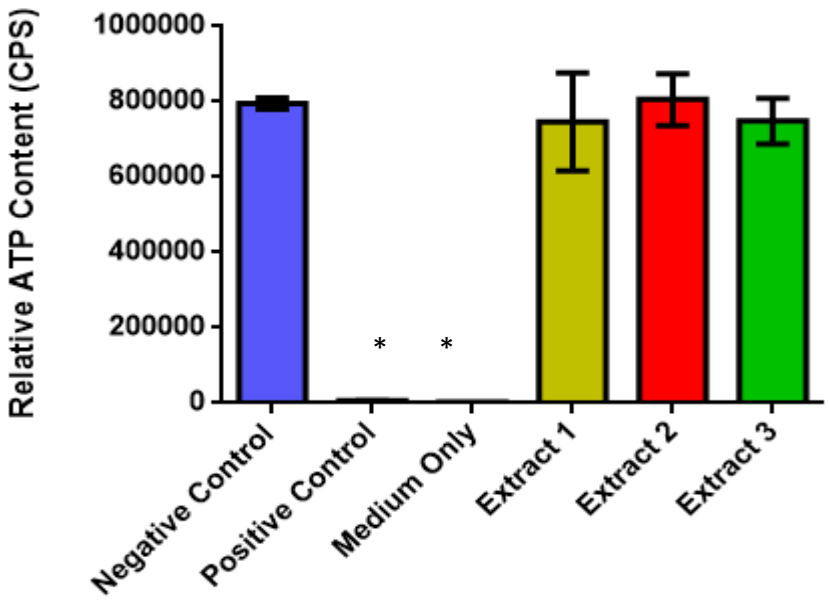

Figure 35. Extract cytotoxicity of decellularised PC arteries to ovine endothelial cells. Data represents mean values ± 95 % confidence limits (n = 3 replicates). ***** Significantly lower than negative control (one-way ANOVA and post hoc testing $p < 0.05$).

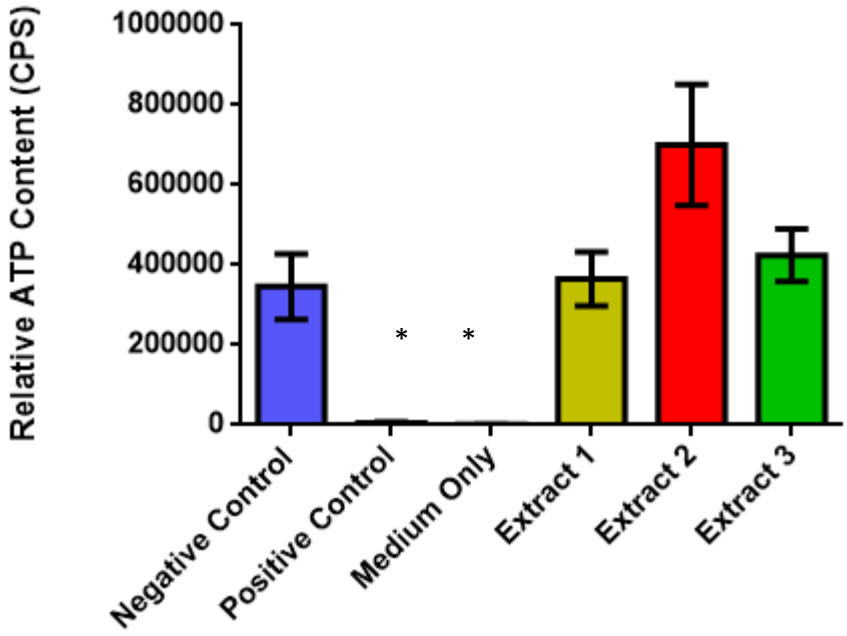

Figure 36. Extract cytotoxicity of decellularised PC arteries to ovine smooth muscle cells. Data represents mean values ± 95 % confidence limits (n = 3 replicates). ***** Significantly lower than negative control (one-way ANOVA and post hoc testing $p < 0.05$).

4.4.5.2 Contact biocompatability

All contact assays demonstrated clear growth of cells to the arterial edges with no evident change in cellular morphology. The results demonstrated a lack of cytotoxicity of the solid components of the decellularised arteries to ovine EC and SMC (Figures 37-38).

Figure (37) shows clear growth visible to the edge of the artery in (B) with retainment of the cobblestone appearance and size typical of EC monolayers, as seen in photomicrograph A. Confluent growth was visible across collagen gel (C), again demonstrating a cobblestone appearance. No cell growth was visible near cyanoacrylate (D).

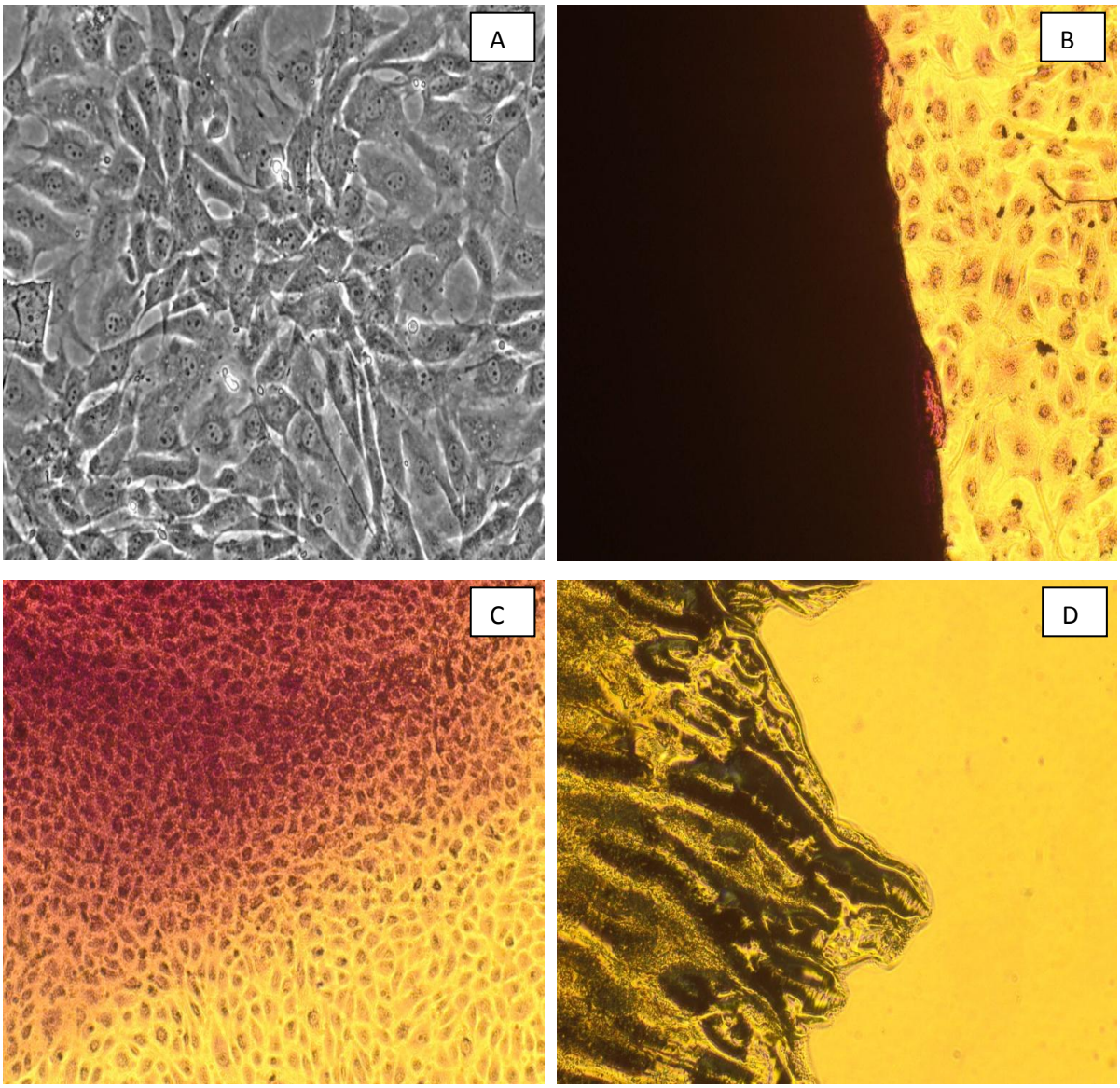

Figure 37. Contact cytotoxicity of decellularised PC arteries to ovine endothelial cells. A; Ovine EC in culture demonstrating cobblestone appearance, B; Decellularised artery, C; Collagen gel, D; Cyanoacrylate.

Figure (38) demonstrates clear growth visible to the edge of the artery in (B) with retainment of the spindle-shaped appearance and size typical of SMC monolayers, as seen in photomicrograph A. Confluent growth was visible across collagen gel (C), again demonstrating a spindle-shaped appearance. No cell growth was visible near cyanoacrylate (D).

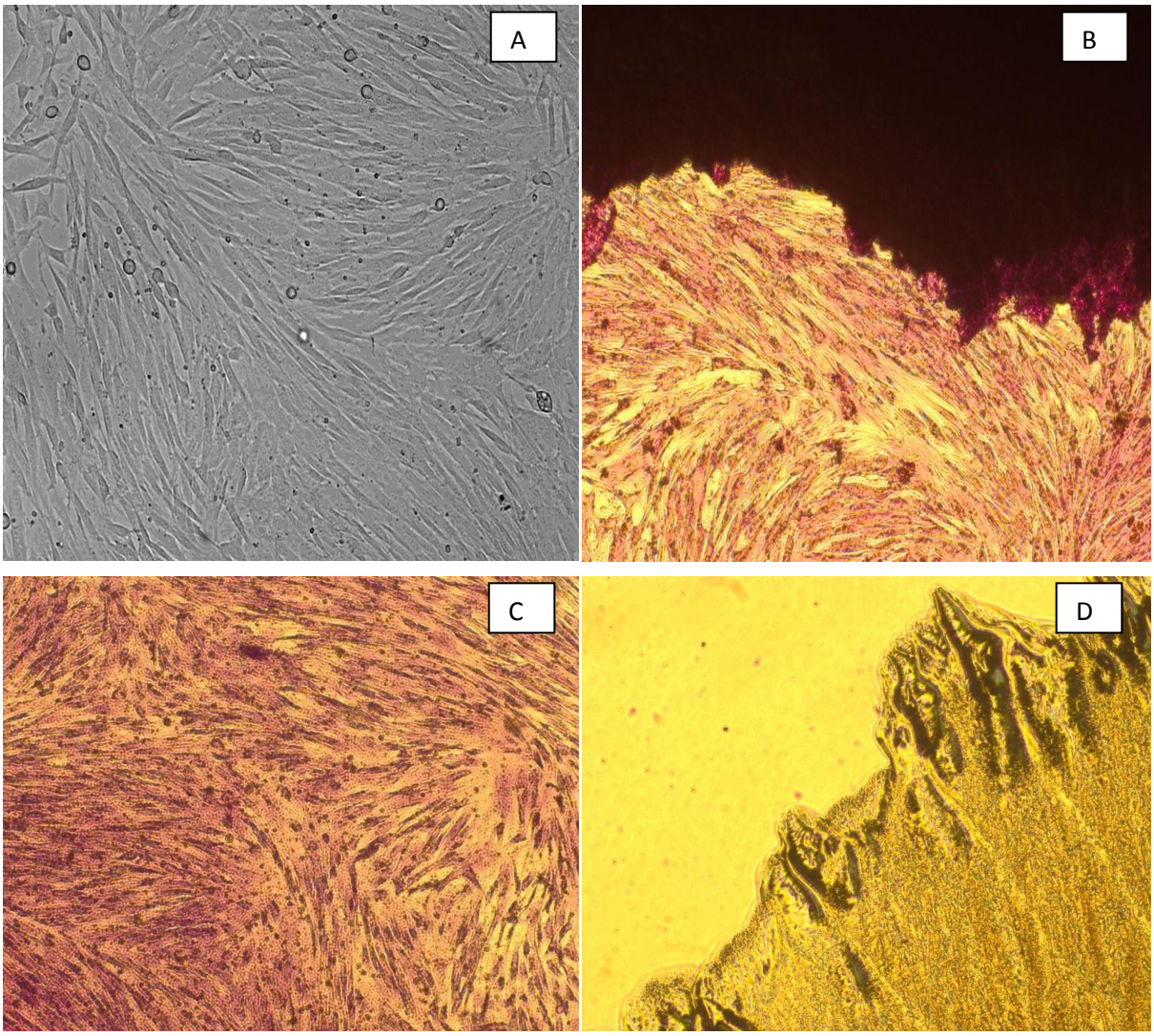

Figure 38. Contact cytotoxicity of decellularised PC arteries to ovine smooth muscle cells. A; Ovine SMC in culture demonstrating spindle-shaped morphology, B; Decellularised artery, C; Collagen gel, D; Cyanoacrylate.

4.5 Discussion

It is intended that any future *in vivo* work with the decellularised PC artery will use an ovine model. To allow accurate experimentation with ovine vascular cells, it was essential to

confirm that harvested vascular cells were pure isolates with the correct vascular cell phenotype prior to commencing further tests.

Standard, well described techniques were used to isolate vascular cells- collagenase degradation to release EC and the explant method of SMC migration onto a surface. Morphologically, both techniques appeared to successfully demonstrate the presence of ovine EC and SMC in culture. In the few experiments available in the literature on ovine vascular cell characterisation, indirect immunoflurescent antibody labeling was the primary technique used to confirm correct cell phenotype and so this was the method adopted in this study (Grooby *et al*., 1997; Orrico *et al*., 2010).

Two well-known EC-specific cell markers are VWF and CD31 and as such were chosen as the primary markers to confirm EC phenotype. Von Willebrand factor is a large glycoprotein made within the Weibal-Palade bodies of mature EC (Orrico *et al*., 2010). It is intimately involved in platelet adhesion. In all characterisation experiments, anti-VWF antibody (rabbit anti-human) showed specificity to both porcine (positive control) and ovine EC, demonstrating that the sequence homology for VWF shares epitopes between mammalian species.

CD31 also known as (PECAM-1) is a protein expressed in high amounts on the surface of endothelial cells and is involved in many processes related to angiogenesis and platelet function. In the first characterisation run, an anti-CD31 primary antibody (mouse anti-human) was used with unknown specificity for ovine CD31. This antibody failed to bind to ovine EC cells confirming that sheep CD31 did not express the same epitope to human CD31. A similar finding has been seen in a previous work on ovine EC characterisation (Hoerstrup *et al*., 2000). In subsequent characterisation runs therefore, an ovine specific anti-CD31 antibody was purchased which did subsequently bind to and show specificity for ovine EC and was used for the remainder of the study.

Based on evidence in the literature for the characterisation of vascular SMC (Abdi *et al.*, 1995; Grooby *et al.*, 1997; Afting *et al.*, 2003; Zhao *et al.*, 2010) two antibodies were used to characterise the harvested ovine SMC, anti-SMC α-actin antibody and anti-SMC Myosin (Heavy Chain). SMC α-actin and SMC Myosin (Heavy chain) are filamentous proteins heavily involved in the contractility of smooth muscle and are highly conserved across species. In all characterisation experiments antibodies to both proteins demonstrated specificity to both porcine (positive control) and ovine SMC.

Unfortunately despite developing a successful characterisation protocol for ovine SMC and EC, the results from the first two characterisation runs did confirm mixed cell populations of both SMC and EC (Figure 26). This is a well-known and common complication seen when harvesting and isolating cells of all types, including vascular. For future seeding experiments to be accurate, it was essential that cell populations were pure. In order to achieve pure isolates, magnetic-bead separation was chosen as it is one of a number of established biochemical techniques used to achieve pure cell isolates. The technique itself is technically difficult and time-consuming. It was felt that attempting to purify existing harvested vascular cells that had been correctly identified by phenotype was a more sensible and time- saving approach than repeating (and subsequently re-characterising) numerous cell harvestings. It was decided to deplete fibroblasts from all populations in addition to producing pure cell isolates as it is well know that fibroblasts commonly contaminate harvested vascular cell populations. The results from magnetic bead separation were mixed. Magnetic bead separation of ovine EC was not successful as in both experiments, the ovine EC were non-viable following the experiment. This was likely secondary to experimental error or possible toxicity to the reagents used. Ovine SMCs did survive the process and were found to be pure isolates. It is difficult to say here accurately whether magnetic bead separation was successful at all, as characterisation experiments had only demonstrated contamination of EC populations with SMC and not vice versa i.e. harvested SMC populations may have been pure to begin with. Gifted ovine EC however were subsequently shown to be pure following characterisation.

In future, if further cell isolation experiments were required, the approach used would be to use an alternate and ultimately more accurate technique for cell purification such as flow cytometry. In flow cytometry, a fluorescent cell sorter is used to seperate cells suspended in solution that have been antibody labelled, using laser detection.

Table (13) below summarises the immune-reactivity of primary antibodies used in the study to characterise ovine EC and SMC.

Antibody	Ovine EC	Ovine SMC
Anti-CD31: FITC	+	-
Anti- Von Willebrand factor	+	-
Anti-smooth muscle cell myosin (Heavy Chain)	-	+
Anti-smooth muscle cell α-actin antibody	-	+

Table 13. Demonstration of reactivity of laboratory stock and specifically purchased primary antibodies to ovine vascular cells.

As pure isolates of both EC and SMC were available and phenotypically characterised, work could now continue on assessing the biocompatibility of ovine cells to the decellularised PCA scaffolds. Extract and contact cytotoxicity assays were used to assess the biocompatibility of the scaffolds.

The acellular PCA scaffolds were biocompatible to both types of ovine vascular cells, an essential finding when considering that future *in vivo* work with the decellularised porcine carotid arteries will be based upon using an ovine animal model. Both extract and contact cytotoxicity assays clearly demonstrated a lack of cytotoxicity to the ovine cells of the solid and soluble components of the PC arteries. Following the successful purification of ovine vascular cell populations and their biocompatibility with decellularised PC arteries, it was then possible to begin re-cellularisation experiments.

Chapter 5

Cell seeding of acellular porcine scaffolds using ovine vascular cells

5.1 Introduction

The importance of an endothelium lining and the benefits of dual-cell seeding with EC and SMC in the development of a vascular biological graft were discussed in detail in Chapter (1). Based on literature reports, a seeding density between 10^3-10^5 cells.ml^{-1} has been most often used for seeding both biological and synthetic small-diameter conduits [Chapter (1)]. It was therefore decided to seed the cells characterised in Chapter (4) onto the arterial segments produced in Chapter (3) across this range to determine the optimum seeding density. The strategy behind this approach was based on range of cell densities reported in the literature in which both surfaces of decellularised PCA have been used to seed the cells (McFetridge *et al*., 2004; Shimizu *et al*., 2007; Heine *et al*., 2011; Nitsan *et al*., 2012). 2D cell seeding experiments were performed initially to determine whether ovine vascular cells could successfully attach to the surfaces of the acellular porcine scaffolds and secondly, to determine optimal seeding densities for subsequent 3D dynamic cell seeding. If 3D seeding was attempted, it was decided to perform 'dynamic' 3D seeding of the scaffolds (using a roller-mixer) as current literature reports have demonstrated greater seeding efficiencies when this technique is utilised (Hsu *et al*., 2005).

5.2 Aims and Objectives

The aim of this chapter was to assess the ability of ovine vascular cells to successfully adhere to the acellular porcine arterial scaffold. The objectives were:

1) To determine the ability of ovine vascular cells to adhere to the surfaces of decellularised PCA using a two-dimensional static seeding approach.

2) To determine optimal seeding densities should two-dimensional static seeding experiments confirm successful adherence.

3) If two-dimensional seeding was successful, to determine the ability of ovine vascular cells to successfully adhere to the surfaces of decellularised PCA using a dynamic three-dimensional seeding approach.

4) If three-dimensional dynamic seeding was successful, to perform dynamic three-dimensional dual-cell seeding.

5.3 Materials and Methods

5.3.1.Two-dimensional (2D) cell seeding of acellular scaffolds using ovine vascular cells

All methods were performed using full aseptic precautions in a class II safety cabinet.

Six acellular porcine scaffolds from decellularisation batch seven were divided longitudinally along their length using dissecting scissors. Each scaffold was then cut into two 2 cm x 1 cm lengths, giving twelve sections of scaffold in total.

5.3.1.1 Seeding method for ovine SMC

In the initial ovine SMC seeding experiment, seeding was performed on both the luminal and adluminal surfaces of the scaffold.

Each scaffold segment was placed individually into a well of a six-well plate. In two well plates, the luminal surfaces of the scaffolds were facing upwards. In the third, the adluminal surface was facing upwards. In total, four sections of scaffold were placed individually into wells within a six well plate (one control segment for medium only and three ‘test’ segments for cell seeding).

A sterile oval stainless steel seeding ring (Figure 39) was then placed on the surface of each scaffold segment. To ensure an adequate seal was created between segment and ring, 400 µl of cell-specific medium was placed into each seeding ring. Rings were adjusted if any leak of medium was noted. Once all scaffold segments had seeding rings containing medium, the well-plates were incubated for thirty minutes at 37°C

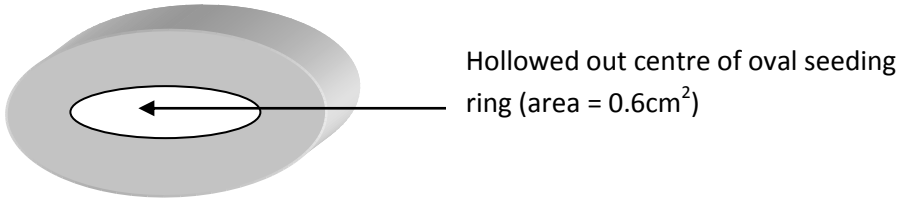

Figure 39. Metallic seeding ring demonstrating hollow centre.

Whilst the well-plates were incubating, ovine SMC were prepared for seeding. Ovine SMC were placed into suspension following the previously described method in Section's 2.7.2 and 2.7.5 and counted using a haemocytometer. Cells were diluted to each cell density using cell-specific medium. For SMC seeding, the two well-plates containing luminal and adluminal scaffold segment surfaces were used. The medium was aspirated from each of the seeding rings within the wells. For both well-plates, the scaffold segment in the top left was used as the control segment/well. Into the control well, 200 µl of SMC medium was placed. Next 200 µl of SMC suspension at each density (7.9 x 10^3cells.ml^{-1}, 7.9 x 10^4cells.ml^{-1}, 7.9 x 10^5 cells.ml^{-1}) was placed into the remaining three seeding rings in each of the two well-plates. Following incubation, all three well plates were labeled with each cell density in preparation for seeding (Figure 40). Once the seeding process was complete, all three well plates were placed in culture at 37°C with 5% (v/v) CO_2 in air for 48 hours. Following incubation, seeded segments were processed for evaluation using scanning electron microscopy (Section 2.3.3).

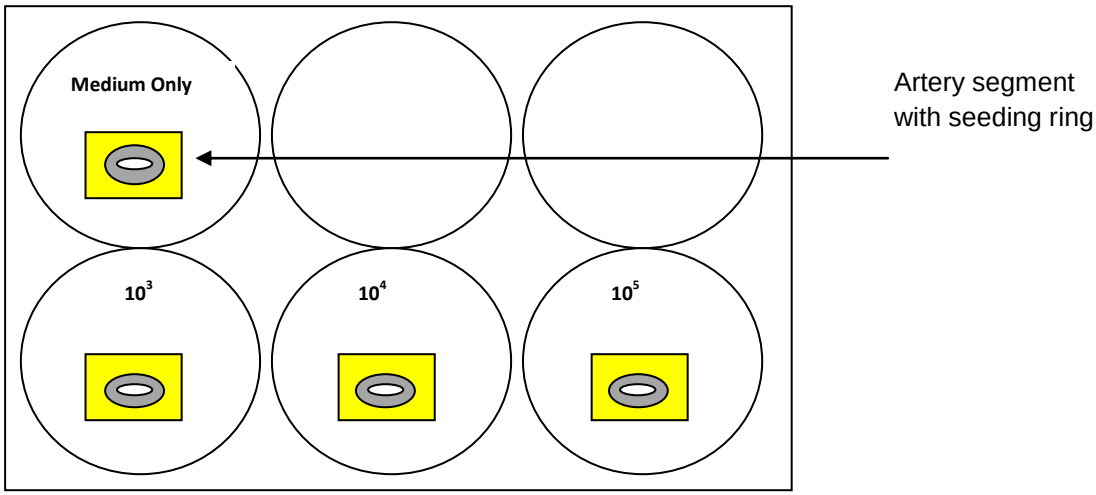

Figure 40. Schematic appearance of acellular arterial segments for 2D seeding.

5.3.1.2 Seeding method for ovine EC

For the ovine EC seeding experiments, only the luminal surface was used. The seeding method and cell-densities used were identical to those described in Section 5.3.1.1.

5.3.1.3 Analysis of cell seeded scaffolds by SEM

It was decided to characterise the 2D seeded scaffolds with SEM using the technique described in Chapter 2, Section 2.3.3. SEM would allow accurate visualisation of the scaffold surface and demonstrate the adherence and level of confluence of seeded cells

5.3.2 Three dimensional dynamic seeding of acellular porcine scaffolds using ovine vascular cells

5.3.2.1 Seeding method for EC and SMC

All methods were performed using full aseptic precautions in a class II safety cabinet.

Results from 2D seeding found that the optimal seeding density was 7.9×10^4 cells.ml^{-1}. In the first experiment six acellular tubular scaffolds were used in total (three for ovine SMC

seeding and three for ovine EC seeding). Prior to seeding, scaffolds were washed overnight at 4°C in sterile DPBSa. Following washing, scaffolds were cut into 8 cm sections. One end of the scaffold was ligated 2 cm from the distal end using a 3/0 silk suture. Cell-specific medium was then injected into the scaffold using a 5 ml syringe to check for any leaks at the ligated end. If leaks were found, a further suture was applied. Next, ovine EC and SMC were placed into suspension following the previously described passage method and diluted to a density of 7.9×10^4 cells.ml^{-1} using freshly made cell-specific medium. Then, 4 ml of cell suspension was injected into each scaffold using a 5 ml syringe at the open end. Next, the open end of the scaffold was ligated with a 3/0 silk suture 2 cm from the open end, leaving a 4 cm section of scaffold containing cell suspension. Next, 12 ml of fresh cell-specific medium was placed into six sterile universals followed by one minute of sparging with 5% (v/v) CO_2 with air to prevent cellular hypoxia. Seeded vessels (n=6) were then placed horizontally within each universal. The universals containing the seeded vessels were then placed horizontally on a roller mixer set at 5 rpm in an incubator at 37°C with 5% (v/v) CO_2 in air. Seeded scaffolds were incubated for 48 hours on the roller mixer and sparged with 5% (v/v) CO_2 in air for one minute every 24 hours to prevent cellular hypoxia.

To assess for the viability of 3D seeded cells, a Live/ Dead ® Assay was used using the techniques described in Section 5.3.2.3.

5.3.2.3 Analysis of cell seeded scaffolds by LIVE/DEAD ® cell assay

A Live/Dead ® assay was used to characterise the 3D seeded scaffolds as in addition to demonstrating the adherence and level of confluence of seeded cells, the assay would also assess the viability of seeded cells. The assay uses two compounds- calcein-AM and ethidium homodimer-1. Calcein is a fluorescent (green) complex that is actively transported across a cell membrane and is such, only transported intra-cellularly in living cells. Ethidium homodimer-1 is a membrane-impermeable fluorescent (red) compound which binds to intra-cellular DNA. It therefore can only enter dead cells (due to a disrupted cell membrane).

5.3.3 Three dimensional dual dynamic cell seeding of decellularised porcine carotid arteries using ovine vascular cells

5.3.3.1 Seeding method for EC and SMC

All methods were performed using full aseptic precautions in a class II safety cabinet.

In total, three acellular scaffolds were used in the experiment. Ovine SMC were seeded first onto the scaffold lumen as they proliferate and adhere faster than ovine EC, laying down a matrix that should allow greater EC adherence and proliferation (see Chapter 1). Prior to seeding, scaffolds were washed overnight at 4°C in sterile DPBSa. Following washing, scaffolds were cut into 8 cm sections. One end of the scaffold was ligated 2 cm from the distal end using a 3/0 silk suture. DPBSa was then injected into the scaffold using a 5 ml syringe to check for any leaks at the ligated end. If leaks were found, a further suture was applied. Next, ovine SMC were placed into suspension following the previously described passage method and diluted to a density of 7.9×10^4 cells.ml^{-1} using freshly made cell-specific medium. Then, 4 ml of cell suspension was injected into each scaffold using a 5 ml syringe at the open end. Next, the open end of the scaffold was ligated with a 3/0 silk suture 2 cm from the open end, leaving a 4 cm section of scaffold containing cell suspension. Next, 12 ml of fresh cell-specific medium was placed into six sterile universals followed by one minute of sparging with 5% (v/v) CO_2 with air to prevent cellular hypoxia. Seeded vessels (n=3) were then placed horizontally within each universal. The universals containing the seeded vessels were then placed horizontally on a roller mixer set at 5 rpm in an incubator at 37°C with 5% (v/v) CO_2 in air. SMC seeded scaffolds were incubated for 48 hours on the roller mixer at 5 rpm and sparged with 5% (v/v) CO_2 in air for one minute every 24 hours to prevent cellular hypoxia.

Following 48 hours of incubation, the scaffolds were removed from culture. The proximal suture from each scaffold was removed and the SMC medium was emptied from the scaffold lumen. Next, a suspension of ovine EC was injected gently into the lumen of the scaffolds using the same technique described above for ovine SMC seeding. The open end was again ligated using a 3/0 silk suture. Scaffolds were then placed into culture for 72 hours with CO_2 and air sparging every 24 hours to prevent cellular hypoxia.

5.3.3.2 Analysis of the cell seeded scaffolds using histological evaluation

A Live / Dead ® assay was initially performed to assess seeded scaffolds for re-cellularisation and cell viability, however this failed to demonstrate the presence of adherent cells. Scaffolds were therefore characterised histologically with H&E and DAPI using staining of tissue sections described in Sections 2.6.2 - 2.6.3. It was decided to assess dual-seeded scaffolds using H&E and DAPI staining as histological analysis would demonstrate the presence of seeded cells and assess the scaffolds in cross-section, thereby assessing the level of penetrance of seeded cells. It would also allow any future immunohistochemical analysis of the seeded scaffolds to confirm vascular cell phenotype.

5.4 Results

5.4.1 Two dimensional cell seeding of acellular scaffolds using ovine vascular cells

The appearance of the luminal and adluminal surfaces of unseeded acellular scaffolds visualised by SEM is shown in Figure (41). Photomicrograph A displays a relatively smooth luminal surface with intimal folds of the basement membrane, with an absence of adhered cells. Photomicrograph B shows an adluminal surface, rough and loosely organised in texture with visible collagen fibrils from the advential surface, again devoid of cells.

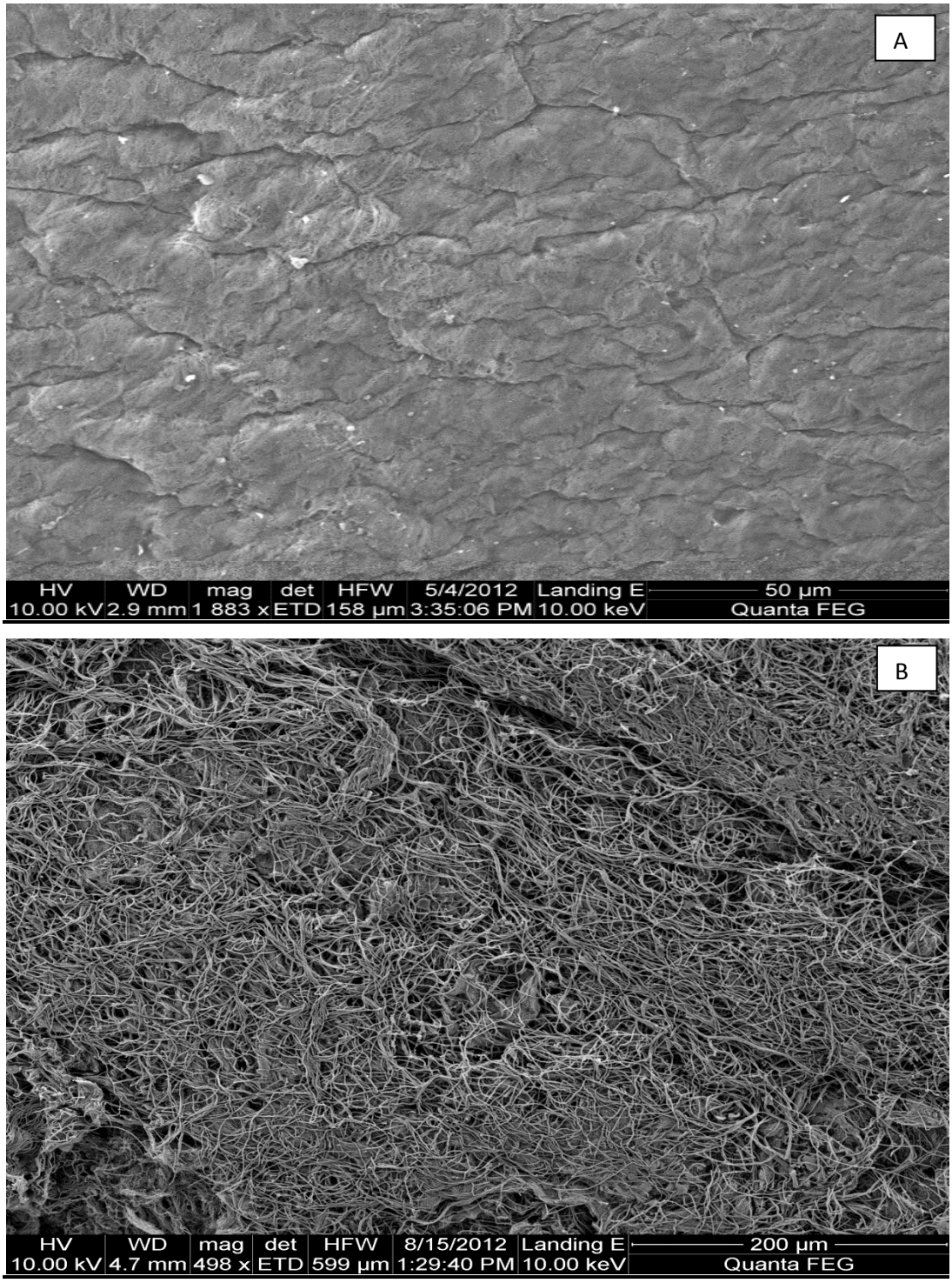

Figure 41. SEM images of acellular porcine scaffolds. A; Control scaffold (luminal). B; Control scaffold (adluminal). Both images show an absence of visible cells.

5.4.1.1 Ovine SMC

The appearances of SMC seeded onto the luminal surfaces of acellular scaffolds using three different seeding densities (7.9 x 10^3, 10^4, 10^5 cells.ml^{-1}) were visualised by SEM and are shown in Figures (42-44).

At a seeding density of 7.9 x 10^3 cells.ml^{-1}, clear colonies of adhered SMC were visualised on the luminal surface of the scaffold by SEM after 48 hours incubation. There was however, a lack of confluence of the seeded cells (Figure 42).

At a seeding density of 7.9 x 10^4 cells.ml^{-1}, complete confluent growth of the seeded area by SMC was visualised on the luminal surface of the scaffold at 48 hours incubation. Confluent growth extending beyond the boundaries of the seeded area was seen (Figure 43).

At a seeding density of 7.9 x 10^5 cells.ml^{-1}, complete confluent growth of the seeded area by SMC was seen on the luminal surface of the scaffold at 48 hours incubation. Evidence of cell debris accumulating on the luminal surface was seen (Figure 44).

Figure (45) clearly demonstrates that the adluminal surface was sub-optimal as compared to the luminal surface for 2D seeding. At each seeding density, cells can be seen on the adluminal surface but do not appear to spread into confluent areas along the matrix to the level seen for luminal seeding.

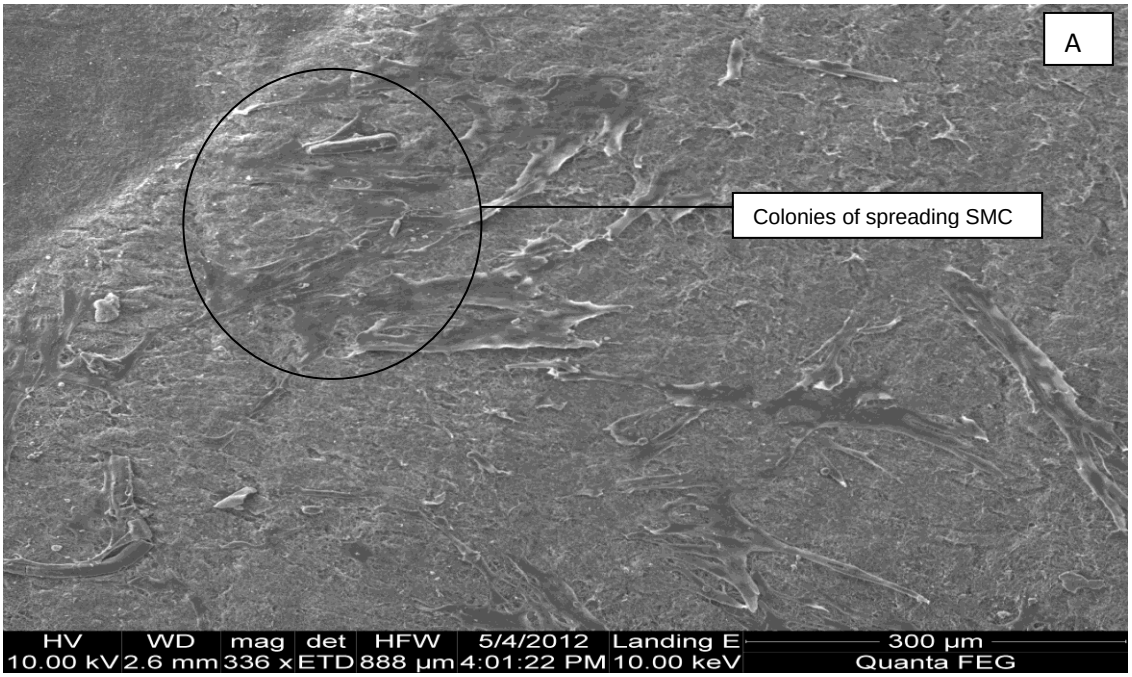

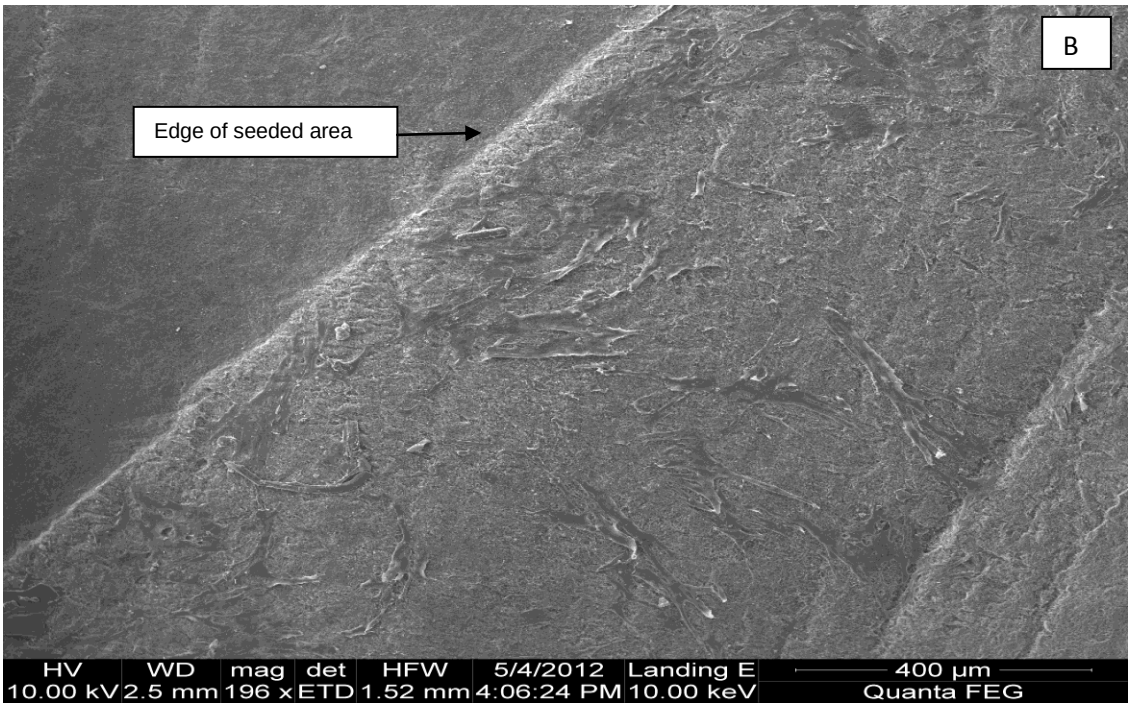

Figure 42. SEM images of SMC seeded (luminal) acellular scaffold using a seeding density of 7.9 x 10^3 cells.ml^{-1} after 48 hours incubation. A & B**;** Seeded scaffold (luminal) demonstrating spreading colonies of SMC but a lack of confluence over the seeded area.

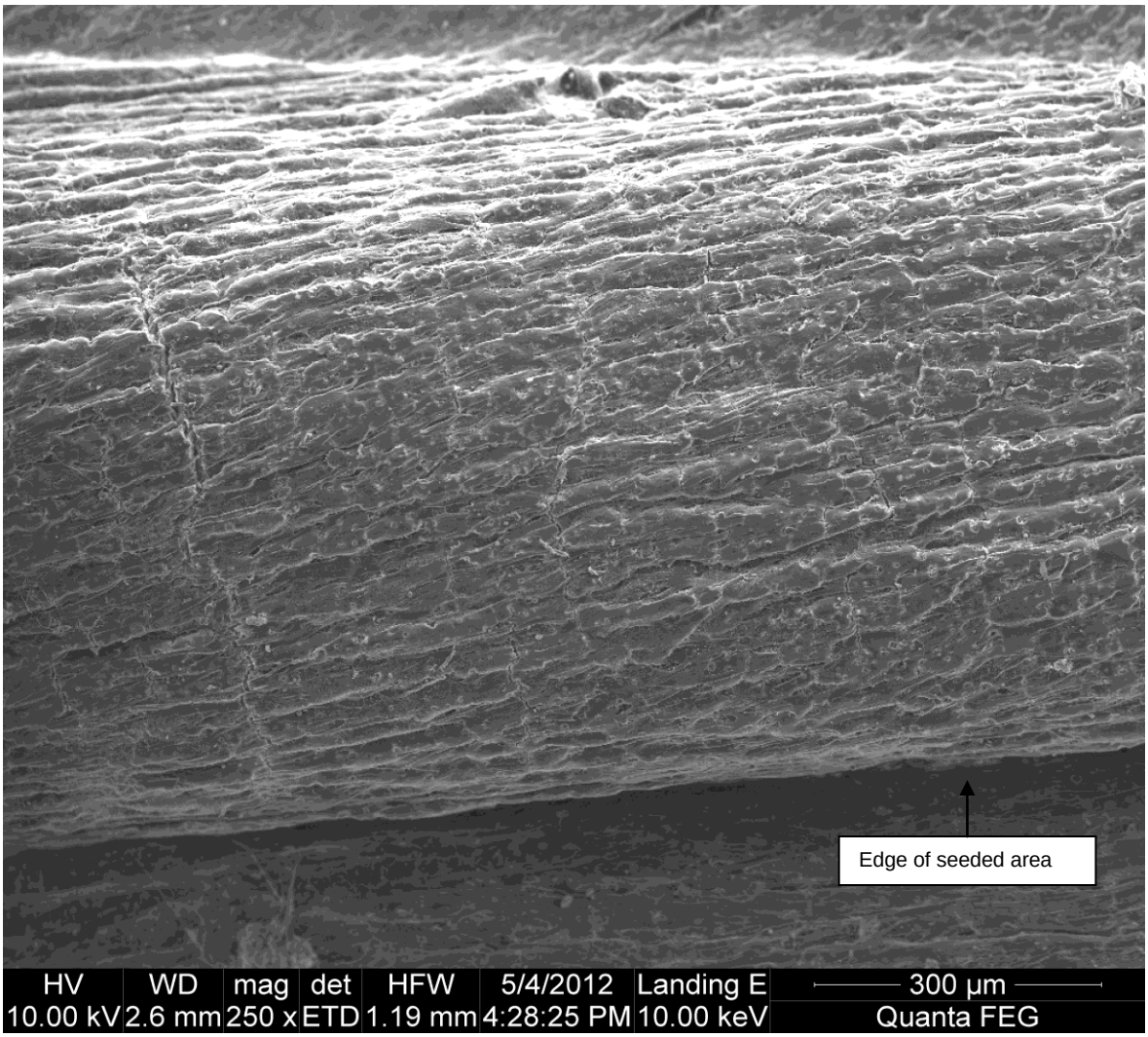

Figure 43. SEM image of SMC seeded (luminal) acellular scaffold using a seeding density of 7.9 x 10^4 cells.ml^{-1} after 48 hours incubation. Confluent growth of SMCs is seen within the seeded area with outward extension of growth.

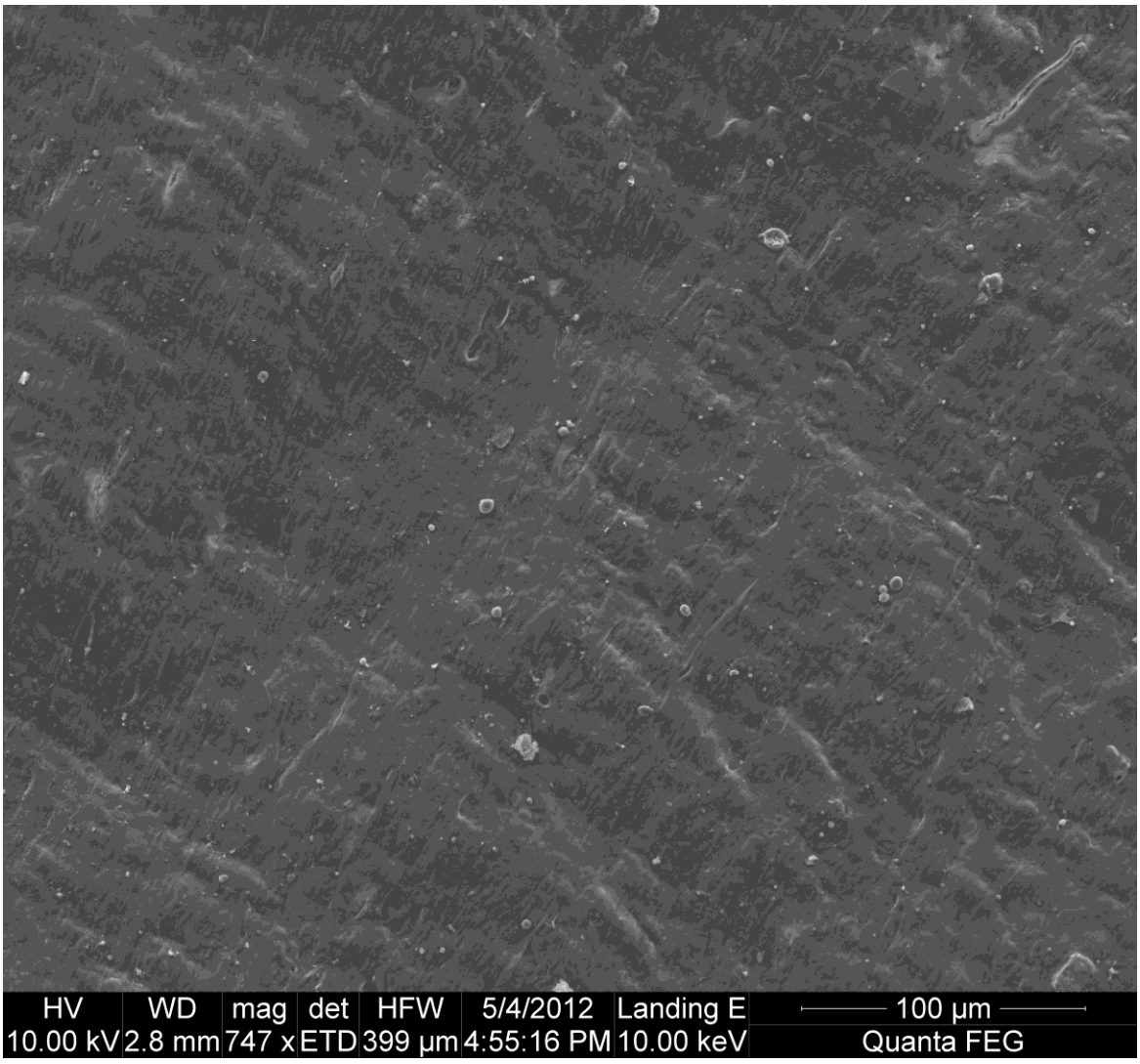

Figure 44. SEM image of SMC (luminal) seeded acellular scaffold using a seeding density of 7.9 x 10^5 cells.ml^{-1} after 48 hours incubation. Confluent growth is seen with accumulation of cellular debris on the luminal surface.

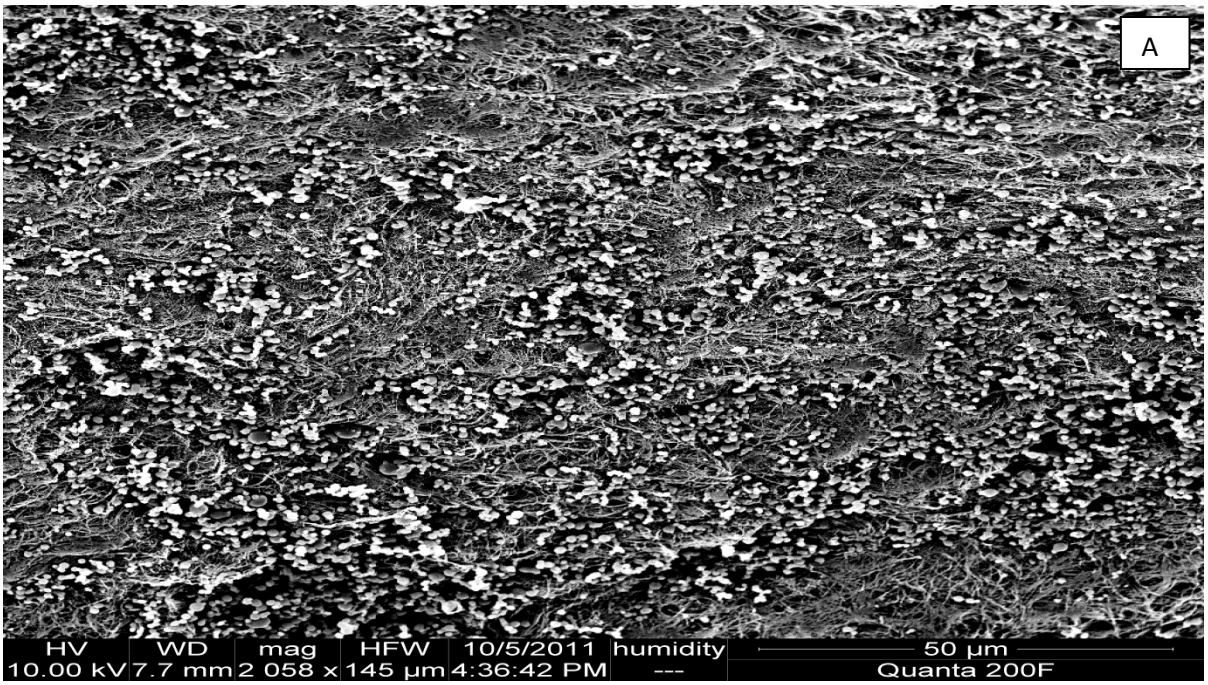
A
HV WD mag HFW 10/5/2011 humidity 50 µm
10.00 kV 7.7 mm 2 058 x 145 µm 4:36:42 PM --- Quanta 200F

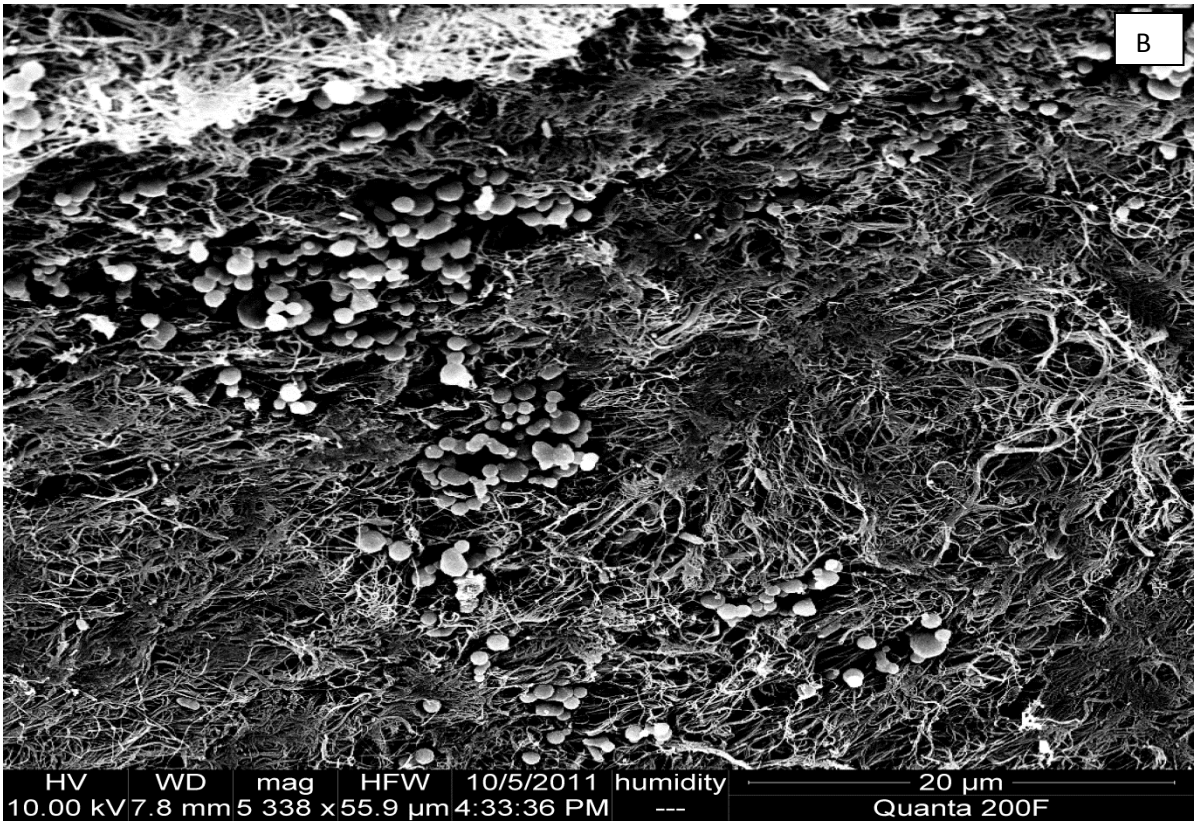
B
HV WD mag HFW 10/5/2011 humidity 20 µm
10.00 kV 7.8 mm 5 338 x 55.9 µm 4:33:36 PM --- Quanta 200F

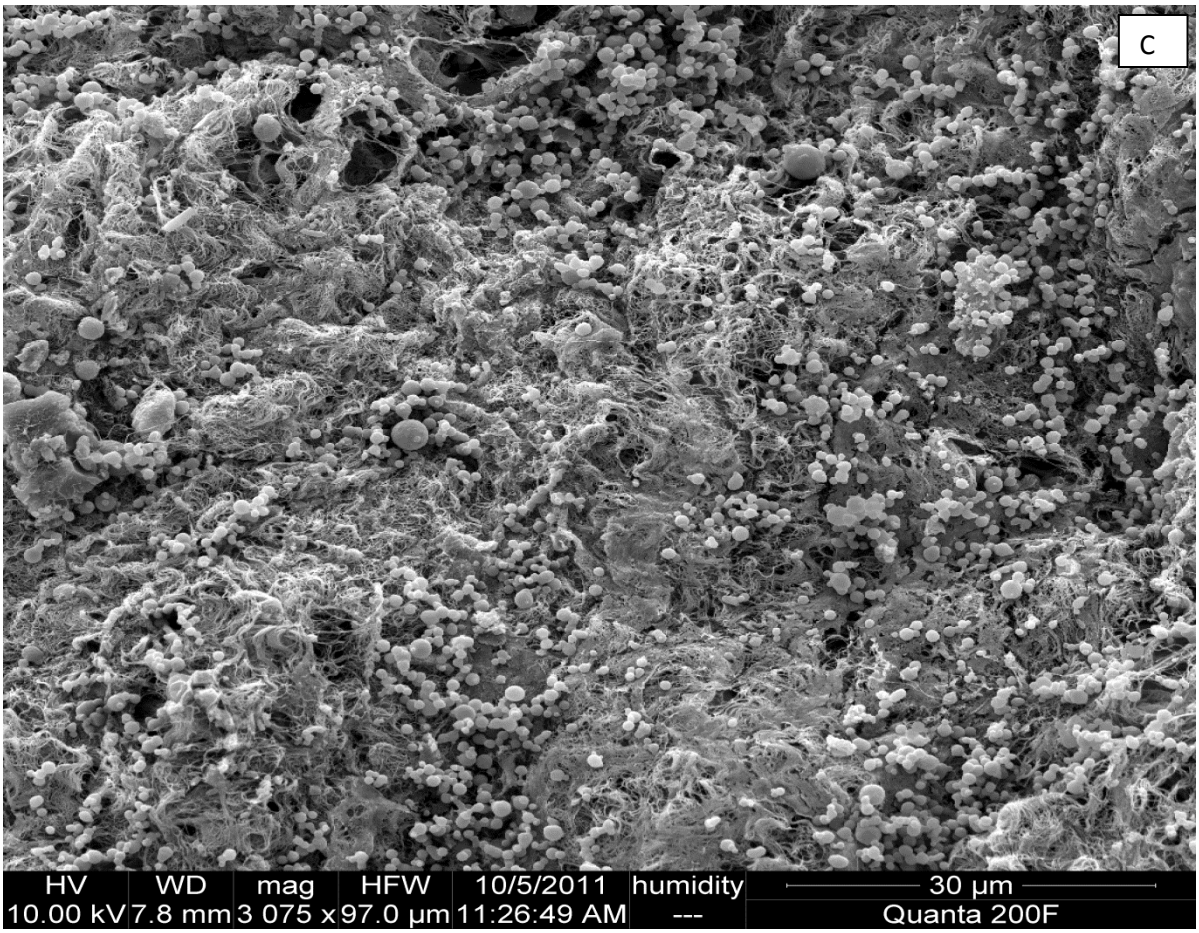

Figure 45. SEM images of SMC seeded (adluminal) acellular scaffold. A; Adluminal surface seeded at a density of 7.9 x 10^3 cells.ml^{-1} after 48 hours incubation. B; Adluminal surface seeded at a density of 7.9 x 10^4 cells.ml^{-1} after 48 hours incubation. C; Adluminal surface seeded at a density of 7.9 x 10^5 cells.ml^{-1} after 48 hours incubation. In all photomicrographs, populations of cells are seen but fail to display areas of spreading, confluent growth and penetration.

A seeding density of 7.9 x 10^3 cells.ml^{-1} of SMC resulted in relatively small areas of cell adherence onto the luminal surface of the scaffolds and would likely result in poor penetration into the scaffold when faced with pulsatile flow in a bioreactor. A seeding density of 7.9 x 10^4 cells.ml^{-1} onto the luminal surface appeared superior, with large areas of spreading cells. A seeding density of 7.9 x10^5 cells.ml^{-1} onto the luminal surface resulted in overconfluence which could potentially lead to over-competition for space, leading to rapid cell death.

Adluminal seeding of ovine SMC cells did not demonstrate the the level of cell adhesion and spreading, the cells appeared very small and rounded indicating lack of adhesion to the scaffold at all three seeding densities.This may well have been due to that fact that the adventitial surface was composed of a matrix that appeared more disorganised as compared to the smooth, ordered, basement membrane of the internal elastic lamina of the intimal surface.

5.4.1.2 Ovine EC

The appearance of EC seeded onto the lumen of acellular scaffolds using three different seeding densities (7.9 x 10^3, 10^4, 10^5 cells.ml^{-1}) and visualised by SEM is shown in Figures (46-48).

At a seeding density of 7.9 x 10^3 cells.ml^{-1}, clear colonies of adhered EC were visualised on the luminal surface of the scaffold by SEM after 48 hours incubation. There was however, a lack of confluence of the seeded cells, highlighted more clearly in photomicrograph B (Figure 46).

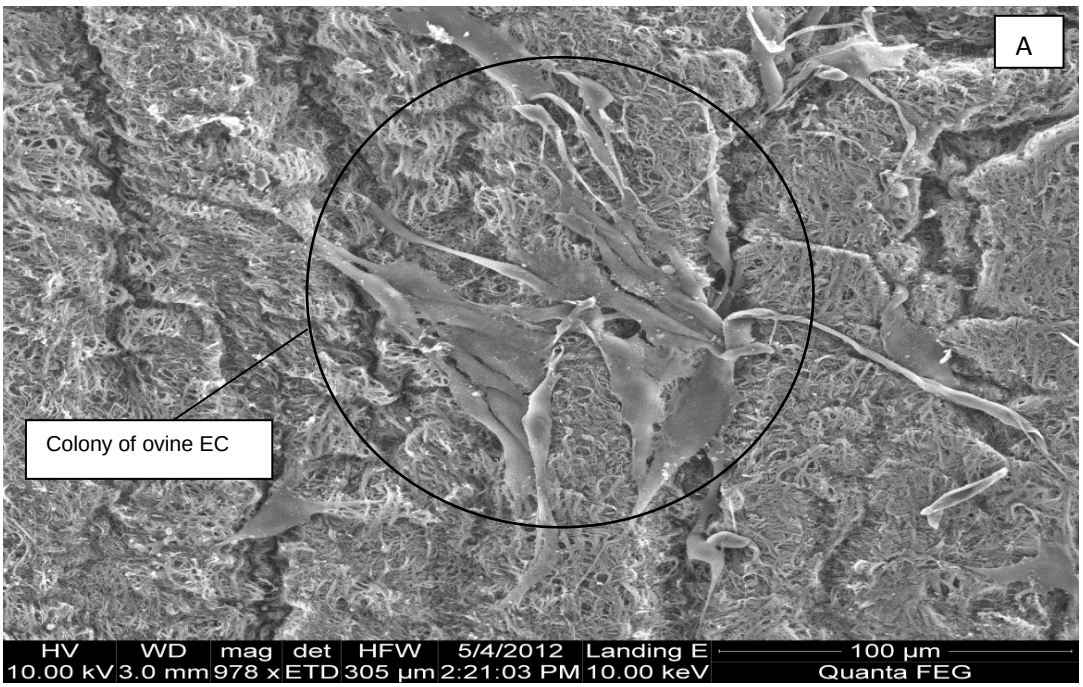

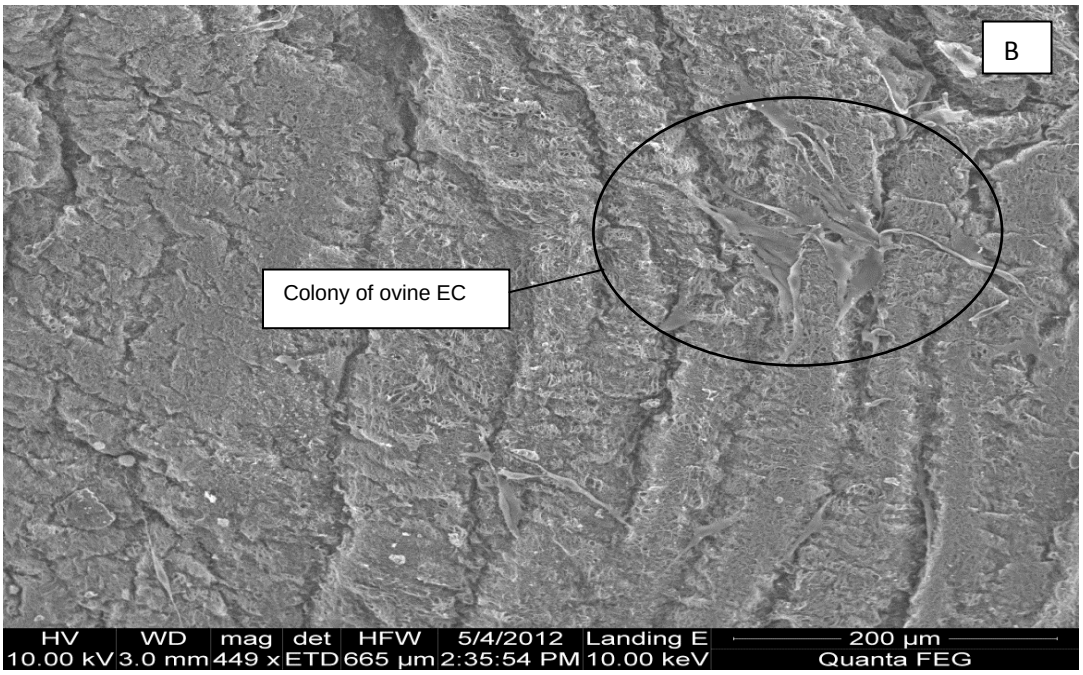

Figure 46. SEM images of EC seeded acellular scaffolds using a seeding density of 7.9 x 10^3 cells.ml^{-1} after 48 hours incubation. A; Luminal surface of seeded scaffold demonstrating colony of EC. B; Seeded scaffold, lower magnification than A.

At a seeding density of 7.9 x 10^4 cells.ml^{-1}, the EC are spreading out and developing much greater areas of confluence on the luminal matrix (area bound by rectangle) than at a density of 7.9 x 10^3 cells.ml^{-1} (Figure 47).

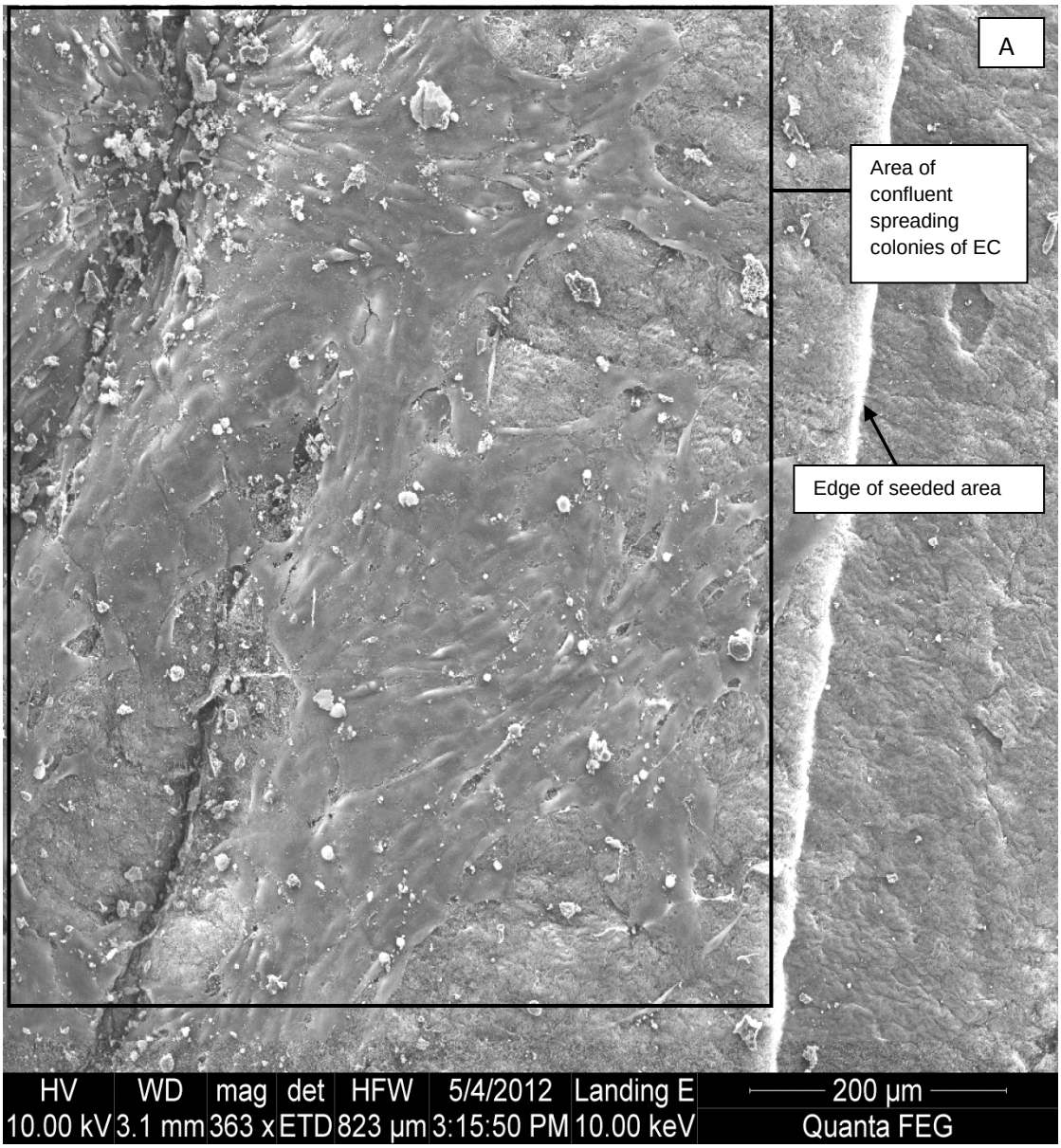
A
Area of confluent spreading colonies of EC
Edge of seeded area
HV WD mag det HFW 5/4/2012 Landing E 200 µm
10.00 kV 3.1 mm 363 x ETD 823 µm 3:15:50 PM 10.00 keV Quanta FEG

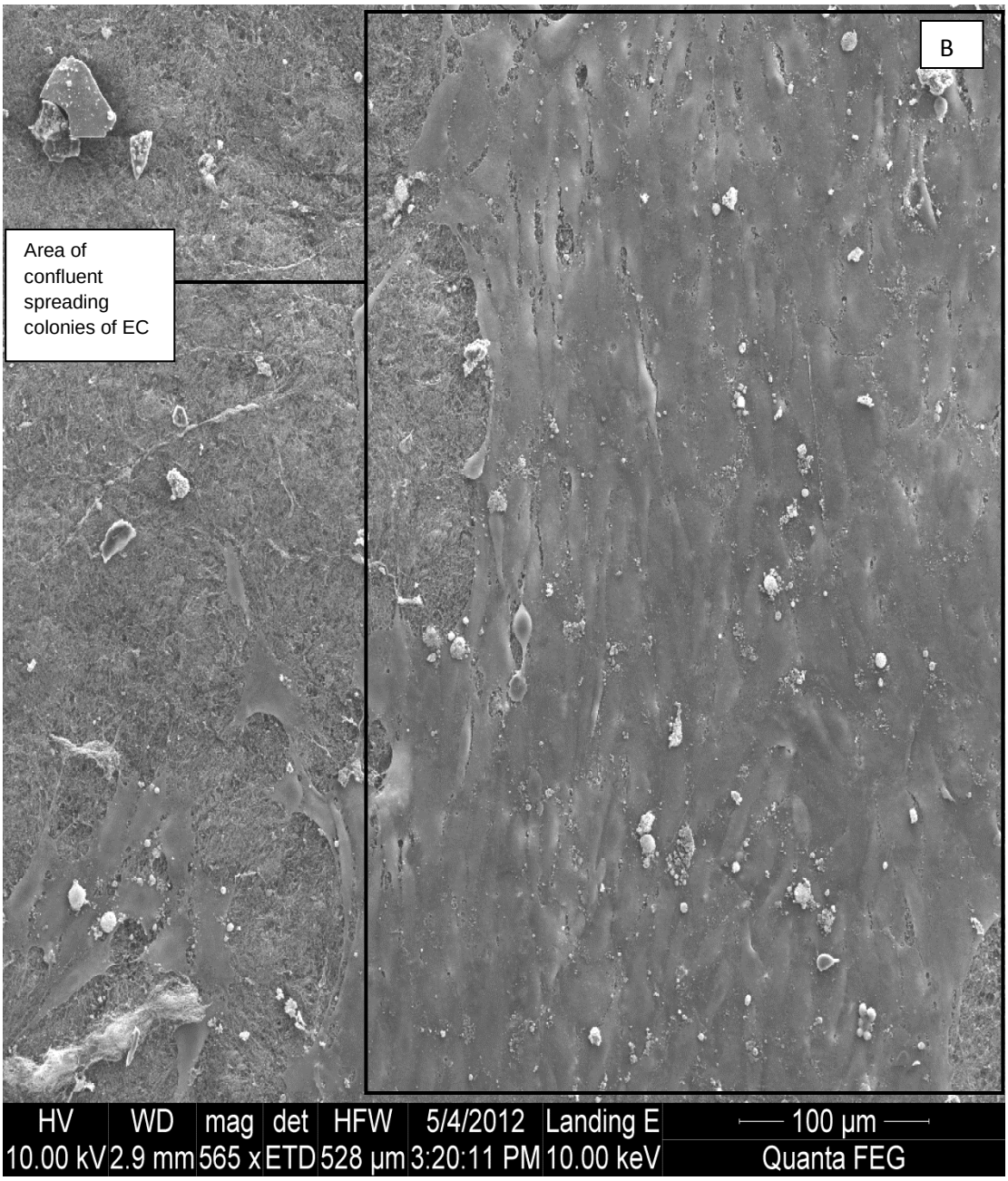

Figure 47. SEM images of EC seeded acellular scaffold using a seeding density of 7.9 x 10^4 cells.ml^{-1} after 48 hours incubation. A; Luminal surface of seeded scaffold demonstrating large area of spreading, confluent growth of EC. B; Seeded scaffold as A, higher magnification.

At a seeding density of 7.9 x 10^5 cells.ml^{-1}, overconfluent growth of the seeded area by EC was seen, with scattered areas of cell clustering on the luminal surface of the scaffold at 48 hours incubation (Figure 48).

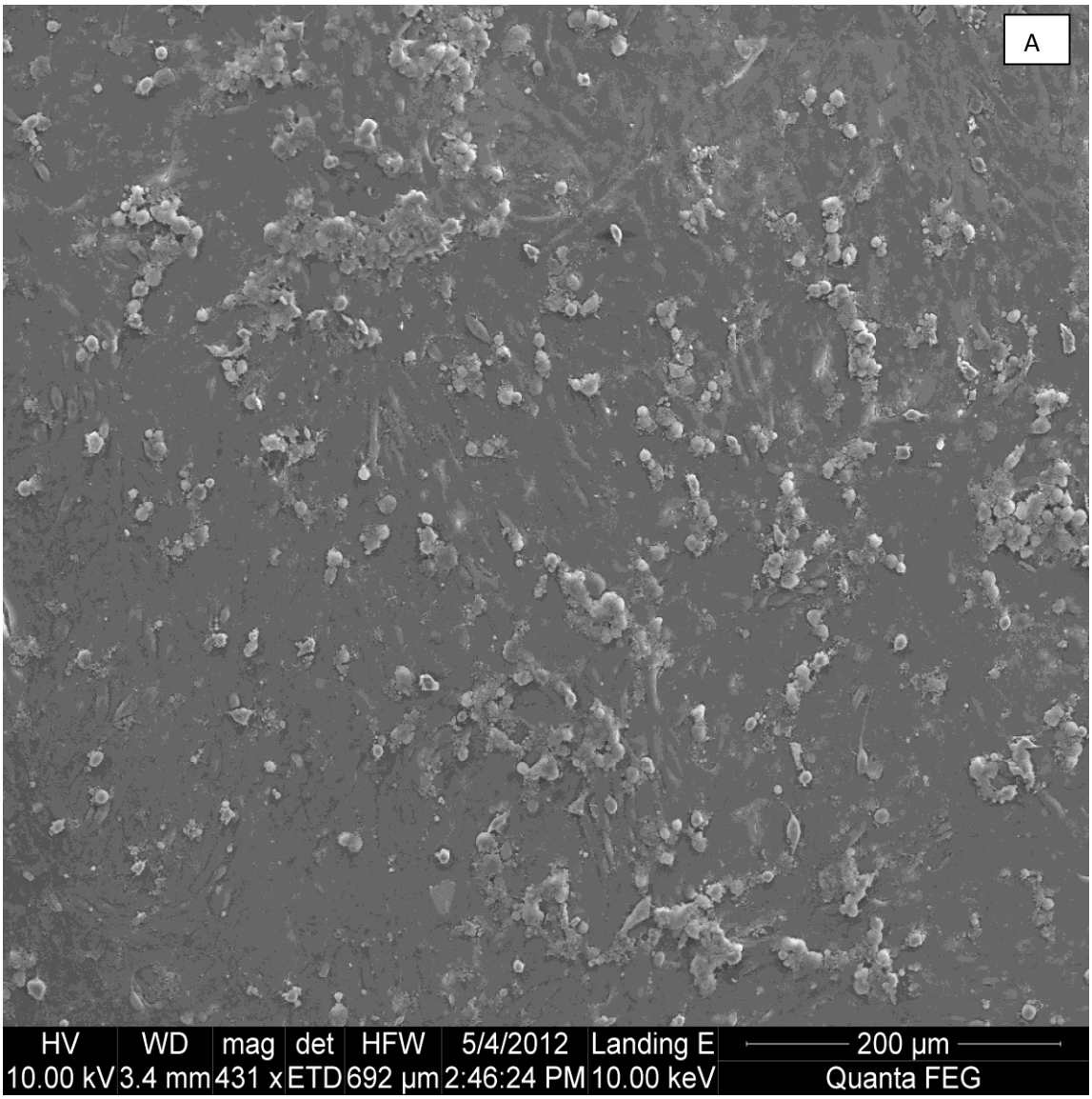

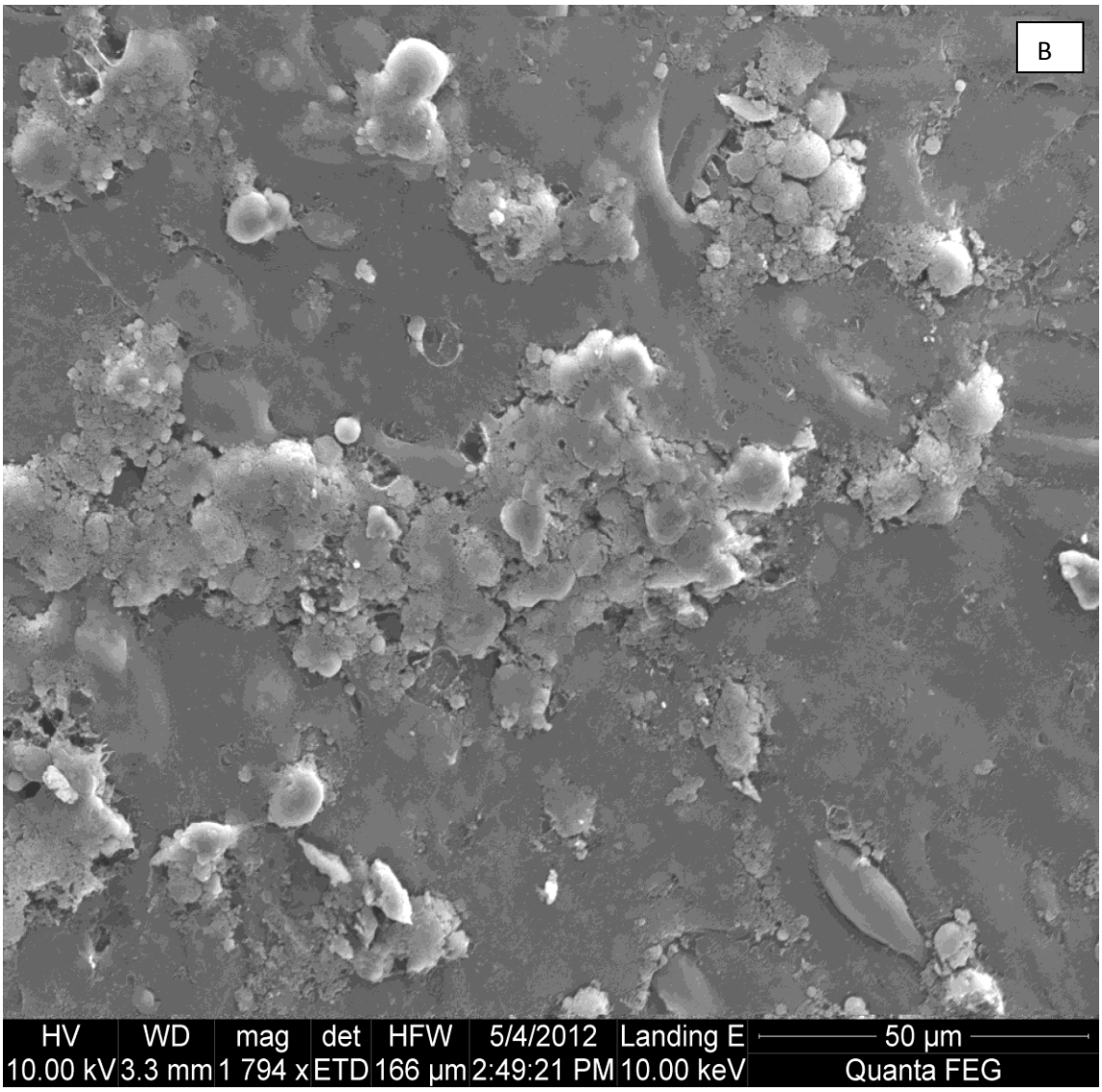

Figure 48. SEM images of EC seeded acellular scaffold using a seeding density of 7.9 x 10^5 cells.ml^{-1} after 48 hours incubation. A; Luminal surface of seeded scaffold demonstrating overconfluent growth and cell clustering. B; Seeded scaffold as A, higher magnification.

Similar findings were seen to those of the SMC seeding experiments. A seeding density of 7.9 x 10^3 cells.ml^{-1} resulted in relatively small areas of cell adherence onto the surface of the scaffolds. A seeding density of 7.9 x 10^4 cell.ml^{-1} appeared superior, with large areas of spreading cells. A seeding density of 7.9 x10^5 cells.ml^{-1} resulted in overconfluence potentially leading to over-competition for space.

5.4.2 Three dimensional cell seeding of acellular scaffolds using ovine vascular cells

A seeding density of 7.9 X 10^4 cells.ml^{-1} for both cell types, seeded onto the luminal surface of the acellular scaffolds was felt to be the most suitable surface and density for 3D cell seeding; as experimental results had clearly demonstrated a significant number of cells adhered to the luminal surface and would be more likely to stand up to the forces of pulsatile flow within a bioreactor whilst having space for proliferation.

5.4.2.1 Ovine EC

Ovine EC successfully seeded onto the luminal surface in all three scaffolds as seen by the typical “cobblestone” appearance of a confluent EC monolayer on the luminal surface of each scaffold (Figures 49-51). In all three replicate scaffolds, the majority of cells were stained with calcein-AM (green), indicating that these EC were viable at 48 hours. In Figure (40), red staining from ethidium homodimer-1 was not seen indicating that no dead cells were present in the characterised area.

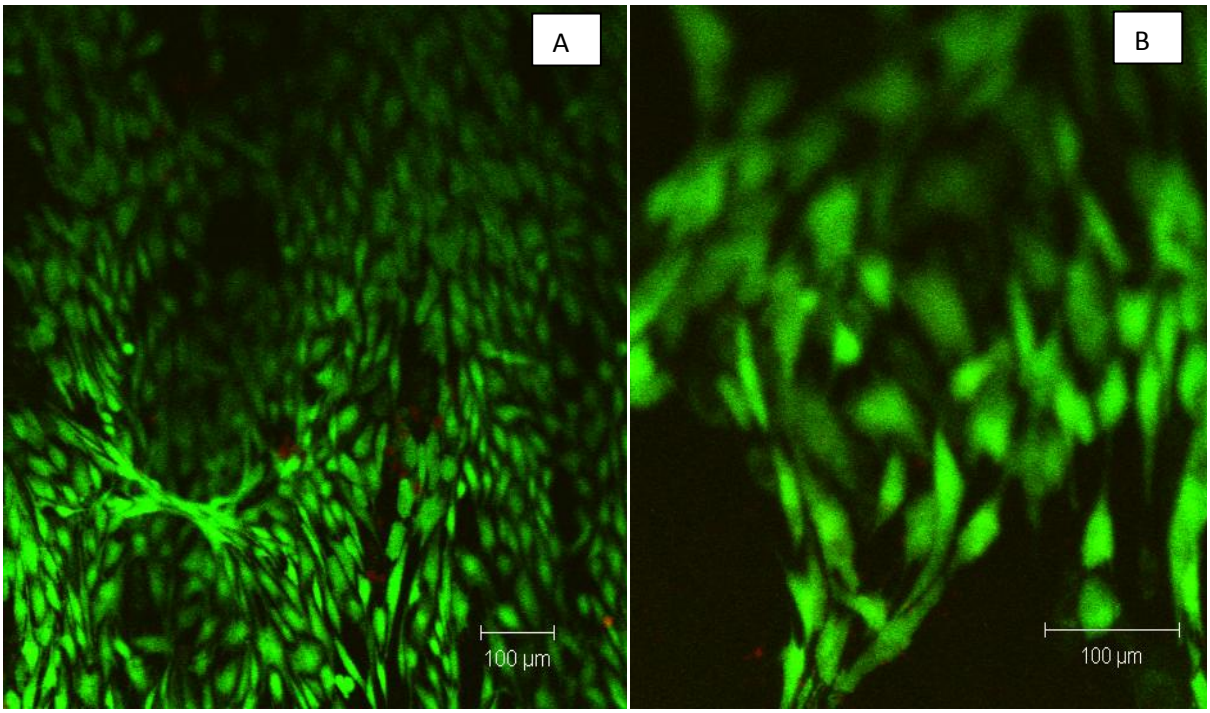

Figure 49 . Photomicrographs of scaffold (1) seeded with EC and stained using the Live / Dead ® assay. Photomicrographs A + B demonstrate confluent EC staining with calcein AM.

Photomicrographs A + B in Figure (50) show large areas of confluent EC stained with calcein AM (green) indicating that the majority of seeded cells were viable on this scaffold. There are small areas of ethidium staining (red) indicating the presence of dead cells on the scaffold.

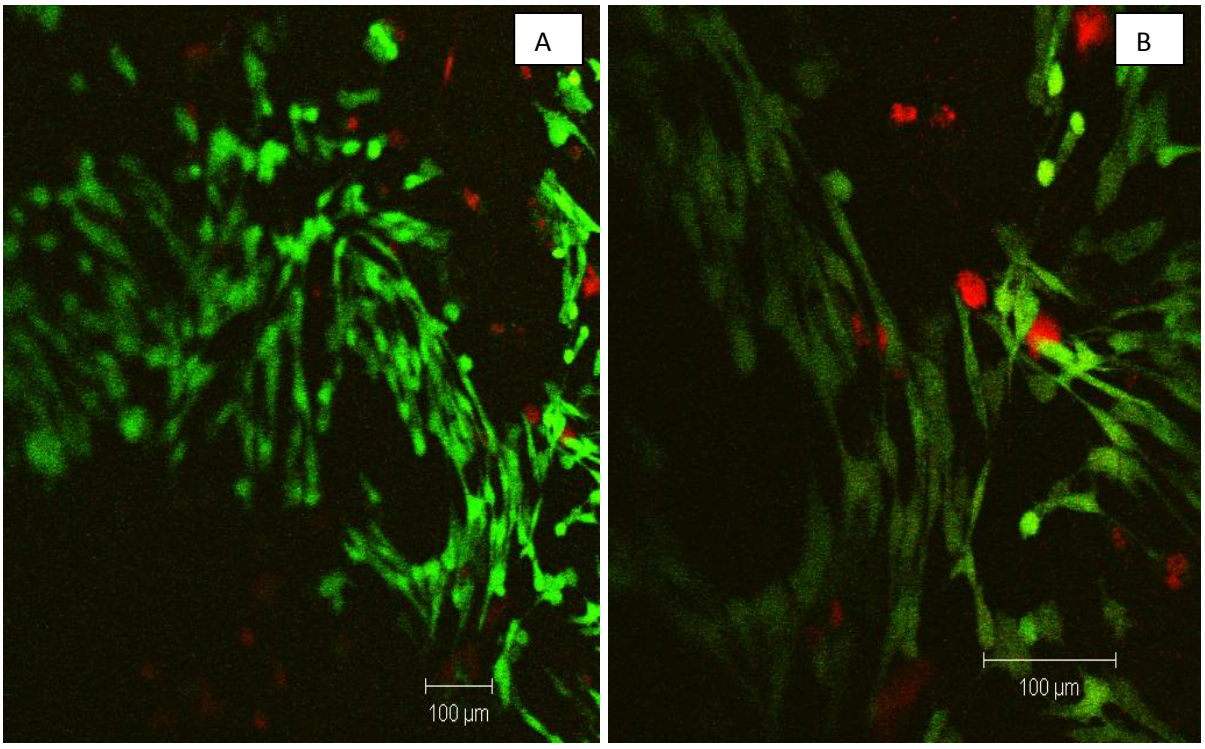

Figure 50. Photomicrographs of scaffold (2) seeded with EC and stained using the Live / Dead ® assay.

Photomicrographs A + B in Figure (51) again show large areas of confluent EC stained with calcein AM (green) indicating that the majority of seeded cells are viable on this scaffold. Again, there were only small areas of ethidium staining (red) indicating the presence of dead cells on the scaffold.

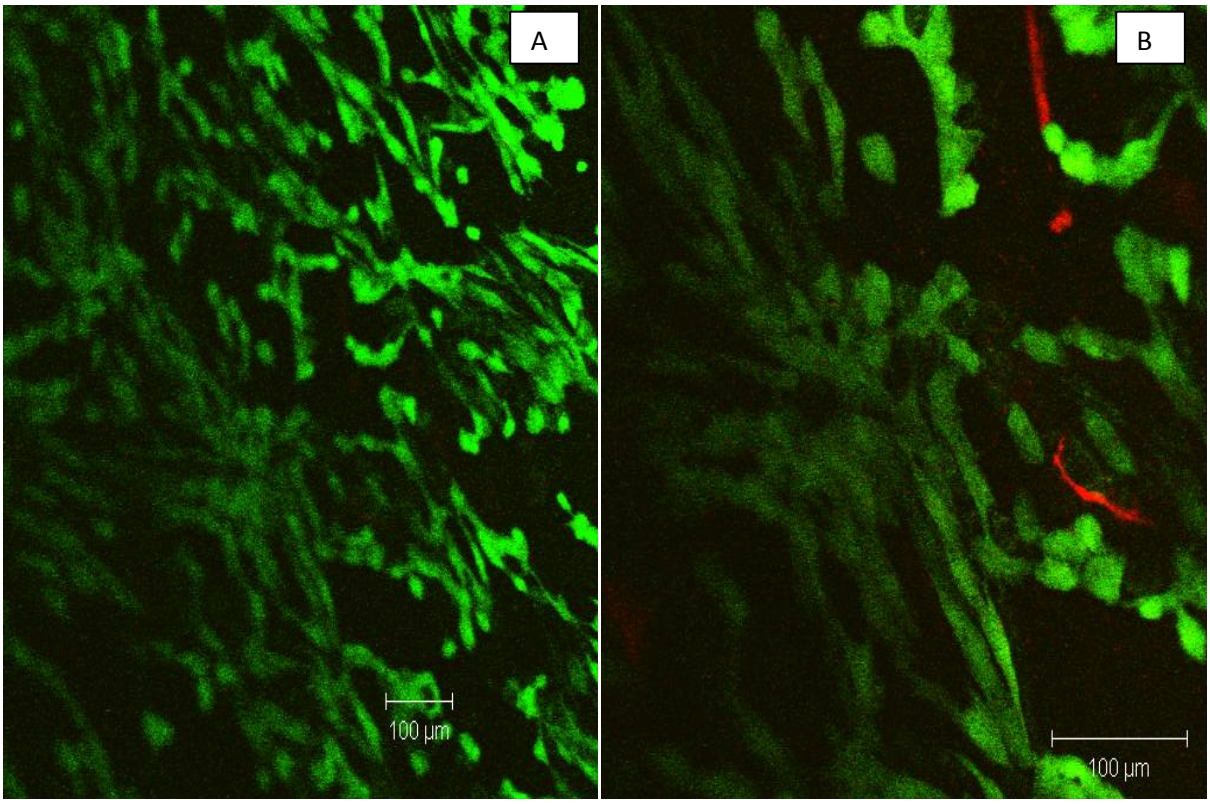

Figure 51. Photomicrographs of scaffold (3) seeded with EC and stained using the Live / Dead ® assay.

The results confirmed that EC successfully adhered to all three scaffolds at a density of 7.9 x 10^4 cells.ml^{-1} using the dynamic 3D seeding technique. Seeded cells were confluent on all scaffolds at 48 hours sampling. Live / Dead ® staining confirmed that the majority of EC cells were viable at 48 hours post seeding. Some dead cells were present in scaffolds two and three and this was not unexpected given that seeded cells would have been in differing phases of the cell "life" cycle.

5.4.2.2 Ovine SMC

Ovine SMC were also successfully seeded onto the luminal surface of all three replicate scaffolds as seen by the typical "spindle-shape" appearance of a confluent SMC monolayer on the luminal surface of each scaffold (Figures 52-54). In all three scaffolds, the majority of cells were stained with calcein-AM (green), indicating that these SMC were viable at 48 hours. In Figure (52), red staining from ethidium homodimer-1 was not seen indicating that no dead cells were present in the characterised area.

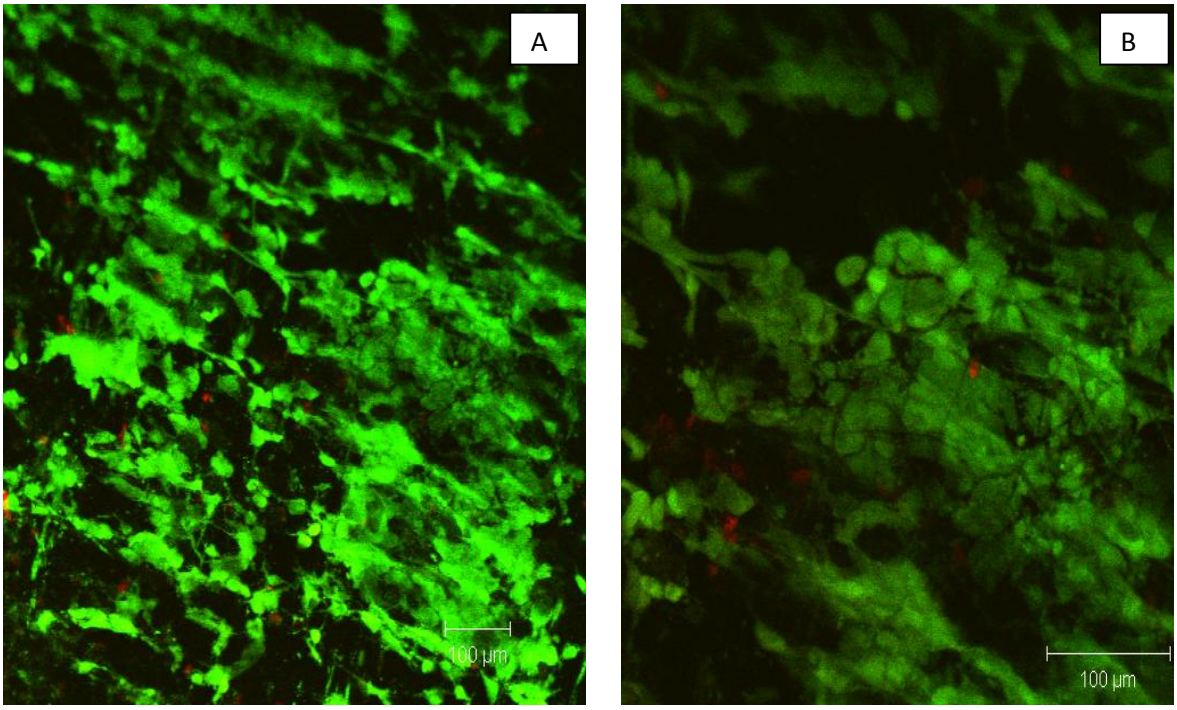

Figure 52. Photomicrographs of scaffold (1) seeded with SMC and stained using the Live / Dead ® assay. Photomicrographs A + B demonstrate large areas of confluent staining with calcein AM.

Photomicrographs A + B in Figure (53) show large areas of confluent SMC stained with calcein AM (green) indicating that the majority of seeded cells were viable on this scaffold. There were minimal areas of ethidium staining (red) indicating the presence of dead cells on the scaffold.

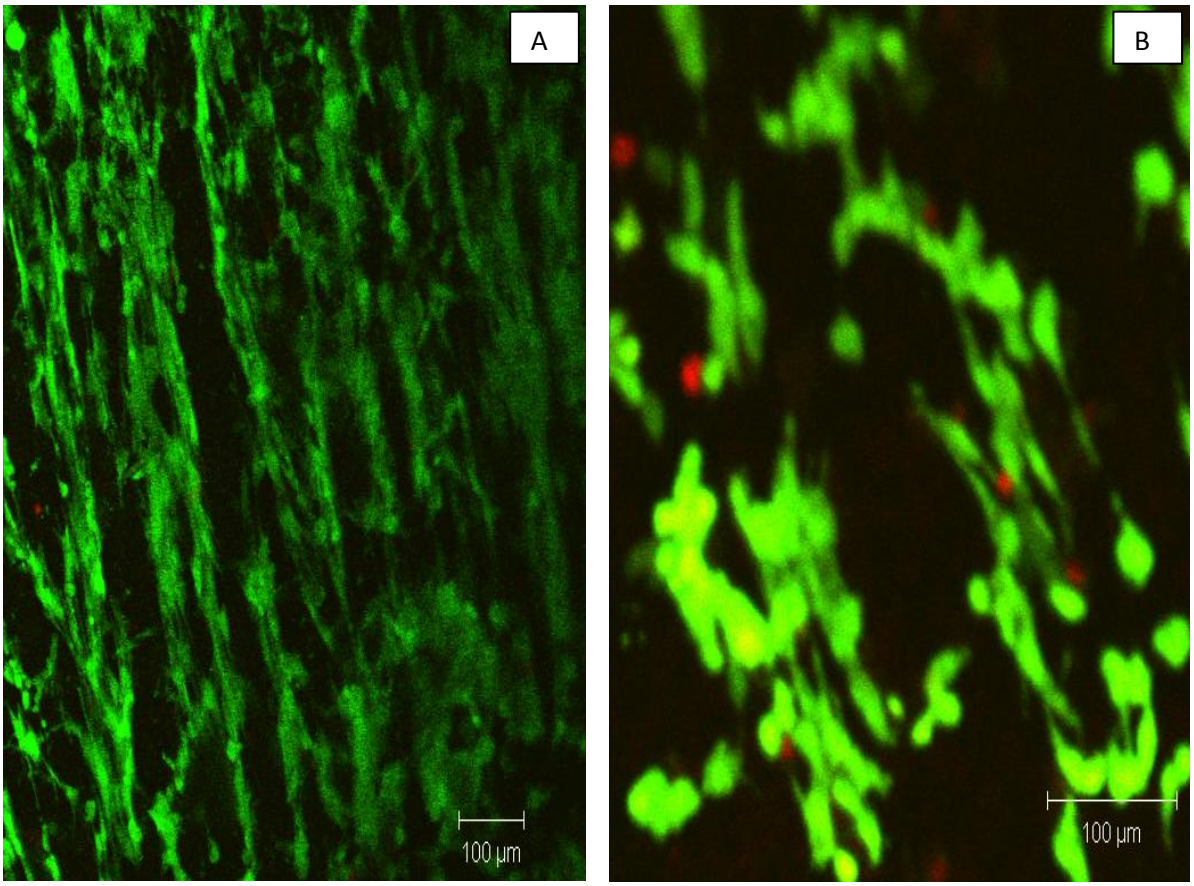

Figure 53. Photomicrographs of scaffold (2) seeded with SMC and stained using the Live / Dead ® assay.

Photomicrographs A + B in Figure (54) again show large areas of confluent staining with calcein AM (green) indicating that the majority of seeded cells were viable on this scaffold. There were minimal areas of ethidium staining (red) indicating the presence of dead cells on the scaffold.

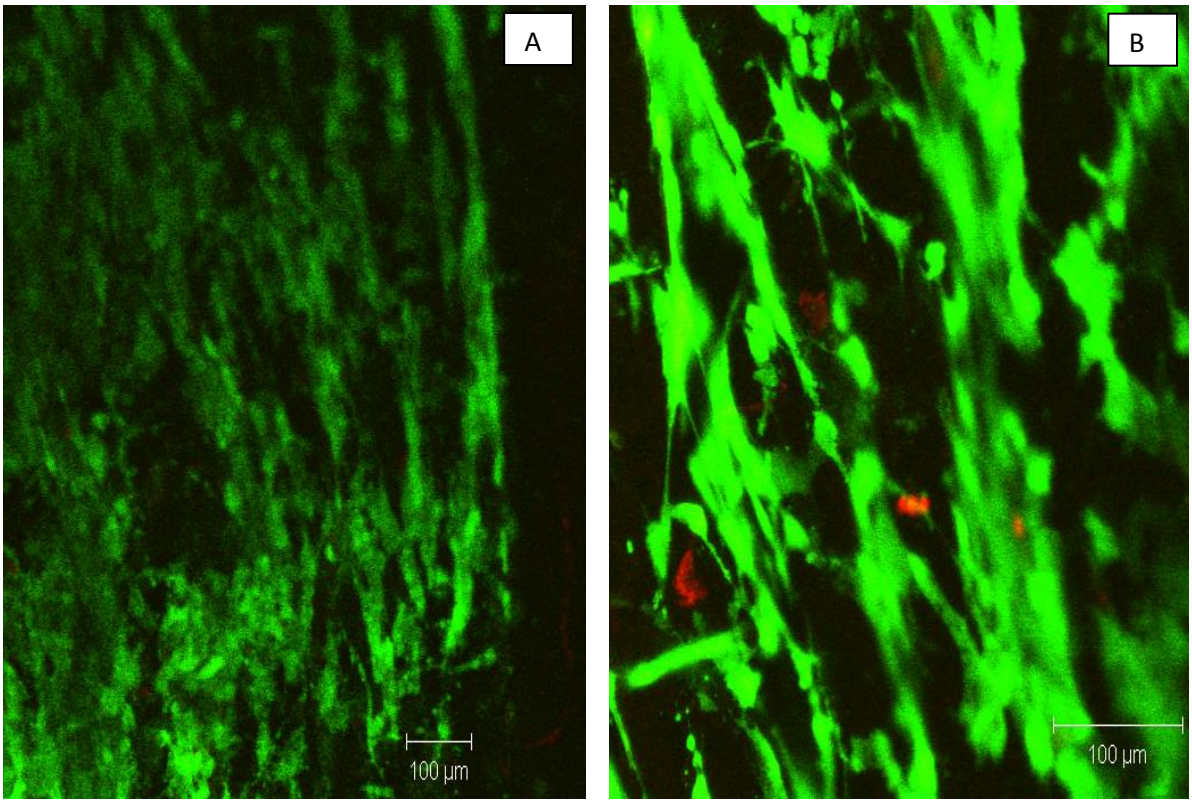

Figure 54. Photomicrographs of scaffold (3) seeded with SMC and stained using the Live / Dead ® assay.

The results confirmed that SMC successfully adhered to all three scaffolds in a confluent manner at a density of 7.9 x 10^4 cells.ml^{-1} using the dynamic 3D seeding technique. Live/Dead ® staining confirmed that the majority of cells were viable at 48 hours post seeding. Again, some dead cells were present in scaffolds two and three and this was not unexpected given that seeded cells will be in differing phases of the cell “life” cycle.

5.4.3 Three dimensional dual dynamic cell seeding of decellularised porcine carotid arteries using ovine vascular cells

Following successful dynamic 3D seeding for both types of ovine vascular cells, the next stage was to attempt dual seeding of SMC and EC onto the luminal surface. SMC were seeded first for 72 hours, followed by EC seeding for 48 hours.

A Live / Dead ® assay was performed but did not demonstrate the presence of adherent cells. This could have occurred for three possible reasons; experimental error, loss of the

cell monolayer during processing or simply, a lack of cell adherence. Histological assessment was therefore performed to assess for the presence of adherent cells. H&E and DAPI staining of the seeded scaffolds confirmed the presence of cells on the surface of the scaffolds, however they were minimal in number and certainly well below confluence.

Figure's (55-56) show a small number of cells attached to the intimal surface with minimal penetration of cells into the medial layer.

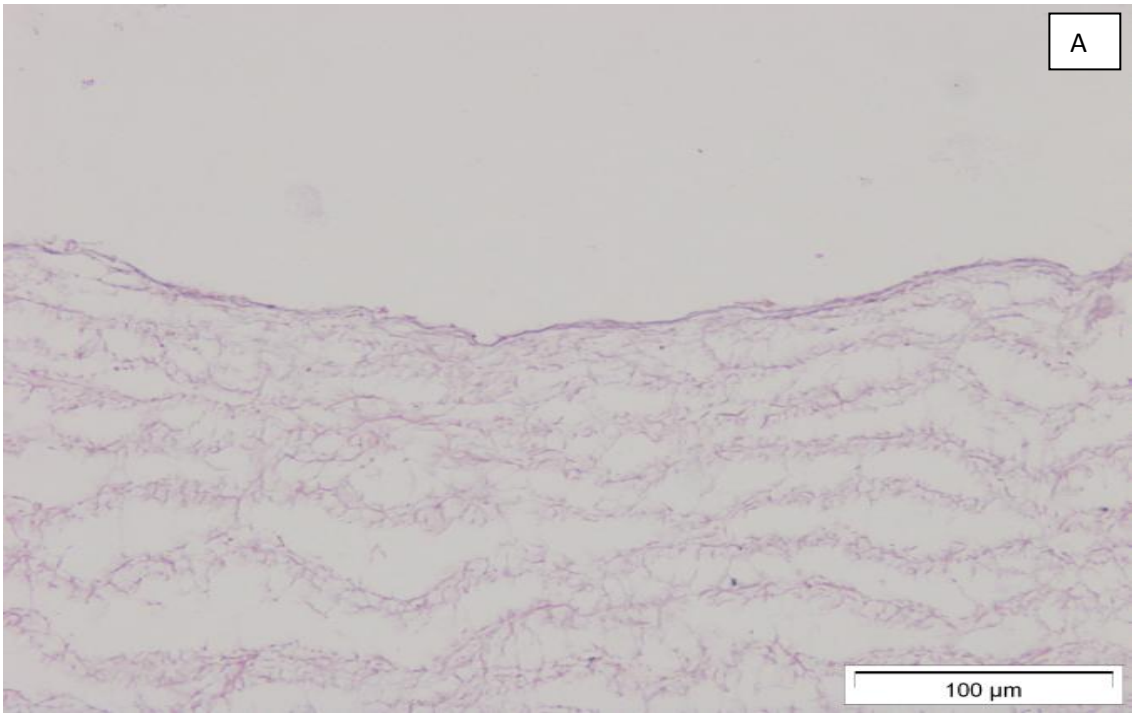

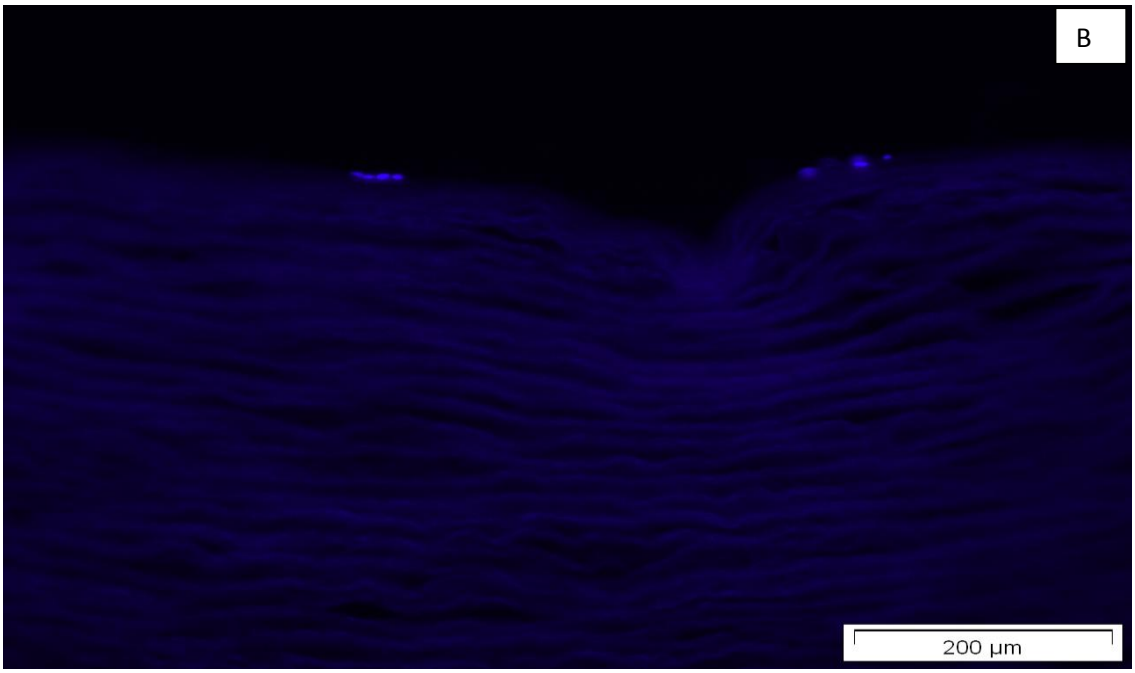

Figure 55. Images of H&E and DAPI stained sections of acellular scaffold (1) seeded with both SMC and EC. A + B; H&E and DAPI assessment both confirm the presence of cells on the intimal surface of the scaffold only.

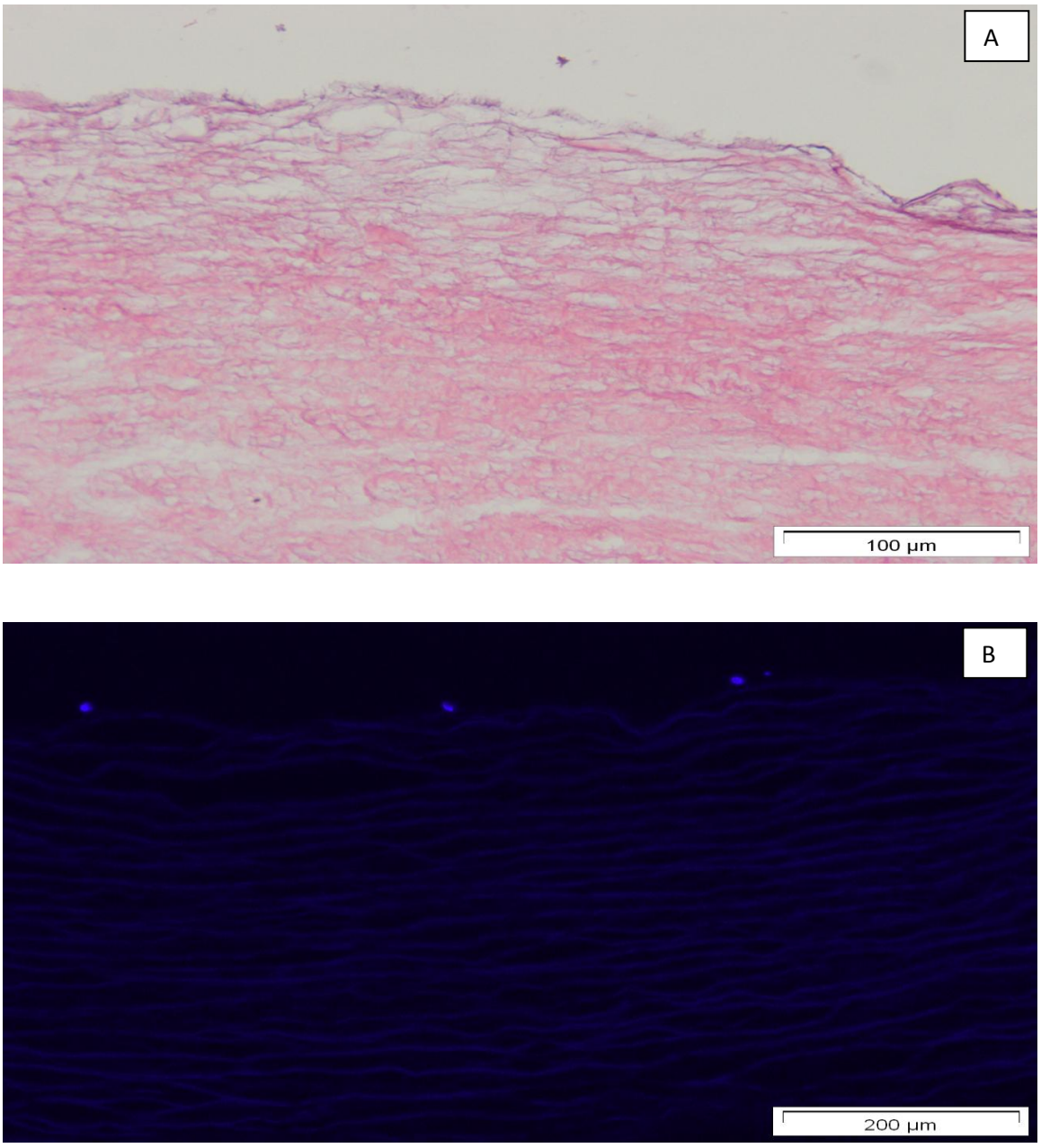

Figure 56. Images of H&E and DAPI stained sections of acellular scaffold (2) seeded with both SMC and EC. A + B; H&E and DAPI assessment both confirm the presence of cells on the intimal surface of the scaffold only.

Figure (57) does show the presence of cells both on the intimal surface of scaffold three, but unlike scaffolds one and two, there was evidence of cell penetration into the deeper medial layers. Again however, cells were minimal in number and failed to show any degree of confluent growth.

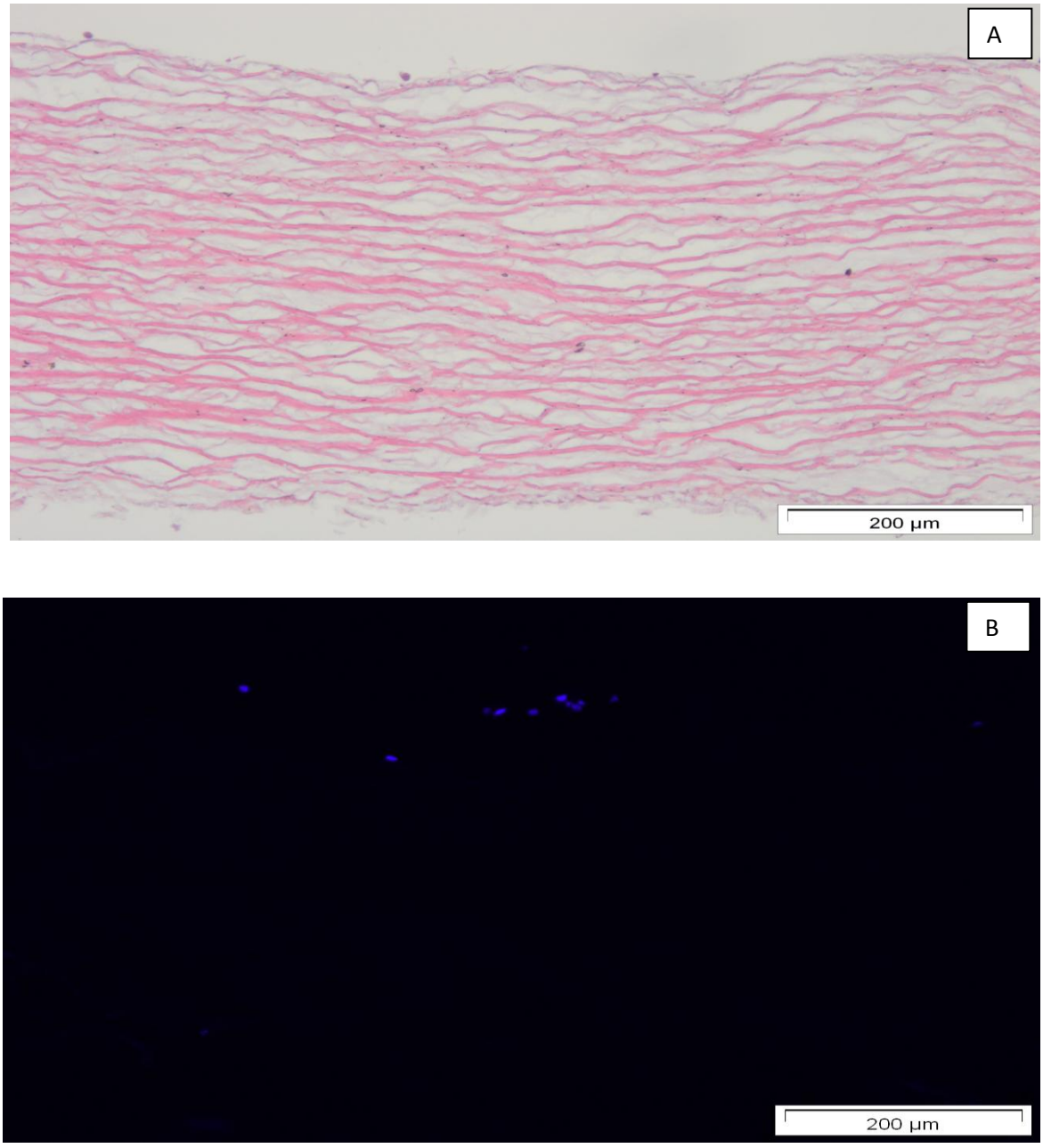

Figure 57. Images of H&E and DAPI stained sections of acellular scaffold (3) seeded with both SMC and EC. A; H&E assessment of scaffold (3) confirms penetration of cells below intimal layer. B; DAPI assessment confirms the presence of cells on the intimal surface of the scaffold only.

Overall, the results for dual (3D) seeding of the scaffolds was disappointing when compared to the results for 2D and 3D single-layer seeding. Scaffolds failed to show significant levels of cell adherence with cell density well below confluence.

5.5 Discussion

It was decided to start seeding experiments with a 2D "static" approach to determine whether ovine vascular cells could successfully attach to the surfaces of the acellular porcine scaffolds. Both luminal and adluminal surfaces were assessed. Furthermore, 2D seeding allowed the determination of optimal seeding densities for subsequent 3D dynamic cell seeding. The seeding densities used in the study were based on densities used in successful seeding experiments on decellularised porcine arterial tissue reported in the literature (McFetridge *et al*., 2004; Shimizu *et al*., 2007; Heine *et al*., 2011; Nitsan *et al*., 2012).

Results from 2D seeding confirmed successful attachment of both types of ovine vascular cells to the luminal matrix of the acellular scaffolds. This was an important finding as firstly, successful cell seeding was paramount in order to allow future experiments to continue, and secondly, the cells and scaffold required no functionalisation in order for cell adherence to occur. The latter was a particularly key finding if the graft were to become a clinically viable product as not having to modify cell adherence would reduce the time and expense required to seed the scaffold in a commercial setting.

For both types of cells, a seeding density of 7.9×10^4 cell.ml^{-1} appeared superior, with large areas of spreading, subconfluent cells. This was consistent with similar experiments reported in the literature that focus on the seeding of vascular cells onto decellularised PCA. McFetridge *et al* (2004) and Heine *et al* (2011) for example, successfully seeded human EC and SMC seeded onto PCA using a seeding density of 10^3-10^4cells.ml^{-1}.
In this study, a seeding density of 7.9×10^3 cells.ml^{-1} resulted in areas of under-confluent cell growth following culture whilst a density of 10^5 cell.ml^{-1} resulted in overconfluence, potentially leading to over-competition for space and subsequent cell death. A seeding density of 7.9×10^4 cells.ml^{-1} was felt to be optimal and therefore used for subsequent 3D seeding experiments. SMC growth on the luminal surface was superior to the adluminal surface so it was decided that future 3D seeding experiments would be limited to the luminal surface only. The reduced cell adherence seen on the adluminal surface was likely secondary to the loose arrangement of collagen matrix found in the adventia as compared

to the basement membrane of the internal elastic lamina. A more loose arrangement of the collagen matrix would have reduced the effectiveness and increased the time required for cellular integration and adherence. Furthermore, the SMC would have to penetrate through the adventia, medial layer and through the basement membrane of the internal elastic lamina before reaching the intimal surface, significantly increasing the culture time if dual-seeding is to be performed.

Following successful 2D seeding of acellular scaffolds and development of an optimal seeding density, 3D dynamic seeding experiments began. If the scaffold is to be successful as a SD graft, it is essential that the entire (3D) luminal surface is effectively seeded with vascular cells. The first set of dynamic 3D seeding experiments were performed on the luminal surfaces of the acellular scaffolds, seeding EC and SMC separately. This stage was performed to help determine efficacy of the dynamic seeding technique, determine seeded cell viability and to act as a control for potential future dual seeding experiments. A dynamic seeding approach was used to provide shear stress to the vascular cells which has been shown to increase cell adherence and proliferation in the literature (Bader *et al*., 2000; Hsu *et al*., 2005; Amiel *et al*., 2006; Nitsan *et al*., 2012). Using a dynamic seeding technique, again the scaffold surfaces became populated with seeded, viable cells as demonstrated with confluent cells stained with the Live/Dead® assay. As it was clear that the scaffolds could be successfully seeded in a 3D dynamic fashion, experiments then began to establish a dual seeding method. The rationale for dual-seeding was derived from current literature on vascular cell-seeding of a variety of biological scaffolds.

As previously discussed, the formation of ECM on a graft surface is important for cell attachment and is secreted by both EC and SMC. Studies have shown that lining a graft with SMC prior to the seeding of EC improves the subsequent retention of EC to the graft (Yu *et al*., 2001, 2003; Stephan *et al*., 2006; Aper *et al*., 2007). The ECM laid down by SMC provides the graft with elastic recoil and tensile strength (Stephan *et al*., 2006), whilst the EC reciprocally interact with SMC, to maintain the ECM (Aper *et al*., 2007).

The dual-seeding experiments failed to demonstrate that the scaffolds could be successfully dynamically seeded using the developed technique. Overall, a distinct lack of penetration of the SMC through the scaffold layers was seen, with only a small number of cells seeding onto the luminal surface. Many factors exist that may explain why the results

seen in static seeding were not reproduced in dual-seeding. Unfortunately, a lack of time severely limited the progress of dual-seeding experiments. If further time was available, longer incubation times prior to EC seeding may have allowed deeper penetration of the SMC into the scaffold layers and subsequently, a higher chance of EC adherence. Another possibility was that the SMC could not penetrate easily past the basement membrane of the intimal surface. Repeat experiments using longer seeding times would help clarify these two possibilities. Furthermore, immunohistochemical analysis of the scaffolds would demonstrate what population of cells had adhered to the scaffold and to what area. Although *in vivo* ovine SMC and EC are intimately related, it is unknown whether following the harvesting and seeding processes, the cells remain biocompatible to one another. It is also apparent in the literature that the interactions of EC and SMC show different species-specific behavior (Wallace *et al*., 2007; Pang *et al*., 2010; Zhao *et al*., 2010). Again if further time was available, static 2D seeding of the vascular cells would help establish that both sets of cells remain biocompatible to one another following harvesting and can proliferate as a co-culture. In retrospect, performing this experiment prior to commencing dynamic 3D seeding would have provided useful information regarding biocompatibility and incubation times, helping to plan dynamic 3D experiments more accurately.

In view of the numerous variables that may have affected the results of dynamic 3D seeding, if further time had been available, it would have been important to refine the technique (using some of the changes mentioned above) before declaring the technique unsuitable and attempting a different method. Certainly the dual-seeded scaffolds would have to show greater cell retention and scaffold penetration before pre-conditioning experiments in a vascular bioreactor could proceed.

The key and exciting finding in this part of the study was that the acellular surface of the scaffolds did not require functionalisation prior to seeding, for example with adhesive proteins such as fibrin or alteration in chemistry such as collagen crosslinking. This finding alone provides good support for the use of decellularised PCA as a suitable conduit for cell seeding and possible use as a vascular graft as it minimizes both production time and costs whilst maximizing reproducibility.

Chapter 6

Development of a perfusion bioreactor system

6.1 Introduction

Bioreactor's have become essential hardware in the development of tissue-engineered constructs. They are designed to maintain a culture environment to help maintain correct cellular phenotypes e.g temperature, humidity, O_2 and CO_2 levels and circulation of media to provide nutrition to cells and to remove waste products of cellular metabolism. They may also be designed to provide biomechanical functions such as flow, pulsatility and shear stress which pre-condition the cells and construct (Rademacher *et al*., 2001; Rashid *et al*., 2008). Ultimately, the main design of a bioreactor for tissue engineering purposes is to closely mimic the *in vivo* physiological conditions in order to assess the performance and function of tissue engineered constructs in such an environment.

When studying a conduit for potential use in the human circulation, the bioreactor should be designed to match the physiological parameters of a typical fit, thirty year old, 70Kg male (the accepted model used in science used when performing studies pertaining to human physiological parameters). Such conditions would therefore require an environmental temperature of between 36.5-37ºC, pulsatile flow of between 70-80 strokes per minute generating a pressure of 100-120 mmHg. As such, many studies in the literature involving the use of bioreactors will aim for the parameters described (Bader *et al*.,2000; Yu *et al*.,2001; Hsu *et al*., 2004; Liao et al., 2008; Yazdani *et al*., 2008). In many such studies the actual design and set up of the bioreactor is not well described, with often only the parameters and environmental conditions being reported. A few studies such as those of Butler *et al.* (2009) and Williams *et al.* (2004) describe their bioreactor set up in more detail but in all cases, the bioreactors are customised for purpose. In these studies, the only single common denominator of each bioreactor is that a peristaltic pump is used, but set up and design after that remains highly variable and experiment specific.

A simple bioreactor developed by Wake Forest Institute for Regenerative Medicine, North Carolina in the United States was used in the study. The bioreactor has been used previously for exploratory experiments within IMBE and the rationale for its use in this study was that it was simple in design, would allow initial basic experiments to be

performed e.g assembly and sterility and that the components were safe to sterilise for repeated use and consumable components were cheap to purchase. Due to the complexity of more sophisticated bioreactors, it was felt appropriate to become familiar with a bioreactor, simple in its design to perform initial experiments before progressing to the use of more complex systems and experiments.

6.2 Aims and Objectives

The aims and objectives of the chapter were the following:

1) To assemble and operate the Wake Forest Vascular Bioreactor under aseptic conditions

2) To evaluate the sterility and performance of the Wake Forest Vascular Bioreactor over an extended period of time

6.3 Materials and Methods

6.3.1 Bioreactor circuit

The bioreactor perfusion circuit was simple in its design. A central pump circulated fluid / culture medium from a reservoir through the perfusion chamber (Figure 58).

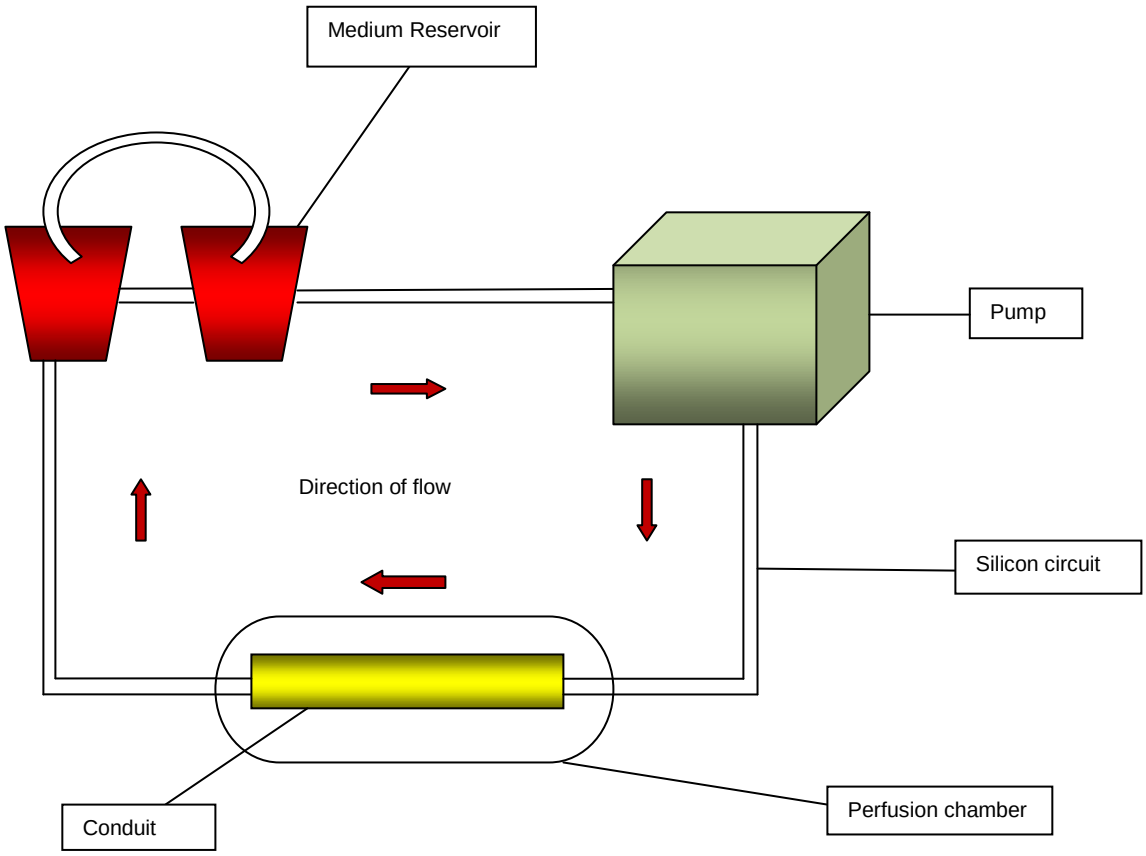

Figure 58. Basic schematic of the Wake Forest bioreactor perfusion system.

6.3.2 Bioreactor components

The various components of the bioreactor are shown in Figure 59.

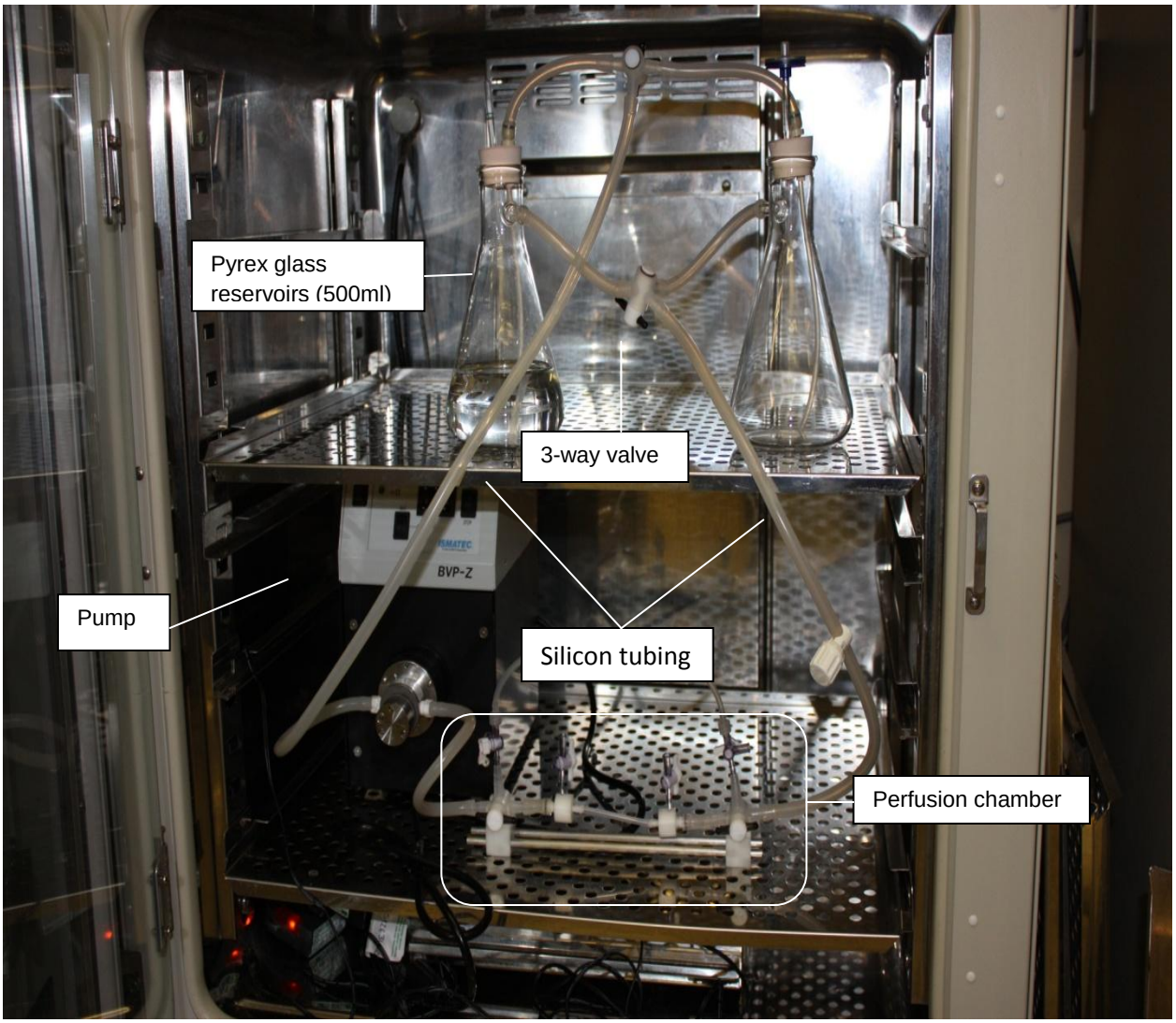

Figure 59. Photograph of assembled Wake Forest bioreactor housed within an incubator.

The pump circulated medium housed in two x 500ml Pyrex glass reservoirs. To ensure an adequate supply of fresh medium, a 3-way valve controlled which reservoir medium was circulated from. Medium was then circulated through the perfusion chamber and back to the reservoir. Assembly and components of the perfusion chamber are shown in Figure (60).

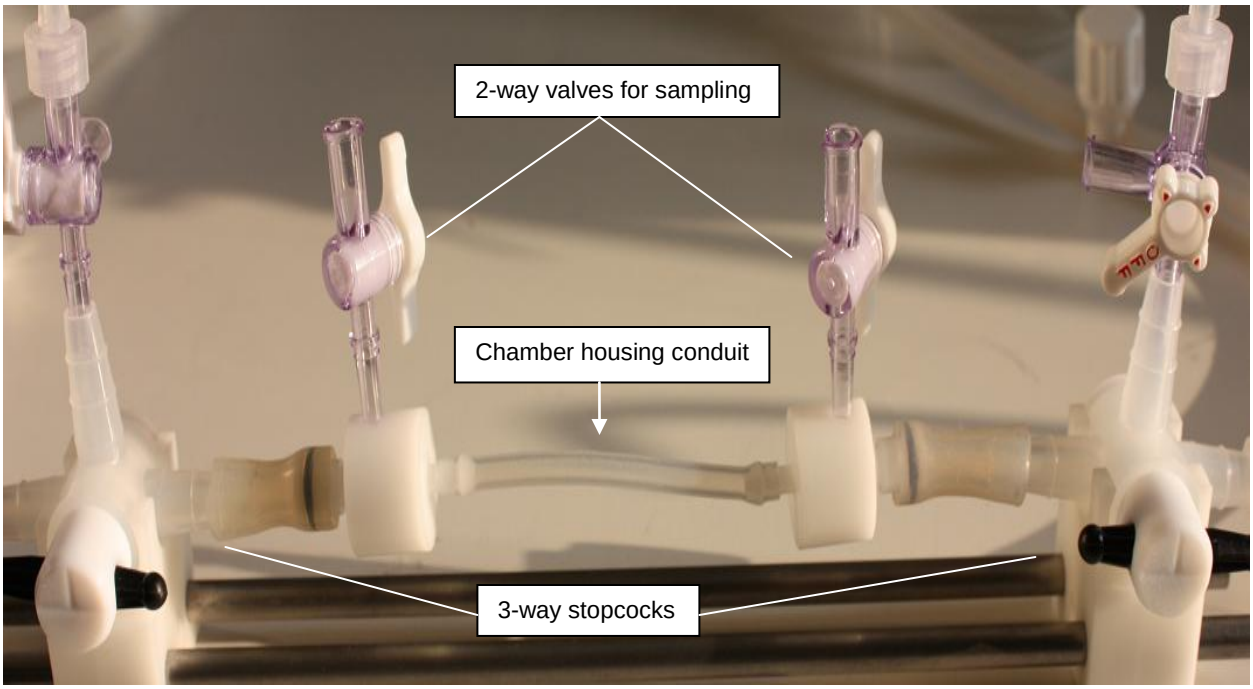

Figure 60. Photograph demonstrating key components of the perfusion chamber.

The presence of 3-way stopcocks allowed the temporary cessation of flow through the chamber (should the conduit need to be changed for example). The 2-way valves allowed sampling of the medium without having to cessate flow.

6.3.3. Bioreactor assembly

All bioreactor components were autoclaved at 121º, 15 psi for 20 minutes prior to use. The Class II safety cabinet and incubator were cleaned extensively with Virkon and then Trigene prior to use. Components were then assembled aseptically in the Class II safety cabinet (Figure 61). Once assembled, the bioreactor components were transferred into the incubator and attached to the pump. DMEM (500 ml) was placed into each of the medium reservoirs and 50 ml was injected into the system to prime the pump. After the pump had started and medium was circulating, the system was checked for leaks. Once the system had been checked for leaks, the whole system was sprayed with Trigene and incubated at 37°C with 5% (v/v) CO_2 in air.

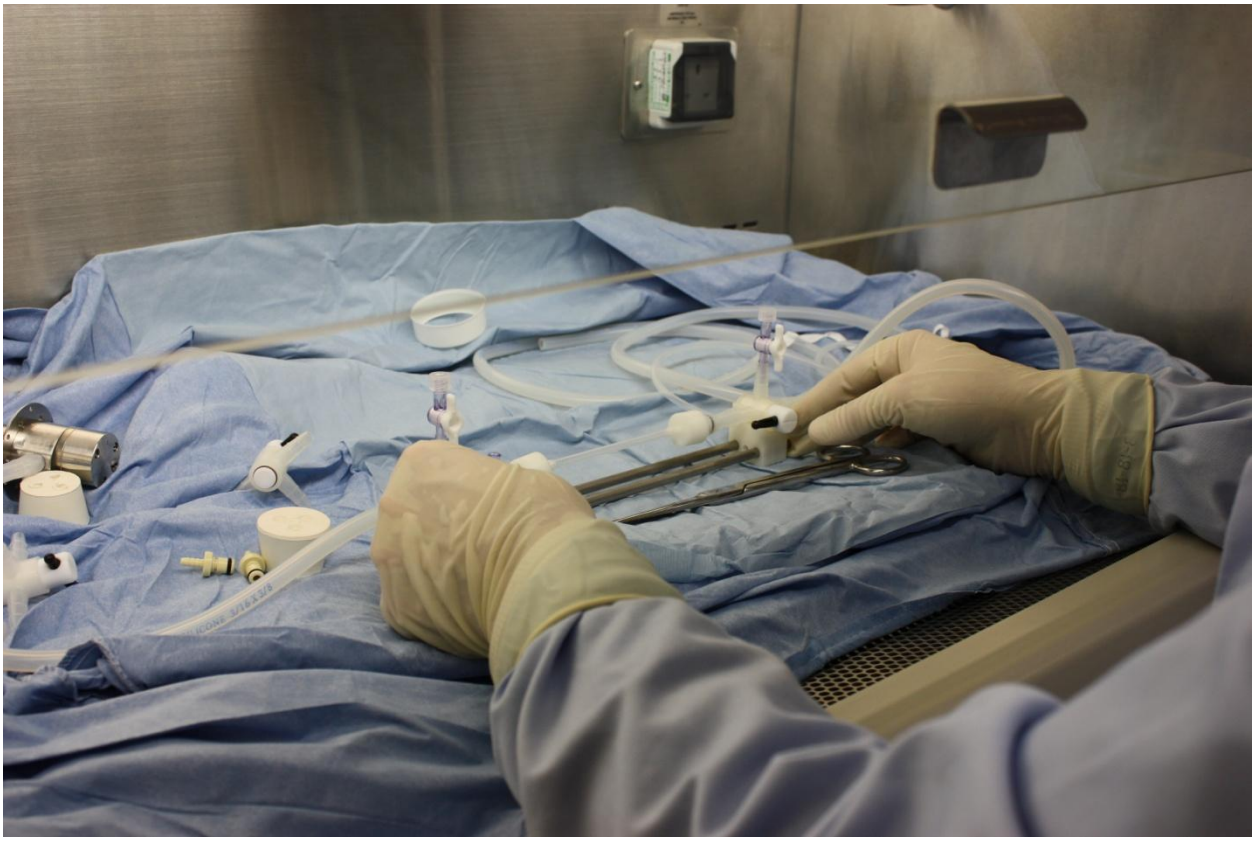

Figure 61. Photograph demonstrating aseptic assembly of bioreactor components (note sterile drapes, gloves and gown).

6.3.4 Sampling of Bioreactor for sterility assessment

During all bioreactor runs, the bioreactor was kept within a closed incubator that was only opened during sampling to limit contamination. In addition to inspection of the medium for obvious contamination (cloudiness), 5 ml samples of medium were taken from the bioreactor at 24 hrs and 48 hours. Medium was aspirated from the two-way valves situated above the housing chamber (Figure 60) and this was performed as aseptically as possible using sterile gloves and syringes. Samples were plated out onto four different agar plates and incubated to assess for bacterial and fungal growth (nutrient, fresh blood, heated blood, sabouraud agar).

6.4 Results

The bioreactor was assembled with medium three times and assessed for sterility. The first run with DMEM alone and the second and third runs with DMEM and antibiotics.

6.4.1 Sterility of Bioreactor Run (1). DMEM only

It was clear at 48 hours that the medium was contaminated as it had become cloudy. Following incubation for 48 hours, it was evident that plates from both samples at 24 and 48 hours had become contaminated with micro-organisms (Figure 62).

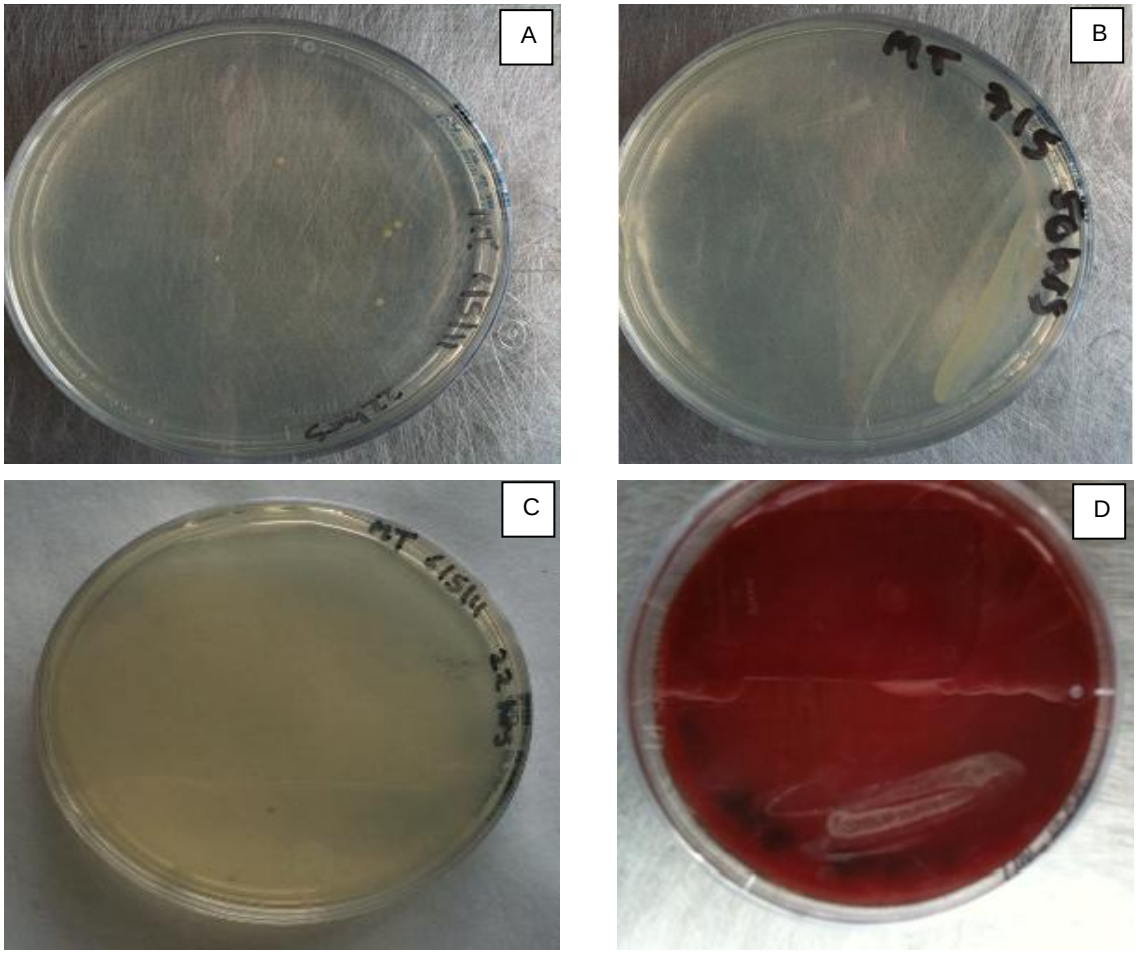

Figure 62. Representative plates from samples at 24 hours and 48 hours demonstrating bacterial and fungal growth. A+C; Nutrient agar showing colonies of bacterial growth, B; Sabouraud agar showing fungal growth, D; Fresh blood agar showing colonies of bacterial growth.

6.4.2 Sterility of Bioreactor Run (2). DMEM and antibiotics

It was evident from run 1 that the bioreactor perfusion system rapidly became contaminated with micro-organisms. For the second run, 15 ml of 100 $U.ml^{-1}$ penicillin and 100µg.ml^{-1} streptomycin was added to 500 ml of DMEM in an attempt to reduce contamination (300 $U.ml^{-1}$ streptomycin, 300 $U.ml^{-1}$ penicillin). Anti-fungals were not added to the medium at this stage. It was decided to not sample the circulating medium as frequently as sampling itself may have been a contributing factor towards contamination. Therefore the medium was viewed daily to asses for gross contamination and sampled at one week. Daily inspection of medium did not demonstrate evidence of gross contamination at one week. Samples were taken at seven days and again, plated onto four different agar plates (nutrient, fresh blood, heated blood and sabouraud agar) and incubated to assess for microbial growth for 48 hours (Figure 63).

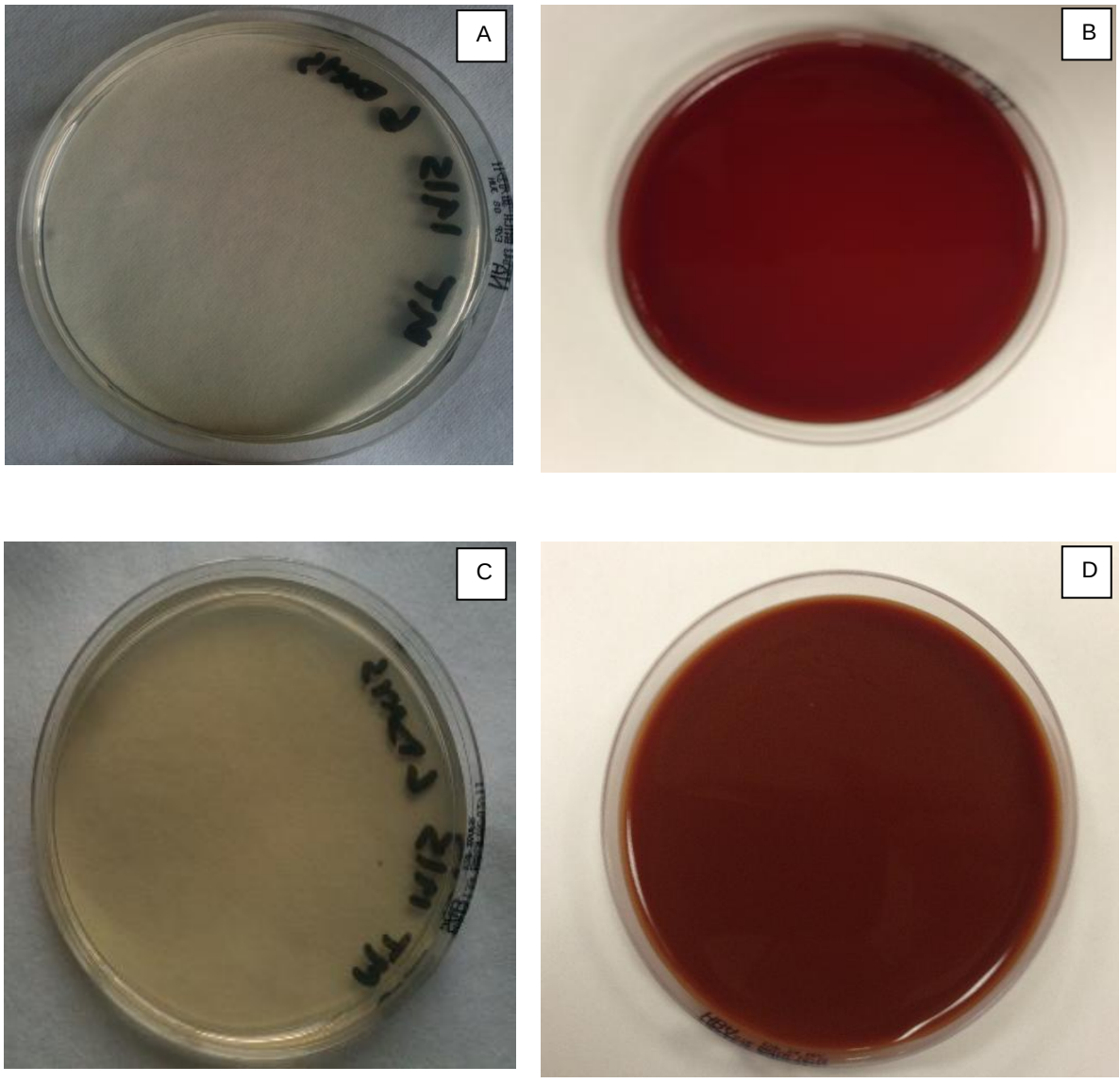

Figure 63. Agar plates demonstrating a lack of micro-organism growth at one week post sampling at 48 hours post incubation. A; Nutrient agar, B; Fresh blood agar, C; Sabouraud agar; D; Heated blood agar. No microbial growth is visible on any of the four plates.

At seven days, there was no evidence of microbial contamination of medium, therefore the run was continued for a further week. At day 18, medium appeared cloudy and so repeat samples were taken and plated onto agar to assess for microbial growth (Figure 64).

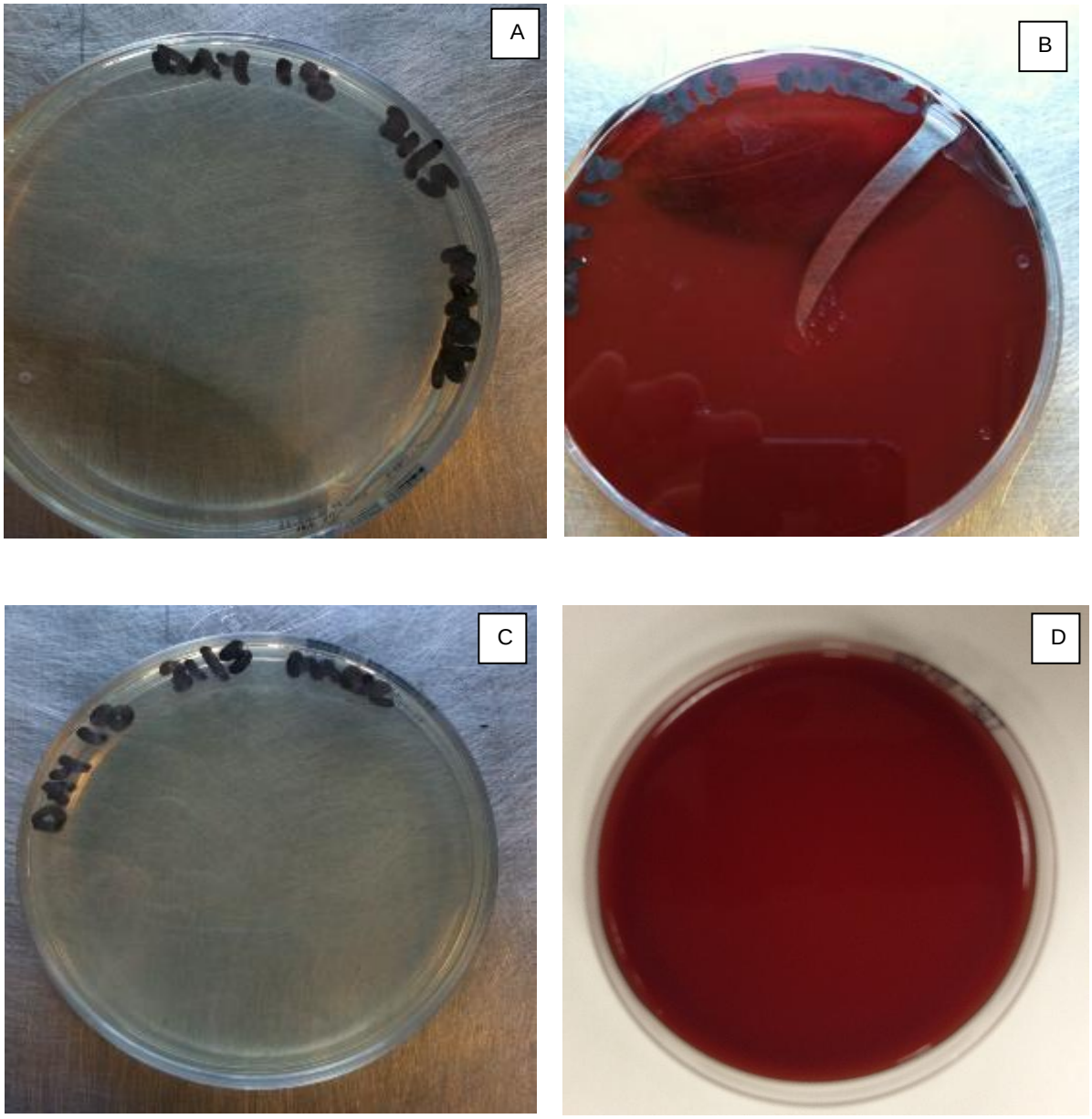

Figure 64. Agar plates demonstrating a lack of micro-organism growth at Day 18 post sampling at 48 hours post incubation. A; Nutrient agar, B; Fresh blood agar (cracked due to heat), C; Sabouraud agar. D; Heated blood agar. No microbial growth is visible on any of the four plates.

Results of run 2 confirmed that the addition of antibiotics to the circulating medium improved the contamination-free period from 24 hours to 18 days.

A third run was performed to determine if the results seen in run 2 were reproducible.

6.4.3 Sterility of Bioreactor Run (3). DMEM and antibiotics

Based on the success of run 2, it was decided to repeat the sterility run under the same bioreactor conditions to determine if sterility of the system was reproducible. As for the second run, 15 ml of 100 $U.ml^{-1}$ penicillin and 100$\mu g.ml^{-1}$ streptomycin was added to 500ml of DMEM. Anti-fungals were not added to the medium. Again, the circulating medium was viewed daily to asses for gross contamination and sampled at one week. Daily inspection of medium did not demonstrate evidence of gross contamination at one week. Samples were taken at seven days and again, plated onto four different agar plates (nutrient, fresh blood, heated blood and sabouraud agar) and incubated to assess for microbial growth for 48 hours (Figure 65).

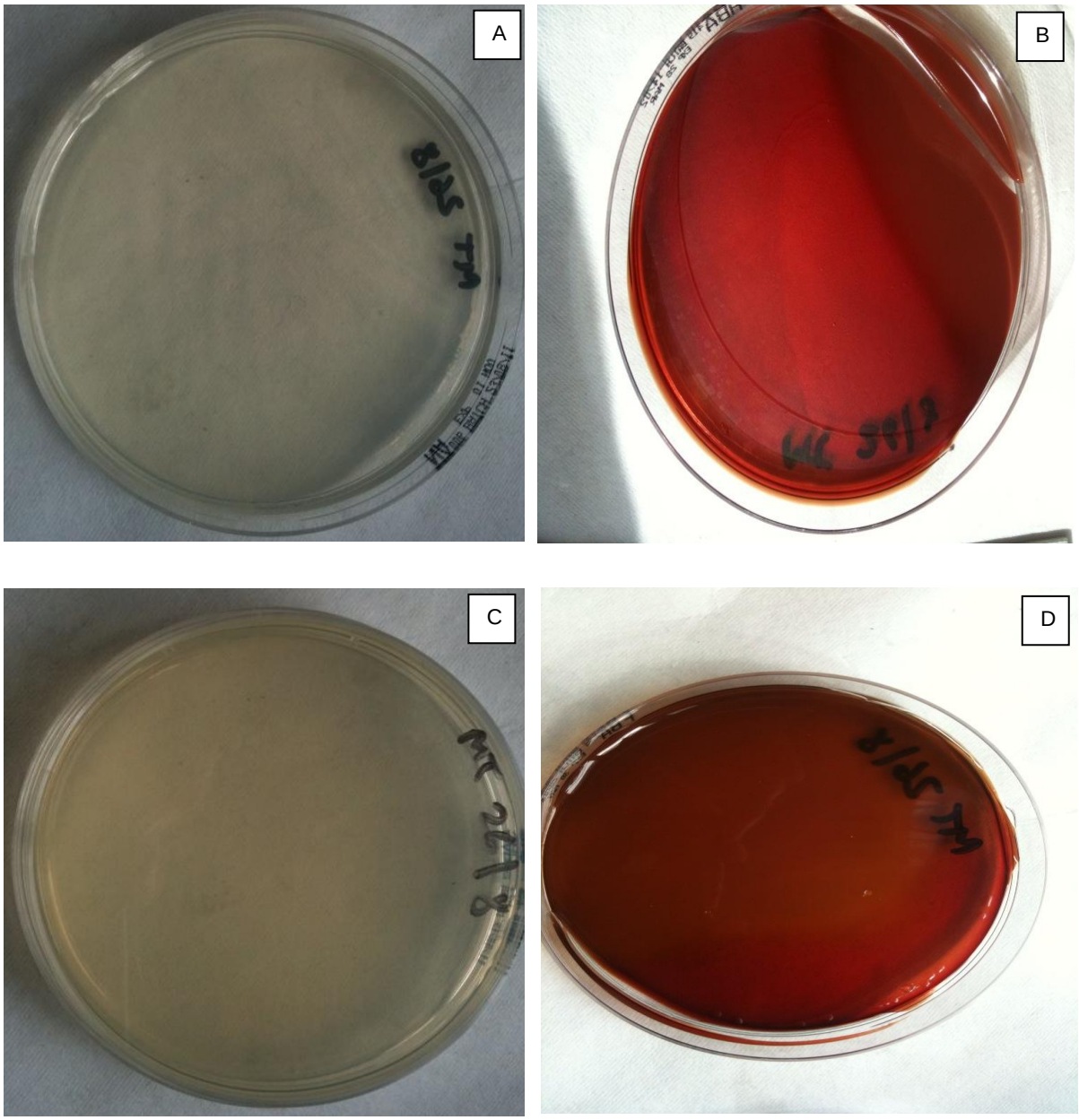

Figure 65. Agar plates demonstrating a lack of micro-organism growth at 48 hours post incubation. A; Nutrient agar, B; Fresh blood agar (cracked due to heat), C; Sabouraud agar. D; Heated blood agar (cracked due to heat). No microbial growth is visible on any of the four plates.

At seven days, there was no evidence of microbial contamination of the medium, therefore the run was continued for a further week. At day 14, medium appeared clear and repeat samples were taken and plated onto agar to assess for microbial growth.

No growth was visible on the agar plates at 48 hours post incubation (Figure 66) confirming a lack of contamination of medium. Unfortunately there was a disturbance to the power supply to the bioreactor pump on the night of day 15 and so the experiment could not continue.

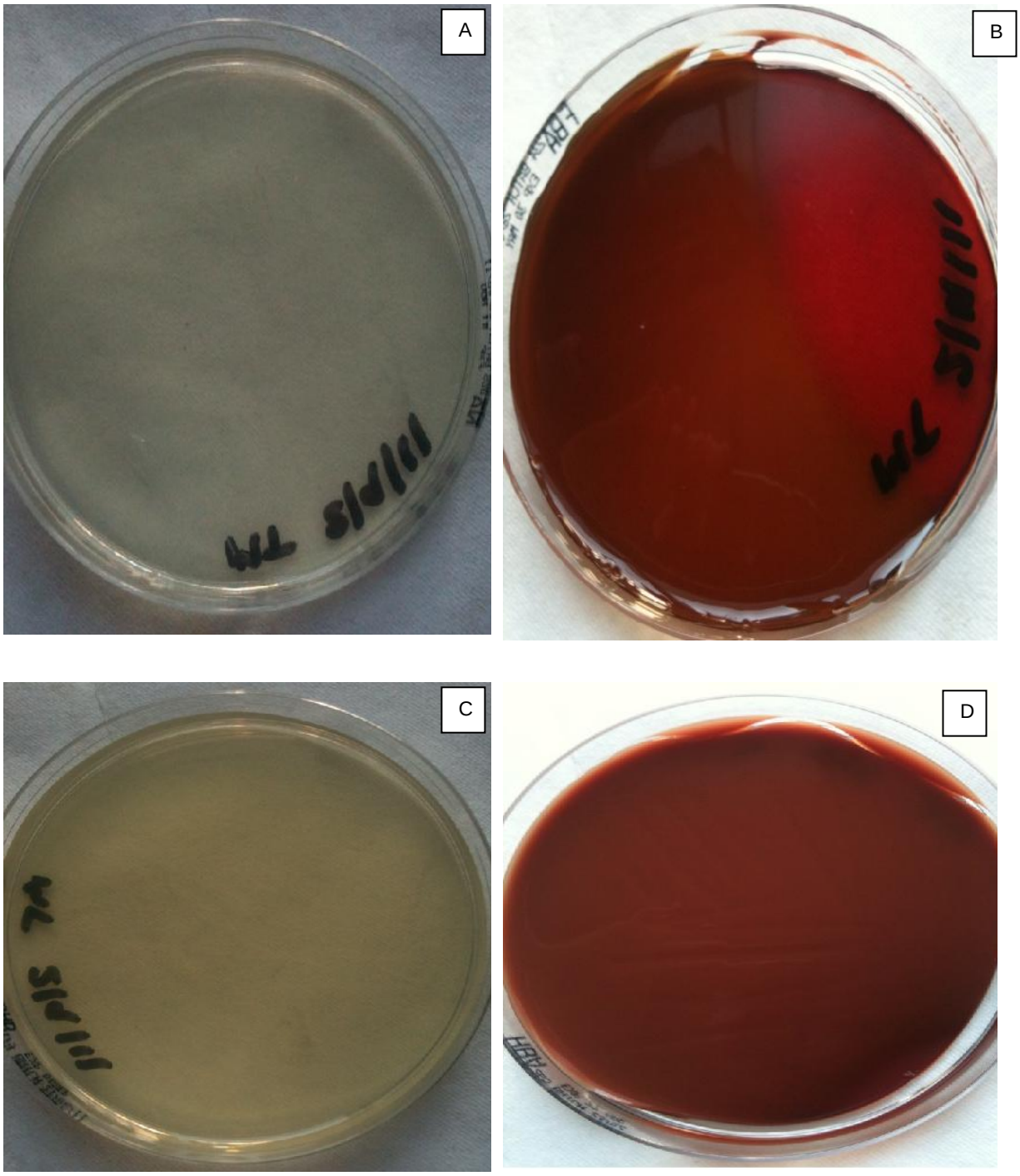

Figure 66. Agar plates demonstrating a lack of micro-organism growth at 48 hours post incubation. A; Nutrient agar, B; Fresh blood agar (cracked due to heat), C; Sabouraud agar. D; Heated blood agar (cracked due to heat). No microbial growth is visible in any of the four plates.

6.5 Discussion

The aims of this part of the study were achieved, namely that it was possible to assemble a simple bioreactor circuit that could be kept free from bacterial and fungal contamination for approximately two weeks. Keeping circulating medium free from microbial growth is essential in any bioreactor to prevent the experiment and any subsequent data from being compromised. Housing the bioreactor within an incubator situated in a busy working laboratory was not ideal however and likely contributed to the speed of contamination found in the bioreactor run without antibiotics. On this matter alone, if further experiments were to be conducted using the Wake Forest bioreactor, especially using seeded grafts, it would need to be housed under more aseptic conditions.

Ultimately, future experimentation on the seeded conduits would assess scaffold maintenance, pre-conditioning, cellular proliferation, viability and phenotype of the seeded cells once submitted to circumferential and shear stress. In order for these experiments to be performed, it would be necessary to upgrade the bioreactor system significantly with monitoring equipment to allow parameters such as flow rate and pressure to be measured which would allow for accurate biomechanical assessment and to develop optimal biomechanical parameters for the seeded conduits. I believe that firstly, due to the simplicity of its design, it would not be possible to upgrade the Wake Forest bioreactor with such equipment. Secondly, the development, purchasing and procurement of sophisticated monitoring systems would require a large amount of time and expense. Designing and procuring a more sophisticated bioreactor system with such monitoring built within (although it would be more expensive) would ultimately make further experiments on seeded scaffolds proceed in a more timely manner and provide much more robust, accurate and reliable data- essential requirements for the ongoing development of the scaffold as a potential TEVG. As previously discussed, no single universal bioreactor system exists for the specific use of assessing SD tissue-engineered scaffolds.

Unfortunately, due to time constraints, it was not possible to proceed to further experiments to assess cell-seeded scaffolds in the bioreactor, however future projects within IMBE will use and take these preliminary results forward.

Chapter 7

General Discussion

To treat the increasing incidence of atherosclerosis, surgical bypass remains one of the standard surgical techniques (Nalysnyk, 2003; Klinkert *et al*., 2004). To date, autologous vein remains the gold standard graft of choice, mainly due it its length, ease of access and handling properties. Despite this, autologous vein may be unavailable or unsuitable to use in up to 30% of patients and in this scenario, surgeons often have to turn to the use of synthetic grafts to enable effective surgical bypass (Sayers *et al*.,1998). Synthetic materials (particularly as their diameter gets smaller) possess many drawbacks when compared to their venous counterparts, namely, thrombogenicity, reduced tissue handling, infection and biomechanical disadvantages such as compliance mismatch, a major cause of neointimal neoplasia and subsequent graft failure (Kannan *et al*., 2004). Such drawbacks are clearly seen when comparing the patency rates of autologous vein versus synthetic grafts such as ePTFE and Dacron. In AK and BK bypass for example, 5-year primary patency rates of 39% and 50% have been reported for ePTFE compared to 74% for saphenous vein (Albers *et al*., 2003; Klinkert *et al*., 2004).

In order to overcome these limitations when autologous vein is not available, surgeons and scientists have attempted to create a wide range of vascular grafts utilising three main strategies: to modify existing synthetic grafts, create new synthetic grafts or create blood vessels using tissue engineering. Tissue engineering strategies continue to evolve but mainly focus on the manipulation of tissues and cells to create a functional, living graft capable of remodeling and repair. In vascular tissue engineering such techniques include: the seeding of “old” and new synthetic materials with vascular cells (Meinhart *et al*, 2001; Rashid *et al*., 2004; Sarkar *et al*., 2007), the decellularisation and subsequent recellularisation of allogeneic and xenogeneic tissue (Schaner *et al*, 2004; Shimizu *et al*., 2007; Zhao *et al*., 2010) and the creation of assembled constructs capable of cellular ingrowth and remodeling (Campbell *et al*., 1999; Aper *et al*., 2007;). All techniques to date however have failed to achieve wide-spread clinical use.

The tissue engineering strategy used in this study was the decellularisation and subsequent re-cellularisation of porcine arterial tissue. The aim of the study was to create

a decellularised scaffold using PCA and assess its ability for re-cellularisation with xenogeneic vascular cells to aid in the development of a tissue engineered vascular graft.

7.1 Creation of acellular PCA scaffolds

The first objective of the study was to treat PCA with the established iMBE decellularisation protocol to produce acellular scaffolds and assess their biocompatability. Initial decellularisation runs failed to achieve acellular scaffolds but following modification of the protocol, histological analysis confirmed a lack of cell nuclei and double-stranded DNA within the treated arteries. DNA quantification confirmed a net DNA removal of between 90-99% ($ng.mg^{-1}$) in treated arteries following the protocol modification confirming successful decellularisation. Preservation of native arterial histioarchitecture was also well demonstrated. Biocompatibility of the acellular scaffolds was confirmed using the ISO standard cell lines for the assessment of medical devices, BHK and 3T3 cells (10993-p5, 2005).

7.2 Isolation and characterisation of primary [xenogeneic] ovine vascular cells

The next objective in the study was to isolate ovine vascular cells for future seeding experiments as such cells are not commercially available and ultimately it is intended that an ovine *in vivo* model will be used for future experiments. Isolation of ovine EC and SMC began in Chapter (4) and proved difficult as following harvesting and incubation, mixed cell populations of EC and SMC were seen on characterisation. Isolation of cells using magnetic beads was successful in isolating SMC but resulted in the death of EC isolates. To allow a timely continuation of the study, a peer within iMBE kindly gifted a population of pure ovine EC isolates. Before the ovine cells could be used experimentally, it was necessary to develop a reproducible, characterisation protocol to ensure correct cell phenotype and pure isolates. Very little work had been published on the characterisation of ovine vascular cells but what did exist focused heavily on indirect immunofluorescence and as such, was the technique used in this study. Anti-VWF antibody was the most commonly used antibody to identify ovine EC and for ovine SMC, anti-SMC α-actin antibody was the most commonly used. (Abdi *et al.*, 1995; Grooby *et al.*, 1997; Afting *et al.*, 2003; Zhao *et al.*, 2010;). These antibodies were used in the study alongside two antibodies to traditional markers of EC and SMC phenotype, namely CD31 and SMC-Myosin Heavy Chain respectively. (Hutanu *et al*., 2007; Walpoth *et al*., 2007). Both sets of

antibodies for each cell type stained in a specific fashion and so a successful characterisation protocol was developed to identify ovine vascular cells.

7.3 Ovine vascular cell-seeding of acellular scaffolds

The objective of this part of the study was to seed ovine vascular cells characterised in Chapter (4) onto the luminal surfaces of the acellular scaffolds in a (static) 2D and (dynamic) 3D fashion. 2D cell seeding experiments were performed initially and confirmed that ovine vascular cells could successfully adhere to the surface of the acellular scaffolds and display subsequent confluent growth across it. Optimal seeding densities for subsequent 3D dynamic cell seeding were developed and were consistent with current literature reports (McFetridge *et al*., 2004; Shimizu *et al*., 2007; Heine *et al*., 2011; Nitsan *et al*., 2012). 'Dynamic' 3D seeding of the scaffolds was performed using a roller-mixer. A rotational seeding technique was used in the study to seed the acellular scaffolds as literature reports had demonstrated greater seeding efficiencies when this technique is utilised. Hsu *et al.* (2005) used a rotational dynamic seeding technique to seed human EC onto the surface of SD polyurethane using a roller-mixer. Compared to static seeding, dynamic seeding lead to a greater GAG content in the scaffolds and a seeding efficiency of up to 90%, compared to10% for static. Rotational seeding subjects cells to shear stress, which leads to release of mediators that aid ECM formation, such as NO and calcium (Hsu *et al*., 2005).). In this current study, rotational seeding was effective in seeding individual populations of ovine vascular cells (EC or SMC) onto the luminal surface of the acellular scaffolds, suggesting that the findings of Hsu *et al.* may also apply to biological grafts.

Studies have demonstrated that EC retention on the luminal surface of prosthetic grafts is enhanced when the lumen is pre-seeded with SMC as they secrete more ECM and allow for greater adherence (Yu *et al*., 2001; Yu *et al*., 2003). It was the results of these studies that lead to the decision to dual-seed the scaffolds with SMC first and then EC. In the dual-seeding experiments, seeding was minimal and in a disorganised fashion with no evidence of monolayer formation seen in the experiments by Yu *et al*. (2003). One possibility is that as prosthetic grafts do not contain layers (just a porous matrix) the penetration of SMC is not limited. As histological assessment demonstrated, the internal elastic lamina was preserved in the acellular scaffolds and it may have been this structure that limited the penetration of SMC into deeper layers in this study.

7.4 Bioreactor development

The final objective of the study was to assemble and develop a bioreactor that would augment 3D seeding of the acellular scaffolds by subjecting them to pre-conditioning. Unfortunately time constraints only allowed time for bioreactor assembly and sterility runs to be performed. It was clear at this stage that the Wake Forest bioreactor was too primitive to allow the accurate assessment and determination of optimal pre-conditioning parameters for the seeded scaffolds and that microbial contamination would limit any experimentation time to approximately two weeks.

7.5 Discussion

To a large extent, the main aims of the study were achieved and had more time been available, such aims could have been further met in assessing the efficacy of a re-cellularised PCA being a potential candidate as a SD vascular bypass graft. The data that was generated from this study correlated with findings from similar tissue engineering studies using porcine tissue, in particular PCA, that have been reported in the literature. It is clear from this study and others reported that decellularised porcine arterial tissue demonstrates a high level of biocompatibility with autologous and xenogeneic vascular cells and provides a suitable environment for subsequent cell adherence (Conklin *et al*., 2002; McFetridge *et al*., 2004; Roy *et al*., 2005; Shimizu *et al*., 2007; Heine *et al*., 2011; Nitsan *et al*., 2012;). The ability of cells to adhere to a scaffold surface and in particularly in this case, form an endothelial monolayer, is a key attribute towards the development of an effective SD bypass graft.

Unfortunately, severe time pressure prevented continuation of further planned experiments. A significant amount of further study and assessment is required to determine whether a tissue engineered, cell-seeded PCA can be developed using the strategy used in this study, in order to create a substitute graft for small-diameter arterial bypass.

Decellularisation has been shown to be an effective technique with which to begin development of a SD tissue engineered graft. Removing host cells from a tissue ‘made-for-purpose’, leaving behind a scaffold matrix largely unaltered both biochemically and biomechanically, carries many advantages. Effective removal of cells should render the scaffold non-immunogenic which would prevent rejection following implantation. The

biological nature of the scaffold should allow effective integration and remodeling within host tissues following implantation and carry a significantly reduced risk of infection compared to synthetic material. Provided the decellularisation process does not significantly alter the ECM of the tissue, the acellular scaffold created should provide a favourable environment for subsequent re-cellularisation and the re-instigation of scaffold functionality. The decellularisation protocol developed by iMBE and used in this study creates non-immunogenic, acellular scaffolds that retain their histioarchitecture and biomechanical properties providing a useful starting material onto which further engineering and scaffold functionalisation can take place (Derham *et al*., 2008; Wilshaw *et al*., 2011). The scaffolds generated using this technique have also been shown to regenerate *in vivo* and some are used clinically now in Europe and the USA (Stapleton *et al*., 2011; Gutierrez *et al*., 2015).

The data presented in chapter five demonstrated that the current seeding strategy could work, but requires modifications in the technique. Firstly, further seeding work would be required with ovine vascular cells to assess whether a luminal dual-seeding approach is possible. Based on the results from the current study, greater seeding times would be required to help ascertain this. If luminal dual-seeding proved unsuccessful, then luminal seeding with EC and adluminal seeding with SMC could be attempted. Failing this, luminal seeding only of EC is an option, as the presence of a functioning endothelium is now well-established as the gold-standard for achieving short and long-term vascular graft efficacy (Zilla *et al*., 1994; Clowes *et al*., 1997; Meinhart *et al*., 2001; Sarkar *et al*., 2007).

With more time available, the study would have progressed to development of an effective 3D seeding protocol and the beginning of preconditioning experiments with the Wake Forest bioreactor. For the current study, the Wake Forest bioreactor would have been useful in assessing how well cells adhered to the scaffold under pulsatile flow but would not have provided much more information. The Wake Forest bioreactor used in this study was deemed to be too primitive in its design to allow sophisticated measurements of flow, pressure and shear stress to be performed. Knowledge of such parameters would be vital for an effective pre-conditioning protocol to be developed for the seeded scaffolds. It was also clear from this study that microbial contamination was an ongoing issue and positioning the bioreactor within an incubator in a busy laboratory likely contributed to the contamination. For future work to progress effectively, a more sophisticated bioreactor

situated in a clean, minimal access area, capable of measuring key parameters is essential.

7.5.1 Future work that is required

The development of a successful 3D seeding technique is essential for the progression of the study. If a 3D seeding technique was achieved then it would be important to assess the biomechanical integrity of the scaffold at this stage before further studies were commenced. In particular, burst pressure, compliance and suture-retention strengths should be measured. Burst pressure is used as a surrogate marker of long-term graft durability and can be used to predict the risk of graft complications such as aneurysmal dilatation and rupture. Compliance is a measure of the distensibility or stiffness of the graft. A non-compliant graft would lead to a significant compliance mismatch at the anastomosis with native artery, predisposing the graft to NIH and subsequent mid-term graft failure. Knowledge of the suture-retention strength of the grafts is required to ensure the anastomotic ends of the implanted grafts could withstand physiological systolic pressures.

If a successful 3D seeding and pre-conditioning protocol for the scaffolds could be developed, the next stage would be implant / explant of the scaffold into an *in vivo* ovine model to assess its efficacy as a vascular graft. An ovine model is suitable as the circulation in sheep is similar to humans; sheep possess a clotting system close to that of humans and also possess similar systolic and diastolic blood pressures and heart rates (Bianco *et al.*, 2004; Konya *et al.*, 2008). Ideally seeded grafts would be implanted as interposition grafts or extra-anatomic grafts in similar sized native vessels e.g ovine carotid artery or femoral artery to reduce compliance mismatch between graft and artery, which could otherwise predispose to thrombosis and NIH. The ‘common’ failures of vascular grafts are known to arise at specific time-points e.g early, mid-term and late, so it would be important to assess the grafts at these intervals, particularly the first two. Late failure in humans is secondary to atherosclerosis developing in the graft and so would be less important to assess in an animal model, particularly given the difficulties and costs involved in caring for an experimental animal model for up to five years. The primary endpoints to assess would be length of graft patency, and levels of thrombosis and neointimal hyperplasia. One protocol could be graft explantation at 30 days to assess for thrombosis and at one year for graft patency and for evidence of NIH. Secondary endpoints could be to determine the position of cells within their graft and their expressed

phenotype (does it possess a functioning endothelial monolayer) and graft function i.e does it possess vasomotor reactivity? The next stage following an ovine model should the scaffold demonstrate efficacy would ultimately be the seeding of acellular scaffolds with human vascular cells and if successful, reproducing the stages above. The final stage of the study would ultimately involve the implantation of a scaffold seeded with human vascular cells in human *in vivo* studies.

Tissue engineering is a promising approach to tackling the difficulties faced with SD bypass, in particular, the approach of seeding grafts with cells. Studies using cell-seeded synthetic grafts have clearly shown efficacy over un-seeded grafts in terms of short and long-term graft patency and I believe such results can be achieved using acellular scaffolds. (Zilla *et al*.,1994 ; Meinhart *et al*., 1997, 2001; Deutsch *et al*., 1997,1999; Laube *et al*., 2000). One of the significant drawbacks of using synthetic grafts remains the risk of infection, a risk that would largely be resolved if biological grafts were used.

In order to develop a graft that could display clinical and commercial success, it is vital that both costs and the time to produce the graft are kept as minimal as possible. The data presented in this thesis has demonstrated that the process of decellularising and re-cellularising porcine arterial tissue is a viable start in the development of a tissue engineered graft. PCA in particular are cheap to acquire as they can be harvested from pigs slaughtered for human consumption at a minimal cost as they are not specifically bred or maintained for purpose. Furthermore with animal tissue comes an essentially unlimited supply. The decellularisation process is short at two weeks and large batches could be decellularised together on a more industrial scale, improving production efficiency.

The scaffolds have demonstrated good initial seeding potential with xenogeneic cells without the need for functionalisation to improve seeding efficiency, again a major advantage in keeping production times and costs down. Despite this however, it is clear from the literature and my own personal view, that cell-seeding of grafts is the major barrier to the translation of this specific form of tissue engineering from getting from the bench to the bedside. Cell procurement from the patient, expansion of cells in culture and the seeding of grafts does take time (although as I have described, techniques are constantly evolving to improve this) and therefore excludes the cohort of patients that require coronary and peripheral arterial bypass in an urgent or semi-elective fashion. Should *in-situ* cell adhesion strategies improve so that grafts rapidly endothelialise

following implantation, then such a product could become an “off the shelf” medical device in the future. The reality is that this technology is still far away from achieving widespread success and for the current time, cell-seeded grafts remain a highly personalised, patient-specific item.

With regards to the scaffold itself as a bypass conduit, it does display excellent tissue handling properties would make it highly desirable to surgeons. It would be an excellent graft for coronary bypass but may have limited use in peripheral arterial bypass. The main drawback of PCA is its length and caliber change. At its origin from the aortic arch, the average length of PCA’s harvested during the study were approximately 10-12 cm. As it moves more proximally towards the brain, the diameter tapers from approx 6-8mm at its base to approximately 4mm at it’s proximal end. This length would be ideal for bypassing coronary vessels and the tapering would be of minimal consequence as it would match the natural tapering seen in the coronary arteries. It would however be too short in most cases for peripheral bypass, where a length of at least 15-25 cm would usually be required. It would be possible to anastomose two or even three grafts together, but this would significantly increase operating time. More importantly, the tapering would mean that any anastomosed grafts would not be completely uniform in diameter, likely impacting on the haemodynamics of the graft (where laminar flow is essential).

This study and others (Bader *et al*., 2000; Kaushal *et al*., 2001; McFetridge *et al*., 2004; Amiel *et al*., 2006; Hinds *et al*., 2006; Liao *et al*., 2009; Heine *et al*., 2011) have demonstrated many key attributes that porcine arterial tissue does possess that makes it an attractive material for the development of tissue engineered vascular grafts. In addition to the important future work discussed earlier with regards to the development of a cell-seeded PCA, applying and assessing the same techniques using porcine arterial tissues with greater length, such as femoral artery, may prove more suitable for human peripheral arterial bypass.

Clearly at the current position, and not unsurprisingly, the study has not created a scaffold that possesses all the key attributes of the ‘Ideal’ Vascular Graft laid out in Table 1, Chapter 1.

Many of the attributes described in Table (1) remain unknown until further studies with the current scaffolds can be or are performed. At the current time, certainly no scaffolds have been developed that do indeed possess all attributes listed. The decellularisation and

subsequent re-cellularisation of tissue remains one of the most viable techniques we have to date in order to achieve a graft displaying such key attributes as: being non-immunogenic, bacteriostatic, being easy to handle, having a potential unlimited size availability and importantly, retaining the biomechanical properties of native tissue. As the development of tissue engineering techniques increases, we may see improvement in other key areas such as production costs, transportation and storage.

There are unfortunately some limitations that in particular, tissue-engineered grafts have. Firstly the use of animal tissue to create a biological graft for human use will not be accepted by all patient groups. Vegetarians and patients with particular religious faiths for example would be unlikely to accept the implantation of such grafts for vascular bypass. Other patients may be concerned regarding the possible transmission of disease from animal to human or the possibility of contaminated grafts being implanted. Porcine cells for example do contain porcine endogenous retroviruses that can potentially infect human cells. The decellularisation process if performed effectively would remove the risk of disease transmission by removing porcine cells, however stringent safeguards and monitoring would be required throughout the production process to ensure grafts were free from endogenous pathogens. In addition, regular quality assurance and sterility testing would be required to ensure that scaffolds remain clear from microbial contamination. Most sterilisation processes are industrial and use predominantly heat or chemicals. Such processes are unsuitable for cell seeded scaffolds. As such, production of such grafts would have to be performed in aseptic environments, potentially increasing the costs of production.

7.6 Conclusion

In final conclusion, I believe that this study has demonstrated the viability of using a decellularised xenograft for the development of a TEVG. In particular the study has demonstrated that porcine carotid tissue can be successfully decellularised and re-cellularised using xenogeneic vascular cells. The scaffold created from PCA is an ideal size for use as a coronary arterial bypass conduit or as a SD interposition graft, but would be unsuitable for peripheral arterial bypass given its lack of length. Further work is required to establish if porcine scaffolds created by the decellularisation process can develop an endothelial monolayer with functionality and display efficacy as a SD graft in an *in vivo* model.

References

Abdi K, Rogers R, Li X, Lopez P, Rawn J, Mentzer S. **In Situ Fluorescence Labeling Of Sheep Lung Microvascular Endothelium**. *In Vitro Cellular & Developmental Biology. Animal*, 1995; 31: 310-315

Afting M, Stock U, Nasseri B, Pomerantseva I, Seed B, Vacanti J. **Efficient and Stable Retroviral Transfection of Ovine Endothelial Cells with Green Fluorescent Protein for Cardiovascular Tissue Engineering**. *Tissue Engineering*, 2003; **9:** 137-141.

Ahanchi S, Tsihlis N, Kibb M. **The role of nitric oxide in the pathophysiology of intimal hyperplasia**. *Journal of Vascular Surgery*, 2007; **45:** 64A-73A.

Albers M, Battistella V, Romiti M, Rodrigues A, Pereira C. **Meta-analysis of polytetrafluroethylene bypass grafts to infrapopliteal arteries**. *Journal of Vascular Surgery*, 2003; **37:** 1263-1269.

Alexy T, Tucker S, Boyle S, Rowe V, Weaver F, Liebman H. **Heparin-platelet factor 4 antibodies are frequent after vascular surgery but not a frequent cause of graft thrombosis or thrombocytopenia**. *Journal of Vascular Surgery*, 2008; **48:** 377-381.

Allaire E, Clowes A. **Endothelial cell injury in cardiovascular surgery: the intimal hyperplastic response**. *Annals of Thoracic Surgery*, 1997; **63:** 582-591.

Amiel G, Komura M, Shapira O, Yoo J, Yazdani S, Berry J *et al*. **Engineering of Blood Vessels from Acellular Collagen Matrices Coated with Human Endothelial Cells**. *Tissue Engineering*, 2006; **12:** 2355-2365.

Angelini G, Christie M, Bryan A, Lewis M. **Surgical preparation impairs release of endothelium-derived relaxing factor from human saphenous vein**. *Annals of Thoracic Surgery,* 1989; **48:** 417-420.

Aper T, Schmidt A, Duchrow M, Bruch H. **Autologous blood vessels engineered from peripheral blood sample**. *European Journal of vascular and Endovascular Surgery*, 2007; **33:** 33-39.

Ariyoshi H, Okuyama M, Okahara K, Kawasaki T, Kambayashi J, Sakon M et al. **Expanded Polytetrafluoroethylene (ePTFE) Vascular Graft Loses Its**

Thrombogenicity Six Months after Implantation. *Thrombosis Research*, 1997; **88:** 427-433.

Avci-Adali M, Perle N, Ziemer G, Wendel H. **Current Concepts And New Developments For Autologous *In Vivo* Endothelialisation Of Biomaterials For Intravascular Applications**. *European Cells and Materials*, 2011; **21:** 157-176.

Bader A, Steinhoff G, Strobl K, Schilling T, Brandes G, Mertsching H *et al*. **Engineering of human vascular aortic tissue based on xenogeneic starter matrix.** *Transplantation*, 2000; **70:** 7-14.

Baguneid M, Murray D, Salacinski H, Fuller B, Hamilton G, Walker M *et al*. **Shear-stress preconditioning and tissue-engineering-based paradigms for generating arterial substitutes**. *Biotechnology and Applied Biochemistry*, 2004; **39:** 151-157.

Baguneid M, Seifalian A, Salacinski H, Murray D, Hamilton G, Walker M. **Tissue engineering of blood vessels**. *British Journal of Surgery*, 2006; **93:** 282-290.

Benedetto B, Lipkowitz G, Madden R, Kurbanov A, Hull D, Miller M *et al*. **Use of cryopreserved cadaveric vein allograft for hemodialysis access precludes kidney transplantation because of allosensitization**. *Journal of Vascular Surgery*, 2001; **34:**139-142.

Berger K, Sauvage L, Rao A, Wood S. **Healing of arterial prostheses in man: Its incompleteness.** *Annals of Surgery*, 1972; **175:** 118-127.

Biancari F, Railo M, Lundin J, Alback A, Kantonen I, Lehtola A *et al*. **Redo bypass surgery to the infrapopliteal arteries for critical leg ischaemia.** *European Journal of Vascular and Endovascular Surgery*, 2001, **21:** 137-142.

Bianco R, Grehan J, Grubbs B, Mrachek J, Schroeder E, Schumacher *et al*. **Large animal models in cardiac and vascular biomaterials research and testing**. In: Ratner B, Hoffman A, Schoen F, Lemons J, editors. *Biomaterials science: an introduction to materials in medicine*. 2nd ed. San Diego, CA: Academic Press; 2004; 379-395.

Blann A, Nadar S, Lip G. **The adhesion molecule P-selectin and cardiovascular disease.** *European Heart Journal*, 2003; **24:** 2166-2179.

Booth C, Korossis S, Wilcox H, Watterson K, Kearney J, Fisher J *et al*. **Tissue engineering of cardiac valve prostheses I: development and histological characterization of an acellular porcine scaffold**. *Journal of Heart Valve Disease*, 2002; **11:** 457-462.

Bowlin G, Meyer A, Fields C, Cassano C, Makhoul R, Allen C *et al*. **The persistence of electrostatically seeded endothelial cells lining a small diameter expanded polytetrafluroethylene vascular graft**. *Journal of Biomaterials Applications,* 2001; **16:** 157-173.

Broze GJ, Warren LA, Novotny WF, Higuchi DA, Girard JJ, Miletich JP. **The lipoprotein-associated coagulation inhibitor that inhibits the factor VII-tissue factor complex also inhibits factor Xa: insight into its possible mechanism of action**. *Blood*, 1988; **71:** 335-343.

Budd J, Brennan J, Beard J, Warren H, Burton P, Bell P. **Infrainguinal bypass surgery: factors determining late graft patency**. *British Journal of Surgery*, 1990; **77:** 1382-1387.

Burton JR. **Coronary bypass graft fate and patient outcome: Angiographic follow-up of 5,065 grafts related to survival and reoperation in 1,388 patients during 25 years**. *Journal of the American College of Cardiology*, 1996; **28:** 616-626.

Butler D, Hunter S, Chokalingam K, Corday M, Shearn J, Juncosa-Melvin N *et al*. **Using Functional Tissue Engineering and Bioreactors to Mechanically Stimulate Tissue-Engineered Constructs**. *Tissue Engineering: Part A*, 2009; **15:** 741-749.

Camilleri J, Phat V, Bruneval P. **Surface healing and histiological maturation of patent polytetrafluroethylene grafts implanted in patients for up to 60 months**. *Archives of pathology and Laboratory Medicine*, 1985; **109:** 833-837.

Campbell J, Efendy J, Campbell G. Novel **Vascular Graft Grown Within Recipient's Own Peritoneal Cavity.** *Circulation Research*, 1999; **85:** 1173-1178.

Carnagey J, Hern-Anderson D, Ranieri J, Schmidt C. **Rapid Endothelialisation of Photofix Natural Biomaterial Vascular Grafts**. *Journal of Biomedical Materials Research Part B*, 2003; **65B:** 171-179.

Chard R, Johnson D, Nunn G, Cartmill T. **Aorta-coronary bypass grafting with polytetrafluoroethylene conduits. Early and late outcomes in eight patients**. *The Journal of Thoracic and Cardiovascular Surgery*, 1987; **94:** 132-134.

Cho S, Park H, Ryu J, Kim S, Kim Y, Choi C *et al*. **Vascular patches tissue-engineered with autologous bone marrow-derived cells and decellularized tissue matrices**. *Biomaterials*, 2005; **26:** 1915-1924.

Clarke D, Lust R, Sun Y, Black K, Ollerenshaw J. **Transformation of nonvascular acellular tissue matrices into durable vascular conduits**. *Annals of Thoracic Surgery*, 2001; **71(S):** S433-S436.

Clowes A. **Control of neointimal hyperplasia in ePTFE grafts**. *Journal of Vascular Surgery*, 1997; **6:** 1100-1101.

Conklin B, Richter E, Kreutziger K, Zhong D-S, Chen C. **Development and evaluation of a novel decellularized vascular xenograft**. *Medical Engineering & Physics*, 2002; **24:** 173-183.

Conte M, Mann M, Simosa H, Rhynhart K, Mulligan R. **Genetic interventions for vein bypass graft disease: a review**. *Journal of Vascular Surgery*, 2002, **36:** 1040-1052.

Cox J, Chiasson D, Gotlieb A. **Stranger in a strange land: the pathogenesis of saphenous vein graft stenosis with emphasis on structural and functional differences between veins and arteries**. *Progress in Cardiovascular Diseases*, 1991, **34:** 45-68.

d'Audiffret, Soloway P, Saadeh R, Carty C, Bush P, Ricotta J *et al*. **Endothelial Dysfunction Following Thrombolysis *in vitro***. *European Journal of Vascular and Endovascular Surgery*, 1998; **16:** 494-500.

Dahan N, Zarbiv G, Sarig U, Karram T, Hoffman A, Machluf M. **Porcine small diameter arterial extracellular matrix supports endothelium formation and media remodeling forming a promising vascular engineered biograft**. *Tissue Engineering: Part A*, 2012, **18**: 411-422.

Dardik A, Liu A, Ballermann B. **Chronic in vitro shear stress stimulates endothelial cell retention on prosthetic vascular grafts and reduces subsequent in vivo neointimal thickness**. *Journal of Vascular Surgery*, 1999; **29:** 157-167.

Dempsey D, Phaneuf M, Bide M, Szycher M, Quist W, Logerfo F. **Synthesis of a Novel Small Diameter Polyurethane Vascular Graft With Reactive Binding Sites**. *ASAIO Journal*, 1998; **44:** M506-M510.

Derham C, Yow H, Ingram J, Fisher J, Ingham E, Korrosis S *et al*. **Tissue engineering Small-Diameter Vascular Grafts: Preparation of a Biocompatible Porcine Ureteric Scaffold**. *Tissue Engineering: Part A*, 2008; **14:** 1871-1882.

Desai M, Mirzay-Razzaz J, von Delft D, Sarkar S, Hamilton G, Seifalian A. **Inhibition of neointimal formation and hyperplasia in vein grafts by external stent/sheath**. *Vascular Medicine,* 2010; **15:** 287-297.

Detta N, Errico C, Dinucci D, Puppi D, Clarke D, Reilly G *et al*. **Novel electrospun polyurethane/gelatin composite meshes for vascular grafts**. *Journal of Materials Science: Materials in Medicine*, 2010; **21:** 1761-1769.

Deutsch M , Meinhart J, Fischlein T, Preiss P, Zilla P. **Clinical autologous in vitro endothelialisation of infrainguinal ePTFE grafts in 100 patients: a 9-year experience**. *Surgery*, 1999; **126:** 847-855.

Deutsch M, Meinhart J, Vesely M, Fischlein T, Groscurth P, von Oppell U, Zilla P. **In vitro endothelialisation of expanded polytetrafluroethylene grafts: a clinical case report after 41 months implantation**. *Journal of Vascular Surgery*, 1997; **25:** 757-763.

Devine C, Hons B, McCollum C**. Heparin-bonded Dacron or polytetrafluoroethylene for femoropopliteal bypass grafting: a multicenter trial**. *Journal of Vascular Surgery*, 2001; **33:** 533-539.

Dichek D, Anderson J, Kelly A, Hanson S, Harker L. **Enhanced In Vivo Antithrombotic Effects of Endothelial Cells Expressing Recombinant Plasminogen Activators Transduced With Retroviral Vectors**. *Circulation*, 1996; **93:** 301-309.

Dunn P, Newman K, Jones M, Yamada I, Shayani V, Virmani I *et al*. **Seeding of vascular grafts with genetically modified endothelial cells. Secretion of recombinant TPA**

results in decreased seeded cell retention in vitro and in vivo. *Circulation*, 1996; **93:** 1439-1446.

Falk J, Townsend L, Vogel L, Boyer M, Olt S, Wease G. **Improved adherence of genetically modified endothelial cells to small-diameter expanded polytetrafluroethylene grafts in a canine model**. *Journal of Vascular Surgery*, 1998; **27:** 902-908.

Farrar D. **Development of a prosthetic coronary artery bypass graft**. *The Heart Surgery Forum*, 2000; **3:** 36-40.

Farrar D. **Development of a prosthetic coronary artery bypass graft**. *The Heart Surgery Forum*, 2000; **3:** 36-40.

Fields C, Cassano A, Allen C, Meyer A, Pawlowski K, Bowlin G *et al*. **Endothelial cell seeding of a 4-mm I.D. polyurethane vascular graft**. *Journal of Biomaterials Applications,* 2002; **17:** 45-70.

Fillinger M, O'Connor S, Wagner R, Cronenwett J. **The effect of endothelial cell coculture on smooth muscle cell proliferation**. *Journal of Vascular Surgery*, 1993: **17:** 1058-1067.

Fisher A, Chien S, Barakat A, Nerem R. **Endothelial cellular response to altered shear stress**. *American Journal of Physiology – Lung Cellular and Molecular Physiology*, 2001; **281:** L529-L533.

Formichi M, Guidoin R, Jausseran J. **Expanded polytetrafluroethylene arterial prosthesis in humans: Late pathological findings in 73 excised grafts**. *Annals of Vascular Surgery*, 1988; **2:** 14-27.

Furie B, Furie BC. **Molecular and cellular biology of blood coagulation**. *New England Journal of Medicine*, 1992; **326:** 800-806.

Galili U**. The α-gal epitope and the anti-Gal antibody in xenotransplantation and in cancer immunotherapy**. *Immunology and Cell Biology*, 2005; **83:** 674-686.

Gambillara V, Thacher T, Silacci P, Stergiopulos N. **Effects of Reduced Cyclic Stretch on Vascular Smooth Muscle Cell Function of Pig Carotids Perfused *Ex Vivo***. *American Journal of Hypertension*, 2008; **21:** 425-431.

Gao J, Niklason L, Langer R. **Surface hydrolysis of poly(glycolic acid) meshes increases the seeding density of vascular smooth muscle cells**. *Journal of Biomedical Materials Research*, 1998; **42:** 417- 424.

Gauvin R, Ahsan T, Larouche D, Lévesque P, Dubé J, Auger F *et al*. **A Novel Single-Step Self- Assembly Approach for the Fabrication of Tissue-Engineered Vascular Constructs**. *Tissue Engineering: Part A*, 2010; **16:** 1737-1747.

Gilbert T, Sellaro T, Badylak S. **Decellularization of tissues and organs**. *Biomaterials*, 2006; **27:** 3675-3683.

Giudiceandrea A, Seifalian AM, Krijgsman B, Hamilton G. **Effect of prolonged pulsatile shear stress in vitro on endothelial cell seeded PTFE and compliant polyurethane vascular grafts**. *European Journal of Vascular and Endovascular Surgery*, 1998; **15:** 147-154.

Goldstein A, Christ G. **Functional Tissue Engineering Requires Bioreactor Strategies**. *Tissue Engineering: Part A*, 2009; **15:** 739-740.

Gratzer P, Harrison R, Woods T. **Matrix alteration and not residual sodium dodecyl sulfate cytotoxicity affects the cellular repopulation of a decellularised matrix**. *Tissue Engineering*, 2006, **12:** 2975-2983.

Greisler HP. **Arterial regeneration over absorbable prostheses**. *Archives of Surgery,* 1982; **117:** 1425-1431.

Grooby W, Krishnan R, Russ G. **Characterization of ovine umbilical vein endothelial cells and their expression of cell adhesion molecules: Comparative study with human endothelial cells**. *Immunology and Cell Biology*, 1997; **75:** 21-28.

Gross D. **Animal models in cardiovascular research**. 2nd rev ed. Dordrecht, Boston: Kluwer Academic; 1994.

Gulbins H, Dauner M, Petzold R, Goldemund A, Anderson I, Doser M *et al*. **Development of an artificial vessel lined with human vascular cells**. *The Journal of Thoracic and Cardiovascular Surgery*, 2004; **128:** 372-377.

Gumpenberger T, Heitz J, Bäuerle D, Kahr H, Graz I, Romanin C *et al*. **Adhesion and proliferation of human endothelial cells on photochemically modified polytetrafluroethylene**. *Biomaterials*, 2003; **24:** 5139-5144.

Guitierrez J, Berry H, Korossis S, Mirsadraee S, Lopes S, da Costa F *et al*. **Regenerative Potential of Low-Concentration SDS-Decellularized Porcine Aortic Valved Conduits In Vivo.** *Tissue Engineering: Part A*, 2015; **21:** 332-342.

Hagemeyer C, Peter K. **Ex-vivo thrombolytic gene therapy for vein graft patency: The frontier for development of selective, localised therapeutic approaches**. *Thrombosis & Haemostasis*, 2009; **102:** 3-4.

Harris L, O'brien-Irr M, Ricotta J. **Long-term assessment of cryopreserved vein bypass grafting success.** *Journal of Vascular Surgery*, 2001; **33:** 528-532.

Haruguchi H, Teraoka S. **Intimal hyperplasia and hemodynamic factors in arterial bypass and arteriovenous grafts. A review**. *Journal of Artificial Organs*, 2003; **6:** 227-235.

Hata M, Sezai A, Niino T, Yoda M, Wakui S, Chiku M. **What is the optimal management for preventing saphenous vein graft diseases?: early results of intravascular angioscopic assessment**. *Circulation Journal*, 2007; **71:** 286-287.

Hata M, Sezai A, Niino T, Yoda M, Wakui S, Chiku M. **What is the optimal management for preventing saphenous vein graft diseases?: early results of intravascular angioscopic assessment**. *Circulation Journal*, 2007; **71:** 286-287.

Hehrlein F, Schlepper M, Loskot F, Scheld H, Walter P, Mulch J. **The use of expanded polytetrafluroethylene (PTFE) grafts for myocardial revascularization**. *Journal of Cardiovascular Surgery*, 1984; **25:** 549-553.

Heine J, Schmiedl A, Cebotari S, Mertsching H, Karck M, Haverich A *et al*. **Preclinical Assessment of a Tissue-Engineered Vasomotive Human Small-Calibered Vessel Based on a Decellularized Xenogeneic Matrix: Histiological and Functional Characterization**. *Tissue Engineering Part A*, 2011; **17:** 1253-1261.

Heine J, Schmiedl A, Cebotari S, Mertsching H, Karck M, Haverich A *et al*. **Preclinical Assessment of a Tissue-Engineered Vasomotive Human Small-Calibered Vessel Based on a Decellularized Xenogeneic Matrix: Histiological and Functional Characterization**. *Tissue Engineering Part A*, 2011; **17:** 1253-1261.

Herring M, Gardner A, Glover J. **A single staged technique for seeding vascular grafts with autologous endothelium.** *Surgery*, 1978; **84:** 498-504.

Higgins S, Solan A, Niklason L. **Effects of polyglycolic acid on porcine smooth muscle cell growth and differentiation**. *Journal of Biomedical Materials Research Part A,* 2003; **67:** 295-302.

Hilbert SL, Boerboom LE, Livesey SA, Ferrans VJ. **Explant pathology study of decellularized carotid artery vascular grafts**. *Journal of Biomedical Materials Research,* 2004; **69:** 197-204.

Hinds M, Rowe R, Ren Z, Teach J, Wu P-C, Kirkpatrick S *et al*. **Development of a reinforced porcine elastin composite vascular scaffold**. *Journal of Biomedical Materials Research*, 2006; **77A:** 458-469.

Hoerstrup S, Sodian R, Daebritz S, Wang J, Bacha E, Martin D *et al*. **Functional living trileaflet heart valves grow in vitro**. *Circulation*, 2000; **102:** 44-49.

Hoffmann J, Paul A, Harwardt M, Groll J, Reeswinkel T, Klee D *et al*. **Immobilized DNA aptamers used as potent attractors for porcine endothelial precursor cells**. *Journal of Biomedical Materials Research Part A*, 2008; **84A:** 614-621

Hsu S, Sun S, Chen D. **Improved retention of endothelial cells seeded on polyurethane small-diameter vascular grafts modified by a RGD-containing protein**. *Artificial Organs*, 2003; **27:** 1068-1078.

Hsu SH, Chuang SC, Chen CH, Chen DC. **Endothelial cell attachment to the gamma irradiated small diameter polyurethane vascular grafts**. *Biomedical Material Engineering*, 2006; **16:** 397-404.

Hsu S-H, Tsai I-J, Lin D-J, Chen D. **The effect of dynamic culture conditions on endothelial cell seeding and retention on small diameter polyurethane vascular grafts**. *Medical Engineering & Physics*, 2005; **27:** 267-272.

Huber T, Welling T, Sarkar R, Messina L, Stanley J. **Effects of retroviral-mediated tissue plasminogen activated gene transfer and expression on adherence and proliferation of canine endothelial cells seeded onto expanded polytetrafluroethylene**. *Journal of Vascular Surgery*, 1995; **22:** 795-803.

Hutanu C, Cox B, DeSpain K, Liu X-T, Rosenfeld C. **Vascular development in early ovine gestation: carotid smooth muscle function, phenotype, and biochemical markers**. *American Journal of Physiology-Regulatory, Integrative and Comparative Physiology.* 2007; **293:** R323-R333.

Huynh T, Abraham G, Murray J, Brockbank K, Hagan P-O, Sullivan S. **Remodelling of an acellular collagen graft into a physiologically responsive neovessel**. *Nature Biotechnology*, 1999; **17:** 1083-1086.

Ikeda M, Ariyoshi H, Kambayashi J, Sakon M, Kawasaki T, Monden M. **Simultaneous digital imaging analysis of cytosolic calcium and morphological change in platelets activated by surface contact.** *Journal of Cell Biochemistry*, 1996; **61:** 292-300.

Innocente F, Mandracchia D, Pektok E, Nottelet B, Till J-C, de Valence S *et al*. **Paclitaxel-Eluting Biodegradable Synthetic Vascular Prostheses**. *Circulation*, 2009; **120(S1):** S37-S45.

Isenberg B, Williams C, Tranquillo R. **Small-Diameter Artificial Arteries Engineered In Vitro.** *Circulation Research*, 2006; **98:** 25-35.

Ishii Y, Sakomoto S, Kronengold R, Virmani R, Rivera E, Goldman S *et al*. **A novel bioengineered small-caliber vascular graft incorporating heparin and sirolimus: Excellent six-month patency**. *The Journal of Thoracic and Cardiovascular Surgery*, 2008; **135:** 1237-1246.

Iwai S, Sawa Y, Taketani S, Torikai K, Hirakawa K, Matsuda H. **Novel Tissue-Engineered Biodegradable Material for Reconstruction of Vascular Wall**. *Annals of Thoracic Surgery,* 2005; **80:** 1821-1828.

Izzat M, West R, Bryan A. **Coronary artery bypass surgery: current practice in the United Kingdom**. *British Heart Journal*, 1994; **71:** 382-385.

Jones D, Rutherford R, Ikezawa T, Nishikimi N, Ishibashi H, Whitehall T. **Factors affecting the patency of small-caliber prostheses: observations in a suitable canine model**. *Journal of Vascular Surgery*, 1991; **14:** 441-448.

Kannan R, Salacinski H, Butler P, Hamilton G, Seifalian A. **Current Status of Prosthetic Bypass Grafts: A Review**. *Journal of Biomedical Materials Research Part B: Applied Biomaterials,* 2005; **74B:** 570-581.

Kasisis J, Liapis C, Breuer C, Sumpio B. **Artificial blood vessel: The Holy Grail of peripheral vascular surgery**. *Journal of Vascular Surgery*, 2005; **41:** 349-354.

Kaushal S, Amiel G, Guleserian K, Shapira O, Perry T, Sutherland F *et al*. **Functional small-diameter neovessels created using endothelial progenitor cells expanded ex vivo**. *Nature Medicine*, 2001; **7:** 1035-1040.

Kimura H, Sakata Y, Hamada H, Yoshida Y, Sato O, Deguchi J *et al*. **In vivo retention of endothelial cells adenovirally transduced with tissue-type plasminogen activator and seeded onto expanded polytetrafluroethylene**. *Journal of Vascular Surgery*, 2000; **32:** 353-363.

Klinkert P, Post P, Breslau P, van Bockel J. **Saphenous vein versus PTFE for above-knee femoropopliteal bypass. A review of the literature**. *European Journal of Vascular and Endovascular Surgery*, 2004; **27:** 357-362.

Kloner RA, Przyklenk K, Whittaker P. **Deleterious effects of oxygen radicals in ischaemia/reperfusion: resolved and unresolved issues**. *Circulation*, 1989; **80:** 1115-1127.

Knetsch M, Aldenhoff Y, Schraven M, Koole L. **Human endothelial cell attachment and proliferation on a novel vascular graft prototype**. *Journal of Biomedical Materials Research*, 2004; **71A:** 615-624.

Kokubo T, Uchida H, Choi E**. Integrin $\alpha_v\beta_3$ as a target in the prevention of neointimal hyperplasia**. *Journal of Vascular Surgery*, 2007; **45:** 33A-38A.

Konya A, Wright K, Gounis M, Kandarpa K. **Animal models for atherosclerosis, restenosis, and endovascular aneurysm repair**, In: Conn P, editor. *Sourcebook of models for biomedical research*. Totowa, NJ: Humana Press; 2008; 369-384.

Kumar T, Krishnan L. **A stable matrix for generation of tissue-engineered nonthrombogenic vascular grafts**. *Tissue Engineering*, 2002; **8:** 763-670.

L'Heureux N, Pâquet S, Labbé R, Germain L, Auger A. **A completely biological tissue-engineered human blood vessel**. *FASEB Journal*, 1998; **12:** 47-56.

Laube H, Duwe J, Rutsch W, Konertz W. **Clinical experience with autologous endothelial cell-seeded polytetrafluoroethylene coronary artery bypass grafts**. *The Journal of Thoracic and Cardiovascular Surgery*, 2000; **120:** 134-141.

Lee D, Steen J, Jordan J, Kincaid E, Kon N, Atala A *et al*. **Endothelialisation of Heart Valve Matrix Using a Computer-Assisted Pulsatile Bioreactor**. *Tissue Engineering: Part A*, 2009; **15:** 807-814.

Lehoux S, Castier Y, Tedgui A. **Molecular mechanisms of the vascular responses to haemodynamic forces**. *Journal of Internal Medicine*, 2006; **259:** 381-392.

Leung B, Sefton M. **A Modular Tissue Engineering Construct Containing Smooth Muscle Cells and Endothelial Cells**. *Annals of Biomedical Engineering*, 2007; **35:** 2039-2049.

Liao D, Lin P, Yao Q, Chen C. **Vascular smooth cell proliferation in perfusion culture of porcine carotid arteries**. *Biomechanical and Biophysical Research Communications*, 2008; **372:** 668-672.

Liao D, Wang X, Lin P, Yao Q, Chen C. **Covalent linkage of heparin provides a stable anti-coagulation surface of decellularized porcine arteries**. *Journal of Cellular and Molecular Medicine,* 2009; **13:** 2736-2743.

Libby P, Ridker P, Hansson G. **Progress and challenges in translating the biology of atherosclerosis**. *Nature*, 2011; **473:** 317-325.

Loop F, Lytle B, Cosgrove D, Stewart R, Goormastic M, Williams G *et al*. **Influence of the internal-mammary-artery graft on 10-year survival and other cardiac events**. *New England Journal of Medicine*, 1986; **314:** 1-6.

Mann KG, Brummel K, Butenas S. **What is all that thrombin for?** *Journal of Thrombosis and Haemostasis*, 2003; **1:** 1504-1514.

McAllister T, Maruszewski M, Garrido S, Wystrychowski W, Dusserre N, Marini A *et al*. **Effectiveness of haemodialysis access with an autologous tissue-engineered vascular graft: a multicentre cohort study**. *Lancet*, 2009; **373:** 1440-1446.

McFetridge P, Daniel J, Bodamyali T, Horrocks M, Chaudhuri J. **Preparation of porcine carotid arteries for vascular tissue engineering applications**. *Journal of Biomedical Materials Research*, 2004; **70A:** 224-234.

Mehta P, Griendling K**. Angiotensin II cell signaling: physiological and pathological effects in the cardiovascular system**. *American Journal of Physiology: Cell physiology*, 2007; **292**, C82-97.

Meinhart J, Deutsch M, Fischlein T, Howanietz N, Froschl A, Zilla P. **Clinical autologous in vitro endothelialisation of 153 infrainguinal ePTFE grafts.** *Annals of Thoracic Surgery*, 2001; **71:** S327-331.

Meinhart J, Deutsch M, Zilla P. **Eight years of clinical endothelial cell transplantation. Closing the gap between prosthetic grafts and vein grafts**. *ASAIO Journal*, 1997; **43:** M515-M 521.

Mitchell S, Niklason L. **Requirements for growing tissue-engineered vascular grafts**. *Cardiovascular Pathology*, 2003; **12:** 59-64.

Moneta G, Porter J. **Arterial substitutes in peripheral vascular surgery: a review**. *Journal of Long-Term Effects of Medical Implants*, 1995; **5:** 47-67.

Motwani J, Topol E. **Aortocoronary saphenous vein graft disease: pathogenesis, predisposition, and prevention**. *Circulation*, 1998; **97:** 916-931.

Nalysnyk L, Fahrbach K, Reynolds M, Zhao S, Ross S. **Adverse events in coronary artery bypass (CABG) graft trials: a systematic review and analysis**. *Heart*, 2003; **89:** 767-772.

National Center for Health Statistics. Series 13, 1996, No. **139:** 25-28.

Nemcova S, Noel A, Jost C, Gloviczki P, Miller V, Brockbank K. **Evaluation of an Xenogeneic Acellular Collagen Matrix as a Small-Diameter Vascular Graft in Dogs-Preliminary Observations**. *Journal of Investigative Surgery*, 2001; **14:** 321-330.

Nigri G, Kossodo S, Waterman P, Fungaloi P, LaMuraglia G. **Free Radical attenuation prevents thrombosis and enables photochemical inhibition of vein graft intimal hyperplasia**. *Journal of Vascular Surgery*, 2004; **39:** 843-849.

Nitsan D, Gabriel Z, Udi S, Tony K, Hoffman A, Marcelle M. **Porcine Small Diameter Arterial Extracellular Matrix Supports Endothelium Formation and Media Remodeling Forming a Promising Vascular Engineered Biograft**. *Tissue Engineering: Part A*, 2012; **18:** 411-422.

Norgren L, Hiatt W, Dormandy J, Nehler M, Harris K, Fowkes F. **TASC II Working Group. Inter-society concensus for the management of peripheral arterial disease (TASC II)**. *Journal of Vascular Surgery*, 2007; **45:** Supp, S5-S67.

Novokhatny V. **Structure and activity of plasmin and other direct thrombolytic agents**. *Thrombosis Research*, 2008; **122:** S3-S8.

Ogle B, Mooradian D. **Manipulation of remodelling pathways to enhance the mechanical properties of a tissue engineered blood vessel**. *Journal of Biomechanical Engineering*, 2002; **124:** 724-733.

Orrico C, Pasquinelli G, Foroni L, Muscara D, Tazzari P, Ricci F *et al*. **Dysfunctional Vasa Vasorum in Diabetic Peripheral Artery Obstructive Disease with Critical Lower Limb Ischaemia**. *European Journal of Vascular and Endovascular Surgery*, 2010; **40:** 365-374.

Pang Z, Niklason L, Truskey G. **Porcine Endothelial Cells Cocultured with Smooth Muscle Cells Became Procoagulant *In Vitro***. *Tissue Engineering: Part A*, 2010; **16:** 1835-1844.

Panigua Gutierrez J, Berry J, Korossis S, Mirsadraee S, Lopes S, daCosta F *et al*. **Regenerative potential of low concentration SDS decellularised porcine aortic valved conduits in vivo**. *Journal of Tissue Engineering: Part A*, 2015; **21:** 332-342.

Potter van Loon BJ, Rijken DC, Brommer EJ, Van der Maas AP. **The amount of plasminogen, tissue-type plasminogen activator and plasminogen activator inhibitor type 1 in human thrombi and the relation to ex-vivo lysibility**. *Thrombosis and Haemostasis*, 1992; **67:** 101-105.

Powell R, Cronenwett J, Fillinger M, Wagner R, Sampson L. **Endothelial cell modulation of smooth muscle cell morphology and organizational growth pattern**. *Annals of Vascular Surgery*, 1996; **10:** 4-10.

Pratt K, Jarrell B, Williams S, Carabasi R, Rupnick M, Hubbard F. **Kinetics of Endothelial Cell-Surface Attachment Forces**. *Journal of Vascular Surgery*, 1988; **7:** 591- 599.

Pulli R, Dorigo W, Castelli P, Dorrucci V, Ferilli F, De Blasis G *et al*. **Midterm results from a multicenter registry on the treatment of infrainguinal critical limb ischemia using a heparin-bonded ePTFE graft**. *Journal of Vascular Surgery*, 2010; **51:** 1167-1177.

Punshon G, Sales K, Vara D, Hamilton G, Seifalian A. **Assessment of the potential of progenitor stem cells extracted from human peripheral blood for seeding a novel vascular graft material**. *Cell Proliferation*, 2008; **41:** 321-335.

Quiniones M, Leor J, Kloner R, Ito M, Patterson M, Witke W *et al*. **Avoidance of immune response prolongs expression of genes delivered to the adult rat myocardium by replication-defective adenovirus**. *Circulation*, 1996; **94:** 1394-1401.

Rademacher A, Paulitschke M, Meyer R, Hetzer R. **Endothelialisation of PTFE vascular grafts under flow induces significant cell changes**. *International Journal of Artificial Organs*, 2001; **24:** 235-242.

Rashid S, Fuller B, Hamilton G, Seifalian A. **Tissue engineering of a hybrid bypass graft for coronary and lower limb bypass surgery**. *The FASEB Journal*, 2008; **22:** 2084-2089.

Rashid S, Salacinski H, Button M, Fuller B, Hamilton G, Seifalian A. **Cellular engineering of conduits for coronary and lower limb bypass surgery: role of cell attachment peptides and pre-conditioning in optimising smooth muscle cells (SMC) adherence to compliant poly(carbonate-urea)urethane (Myolink trademark) scaffolds**. *European Journal of Vascular and Endovascular Surgery*, 2004; **27:** 608-616.

Rashid S, Salacinski H, Fuller B, Hamilton G, Seifalian A. **Engineering of bypass conduits to improve patency**. *Cell Proliferation*, 2004; **37:** 351-366.

Rosenman J, Kempczinski R, Pearce W, Silberstein E. **Kinetics of Endothelial Cell Seeding**. *Journal of Vascular Surgery*, 1985; **2:** 778-784.

Rotmans J, Heyligers J, Verhagen H, Velema E, Nagtegaal M, de Kleijn D *et al*. **In vivo cell seeding with anti-CD34 antibodies successfully accelerates endothelialisation but stimulates intimal hyperplasia in porcine arteriovenous expanded polytetrafluroethylene grafts**. *Circulation*, 2005; **112:** 12-18.

Roy S, Silacci P, Stergiopulos N. **Biomechanical properties of decellularized porcine common carotid arteries**. *American Journal of Physiology: Heart & Circulatory Physiology*, 2005; **289:** H1567-H1576.

Rubin BG, Toursarkissian B, Petrinec D, Ying Yang L, Eisenberg PR, Abendschein DR**. Preincubation of Dacron grafts with recombinant tissue factor pathway inhibitor decreases their thrombogenicity in vivo**. *Journal of Vascular Surgery*, 1996; **24:** 865-870.

Rutherford RB, Jones DN, Bergentz S, Bergqvist D, Comerota A, Dardik H *et al*. **Factors affecting the patency of infrainguinal bypass**. *Journal of Vascular Surgery*, 1988; **8:** 236-246.

Niklason L. **Requirements for growing tissue-engineered vascular grafts**. *Cardiovascular Pathology*, 2003; **12:** 59-64.

Salacinski H, Tiwari A, Hamilton G, Seifalian A. **Cellular engineering of vascular bypass grafts: Role of chemical coatings for enhancing endothelial cell attachment**. *Medical and Biological Engineering and Computation*, 2001; **39:** 609-618.

Sarkar S, Sales K, Hamilton G, Seifalian A. **Addressing Thrombogenicity in Vascular Graft Construction**. *Journal of Biomedical Materials Research Part B*, 2007; **82:** 100-108.

Sauvage LR, Walker MW, Berger K, Robel SB, Lischko MM, Yates SG *et al*. **Current arterial prostheses: Experimental evaluation by implantation in the carotid and circumflex coronary arteries of dogs**. *Archives of Surgery*, 1979; **114:** 687-691.

Sawyer P, Fitzgerald J, Kaplitt M, Sanders R, Williams G, Leather R *et al*. **Ten year experience with the negatively charged glutaraldehyde-tanned vascular graft in peripheral vascular surgery. Initial multicenter trial**. *American Journal of Surgery*, 1987; **154:** 533-537.

Sayers RD, Raptis S, Berce M, Miller JH. **Long-term results of femorotibial bypass with vein or polytetrafluroethylene**. *British Journal of Surgery*, 1998; **85:** 934-938.

Schachner, T. **Pharmacologic inhibition of vein graft neointimal hyperplasia**. *The Journal of Thoracic and Cardiovascular Surgery*, 2006; **131:** 1065-1072.

Schaner P, Martin N, Tulenko T, Shapiro I, Tarola N, Leichter R *et al*. **Decellularized vein as a potential scaffold for vascular tissue engineering**. Journal *of Vascular Surgery*, 2004; **40:** 146-153.

Scharn D, Oyen W, Klemm P, Verhofstad A, van der Vliet A. **Thrombogenicity and Related Biological Properties of Heparin Bonded Collagen Coated Polyester and Human Umbilical Vein Prosthetic Vascular Grafts**. *Journal of Surgical Research*, 2006; **134:** 182-189.

Seifu D, Purnama A, Mequanint K, Mantovani D. **Small-diameter vascular tissue engineering**. *Nature Reviews: Cardiology*, 2013; **10:** 410-421.

Shi Q, Aida K, Vandeberg J, Wang XL. **Passage-dependent changes in baboon endothelial cells- relevance to in vitro ageing**. *DNA and Cell Biology*, 2004; **23:** 502-509.

Shi Q, Bhattacharya V, Hong-De Wu M, Sauvage L. **Utilizing granulocyte colony-stimulating factor to enhance vascular graft endothelialisation from circulating blood cells**. *Annals of Vascular Surgery*, 2002; **16:** 314-320.

Shimizu K, Ito A, Arinobe M, Murase Y, Iwata Y, Narita Y *et al*. **Effective Cell-Seeding Technique Using Magnetite Nanoparticles and Magnetic Force onto Decellularized Blood Vessels for Vascular Tissue Engineering**. Journal *of Bioscience and Bioengineering*, 2007; **103:** 472-478.

Sottiurai V, Yao J, Flinn W, Batson R. **Intimal hyperplasia and neo intima: an ultrastructoral analysis of thrombosed grafts in humans**. *Surgery*, 1983; **93:** 809-817.

Spijker HT, Bos R, Busscher HJ, Van Kooten TG, van Oeveren W. **Platelet adhesion and activation on a shielded plasma gradient prepared on polyethylene**. *Biomaterials*, 2002; **23:** 757-766.

Spijker HT, Busscher HJ, van Oeveren W. **Influence of abciximab on the adhesion of platelets on a shielded plasma gradient prepared on polyethylene**. *Thrombosis Research*, 2003; **108:** 57-62.

Sprague E, Palmaz J. **A Model System to Assess Key Vascular Responses to Biomaterials**. *Journal of Endovascular Therapy*, 2005; **12:** 594-604.

Stapleton, T, Ingram J, Fisher J, Ingham, E**. Investigation of the regenerative capacity of an acellular porcine medial meniscus for tissue engineering applications**. *Tissue Engineering Part A*, 2011; **17:** 231-242 (2011)

Stegemann J, Kaszuba S, Rowe S. **Advances in Vascular Tissue Engineering Using Protein-Based Biomaterials**. *Tissue Engineering*, 2007; **13:** 2601-2613.

Stephan S, Ball S, Williamson M, Bax D, Lomas A, Shuttleworth C *et al*. **Cell-matrix biology in vascular tissue engineering**. *Journal of Anatomy*, 2006; **209:** 495-502.

Strobel R, Wengerter K, Qin F, Pangilinan A, Silvestri F, Wolodiger F *et al*. **Aneurysm formation in modified human umbilical vein grafts**. *European Journal of Vascular and Endovascular Surgery,* 1996; **11:** 417-420.

Suma H. **Arterial grafts in coronary bypass surgery**. *Annals of Thoracic & Cardiovascular Surgery*, 1999; **5:** 141-145.

Suzuki H, Yamazaki H, Tanoue K. **Immunocytochemical aspects of platelet membrane glycoproteins and adhesive proteins during activation**. *Progress in Histochemistry and Cytochemistry,* 1996; **30:** 1-106.

Swartz D, Russell J, Andreadis S. **Engineering of fibrin-based functional and implantable small diameter blood vessels**. *American Journal of Physiology. Heart and Circulatory Physiology*, 2005; **288:** H1451-H1460.

Teebken O, Haverich A. **Tissue Engineering of Small Diameter Vascular Grafts**. *European Journal of Vascular and Endovascular Surgery*, 2002; **23:** 475-485.

Thomas A, Campbell G, Campbell J. **Advances in vascular tissue engineering**. *Cardiovascular Pathology*, 2003; **12:** 271-276.

Thomas A, Wyatt M, Newby A. **Reduction of early vein graft thrombosis by tissue plasminogen gene transfer**. *Thrombosis and Haemostasis*, 2009; **102:** 145-152.

Tiwari A, Salacinski H, Hamilton G, Seifalian A. **Tissue engineering of vascular bypass grafts: role of endothelial cell extraction**. *European Journal of Vascular and Endovascular Surgery*, 2001; **21:** 193-201.

Torikai K, Ichikawa H, Hirakawa K, Matsumiya G, Kuratani T, Iwai S, Saito A *et al*. A **self-renewing, tissue-engineered vascular graft for arterial reconstruction**. *The Journal of Thoracic and Cardiovascular Surgery*, 2008; **136:** 37-45.

Toursarkissian B, Eisenberg PR, Abendschein DR, Rubin BG. **Thrombogenicity of small diameter prosthetic grafts: Relative contributions of graft-associated thrombin and factor Xa**. *Journal of Vascular Surgery*, 1997; **25:** 730-735.

Twine C, McLain A. **Graft type for femoro-popliteal surgery**. *Cochrane Database of Systematic Reviews*, 2010; **CD001487**.

Verhagen H, Heijnen-Snyder G, Pronk A, Vroom T, van-Vroonhoven T, Eikelboom B *et al*. **Thrombomodulin activity on mesothelial cells: perspectives for mesothelial cells as an alternative for endothelial cells for cell seeding on vascular grafts**. *British Journal of Haematology*, 1996; **95:** 542-549.

Vroman, L. **Effect of Adsorbed Proteins on the Wettability of Hydrophilic and Hydrophobic Solids**, *Nature*, 1962; **196:** 476-477.

Wallace C, Champion J, Truskey G. **Adhesion and function of human endothelial cells co-cultured on smooth muscle cells**. *Annals of Biomedical Engineering,* 2007; **35: 375-**

Wallace C, Strike S, Truskey G. **Smooth muscle cell rigidity and extracellular matrix organization influence endothelial cell spreading and adhesion formation in coculture**. *American Journal of Physiology: Heart and Circulatory Physiology*, 2007; **293:** H1978.

Walles T, Puschmann C, Haverich A, Mertsching H. **Acellular scaffold implantation- no alternative to tissue engineering**. *International Journal of Artificial Organs*, 2003; **26:** 225-234.

Walpoth B, Zammaretti P, Cikirikcioglu M, Khabiri E, Djebaili M, Pache J-C *et al.* **Enhanced intimal thickening of expanded polytetrafluroethylene grafts coated with fibrin or fibrin-releasing vascular endothelial growth factor in the pig carotid artery interposition model**. *Journal of Thoracic and Cardiovascular Surgery*, 2007; **133:** 1163-1170.

Wang X-N, Chen C-Z, Yang M, Gu Y. **Implantation of Decellularized Small-caliber Vascular Xenografts With and Without Surface Heparin Treatment**, *Artificial Organs*, 2007; 31: 99-104.

Weinberg C, Bell E. **A blood vessel model constructed from collagen and cultured vascular cells.** *Science*, 1986; **231:** 397-400.

Weitz JI, Hudoba M, Massel D, Maragnore J, Hirsch J. **Clot-bound thrombin is protected from inhibition by heparin-antithrombin III but is susceptible to inactivation by antithrombin III-independent inhibitors**. *Journal of Clinical Investigation*, 1990; **86:** 385-391.

Weyand M, Kerber S, Schmid C, Rolf N, Scheld H. **Coronary artery bypass grafting with an expanded polytetrafluroethylene graft**. *Annals of Thoracic Surgery*, 1999; **67:** 1240-1245.

Widmer M, Aregger F, Stauffer E, Savolainen H, Heller G, Hakki H *et al*. **Intermediate outcome and risk factor assessment of bovine vascular heterografts used as AV-fistulas for hemodialysis access**. *European Journal of Vascular and Endovascular Surgery*, 2004; **27:** 660-665.

Wilcox H, Korossis S, Booth C, Watterson K, Kerney J, Fisher J *et al.* **Tissue engineering a living heart valve : biological and biomechanical assessment of an acellular, porcine valve matrix**. *European Cells and Materials*, 2003**; 6 (S2)**: 8.

Williams C, Wick T. **Perfusion Bioreactor for Small Diameter Tissue-Engineered Arteries**. *Tissue Engineering*, 2004; **10:** 930-941.

Wilshaw S-P, Kearnery J, Fisher J, Ingham E. **Production of an acellular amniotic membrane matrix for use in tissue engineering**. *Tissue Engineering*, 2006; **12:** 2117-2129.

Wilshaw S-P, Rooney P, Berry H, Kearney J, Homer-Vanniasinkam S, Fisher J *et al*. **Development and Characterization of Acellular Allogeneic Arterial Matrices**. *Tissue Engineering: Part A*, 2012; **18:**471-483.

Wippermann J, Schumann D, Klemm D, Kosmehl H, Salehi-Gelani S, Wahlers T. **Preliminary Results of Small Arterial Substitute Performed with a New Cylindrical Biomaterial Composed of Bacterial Cellulose**. *European Journal of Vascular and Endovascular Surgery,* 2009; **37:** 592-596.

Wissink M, Beernink R, Poot A, Engbers G, Beugeling T, van Aken W *et al*. **Improved endothelialisation of vascular grafts by local release of growth factor from heparinized collagen matrices**. *Journal of Controlled Release*, 2000; **64:** 103-114.

Writing Group Members *et al*. **Heart Disease and Stroke Statistics 2010 Update: A Report From the American Heart Association**. *Circulation*, 2010; **121:** 1-173.

Yang D, Guo T, Nie C, Morris S. **Tissue-Engineered Blood Vessel Graft Produced by Self-Derived Cells and Allogenic Acellular Matrix**. *Annals of Plastic Surgery*, 2009; **62:** 297-303.

Yang Z, Ruschitzka F, Rabelink TJ, Noll G, Julmy F, Joch H *et al*. **Different effects of thrombin receptor activation on endothelium and smooth muscle cells of human coronary bypass vessels. Implications for venous bypass failure.** *Circulation*, 1997; **95:** 1870-1876.

Yao L, Swartz D, Gugino S, Russell J, Andreadis S. **Fibrin-based tissue-engineered blood vessels: differential effects of biomaterial and culture parameters on mechanical strength and vascular reactivity**. *Tissue Engineering*, 2005; **11:** 991-1003.

Yazdani S, Tillman B, Berry J, Soker S, Geary R. **The fate of an endothelium layer after preconditioning**. *Journal of Vascular Surgery*, 2010; **51:** 174-183.

Yazdani S, Watts B, Machingal M, Jarajapu Y, Van Dyke M, Christ G. **Smooth Muscle Cell seeding of Decellularized Scaffolds: The Importance of Bioreactor Preconditioning to Development of a More Native Architecture for Tissue-Engineered Blood Vessels**. *Tissue Engineering: Part A*, 2009; **15:** 827-840.

Yu H, Dai W, Yang Z, Kirkman P, Weaver F, Eton D *et al*. **Smooth muscle cells improve endothelial cell retention on polytetrafluoroethylene grafts in vivo**. *Journal of Vascular Surgery*, 2003; **38:** 557-563.

Yu H, Wang Y, Eton D, Rowe V, Terramani T, Cramer DV *et al*. **Dual cell seeding and the use of zymogen tissue plasminogen activator to improve cell retention on polytetrafluoroethylene grafts**. *Journal of Vascular Surgery*, 2001; **34:** 337-343.

Zhan F, Fan Y, Deng X. **Swirling flow created in a glass tube suppressed platelet adhesion to the surface of the tube: Its implication in the design of small-caliber arterial grafts.** *Thrombosis Research*, 2010; **125:** 413-418.

Zhang Z, Wang Z, Liu S, Kodama M. **Pore size, tissue ingrowth, and endothelialisation of small-diameter microporous polyurethane vascular prostheses**. *Biomaterials*, 2004; **25:** 177-187.

Zhao Y, Zhang S, Zhou J, Wang J, Zhen M, Liu Y *et al*. **The development of a tissue-engineered artery using decellularized scaffold and autologous ovine mesenchymal stem cells**. *Biomaterials*, 2010; **31:** 296-307.

Ziegler T, Nerem R. **Tissue engineering a blood vessel: regulation of vascular biology by mechanical stresses**. *Journal of Cell Biochemistry*, 1994; **56:** 204-

Zilla P, Deutsch M, Meinhart J, Puschmann R, Eberl T, Minar E *et al*. **Clinical in vitro endothelialisation of femoropopliteal bypass grafts: an actuarial follow-up over three years**. *Journal of Vascular Surgery*, 1994; **19:** 540-548.

Appendix A

Accepted Abstracts and Publications

1) Presented at the Vascular Society of Great Britain and Ireland AGM, Edinburgh 2011 (BJS Prize Session). Oral presentation.

"Tissue engineering small-diameter vascular grafts: decellularisation of porcine arteries"

M Tatterton, SP Wilshaw, H Berry, JN Kearney, J Fisher, E Ingham, S Homer-Vanniasinkam .

2) Presented at the Society of Academic and Research Surgery (SARS) Annual Conference, Nottingham 2012. Oral presentation.

"Tissue engineering small diameter bypass grafts: decellularisation and biocompatibility of porcine internal carotid arteries".

M Tatterton, SP Wilshaw, S Korrosis, E Ingham, S Homer-Vanniasinkam.

3) Presented at the Arteriosclerosis, Thrombosis and Vascular Biology (ATVB) Conference in Chicago, USA, April 2012. Poster presentation.

"Tissue engineering a small diameter vascular graft".

Tatterton M, Wilshaw S-P Ingham E, Homer-Vanniasinkam S.

4) Presented at the Vascular Society of Great Britain and Ireland AGM, Manchester 2012 (SARS Prize Session). Oral presentation.

"Tissue engineering a small diameter vascular graft- cell seeding of a decellularised porcine arterial scaffold"

Tatterton M, Wilshaw S-P, Ingham E, Vanniasinkam, S.

5) Review published in The Journal of Vascular and Endovascular Surgery.

M. Tatterton, S-P Wilshaw, E.Ingham, S Homer-Vanniasinkam. **The use of antithrombotic therapies in reducing synthetic small-diameter vascular graft thrombosis, Journal of Vascular and Endovascular Surgery, 2012; 46:3; 212-222.**

6) **Presented at the Tissue Engineering and Regenerative Medicine International Society, Atlanta, USA, 2013. Poster presentation.**

"Tissue engineering a Small Diameter Cell Seeded vascular Graft"

Tatterton M, Wilshaw S-P, S-P Ingham E, Homer-Vanniasinkam S.